Karlsruhe Institute of Technology

PADF-2. Data for stable isotopes of Cl, K, Sc, and Ti

A.Yu. Konobeyev[1], A. Stankovskiy[2], D. Leichtle[1], D. Koliadko[1], A. Klix[1]

KIT SCIENTIFIC WORKING PAPERS 266

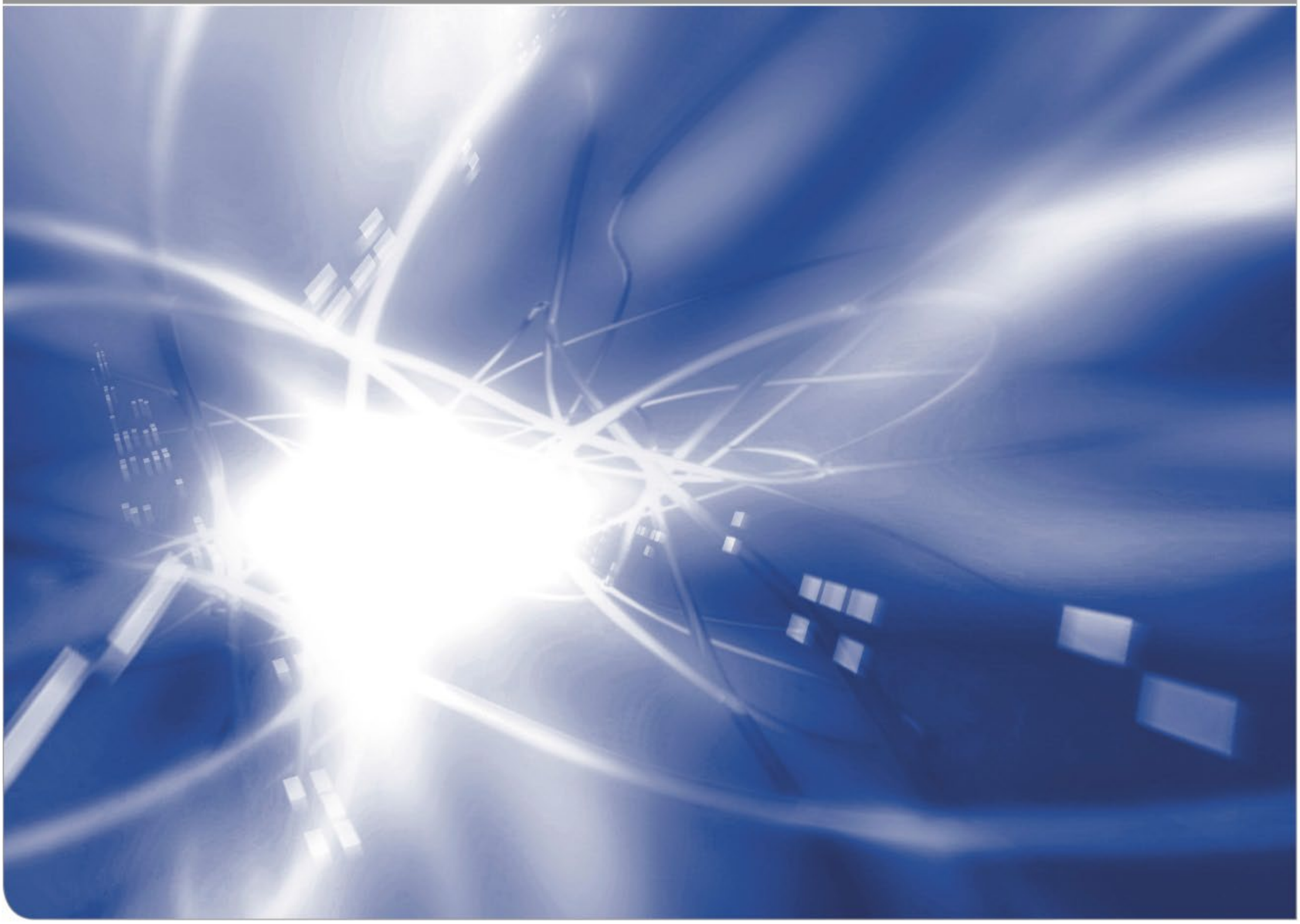

[1] Institute for Neutron Physics and Reactor Technology, Karlsruhe Institute of Technology, 76344 Eggenstein-Leopoldshafen, Germany

[2] Belgian Nuclear Research Centre, SCK CEN, Boeretang 200, B-2400 Mol, Belgium

Impressum

Karlsruher Institut für Technologie (KIT)
www.kit.edu

2025

ISSN: 2194-1629

Abstract

The cross-sections for proton interactions with stable isotopes of chlorine, potassium, scandium, and titanium were obtained for energies ranging from the reaction threshold up to 200 MeV. The study comprised model-based calculations, analysis of experimental data, and evaluation of resulting cross-sections.

For reactions lacking experimental data, the cross-sections were estimated based on calculated results, considering the accuracy and predictive capability of different models across various energy ranges.

The resulting data files can be accessed and downloaded from the KIT Cloud at https://bwsyncandshare.kit.edu/s/YwCwKH5qSjBPjfx

CONTENTS

page

1. INTRODUCTION

This work is a continuation of other published works [1-3] dedicated to the creation of the PADF-2 file.

The report describes the evaluation of cross-sections for stable isotopes of chlorine $^{35,37}Cl$, potassium $^{39,40,41}K$, scandium ^{45}Sc, and titanium $^{46,47,48,49,50}Ti$ at incident proton energies up to 200 MeV.

In this work, as in Refs. [1-3], all available experimental data for the targets under consideration were used - independent and cumulative measurements were utilized for individual target isotopes, as well as for natural isotopic mixtures.

The calculations were performed using advanced methods and the most recent releases of the computer codes applied also in Refs. [1-3].

The resulting files contain cross-sections of all observed reactions, provided and not provided by experimental data. They also include the total production cross-sections of neutrons, protons, deuterons, ^{3}He, α-particles, and heavy fragments.

Section 2 describes the cross-section calculation methods, Section 3 discusses the use of experimental data, Section 4 details the cross-section evaluation, and Section 5 presents the results.

2. CROSS-SECTION CALCULATION

As in works [1-3] the calculations were performed using current versions of the codes ALICE/ASH [4-6], CEM [7,8], PHITS [9,10], TALYS [11,12], and TALYS-G [13-15]. The calculations using TALYS-2.0 [12] were carried out using various models describing the level density of excited states and corresponding to the input code parameters *ldmodel* equal to *1, 2, and 3*. The optimal parameters of the models obtained by the authors [12] were applied by including the value "*fit y*" for the parameters *ldmodel* equal to *1 and 2* in the input data fille.

The spread of the calculation results and the use of different methods and codes in various ranges of energies and residual nuclei are discussed in work [3]. This includes an explanation of the use of a weighted sum of calculated cross-sections.

3. EXPERIMENTAL DATA

The experimental data were taken from EXFOR [16]. Auto-corrections, available on the website, were applied for the monitor cross-sections and decay data.

Before use, the experimental data were analysed by consulting the original publications and, in some cases, the results of theoretical calculations. The following considerations needed to be addressed, and the necessary cross-section corrections performed if required:

- Is the reaction cross-section independent or cumulative in the energy range under consideration? The results of calculations performed using CEM, PHITS, and TALYS were used as a basis for the answer.
- If comprehensive information on the used monitor reaction cross-sections is available, the measured cross-section should be corrected using the new monitor cross-sections, if exist. For some reactions, the automatic renormalization of cross-sections available on the EXFOR website was applied. For other reactions the corrections were made in this work.
- If a cross-section is presented in EXFOR as "partial" (PAR,SIG), can it be used as the total cross-section within a certain energy range of primary protons? The results of calculations using the TALYS code [12] were used to answer this question.

Below are comments explaining the use of measured data in specific cases.

Only publications, reactions, and nuclides for which changes have been made or the information about which is necessary for the explanations given below are considered here. If the changes were applied using the auto-correction feature on the EXFOR website or were not made at all, the measurement is not mentioned here. Experimental works [17-49] are cited mainly based on EXFOR entries and are listed in the bibliography alphabetically.

3.1 Chlorin

Following the analyses with TALYS, PHITS, and CEM, all available measurements of ^{22}Na and ^{24}Na yields were considered cumulative, due to potential contributions from their precursors, ^{22}Mg and ^{24}Ne, respectively.

R.Bimbot, H.Gauvin (1971) [19]. Data measured for ^{34m}Cl were corrected at 50 MeV using new cross-section [50] for the monitor reaction $^{27}Al(p,x)^{22}Na$.

R.G.Korteling, A.A.Caretto (1970) [31]. The cross-sections for the $^{nat}Cl(p,x)^{22}Na$ and $^{nat}Cl(p,x)^{24}Na$ reaction were adjusted based on the updated monitor reaction cross-section value for $^{27}Al(p,x)^{22}Na$ and $^{27}Al(p,x)^{24}Na$ from IAEA NDS at 100 MeV [50] and PADF-2 at 200 MeV [51-53]. The authors of Ref.[31] had used a monitor cross-section for $^{27}Al(p,x)^{22}Na$ at 100 MeV that is 20% lower than the updated value [50]. As a result, the cross-sections here are higher than those in Ref.[31].

The evaluated data for ^{22}Na production are based on the assumption that the $^{27}Al(p,x)^{22}Na$ reaction was used to determine the ^{22}Na yield for all target nuclei in Ref.[31], while the $^{27}Al(p,x)^{24}Na$ reaction was used for the ^{24}Na yield. This assumption is also reflected in the corresponding EXFOR file entries. However, the authors of Ref.[31] did not specify how exactly the $^{27}Al(p,x)^{22}Na$ and $^{27}Al(p,x)^{24}Na$ monitor reactions were applied. If the assumption is incorrect and both monitor reactions were actually used to determine the ^{22}Na yield, then the currently evaluated ^{22}Na production cross-section would be somewhat overestimated.

H.Lundqvist, P.Malmborg (1979) [35]. The measured ^{24}Na cross-sections using the monitor reaction cross-section $^{27}Al(p,x)^{24}Na$ of J.B. Cumming [22] were corrected using cross-section from Ref.[50] below 100 MeV and from Ref.[51] above 100 MeV.

The measurements of ^{28}Mg were treated as independent, based on an analysis of potential precursor contributions using nuclear modelling codes.

G.F.Steyn et al (2007) [48]. The yield of ^{28}Mg was considered as independent after the analysis using results of calculations.

3.2 Potassium

3.2.1 Natural potassium

M.Imamura et al. (1997) [28]. The data, originally obtained using $^{27}Al(p,x)^{22}Na$ monitor cross-sections from Ref.[47], were improved by applying IAEA monitor cross-sections [50].

R.G.Korteling, A.A.Caretto (1970) [31]. Based on the analysis using TALYS, PHITS, and CEM, the measurements of ^{22}Na and ^{24}Na were interpreted as cumulative, reflecting contributions from their respective precursors, ^{22}Mg and ^{24}Ne.

The cross-sections were adjusted based on the updated monitor reaction cross-sections for $^{27}Al(p,x)^{22}Na$ and $^{27}Al(p,x)^{24}Na$. See comments in Section 3.1.

H.Lundqvist, P.Malmborg (1979) [35]. The data for ^{24}Na were considered as cumulative and for ^{28}Mg as independent basing on codes calculations. All measurements were corrected using new values of monitor reaction cross-section, see comments in Section 3.1.

3.2.2 Potassium-39

M.Imamura et al. (1997) [28]. The data were improved by applying new monitor cross-sections [50].

3.2.3 Potassium-40

M.E.Sevior et al. (1986) [45]. Data for investigated reactions were transformed from the CM to the lab system.

Measured data for the (p,α) reaction for the ground state and first excited state of ^{38}Ar were summed to obtain the total (p,α) cross-section at proton energies up to 2.6 MeV.

Measured data for the (p,p') reaction for first five excited states were summed to obtain the total (p,p') cross-section at proton energies up to 1.86 to 2.6 MeV. The necessary correction was made using TALYS calculations with the input parameter *ldmodel* equal to *1* and *2*.

M.E.Sevior et al. (1982) [44]. The data for all reactions were not used, as the authors of Ref. [45] stated that their work repeats the earlier measurements [44] with better statistics.

3.3 Scandium

L.Daraban et al. (2009) [23]. The measured data were normalized using new cross-section values [50] for the monitor reaction $^{nat}Ti(p,x)^{48}V$. The monitor cross-sections used in the Ref.[23] were taken from Refs.[54,55]

T.McGee et al. (1970) [27]. All measurements were normalized using PADF-2 cross-sections [51]. Old monitor data were taken from Table 2 [27]. The sum of two cross-sections $^{63}Cu(p,2n)^{62}Zn$ and $^{65}Cu(p,4n)^{62}Zn$ was calculated taken into account the contributions of ^{63}Cu and ^{65}Cu in natural copper mixture.

M.Lagarde-Simonoff et al. (1975) [33]. All measurements were normalized using cross-sections for monitor reaction $^{27}Al(p,x)^{22}Na$ from Ref.[50].

V.N.Levkovskij (1979) [34]. Data were corrected for ^{45}Sc target using the recommended value of 192.8 mb for the reaction $^{nat}Mo(p,x)^{96}Tc$ at 30 MeV [50].

For the other targets considered in this report, the cross-sections measured in Ref.[34] were normalized to the 190.8 mb value used in the auto-correction on the EXFOR page. At the same time, there is every reason to believe that the value of 192.8 mb is more accurate.

3.4 Titanium

Various works. All measurements of ^{43}K and ^{41}Ca production were considered as independent.

The calculated total contribution of ^{43}Ar and ^{43}Cl at proton energies up to 200 MeV does not exceed 0.21% (TALYS), 0.49% (PHITS), and 0.51% (CEM) of the production of ^{43}K. The contribution of ^{41}Sc in ^{41}Ca yield at proton energies up to 150 MeV, which is the maximum energy of measurements relevant for this work, is less than 0.45% (TALYS), 0.23% (PHITS), and 0.24% (CEM).

Based on the analysis of experimental data, all measurements of the ^{47}Sc yield were treated as independent for proton energies up to 200 MeV. This also includes the measurements labelled as “cumulative” in EXFOR.

All measurements of the ^{44}Ti production were considered as independent, including those which were marked as “CUM” or “(CUM)” in the reaction description in EXFOR. The reason is that the contribution of ^{44}V for natural titanium up to 200 MeV does not exceed 0.012% (TALYS), 0.16% (PHITS), and 0.15% (CEM) of the production of ^{44}Ti.

A. Azzam et al. (2020) [17]. The yield of ^{44}Sc presented in EXFOR file D0978003 was interpreted as ^{44g}Sc.

C.M.Bäcker et al (2021) [18]. Data for the reactions $^{nat}Ti(p,x)^{38}Cl$, $^{nat}Ti(p,x)^{39}Cl$, $^{nat}Ti(p,x)^{41}Ar$, and $^{nat}Ti(p,x)^{44}K$ were adopted as independent after the analysis of results of calculations.

R.L.Brodzinski et al. (1971) [20]. Data at 118 MeV were corrected using monitor cross-section for $^{27}Al(p,x)^{24}Na$ from PADF-2 [51] equal to 10.69 mb.

Data at 45 MeV were not changed due to the absence of information about monitor cross-section.

J.P.Cohen et al. (1965) [21]. The measured cross-sections were renormalized using the new value for the $^{12}C(p,pn)^{11}C$ reaction cross-section [51]. The data were multiplied by 1.22.

D. Fink et al. (1990) [24]. Data in file C0430004 were interpreted as referring to ^{44g}Sc.

M.B.Fox et al. (2021) [25]. The measured cross-sections for ^{43}Sc reported in EXFOR as cumulative (C2702048) were treated as independent, since the contribution of ^{43}Ti for a natural titanium at proton energies up to 200 MeV does not exceed 0.30% (TALYS), 0.76% (PHITS), and 0.91% (CEM) of the ^{43}Sc production.

E.Gadioli et al. (1981) [26]. Measured data were normalized to new values of the monitor reaction cross-sections for the $^{63}Cu(p,n)^{63}Zn$ reaction below 20 MeV and the $^{65}Cu(p,x)^{64}Cu$ reaction above 25 MeV.

Data for ^{50}Ti, presented as "derived data" in EXFOR file D4060, were used for the evaluation. According to the authors, these constitute "recommended experimental data for the pure ^{50}Ti target", Table 5 [26].

M.U.Khandaker et al. (2009) [30]. The measured yields of ^{44g}Sc compiled in the EXFOR file D0569005 as "-G,M+,SIG"- data, were considered as not containing any contribution from ^{44m}Sc.

R.G.Korteling, A.A.Caretto (1970) [31]. After the analysis using TALYS, PHITS, and CEM the measurements for reactions $^{nat}Ti(p,x)^{22}Na$ and $^{nat}Ti(p,x)^{24}Na$ were treated as cumulative, due to possible contributions of precursors, ^{22}Mg and ^{24}Ne.

The measured cross-sections were normalized taking using new value of the monitor reaction cross-section for $^{27}Al(p,x)^{22}Na$ and $^{27}Al(p,x)^{24}Na$ [50,51].

It should be noted that the value of the monitor cross-section of the $^{27}Al(p,x)^{22}Na$ reaction used by the authors of Ref.[31] at an energy of 100 MeV is 20% lower than the new value [50]. Accordingly, the cross-sections used in the present work are noticeably higher than those presented by the authors of Ref.[31].

The present work proceeds from the fact that the $^{27}Al(p,x)^{22}Na$ reaction was used to get the yield of ^{22}Na for all target nuclei studied in Ref.[31] and the $^{27}Al(p,x)^{24}Na$ reaction was used for the yield of ^{24}Na. The compiler of the corresponding EXFOR files also assumes this. At the same time, it should be noted that the authors of Ref.[31] did not provide detailed information on how both monitor reactions $^{27}Al(p,x)^{22}Na$ and $^{27}Al(p,x)^{24}Na$ used in Ref.[31] were applied.

If the assumption made in this report is incorrect and both above mentioned monitor reactions were used to measure yield of ^{22}Na, the value of the ^{22}Na production cross-section should be somewhat lower.

M.S.Lafleur et al. (1966) [32]. Measured ^{7}Be yields were corrected using new monitor cross-sections from IAEA NDS [50].

L.F.Mausner et al.(1998) [36]. Data were corrected using monitor cross-sections [50].

Data from EXFOR file C2614003 (ratios) were applied to derive cross-sections for ^{44m}Sc and ^{46}Sc. Firstly the $^{nat}Ti(p,x)^{47}Sc$ cross-section was evaluated (Section 4) using available experimental data and then the $^{48}Ti(p,x)^{47}Sc$ cross-section, which was used to get values for ^{44m}Sc and ^{46}Sc by irradiation of ^{48}Ti.

R.Michel, R.Stück (1984) [39]. Data were corrected using IAEA NDS monitor cross-section for $^{27}Al(p,x)^{22}Na$ [50]. The monitor cross-sections used by the authors were taken from Ref.[38].

R.Michel et al. (1985) [38]. Data were corrected using new monitor cross-sections from Ref.[50].

R.Michel et al. (1997) [37]. All measured cross-sections were corrected using monitor cross-sections [37] and new data for $^{27}Al(p,x)^{22}Na$ reaction from IAEA NDS [50].

S. Neumann (1999) [40]. Measured data were corrected using monitor cross-section for $^{27}Al(p,x)^{22}Na$ from Ref.[50]. Monitor data used by author were taken from EXFOR file A0497002 [47].

S.M.Qaim et al. (2010) [41]. Data for the reaction $^{nat}Ti(p,x)^{45}Ca$ compiled in EXFOR as independent (D0608002) were considered as cumulative, because of the contribution of ^{45}K for natural titanium up to 200 MeV is up to 0.78% (TALYS), 2.25% (PHITS), and 2.42% (CEM) of the production of ^{45}Ca.

S.Regnier et al. (1977) [43]. Measured cross-sections for $^{nat}Ti(p,x)^{36}Cl$ were corrected as above.

Yields of ^{38}Cl, ^{39}Cl, ^{41}Ar, and ^{44}K were considered as independent. For the $^{nat}Ti(p,x)^{38}Cl$ cross-section, the contribution of ^{38}S up to 130 MeV does not exceed 0.42% (TALYS), 0.55% (PHITS), and 0.47% (CEM) of the production of ^{38}Cl. For $^{nat}Ti(p,x)^{39}Cl$ the part of ^{39}S in the production of ^{39}Cl up to 130 MeV is less than 0.05% (TALYS), 0.14% (PHITS), and 0.10% (CEM). For $^{nat}Ti(p,x)^{41}Ar$ contribution of ^{41}Cl in the yield of ^{41}Ar does not exceed 0.30% (TALYS), 0.61% (PHITS), and 0.56% (CEM). The contribution of ^{44}Ar for each titanium isotope up to 130 MeV does not exceed 0.13% (TALYS), 0.48% (PHITS), and 0.48% (CEM) of the production of ^{44}K.

The ^{44g}Sc yield from the EXFOR file O2560008 marked as “-G,(M),SIG”- data, was considered to be free of contribution from ^{44m}Sc.

S.Regnier (1979) [42]. The EXFOR entry O0095024 defines the data for the reaction ^{nat}Ti(p,x)^{36}Ar as “uncertain if cumulative”. In the present work, at least at 150 MeV, data were adopted as independent. The contribution of ^{36}K f up to 150 MeV does not exceed 0.021% (TALYS), 0.009% (PHITS), and 0.013% (CEM) of the production of ^{36}Ar. The contribution of ^{36}Ca is even much lower.

A similar situation occurs with measurements for the ^{nat}Ti(p,x)^{42}Ar reaction, which also were considered as independent. Here, the contribution of ^{42}Cl is no more than 0.059% (TALYS), 0.26% (PHITS), and 0.19% (CEM) of the production of ^{42}Ar.

Data for all reactions were corrected at 150 MeV using IAEA NDS monitor cross-section for ^{27}Al(p,x)^{22}Na [50].

M.Shahid et al. (2018) [46]. The measured ^{44g}Sc yields, presented in the EXFOR file D7033005 as “-G,M+,SIG”- data, were considered to be free of contribution from ^{44m}Sc.

L.Valentin (1965) [49]. Measured cross-sections were corrected using new values of cross-sections for monitor reaction ^{12}C(p,pn)^{11}C [51].

4. CROSS-SECTION EVALUATION

Using cross-section values obtained via various methods and codes, "average calculated values" were computed. These values were calculated using weights that reflect the applicability of the models across different energy ranges of primary particles and residual nuclei [3].

Where experimental data were available, the resulting average calculated values and measurement data were used to derive the final evaluated data.

In general, for each reaction, there is a noticeable spread in the values calculated using different models and codes.

To avoid creating a misleading impression regarding the quality of any specific model based on a limited number of illustrations, the Figures below present only the experimental data, the averaged curve derived exclusively from calculation results using various models, and the final evaluated data. The experimental data shown in the Figs.1-8 are taken from Refs. [17-20,23-25,27,29-31,34,35,37,39,40-42,46,48,56-88].

Figures 1-4 show data examples for chlorine, scandium, and titanium. Figures with calculation results obtained using all applied methods and computer codes for all reactions are available upon request [89].

When preparing the evaluated data in this work, information on reaction cross-sections used for medical applications from IAEA NDS [90] was utilized. For some reactions, the data from Ref.[90] were not adopted, and for such reactions a new evaluation of the cross-sections was carried out either over the full energy range or within a limited range. Examples of such evaluations for the reactions ^{45}Sc(p,n)^{45}Ti and ^{45}Sc(p,2n)^{44}Ti are shown in Figs. 5 and 6. The new evaluation reflects the availability of new measurements, the correction of the (p,n) reaction threshold, and was performed over the entire energy range up to 200 MeV.

Another example of a new evaluation is shown for the ^{nat}Ti(p,x)^{48}V reaction in Fig. 7. The cross-sections [90] are available in the range from 3.8 to 100 MeV. Significant differences between the present evaluation and the data [90] are observed below 4.9 MeV. The only contribution to the ^{nat}Ti(p,x)^{48}V reaction at such energies comes from the ^{47}Ti(p,γ)^{48}V reaction. The corresponding cross-section is shown in Fig. 8. The energy range covered by the experimental data [29] extends from 0.76 to 4.1 MeV. The evaluated values of the (p,γ) cross-section presented in Fig. 8 and the results of TALYS calculations support the lower evaluated cross-section values of the ^{nat}Ti(p,x)^{48}V reaction at energies up to 4.9 MeV compared with the evaluation [90], Fig. 7.

5. RESULTS

The evaluation was performed for the cross-sections of all energetically possible reactions.

The resulting data were written in ENDF format in two different ways: in the first case, the files were recorded with MF=10 and MT=5, and in the second case, some of prepared files were integrated into general-purpose JEFF-4.0 files using MF=6 and MT=5 section.

In the file description section (MF=1, MT=451) the experimental data employed are listed in detail, along with information on any cross-sections adopted from Ref.[90], if applicable.

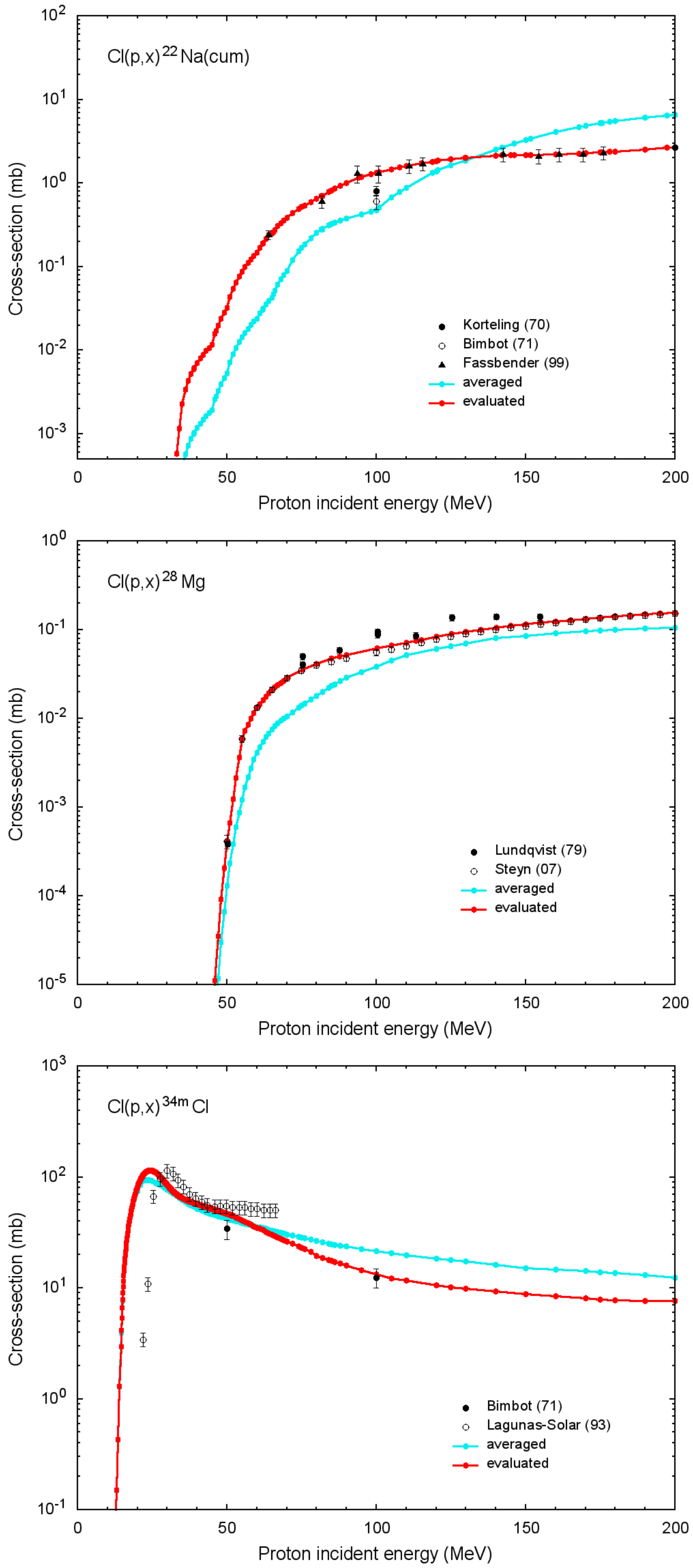

Fig.1 Example of cross-sections evaluated for natural chlorine. "Averaged" is the curve obtained by averaging the calculated data with weights corresponding to the applicability of the codes in different energy and residual nuclei ranges, "evaluated" is the final evaluation. See the explanations in the text.

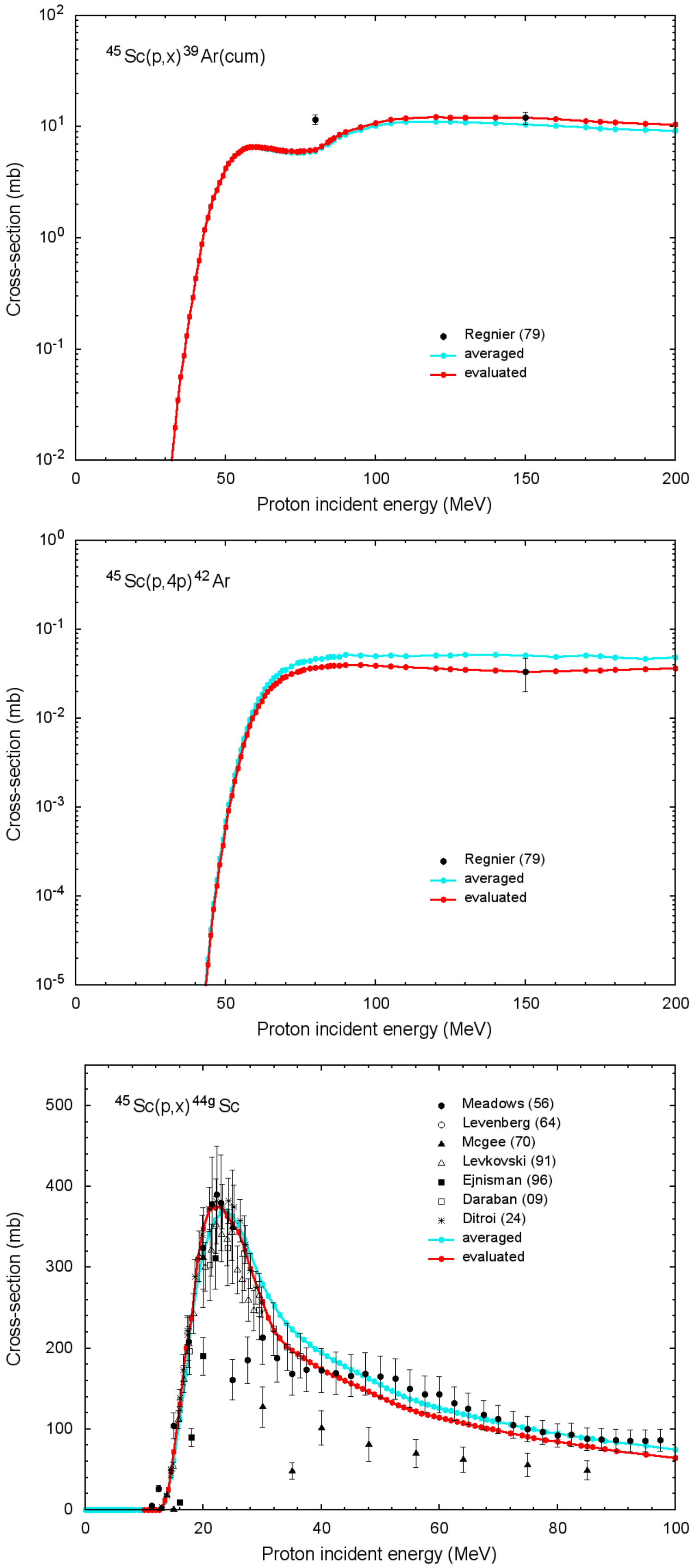

Fig.2 Example of cross-sections evaluated for ^{45}Sc. The data for the ^{45}Sc(p,x)^{44g}Sc reaction are presented on a linear scale and up to 100 MeV for clarity. See comments to Fig.1.

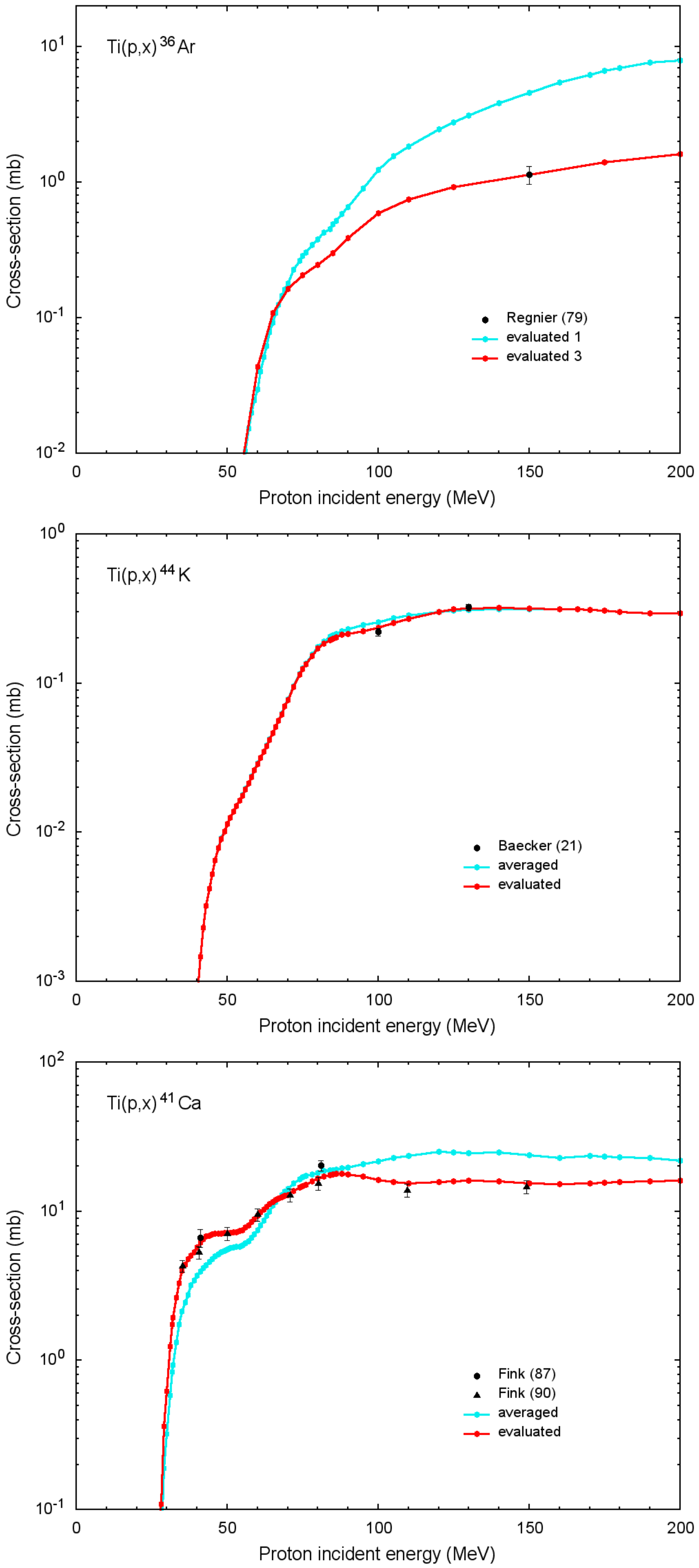

Fig.3 Example of cross-sections evaluated for titanium. See comments to Fig.1.

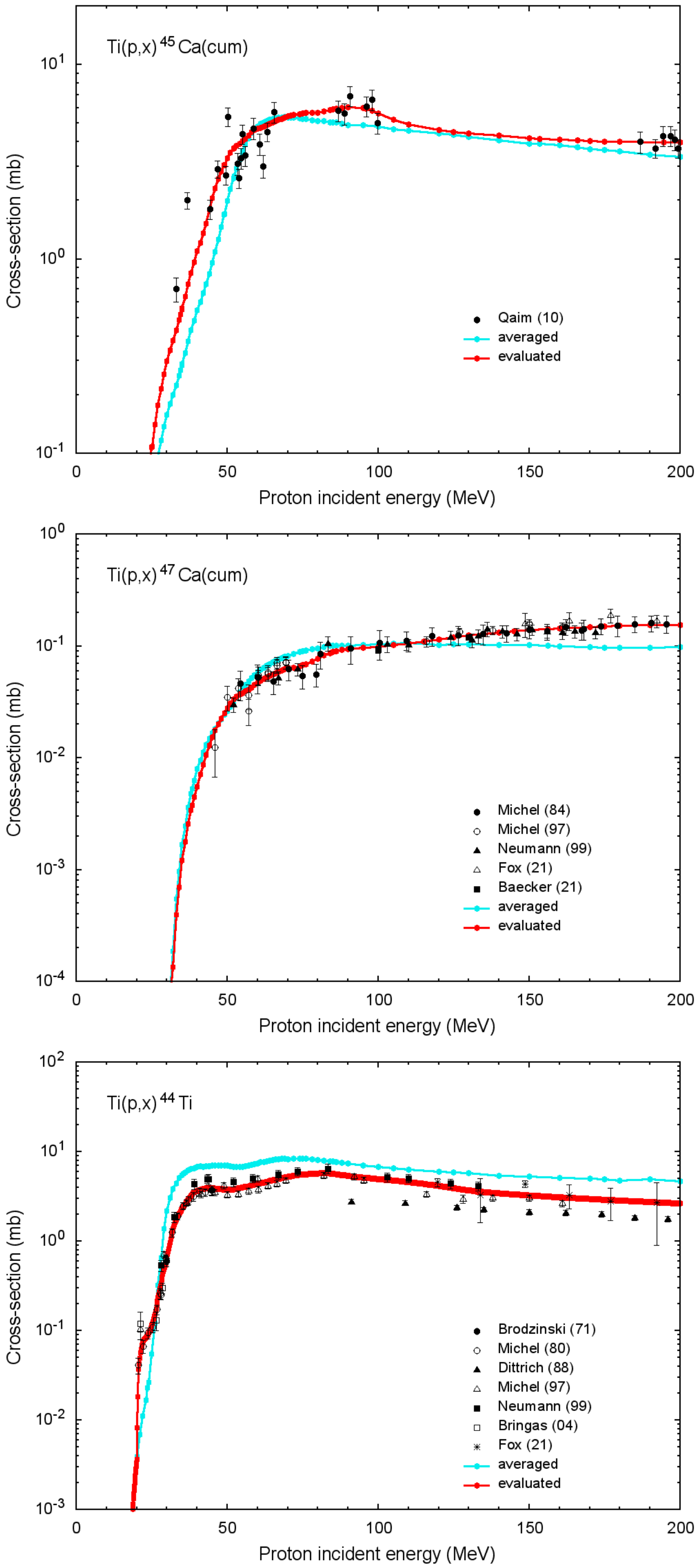

Fig.4 Example of cross-sections evaluated for titanium. See comments to Fig.1.

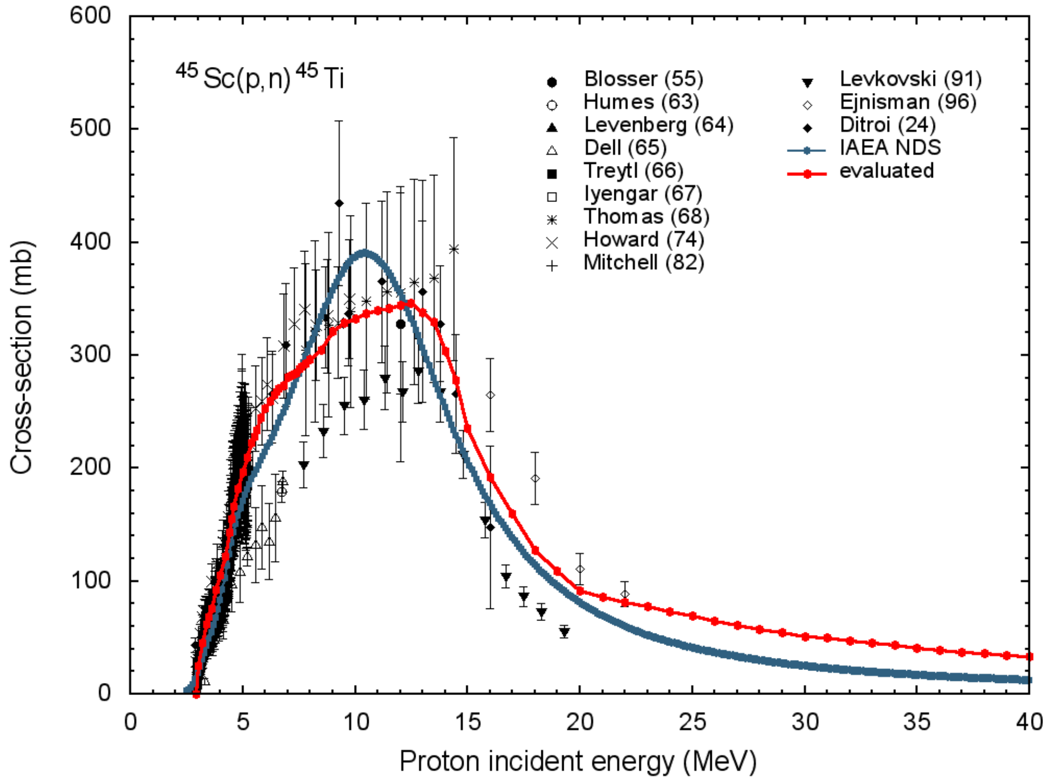

Fig.5 Cross-section for the ^{45}Sc(p,n)^{45}Ti reaction. See the explanations in the text.

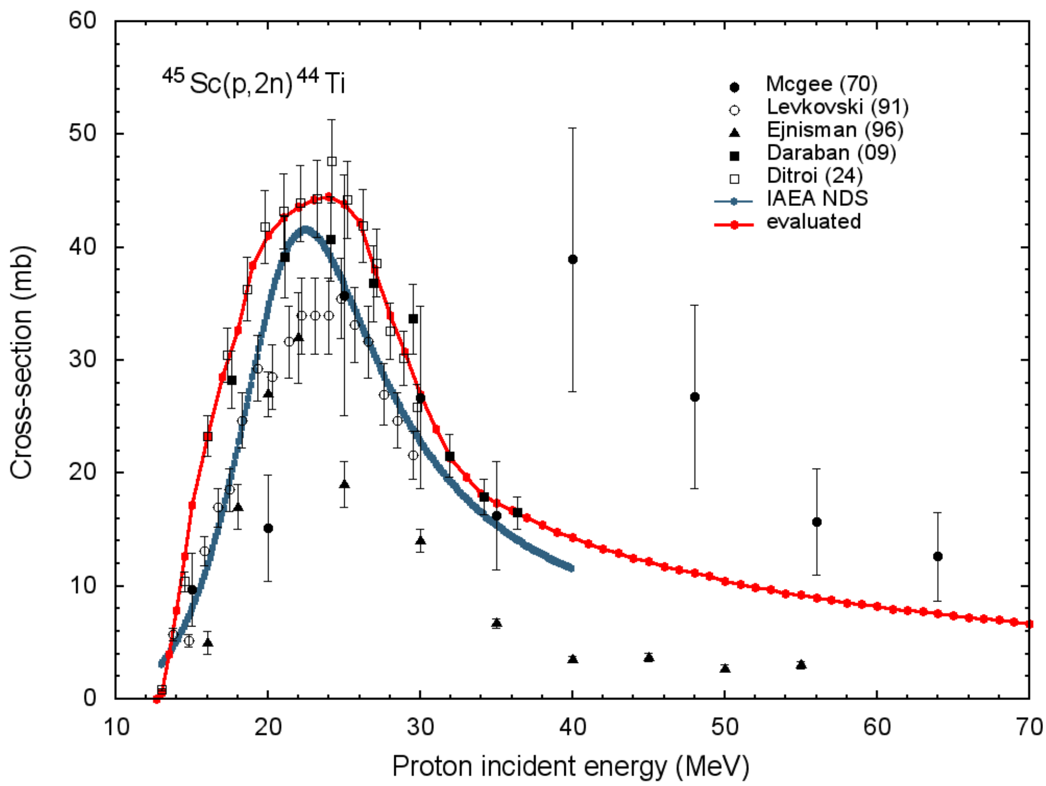

Fig.6 Cross-section for the ^{45}Sc(p,2n)^{44}Ti reaction.

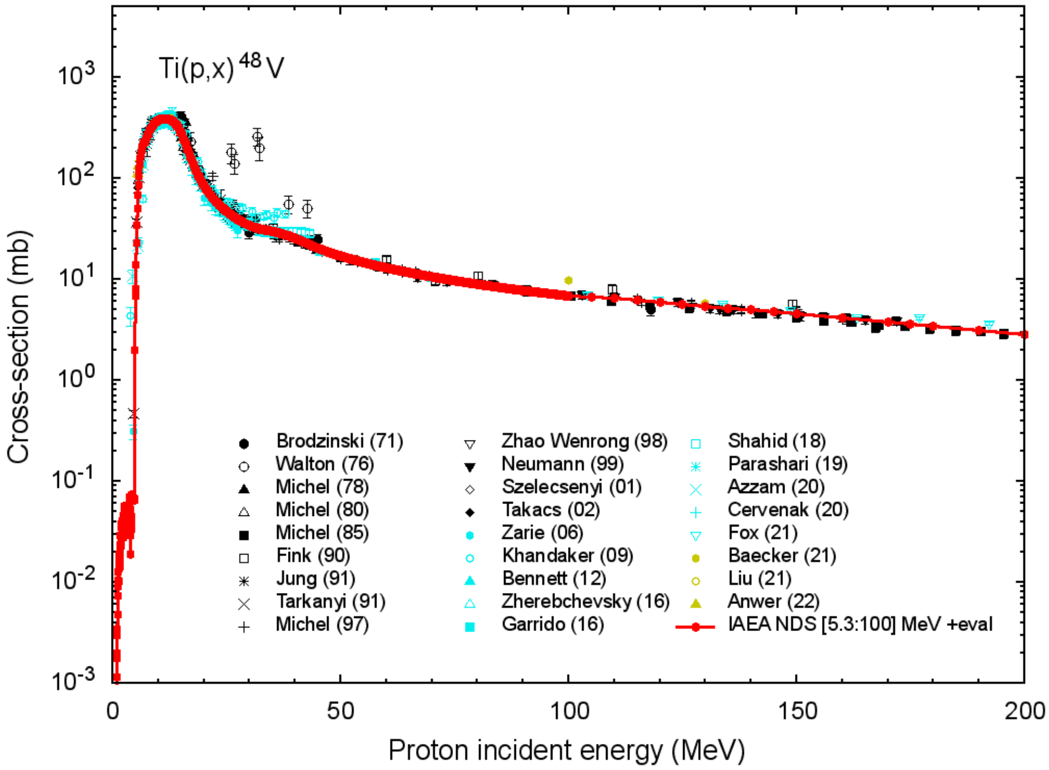

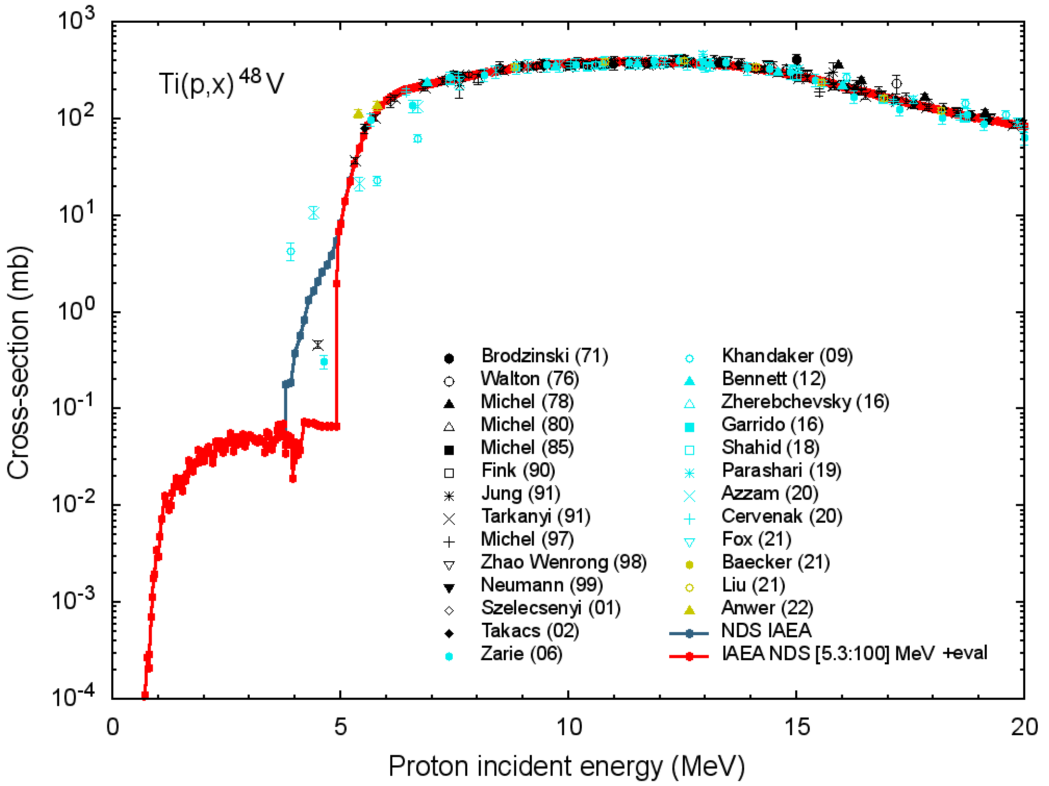

Fig.7 Cross-section for the $^{nat}Ti(p,x)^{48}V$ reaction. The bottom figure shows the cross-sections up to 20 MeV.

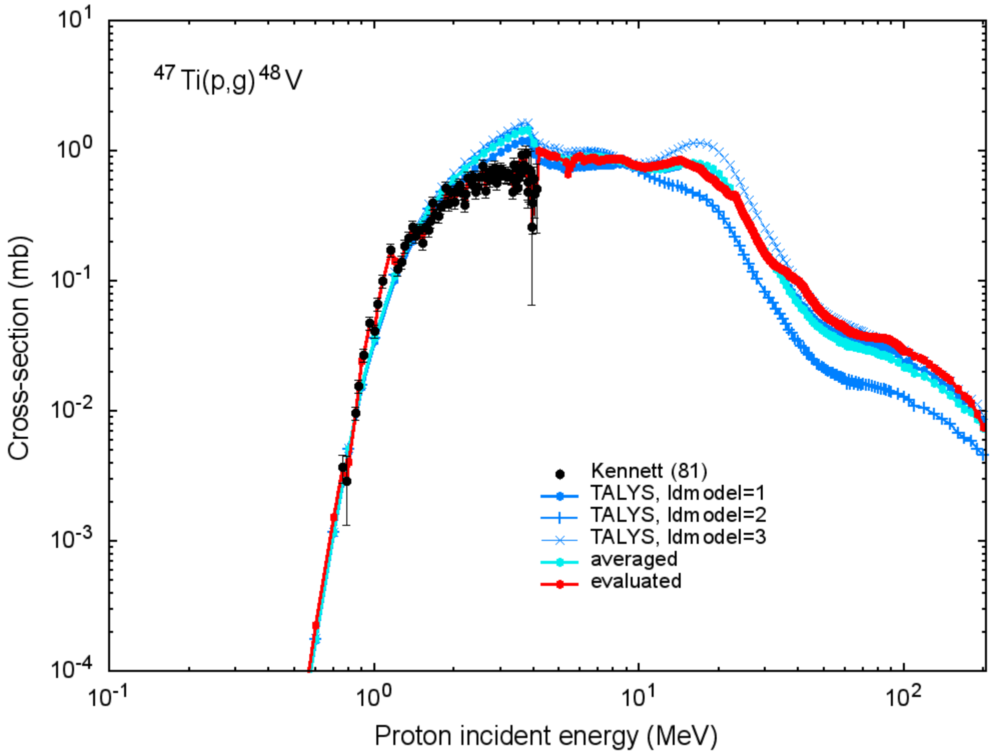

Fig.8 Cross-section for the ^{47}Ti(p,γ)^{48}V reaction.

The resulting data can be downloaded from the website [53].

Plots with the evaluated curves for all reactions for which experimental data exist and for gas production cross-sections are provided in the Appendix.

Detailed information on all steps of the evaluation is available upon request [89]. It includes calculation results obtained with different models and codes, the averaged sum corresponding to the calculated results, the experimental data, and the associated figures.

6. CONCLUSION

Proton-induced reaction cross-sections for stable isotopes of chlorine ^{35,37}Cl, potassium ^{39,40,41}K, ^{45}Sc, and titanium ^{46,47,48,49,50}Ti have been evaluated at energies up to 200 MeV.

The work involved calculations using various models and computer codes, as well as analysis of experimental data.

The resulting files, distributed under the name PADF-2, can be downloaded from Ref. [53].

ACKNOWLEDGEMENT

This work has been carried out within the framework of the EUROfusion Consortium and has received funding from the Euratom research and training programme 2014-2018 and 2019-2020 under grant agreement No 633053. The views and opinions expressed herein do not necessarily reflect those of the European Commission.

REFERENCES

[1] A.Yu.Konobeyev, D.Leichtle, Proton activation data file PADF-2. Targets with atomic numbers from 6 to 15, KIT Scientific Working Papers, 204 (2022), https://dx.doi.org/10.5445/IR/1000152627

[2] A.Yu.Konobeyev, D.Leichtle, PADF-2. Data for stable isotopes of Ca, Cr, Fe, and Ni, KIT Scientific Working Papers, 227 (2023), https://dx.doi.org/10.5445/IR/1000162040

[3] A.Yu.Konobeyev, D.Leichtle, A. Stankovskiy, PADF-2. Data for $^{32,33,34,36}S$, $^{50,51}V$, ^{55}Mn, ^{59}Co, and ^{93}Nb, KIT Scientific Working Papers, 252 (2024), https://dx.doi.org/10.5445/IR/1000176301

[4] C.H.M.Broeders, A.Yu.Konobeyev, Yu.A.Korovin, V.P.Lunev, M.Blann, ALICE/ASH – pre-compound and evaporation model code system for calculation of excitation functions, energy and angular distributions of emitted particles in nuclear reactions at intermediate energies, FZKA 7183, Forschungszentrum Karlsruhe (2006), https://doi.org/10.5445/IR/270064701

[5] A.Yu.Konobeyev, U.Fischer, Simulation of heavy cluster emission in nucleon induced reactions on targets from C to Bi at intermediate energies, KIT Scientific Reports, 7684, 2014, https://doi.org/10.5445/KSP/1000043611

[6] A.Yu.Konobeyev, U.Fischer, P.E.Pereslavtsev, M.Blann, Improved simulation of the pre-equilibrium triton emission in nuclear reactions induced by nucleons, Nuclear Data Sheets, vol.118, p. 280 (2014)

[7] S.G.Mashnik, A.J.Sierk, CEM03.03 User manual, Report LA-UR-12-01364 (2012), https://mcnp.lanl.gov/pdf_files/la-ur-12-01364.pdf

[8] S.G.Mashnik, L.M.Kerby, MCNP6 simulation of light and medium nuclei fragmentation at intermediate energies, EPJ Web of Conferences, vol.117, p.03008 (2016), https://doi.org/10.1051/epjconf/201611703008

[9] PHITS, Particle and heavy ion transport system, https://phits.jaea.go.jp/

[10] T.Sato, Y.Iwamoto, S.Hashimoto, T.Ogawa, T.Furuta, S.Abe, T.Kai, P.-E.Tsai, N.Matsuda, H.Iwase, H.Shigyo, L.Sihver, K.Niita, Features of particle and heavy ion transport code system (PHITS), J. Nucl. Sci. Technol., vol.55, p. 684 (2018), https://doi.org/10.1080/00223131.2017.1419890

[11] A.J. Koning, S. Hilaire, S. Goriely, TALYS: modeling of nuclear reactions, Eur. Phys. J. A59 :131 (2023), https://doi.org/10.1140/epja/s10050-023-01034-3

[12] A.Koning, S.Hilaire, S.Goriely, TALYS-2.0. Simulation of nuclear reactions, https://nds.iaea.org/talys/
[13] TALYS-G code, https://www.inr.kit.edu/english/940.php
[14] A.Yu.Konobeyev, U.Fischer, P.E.Pereslavtsev, A.Koning, M.Blann, Implementation of GDH model in TALYS-1.7 code, KIT Scientific Working Papers, 45 (2016), https://doi.org/10.5445/IR/1000052543
[15] A.Yu.Konobeyev, U.Fischer, A.J.Koning, P.E.Pereslavtsev, M.Blann, Implementation of the geometry dependent hybrid model in TALYS, J. Korean Phys. Soc., vol.59, p. 935 (2011), https://doi.org/10.3938/jkps.59.935
[16] Experimental Nuclear Reaction Data (EXFOR), https://www-nds.iaea.org/exfor/
[17] A.Azzam, M.S.Hamada, S.A.Said, G.Y.Mohamed, M.Al-abyad, Excitation functions for proton-induced reactions on Te and ^{nat}Ti targets: Measurements and model calculations special relevant to the ^{128}Te(p,n)^{128}I reaction, Nucl. Phys. A, vol. 999, 121790 (2020)
[18] C.M.Bäcker, C.Baeumer, A.Bley, P.Fragoso Costa, M.Gerhardt, K.Herrmann, S.Kauer, K.Kroeninger, C.Nitsch, H.M.Siregar, B.Timmermann, N.Verbeek, J.Weingarten, J.Wulff, A.Yazgan, Towards using secondary gamma-rays from proton-induced radioactivation of titanium implants for off-line field verification, Nucl. Instrum. Methods in Physics Res., Sect.B, vol.492, p.56 (2021)
[19] R.Bimbot, H.Gauvin, Spallation reactions of light nuclei induced by protons from 50, 100 to 153 MeV. Comptes Rendus, Serie B, Physique, Vol.273, p.1054 (1971)
[20] R.L.Brodzinski, L.A.Rancitelli, J.A.Cooper, N.A.Wogman, High-energy proton spallation of titanium, Physical Review, Part C, vol.4, p.1250 (1971)
[21] J.P.Cohen, G.Albouy, N.Poffe, Reaction (p,2p) on some titanium isotopes, Journal de Physique, vol.26, p.427 (1965)
[22] J.B.Cumming, Monitor Reactions for High Energy Proton Beams. Ann. Rev. Nucl. Sci, vol.13, 261(1963)
[23] L.Daraban, R. Adam Rebeles, A.Hermanne, F.Tárkányi, S.Takács, Study of the excitation functions for ^{43}K, ^{43,44,44m}Sc and ^{44}Ti by proton irradiation on ^{45}Sc up to 37 MeV, Nucl. Instrum. Methods in Physics Res., Sect.B, vol. 267, p.755 (2009)

[24] D.Fink, J.Sisterson, S.Vogt, G.Herzog, J.Klein, R.Middleton, A.Koehler, A.Magliss, Production of ^{41}Ca and K, Sc and V short-lived isotopes by the irradiation of Ti with 35 to 150 MeV protons: applications to solar cosmic ray studies, Nucl. Instrum. Methods in Physics Res., Sect.B, vol.52, p.601 (1990)

[25] M.B.Fox, A.S.Voyles, J.T.Morrell, L.A.Bernstein, J.C.Batchelder, E.R.Birnbaum, C.S.Cutler, A.J.Koning, A.M.Lewis, D.G.Medvedev, F.M.Nortier, E.M.O'Brien, Ch.Vermeulen, Measurement and modeling of proton-induced reactions on arsenic from 35 to 200 MeV, Physical Review, Part C, vol.104, p.064615 (2021)

[26] E.Gadioli, E.Gadioli-Erba, J.J.Hogan, K.I.Burns, Emission of alpha particles in the interaction of 10-85 MeV protons with ^{48,50}Ti, Zeitschrift für Physik A, Hadrons and Nuclei, vol.301, p.289 (1981)

[27] T.McGee, C.L.Rao, G.B.Saha, L.Yaffe, Nuclear Interactions of ^{45}Sc and ^{68}Zn with protons of medium energy, Nucl. Phys. A, vol.150, p.11 (1970)

[28] M.Imamura, K.Nishiizumi, M.W.Caffee, S.Shibata, Measurements of proton-induced production cross sections for ^{36}Cl from Ca and K, Nucl. Instrum. Methods in Physics Res., Sect.B, vol.123, p.330 (1997)

[29] S.R.Kennett, L.W.Mitchell, M.R.Anderson, D.G.Sargood, Cross-section measurements and thermonuclear reaction rates for ^{46}Ti(p,γ)^{47}V, ^{47}Ti(p,γ)^{48}V, ^{47}Ti(p,n)^{47}V and ^{48}Ti(p,γ)^{49}V, Nucl. Phys. A, vol.368, p.337 (1981)

[30] M.U.Khandaker, K.Kim, M.W.Lee, K.S.Kim, G.N.Kim, Y.S.Cho, Y.O.Lee, Investigations of the ^{nat}Ti(p,x)^{43,44m,44g,46,47,48Sc,48}V nuclear processes up to 40 MeV, Applied Radiation and Isotopes, vol.67, p. 1348 (2009)

[31] R.G.Korteling, A.A.Caretto Jr, Energy dependence of ^{22}Na and ^{24}Na production cross-sections with 100- to 400-MeV protons, Physical Review, Part C, vol.1, p.1960 (1970)

[32] M.S.Lafleur, N.T.Porille, L.Yaffe, Formation of ^{7}Be in nuclear reactions induced by 85-MeV protons, Canadian Journal of Chemistry, vol.44, p.2749 (1966)

[33] M.Lagarde-Simonoff, S.Regnier, H.Sauvageon, G.N.Simonoff, F.Brout, Spallation cross sections in high energy nuclear reactions with medium mass targets $21 \leq Z \leq 29$ and 0.15, 0.3 and 0.6 GeV protons, J. Inorg. Nucl. Chem., vol.37, p. 627 (1975)

[34] V.N.Levkovskij, Cross sections of medium mass nuclide activation (A=40-100) by medium energy protons and alpha-particles (E=10-50 MeV), Moscow 1991.

[35] H.Lundqvist, P.Malmborg, Production of carrier-free ^{28}Mg and ^{24}Na by 50-180 MeV protons on Si, P, Cl, S, Ar and K: excitation functions and chemical separation, Applied Radiation and Isotopes, vol.30, p.33 (1979)

[36] L.F.Mausner, K.L.Kolsky, V.Joshi, S.C.Srivastava, Radionuclide development at BNL for nuclear medicine therapy, Applied Radiation and Isotopes, vol.49, p.285 (1998)

[37] R.Michel, R.Bodemann, H.Busemann, R.Daunke, M.Gloris, H.-J.Lange, B.Klug, A.Krins, I.Leya, M.Lüpke, S.Neumann, H.Reinhardt, M.Schnatz-Buettgen, U.Herpers, Th.Schiekel, F.Sudbrock, B.Holmqvist, H.Condé, P.Malmborg, M.Suter, B.Dittrich-Hannen, P.-W.Kubik, H.-A.Synal, D.Filges Cross sections for the production of residual nuclides by low- and medium-energy protons from the target elements C, N, O, Mg, Al, Si, Ca, Ti, V, Mn, Fe, Co, Ni, Cu, Sr, Y, Zr, Nb, Ba and Au, Nucl. Instrum. Methods in Physics Res., Sect.B, vol.129, p.153 (1997)

[38] R.Michel, F.Peiffer, R.Stück, Measurement and hybrid model analysis of integral excitation functions for proton-induced reactions on vanadium, manganese and cobalt up to 200 MeV, Nucl. Phys. A, vol. 441, p.617 (1985)

[39] R.Michel, R.Stück, On the production of cosmogenic nuclides in meteorites by primary galactic particles: cross sections and model calculations, J. Geophysical Research, vol. 89, Supplement, p.B673 (1984)

[40] S. Neumann, Aktivierungsexperimente mit Neutronen mittlerer Energien und die Produktion kosmogener Nuklide in extraterrestrischer Materie, Dissertation, Universität Hannover, (1999), https://edocs.tib.eu/files/e002/267375484.pdf

[41] S.M.Qaim, K.Kettern, Yu.N.Shubin, S.Sudár, H.H.Coenen, Excitation functions of nuclear reactions leading to the soft-radiation emitting radionuclides ^{45}Ca, ^{49}V and ^{204}Tl in beam collimator materials used in proton therapy, Radiochimica Acta, vol.98, p.447 (2010)

[42] S.Regnier, Production of argon isotopes by spallation of Sc, Ti, Fe, Co, Ni and Cu, Physical Review, Part C, vol.20, p.1517 (1979)

[43] S.Regnier, M.Baklouti, M.Simonoff-Lagarde, G.N.Simonoff, Production of ^{36}Cl by high energy spallation, Physics Letters, Section B, vol.68, p.202 (1977)

[44] M.E.Sevior, M.R.Anderson, L.W.Mitchell, S.R.Kennett, D.G.Sargood, Thermonuclear reaction rates for proton induced reactions on ^{41}K and neutron induced reactions on ^{41}Ca, Nucl. Phys. A, vol.378, p.349 (1982)

[45] M.E.Sevior, L.M.Mitchell, C.I.W.Tingwell, D.G.Sargood, Cross sections for proton induced reactions on K-41 and for the reaction ^{62}Ni2(α,p)^{65}Cu, Nucl. Phys. A, vol.454, p.128 (1986)
[46] M.Shahid, K.Kim, G.Kim, H.Naik, Measurement of excitation functions of residual radionuclides, from ^{nat}Ti(p,x) reactions up to 44 MeV, Journal of Radioanalytical and Nuclear Chemistry, vol.318, p.2049 (2018)
[47] G.F.Steyn, S.J.Mills, F.M.Nortier, B.R.S.Simpson, B.R.Meyer, Production of ^{52}Fe via proton-induced reactions on manganese and nickel, Applied Radiation and Isotopes, vol.41, p.315 (1990)
[48] G.F.Steyn, N.P. van der Meulen, T.N. van der Walt, C.Vermeulen, Production of carrier-free ^{28}Mg by 50 - 200 MeV protons on ^{nat}Cl: excitation function and target optimization, Conf.on Nucl.Data for Sci. and Technology, Nice 2007, vol.2, p.1391 (2007)
[49] L.Valentin, (p,n) and (p,pn) reactions of light nuclei at intermediate energies, Nucl. Phys., vol.62, p.81 (1965)
[50] Monitor Reactions 2017, Nuclear Data Section IAEA, https://www-nds.iaea.org/medical/monitor_reactions.html
[51] A.Yu. Konobeyev, A. Stankovskiy, D. Leichtle, A. Klix, D. Koliadko, The proton Activation Data File PADF-2 in ENDF-6 format, https://www-nds.iaea.org/padf2/
[52] Joint Evaluated Fission and Fusion (JEFF) Library version 4.0. Proton data. https://databank.io.oecd-nea.org/data/jeff/40/#proton-data
[53] PADF-2. Proton activation data files (2025), https://t1p.de/3vzun or https://bwsyncandshare.kit.edu/s/YwCwKH5qSjBPjfx
[54] Monitor Reactions 2007, Nuclear Data Section IAEA, https://www-nds.iaea.org/medical/medical-2020-05/monitor_reactions_2007.html
[55] Charged particle cross-section database for medical radioisotope production: diagnostic radioisotopes and monitor reactions, Report Report IAEA-TECDOC-1211, (2001)
[56] M.Anwer, A.Naz, I.Ahmad, M.Usman, J.Hussain, S.Z.Ilyas, M.Shahid, Ion beam activation of ^{nat}Cu, ^{nat}Ti, ^{nat}Ni and measurement of product formation cross sections at low energy (<10 MeV), Radiochimica Acta, vol.110, p.799 (2022)
[57] M.E.Bennett, D.A.Mayorov, K.D.Chapkin, M.C.Alfonso, T.A.Werke, C.M.Folden III, Measurement of the ^{nat}Lu(p,x)^{175}Hf excitation function, Nucl. Instrum. Methods in Physics Res., Sect.B, vol.276, p.62 (2012)

[58] H.G.Blosser, T.H.Handley, Survey of (p,n) reactions at 12 MeV, Physical Review, vol.100, p.1340 (1955)

[59] F.Bringas, M.T.Yamashita, I.D.Goldman, P.R.Pascholati, V.Sciani, Measurement of proton-induced reaction cross sections in Ti, Ni and Zr near the threshold, Conf.on Nucl.Data for Sci.and Techn., Santa Fe 2004, vol.2, p.1374 (2004)

[60] J.Červenák, O.Lebeda, New cross-section data for proton-induced reactions on ^{nat}Ti and ^{nat}Cu with special regard to the beam monitoring, Nucl. Instrum. Methods in Physics Res., Sect.B, vol.480, p.78 (2020)

[61] G.F.Dell, W.D.Ploughe, H.J.Hausman, Total reaction cross sections in the mass range 45 to 65, Nucl. Phys., vol.64, p.513 (1965)

[62] F.Ditrói, S.Takács, M.Aikawa, D.Gantumur, H.Huang, S.Goto, H.Haba, Z.Szücs, F.Tárkányi, Production of ^{45}Ti radioisotope by proton irradiation of natural scandium, Radiation Physics and Chemistry, vol.218, p.111572 (2024)

[63] B.Dittrich, U.Herpers, Th.Schiffmann, Thin-target excitation functions for proton-produced long-lived radionuclides, Report INDC(GER)-32, p.33 (1988)

[64] R.Ejnisman, I.D.Goldman, P.R.Pascholati, M.T.F. Da Cruz, R.M.Oliveira, E.B.Norman, I.Zlimen, F.E.Wietfeldt, R.M.Larimer, Y.D.Chan, K.T.Lesko, A.Garcia, Cross sections for ^{45}Sc(p,2n)^{44}Ti and related reactions, Physical Review, Part C, vol.54, p.2047 (1996)

[65] M.Fassbender, Yu.N.Shubin, S.M.Qaim, Formation of activation products in interactions of medium energy protons with Na, Si, P, Cl, Ca and Fe, Radiochimica Acta, vol.84, p.59 (1999)

[66] D.Fink, M.Paul, G.Hollos, S.Theis, S.Vogt, R.Stueck, P.Englert, R.Michel, Measurements of ^{41}Ca spallation cross sections and ^{41}Ca concentrations in the grant meteorite by accelerator mass spectrometry, Nucl. Instrum. Methods in Physics Res., Sect.B, vol.29, p.275 (1987)

[67] E.Garrido, C.Duchemin, A.Guertin, F.Haddad, N.Michel, V.Metivier, New excitation functions for proton induced reactions on natural titanium, nickel and copper up to 70 MeV, Nucl. Instrum. Methods in Physics Res., Sect.B, vol.383, p.191 (2016)

[68] A.J.Howard, H.B.Jensen, M.Rios, W.A.Fowler, B.A.Zimmerman, Measurement and theoretical analysis of some reaction rates of interest in silicon burning, Astrophysical Journal, vol.188, p.131 (1974)

[69] R.M.Humes, G.F.Dell Jr, W.D.Ploughe, H.J.Hausman, (p,n) cross sections at 6.75 MeV, Physical Review, vol.130, p.1522 (1963)

[70] K.V.K.Iyengar, S.K.Gupta, K.K.Sekharan, M.K.Mehta, A.S.Divatia, Fluctuations in the integrated cross section of the reaction $^{45}Sc(p,n)^{45}Ti$, Nucl. Phys. A, vol.96, p.521 (1967)

[71] P.Jung, Cross sections for the production of helium and long- living radioactive isotopes by protons and deuterons, Conf.on Nucl.Data for Sci.and Technol., Juelich 1991, p.352 (1991)

[72] I.Levenberg, V.Pokrovsky, R.De-Hou, L.Tarasova, I.Yutlandov, The (p,pn) and (p,n) reactions on ^{45}Sc induced by high-energy protons, Nucl. Phys., vol.51, p.673 (1964)

[73] B.Liu, R.Han, C.Yuan, H.Sun, Z.Chen, G.Tian, F.Shi, X.Zhang, P.Luo, H.Jia, Excitation functions of proton induced reactions on titanium and copper, Applied Radiation and Isotopes, vol.173, p.109713 (2021)

[74] J.W.Meadows, R.M.Diamond, R.A.Sharp, Excitation functions and yield ratios for the isomeric pairs ^{80}Br, ^{80m}, ^{58}Co, ^{58m}, and ^{44}Sc, ^{44m} formed in (p,pn) reactions, Physical Review, vol.102, p.190 (1956)

[75] R.Michel, G.Brinkmann, On the depth-dependent production of radionuclides ($44 \leq A \leq 59$) by solar protons in extraterrestrial matter, Journal of Radioanalytical Chemistry, vol.59, p.467 (1980)

[76] R.Michel, G.Brinkmann, H.Weigel, W.Herr, Proton-induced reactions on titanium with energies between 13 and 45 MeV, J. Inorg. Nucl. Chem., vol.40, p.1845 (1978)

[77] L.W.Mitchell, M.R.Anderson, S.R.Kennett, D.G.Sargood, Cross sections and thermonuclear reaction rates for $^{42}Ca(p,\gamma)^{43}Sc$, $^{44}Ca(p,\gamma)^{45}Sc$, $^{44}Ca(p,n)^{44}Sc$ and $^{45}Sc(p,n)^{45}Ti$, Nucl. Phys. A, vol.380, p.318 (1982)

[78] S.Parashari, S.Mukherjee, B.K.Nayak, H.Naik, S.V.Suryanarayana, R.Makwana, N.L.Singh, Excitation function of the $^{nat}Ti(p,x)^{48}V$, $^{47,46,44m}Sc$ reactions within the energy range of 10-22 MeV, Nucl. Phys. A, vol.987, p.128 (2019)

[79] F.Szelecsényi, F.Tárkányi, S.Takács, A.Hermanne, M.Sonck, Yu.Shubin, M.G.Mustafa, Zhuang Youxiang, Excitation function for the $^{nat}Ti(p,x)^{48}V$ nuclear process: evaluation and new measurements for practical applications, Nucl. Instrum. Methods in Physics Res., Sect.B, vol.174, p.47 (2001)

[80] S.Takács, F.Tárkányi, M.Sonck, A.Hermanne, New cross sections and intercomparison of proton monitor reactions on Ti, Ni and Cu, Nucl. Instrum. Methods in Physics Res., Sect.B, vol.188, p.106 (2002)
[81] F.Tárkányi, F.Szelecsényi, P.Kopecký, Cross section data for proton, ^{3}He and α-particle induced reactions on ^{nat}Ni, ^{nat}Cu and ^{nat}Ti for monitoring beam performance, Conf.on Nucl.Data for Sci.and Technol., Juelich 1991, p.529 (1991)
[82] R.G.Thomas, W.Bartolini, Excitation functions for (p,n) and (p,2n) interactions in Sc, Cr, Mo, Cd and W between 8 and 14 MeV, Nucl. Phys. A, vol.106, p.323 (1968)
[83] W.J.Treytl, A.A.Caretto, Study of (p,n) reactions between 100 and 400 MeV, Physical Review, vol.146, p.836 (1966)
[84] J.R.Walton, D.Heymann, A.Yaniv, D.Edgerley, M.W.Rowe, Cross sections for He and Ne isotopes in natural Mg, Al, and Si, He isotopes in CaF_2, Ar isotopes in natural Ca and radionuclides in natural Al, Si, Ti, Cr and stainless steel induced by 12-to 45-MeV protons, J. Geophysical Research, vol.81, p.5689 (1976)
[85] K.Zarie, N.Al-Hammad, A.Azzam, Experimental study of excitation functions of some proton induced reactions on ^{nat}Ti for beam monitoring purposes, Radiochimica Acta, vol.94, p.795 (2006)
[86] Zhao Wenrong, Yu Weixiang, Han Xiaogang, Lu Hanlin, Excitation functions of reactions from d+Ti, d+Mo, p+Ti and p+Mo, Report INDC(CPR)-44, p.17 (1998)
[87] V.I.Zherebchevsky, I.E.Alekseev, K.A.Gridnev, E.B.Krymov, T.V.Lazareva, N.A.Maltsev, R.B.Panin, N.A.Prokofyev, S.Yu.Torilov, A.I.Shtamburg, The study of the nuclear reactions for the production of antimony isotopes, Izv. Rossiiskoi Akademii Nauk, Ser.Fiz., vol.80, p.975 (2016)
[88] M.C.Lagunas-Solar, R.P.Haff, Theoretical and experimental excitation functions for proton induced nuclear reactions on Z=10 to Z=82 target nuclides, Radiochimica Acta, vol.60, p.57 (1993)
[89] Information about the evaluation performed for Cl, K, Sc, and Ti available upon request via email alexander.konobeev@kit.edu
[90] Charged-particle cross section database for medical radioisotope production, https://nds.iaea.org/medical/index.html

Appendix

Chlorine

Potassium

Scandium

Titanium

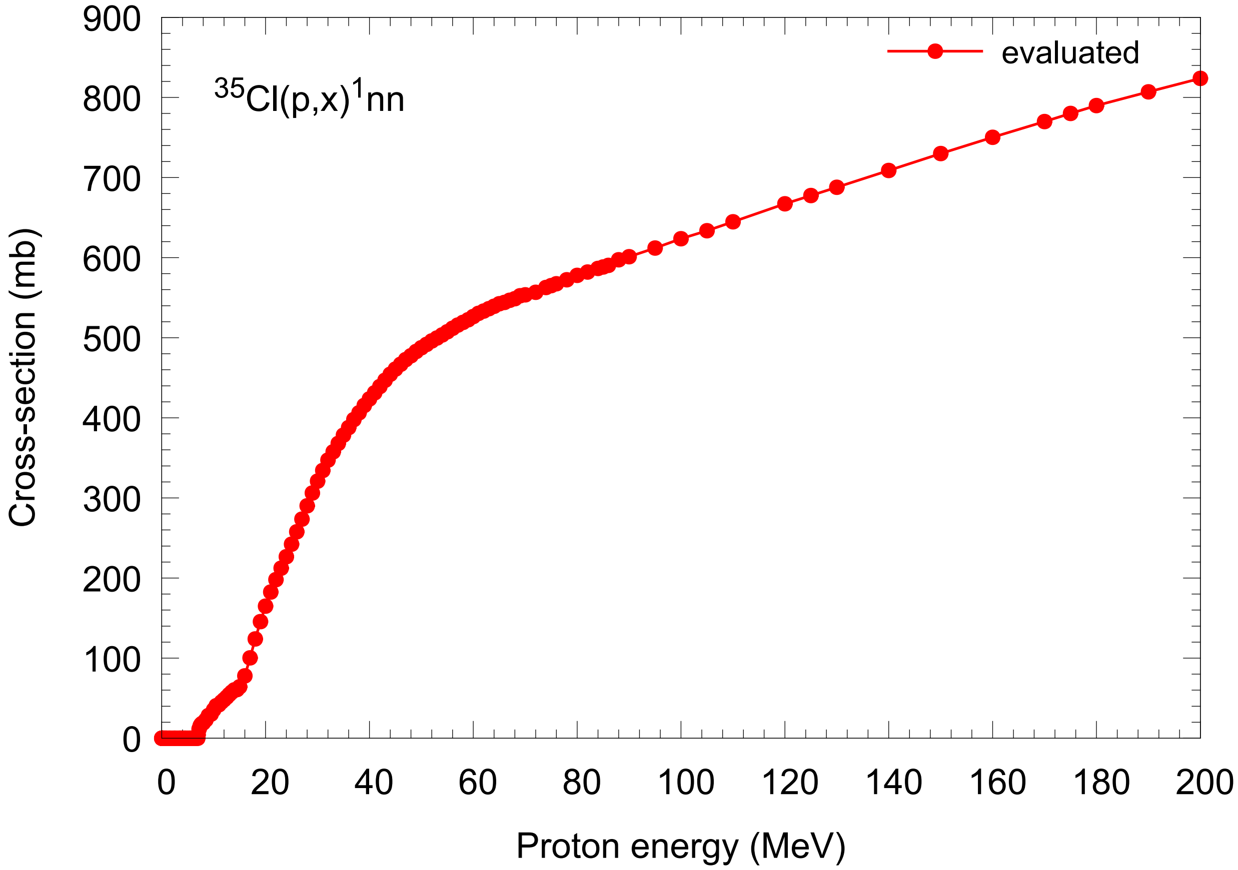

$^{35}Cl(p,x)^{1}nn$
evaluated
Cross-section (mb)
Proton energy (MeV)
0
100
200
300
400
500
600
700
800
900
0
20
40
60
80
100
120
140
160
180
200

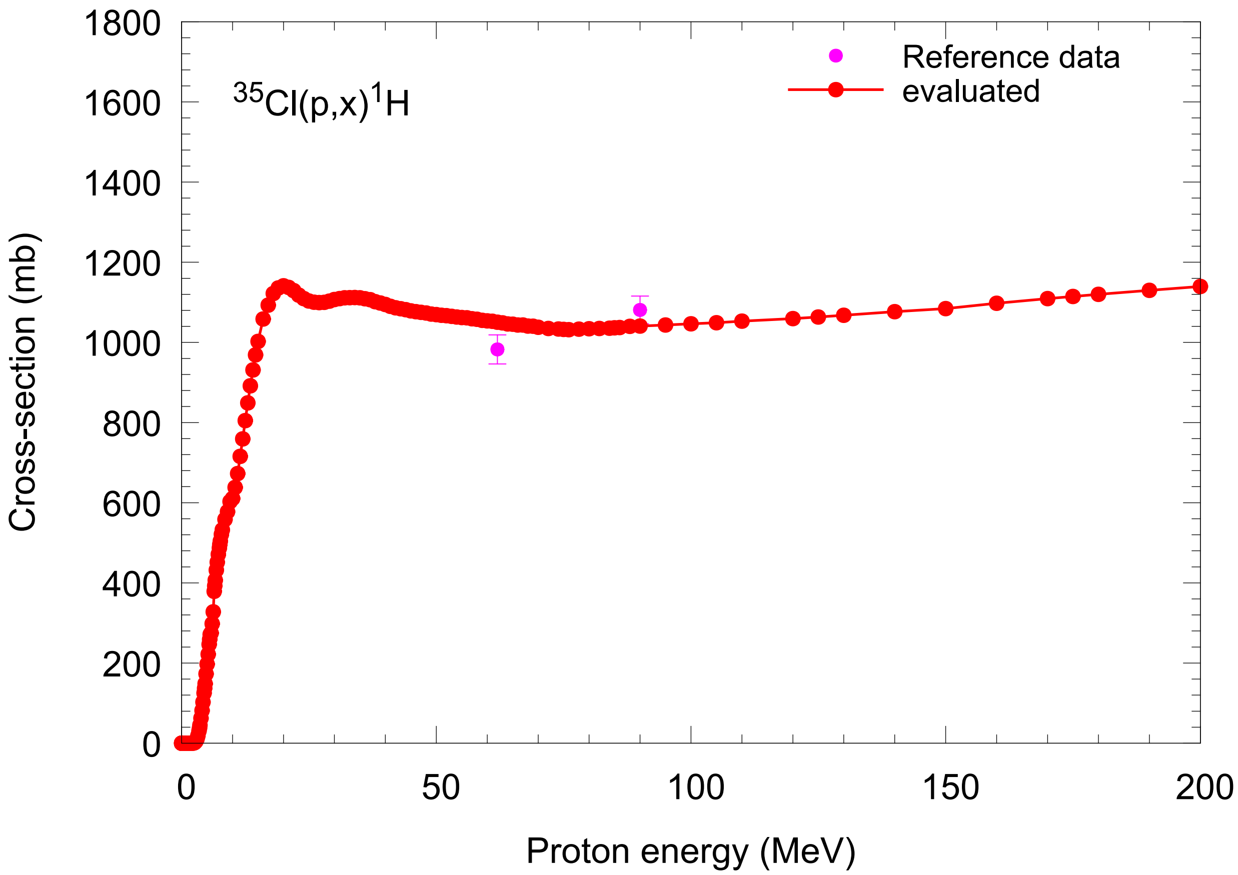

$^{35}Cl(p,x)^{1}H$
Reference data
evaluated
Cross-section (mb)
Proton energy (MeV)
0
200
400
600
800
1000
1200
1400
1600
1800
0
50
100
150
200

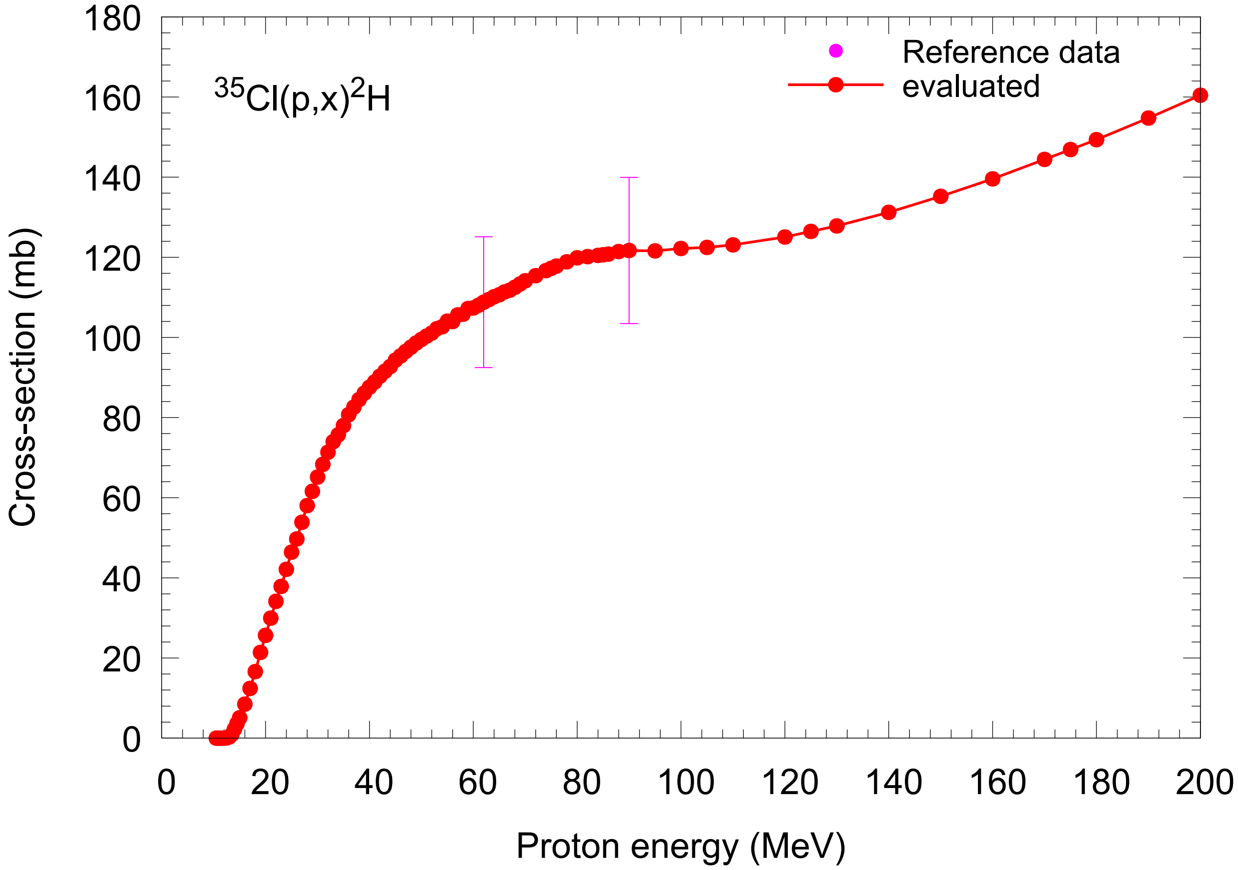

$^{35}Cl(p,x)^{2}H$
Reference data
evaluated
Cross-section (mb)
Proton energy (MeV)
0
20
40
60
80
100
120
140
160
180
200

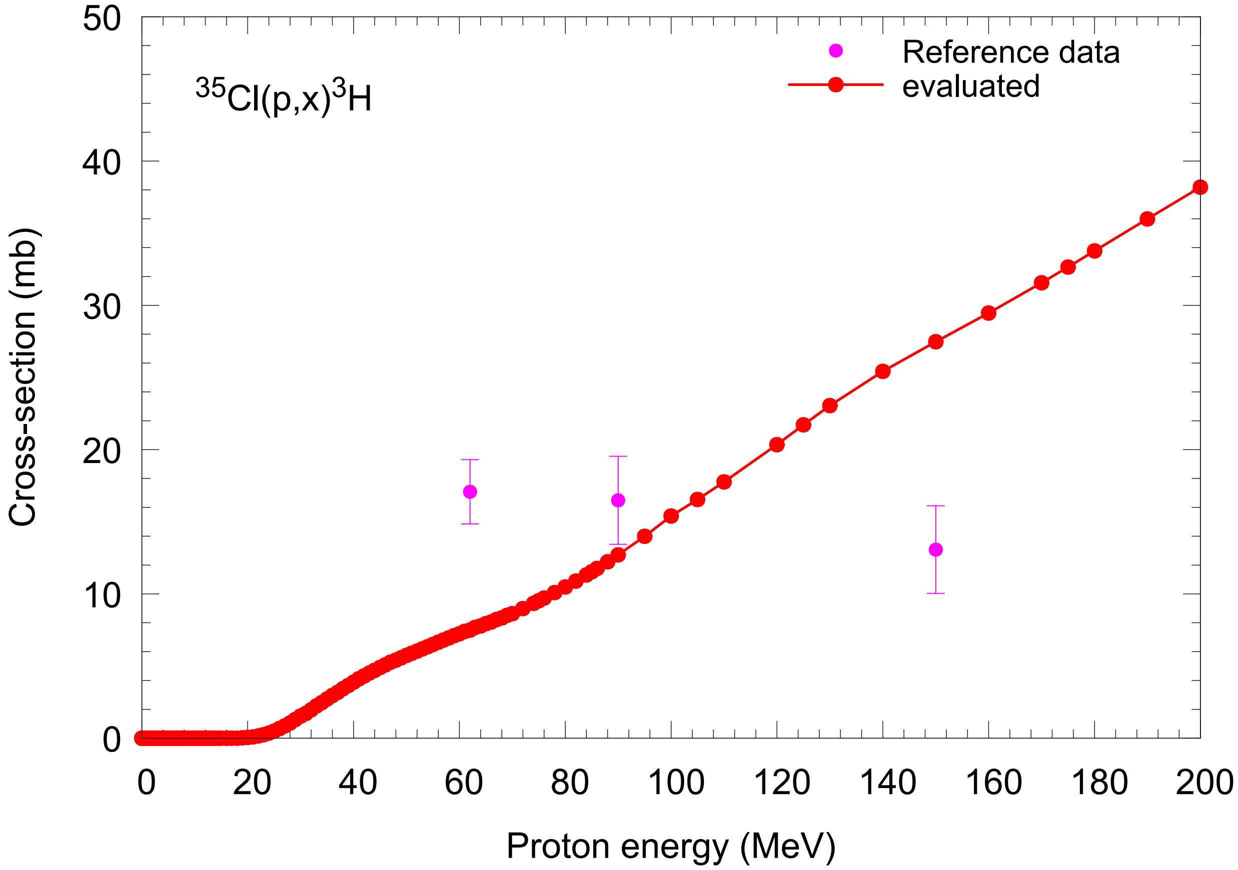

$^{35}Cl(p,x)^{3}H$
Reference data
evaluated
Cross-section (mb)
Proton energy (MeV)
0
10
20
30
40
50

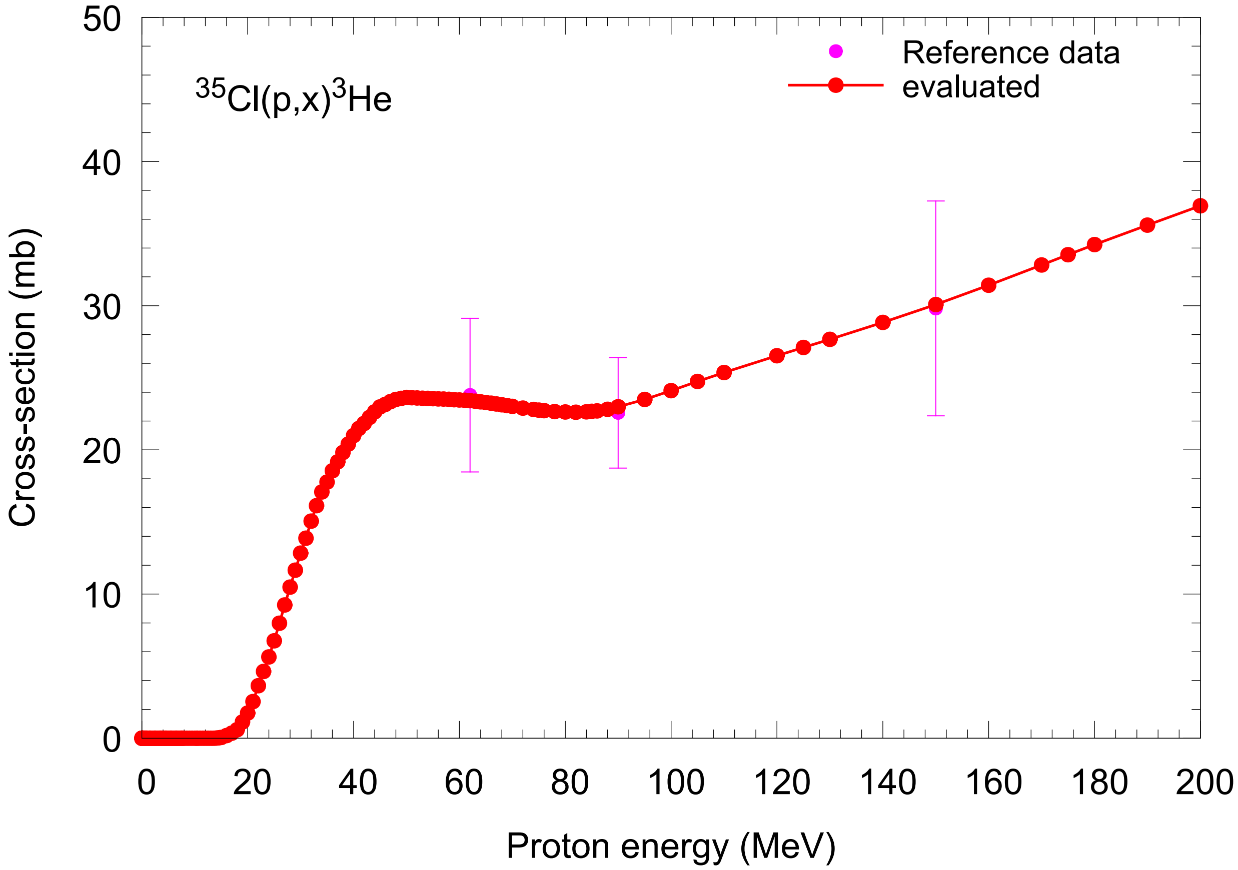

$^{35}Cl(p,x)^{3}He$
Reference data
evaluated
Cross-section (mb)
Proton energy (MeV)
0
10
20
30
40
50
0
20
40
60
80
100
120
140
160
180
200

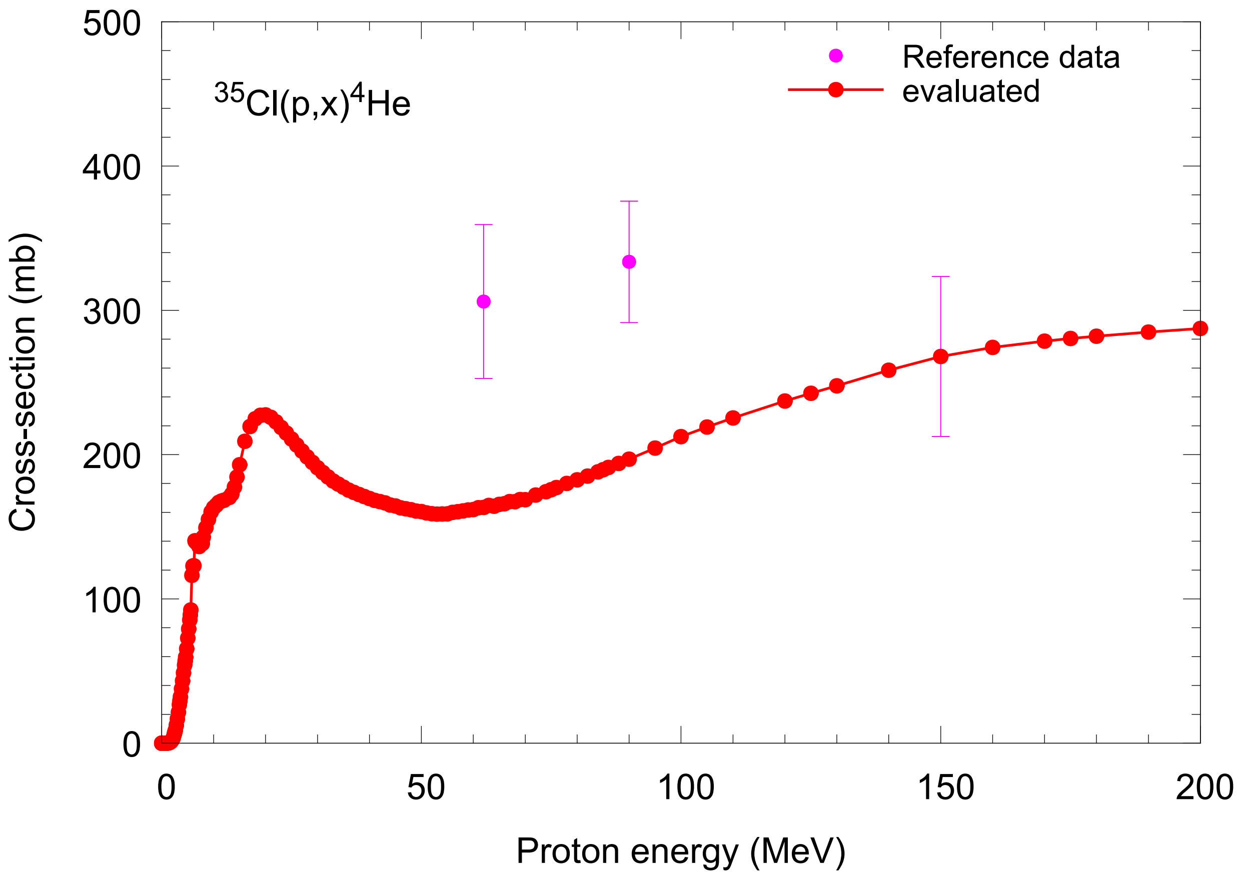

$^{35}Cl(p,x)^{4}He$
Reference data
evaluated
Cross-section (mb)
Proton energy (MeV)
0
100
200
300
400
500
0
50
100
150
200

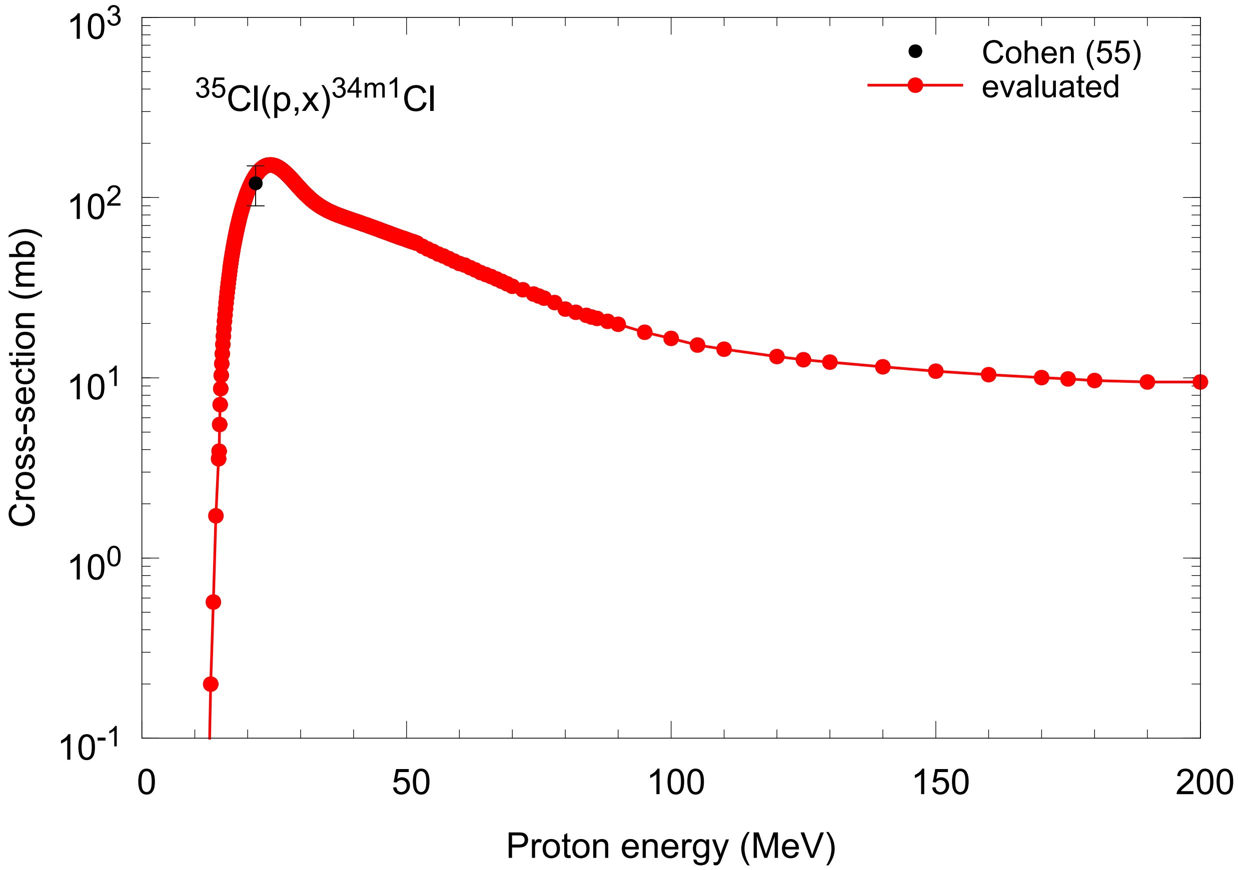

$^{35}Cl(p,x)^{34m1}Cl$
Cohen (55)
evaluated
Cross-section (mb)
Proton energy (MeV)
10^{3}
10^{2}
10^{1}
10^{0}
10^{-1}
0
50
100
150
200

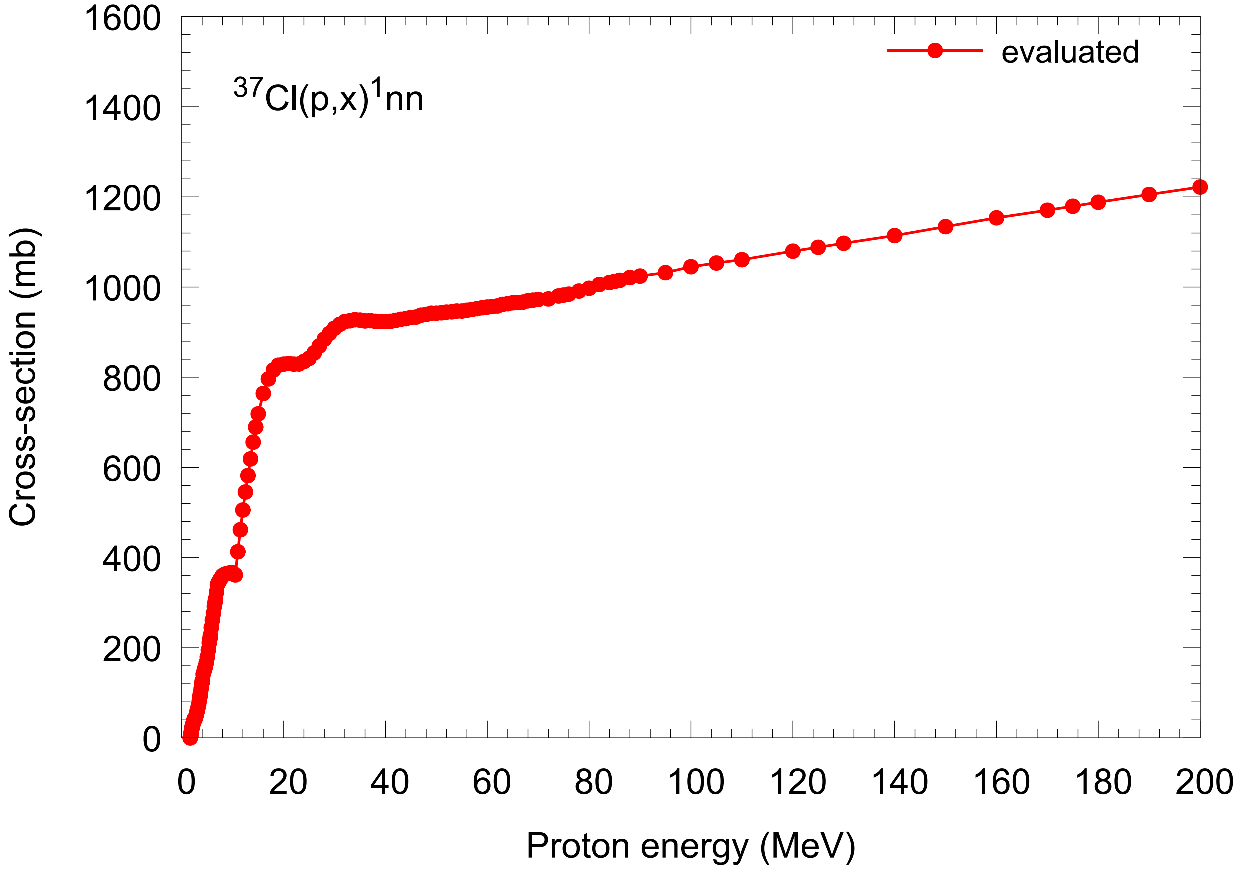

^{37}Cl(p,x)^{1}nn
evaluated
Cross-section (mb)
Proton energy (MeV)
0
200
400
600
800
1000
1200
1400
1600
0
20
40
60
80
100
120
140
160
180
200

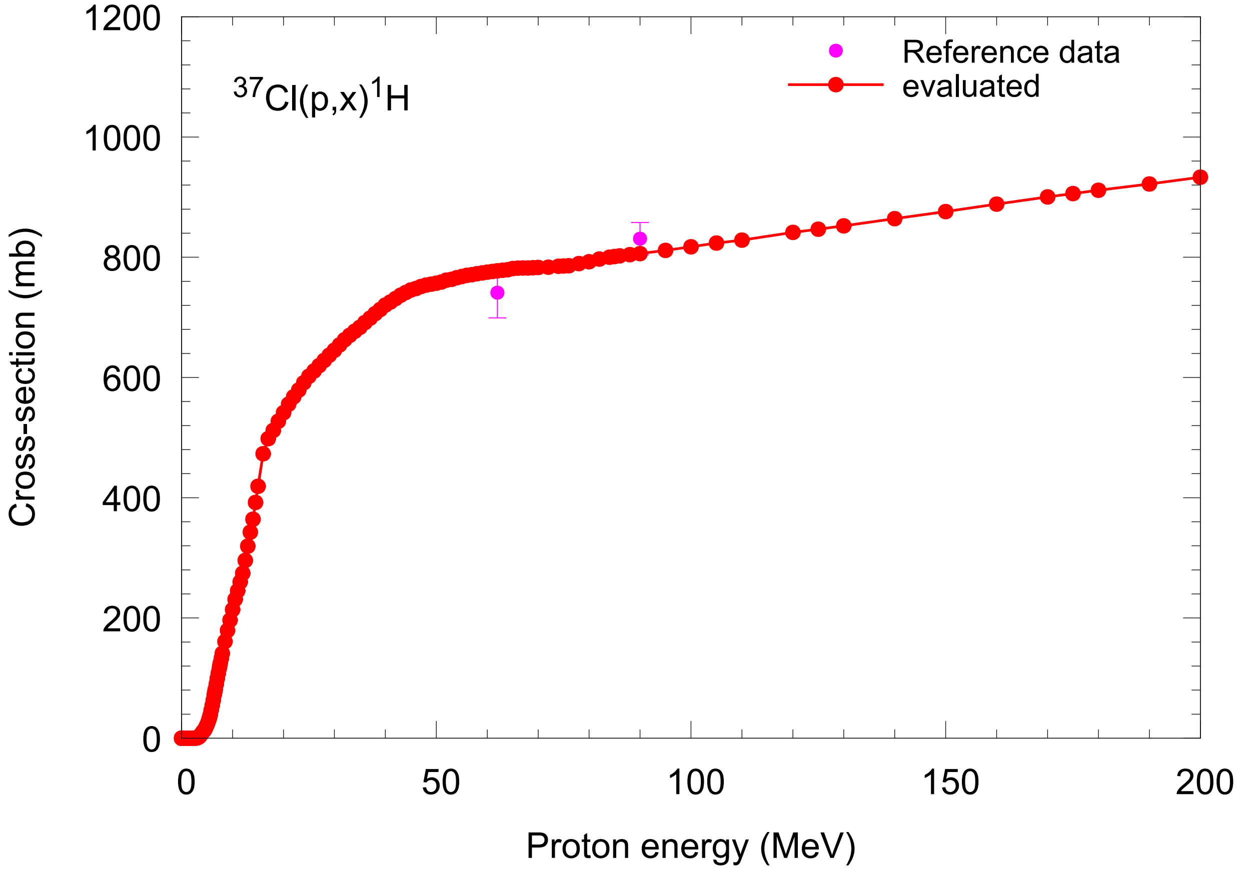

^{37}Cl(p,x)^{1}H
Reference data
evaluated
Cross-section (mb)
Proton energy (MeV)
0
200
400
600
800
1000
1200
0
50
100
150
200

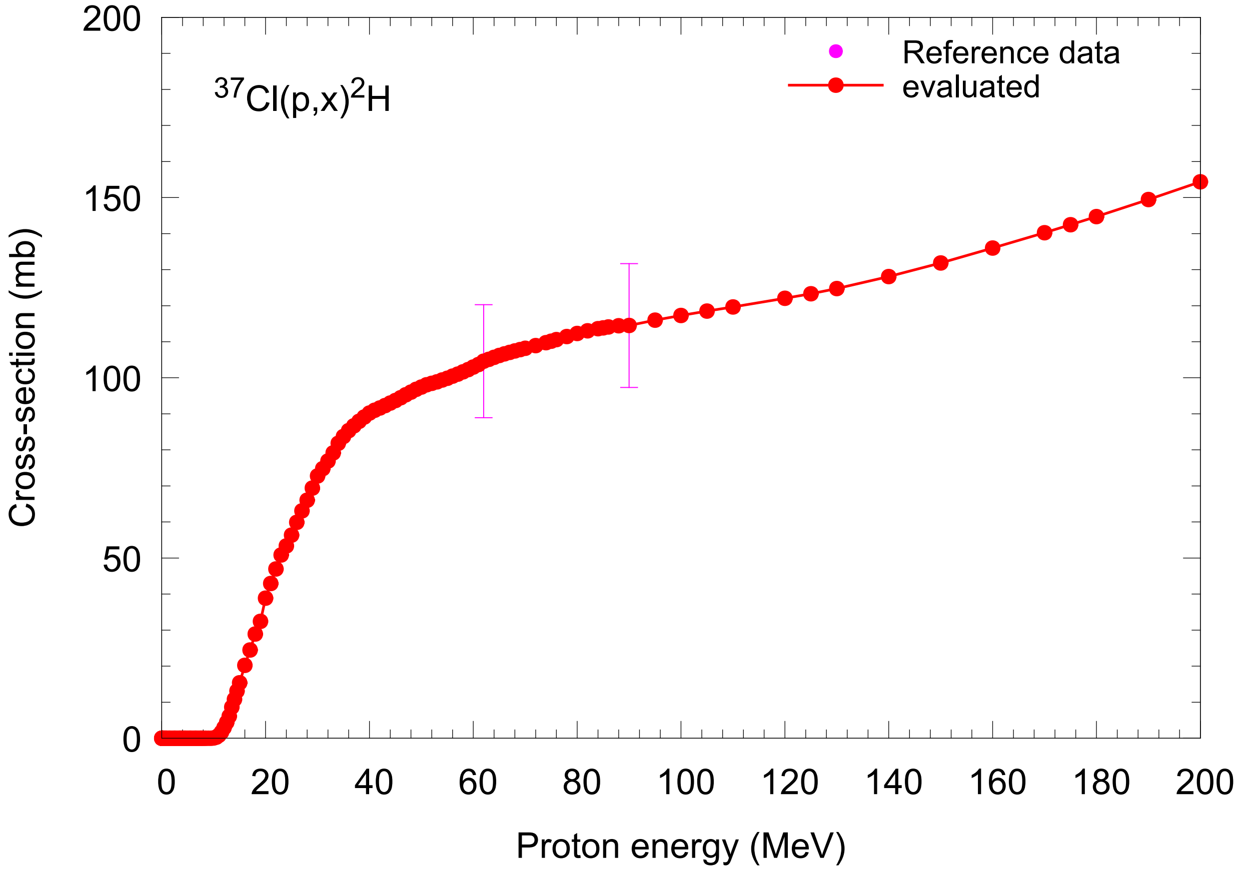
200
150
100
50
0
Cross-section (mb)
^{37}Cl(p,x)^{2}H
Reference data
evaluated
0
20
40
60
80
100
120
140
160
180
200
Proton energy (MeV)

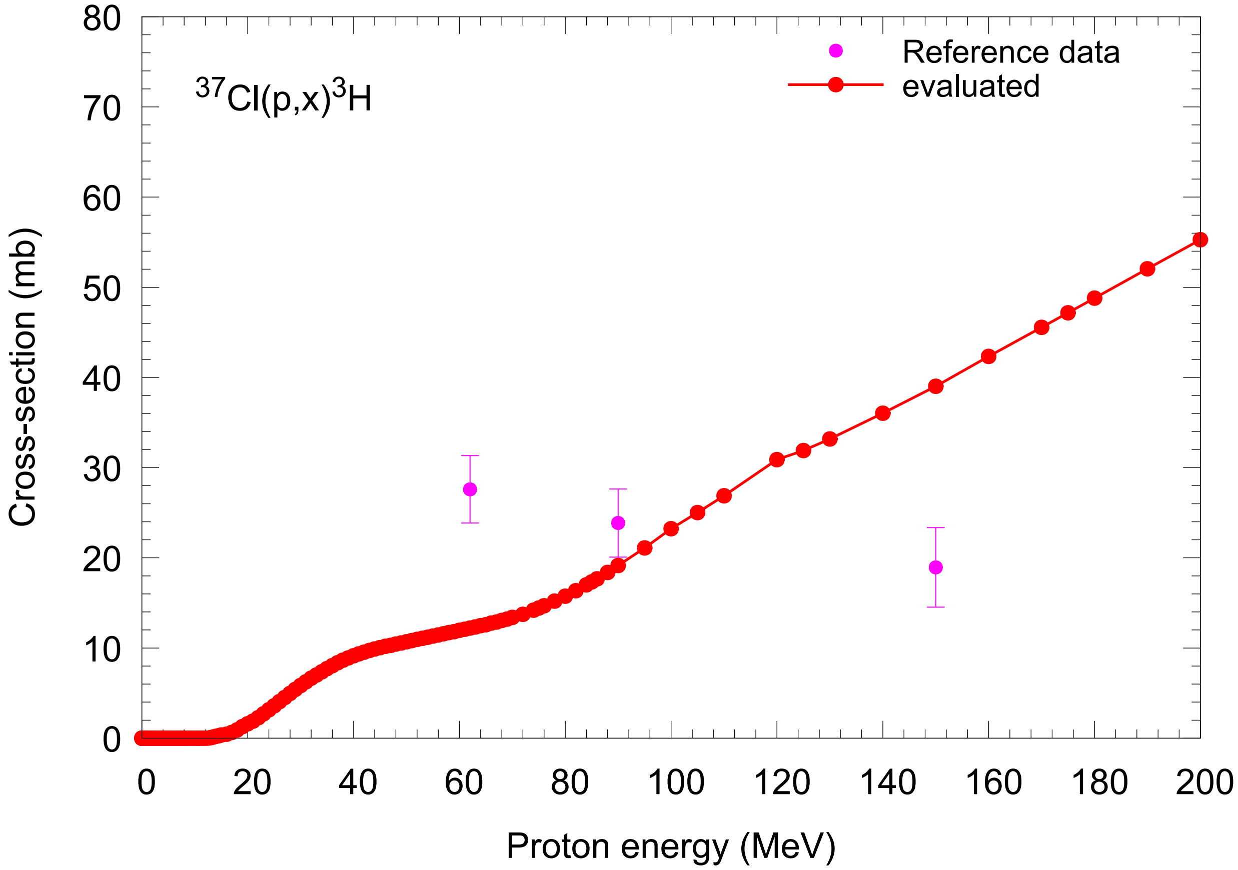
80
70
60
50
40
30
20
10
0
Cross-section (mb)
^{37}Cl(p,x)^{3}H
Reference data
evaluated
0
20
40
60
80
100
120
140
160
180
200
Proton energy (MeV)

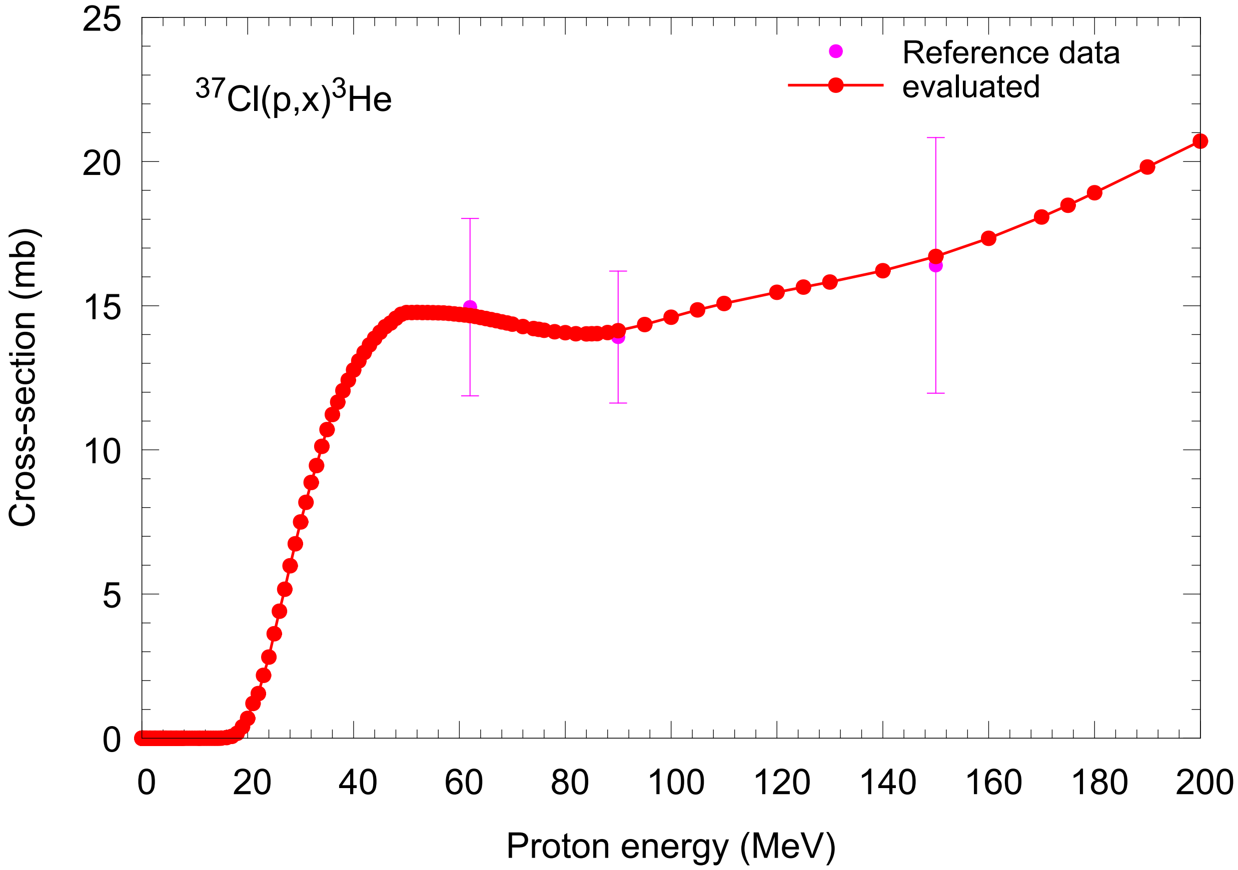

$^{37}Cl(p,x)^3He$
Reference data
evaluated
Cross-section (mb)
Proton energy (MeV)

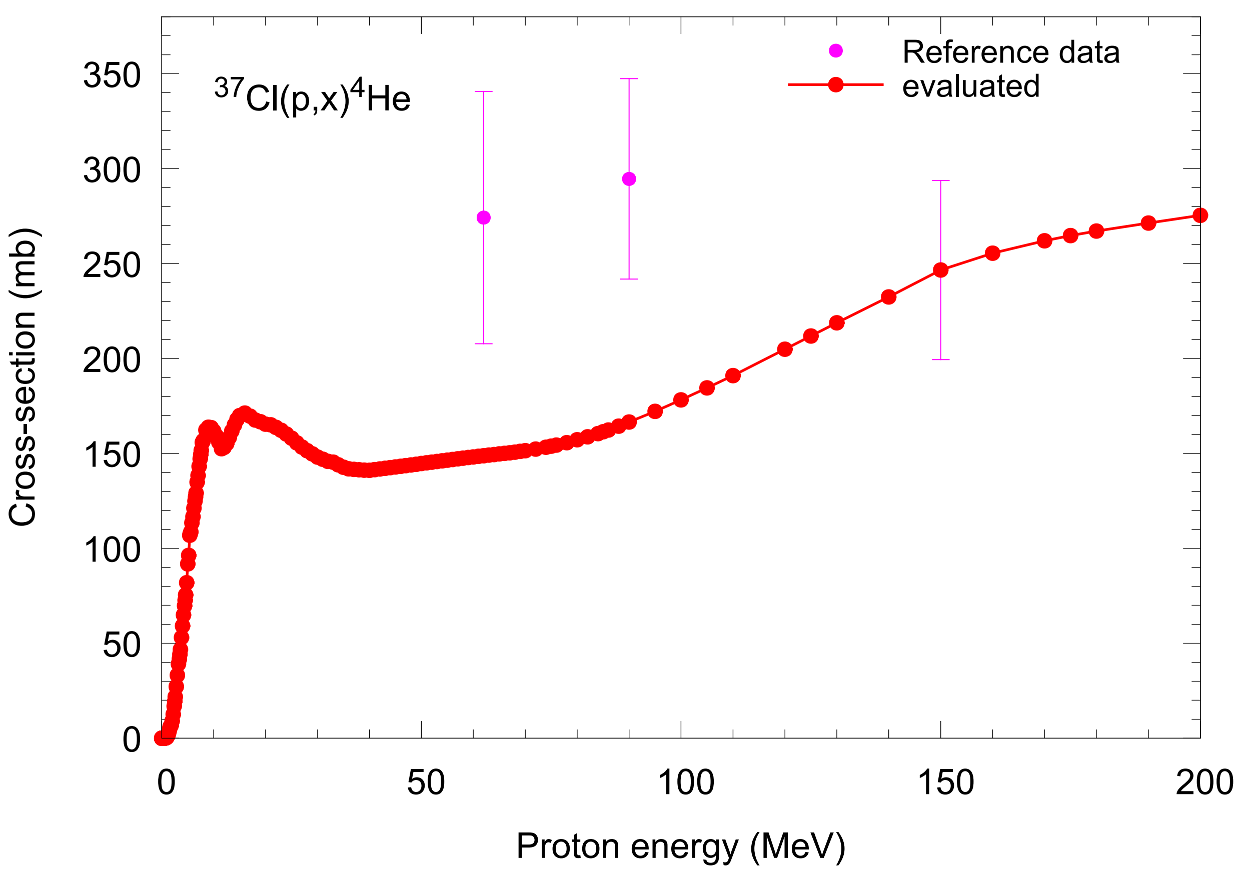

$^{37}Cl(p,x)^4He$
Reference data
evaluated
Cross-section (mb)
Proton energy (MeV)

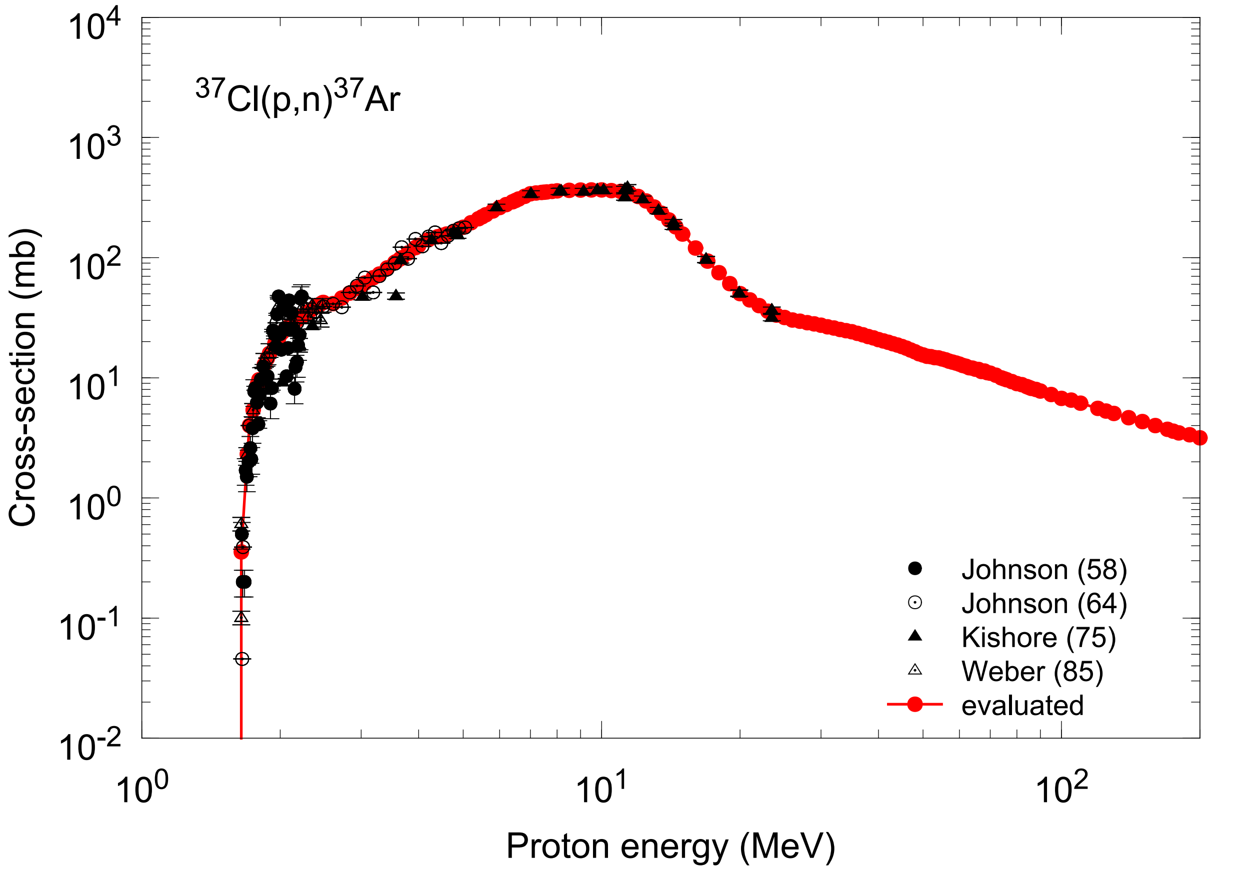

$^{37}Cl(p,n)^{37}Ar$
Cross-section (mb)
Proton energy (MeV)
Johnson (58)
Johnson (64)
Kishore (75)
Weber (85)
evaluated
10^{4}
10^{3}
10^{2}
10^{1}
10^{0}
10^{-1}
10^{-2}
10^{0}
10^{1}
10^{2}

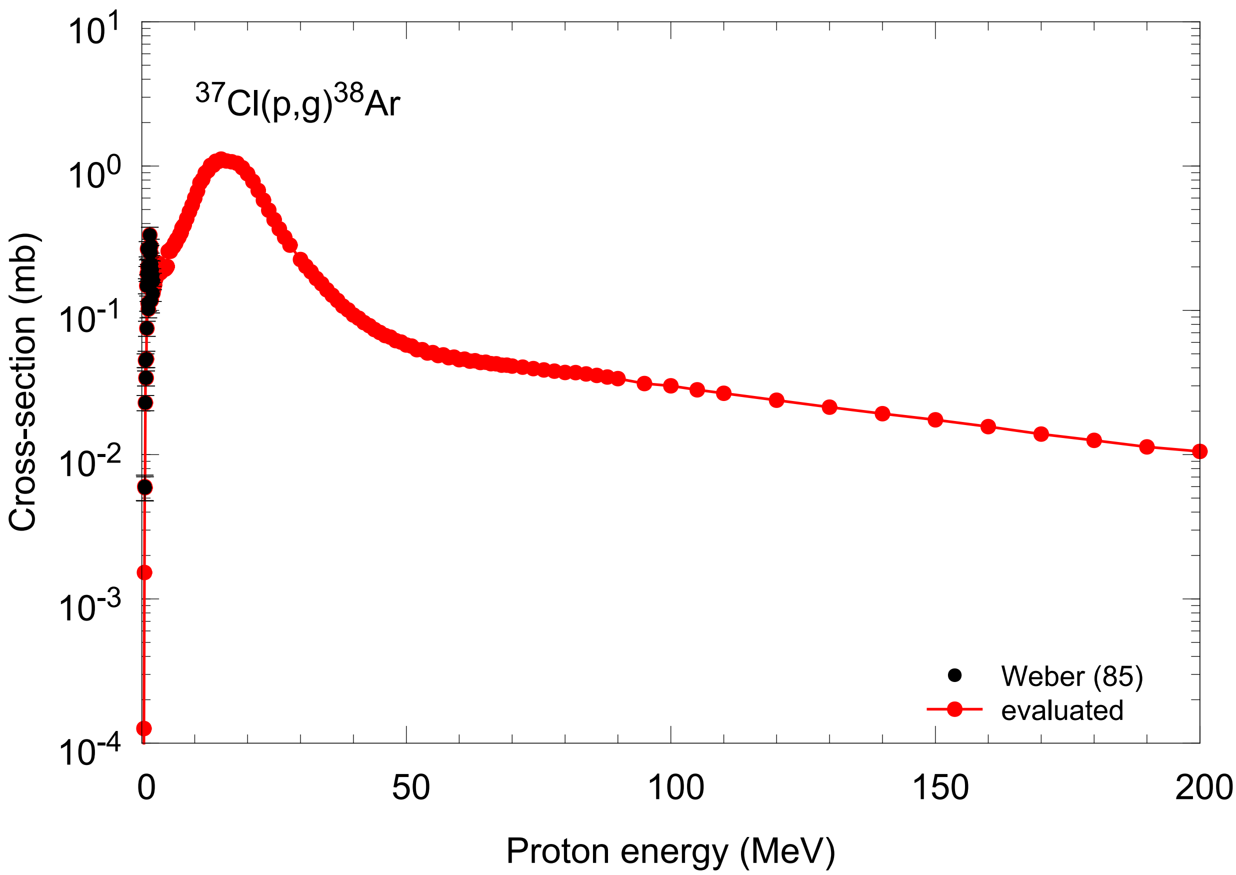

$^{37}Cl(p,g)^{38}Ar$
Cross-section (mb)
Proton energy (MeV)
Weber (85)
evaluated
10^{1}
10^{0}
10^{-1}
10^{-2}
10^{-3}
10^{-4}
0
50
100
150
200

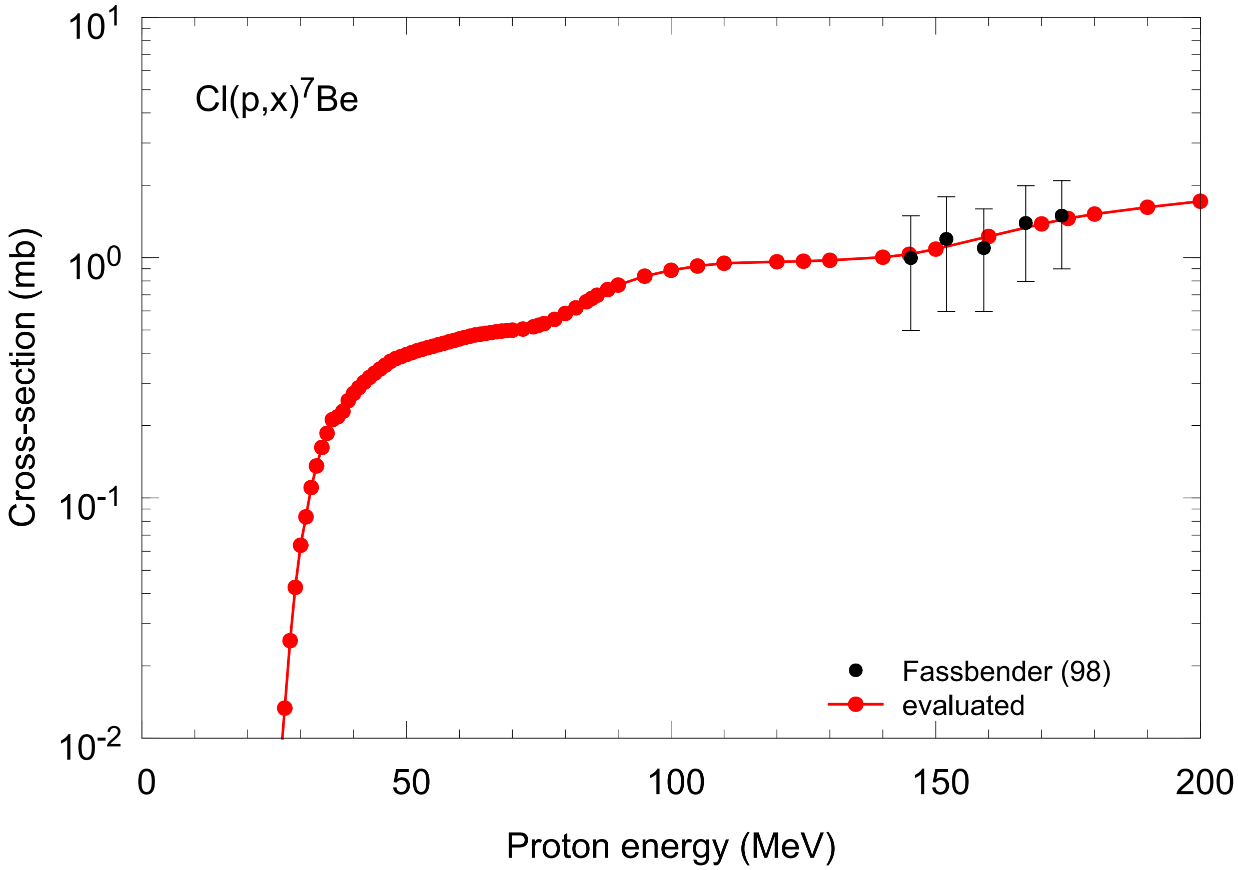

10^1
10^0
10^{-1}
10^{-2}
0
50
100
150
200
Cross-section (mb)
Proton energy (MeV)
Cl(p,x)^{7}Be
Fassbender (98)
evaluated

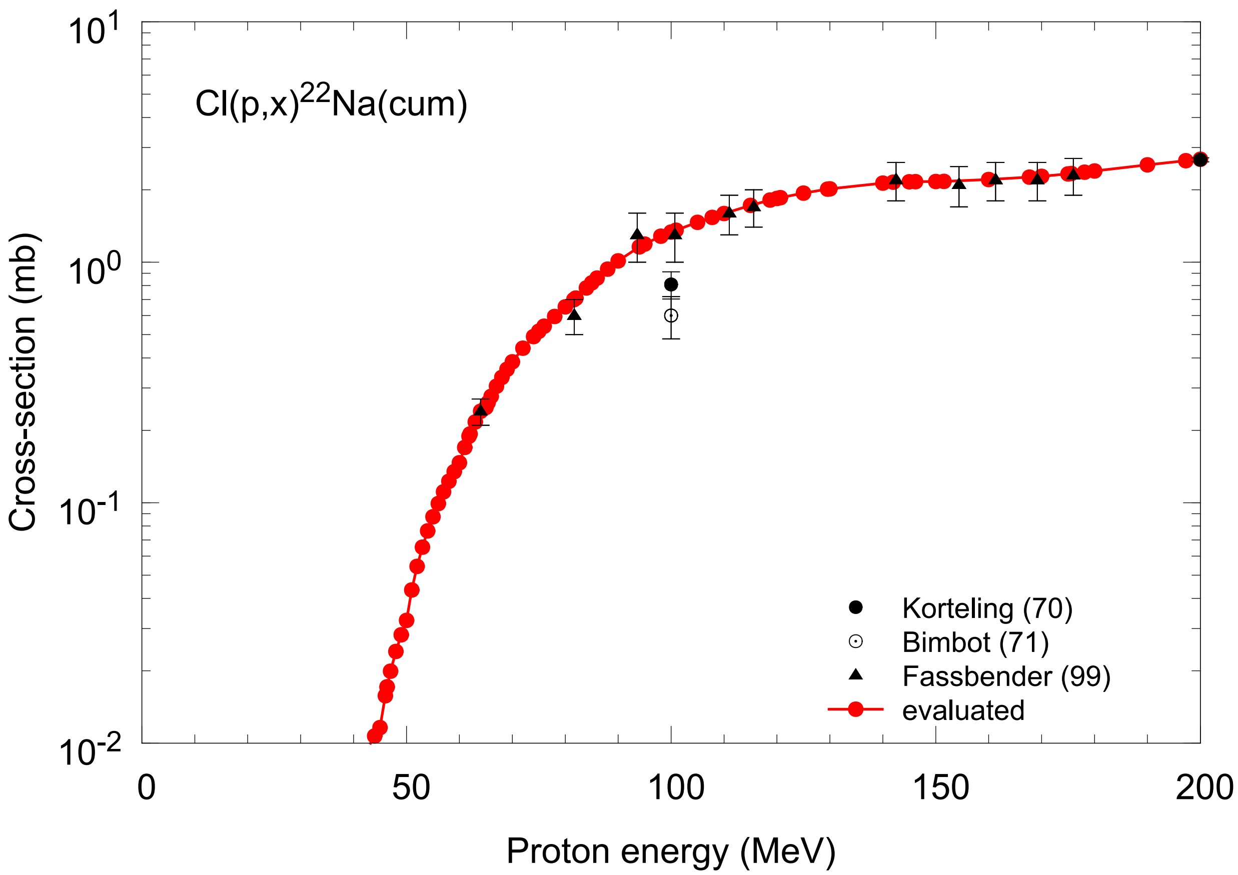

10^1
10^0
10^{-1}
10^{-2}
0
50
100
150
200
Cross-section (mb)
Proton energy (MeV)
Cl(p,x)^{22}Na(cum)
Korteling (70)
Bimbot (71)
Fassbender (99)
evaluated

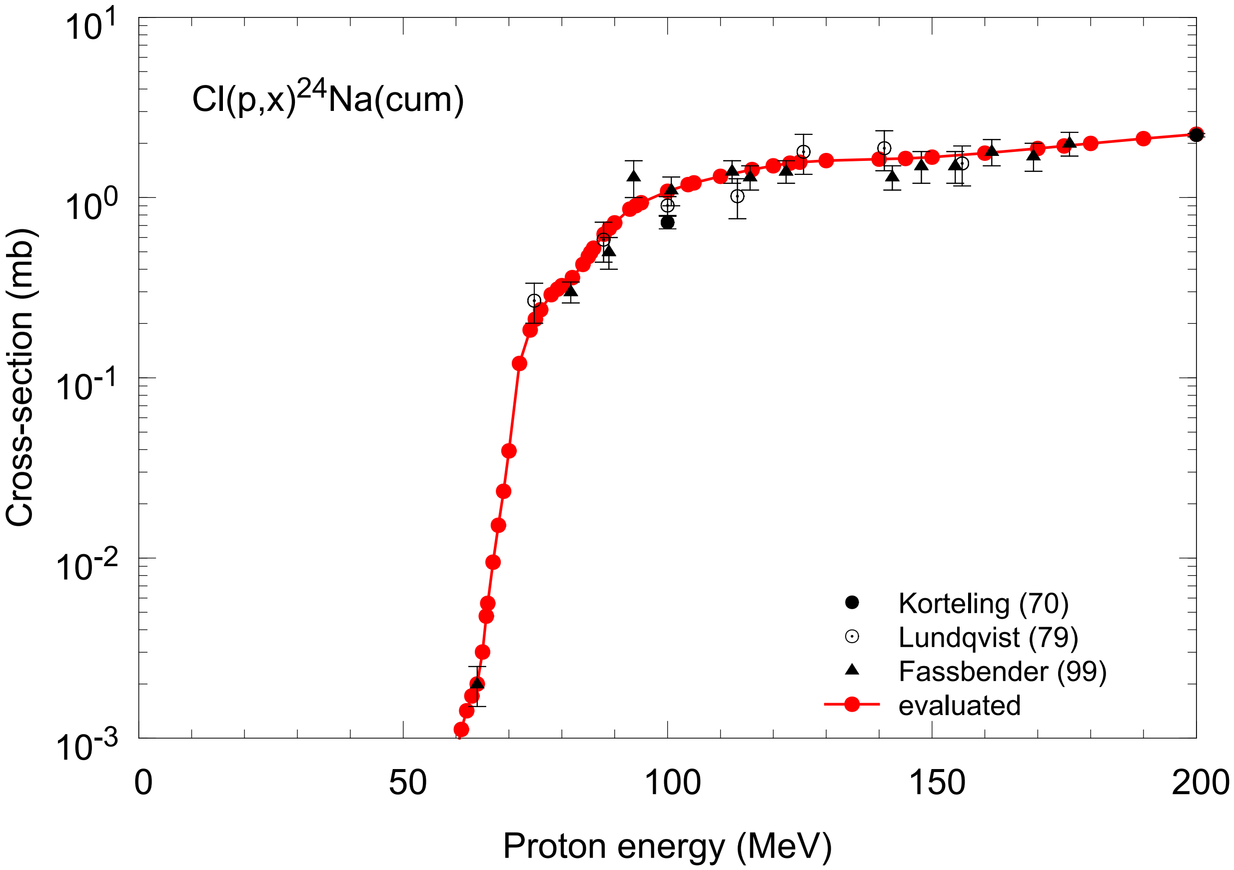

Cl(p,x)24Na(cum)
Cross-section (mb)
Proton energy (MeV)
Korteling (70)
Lundqvist (79)
Fassbender (99)
evaluated

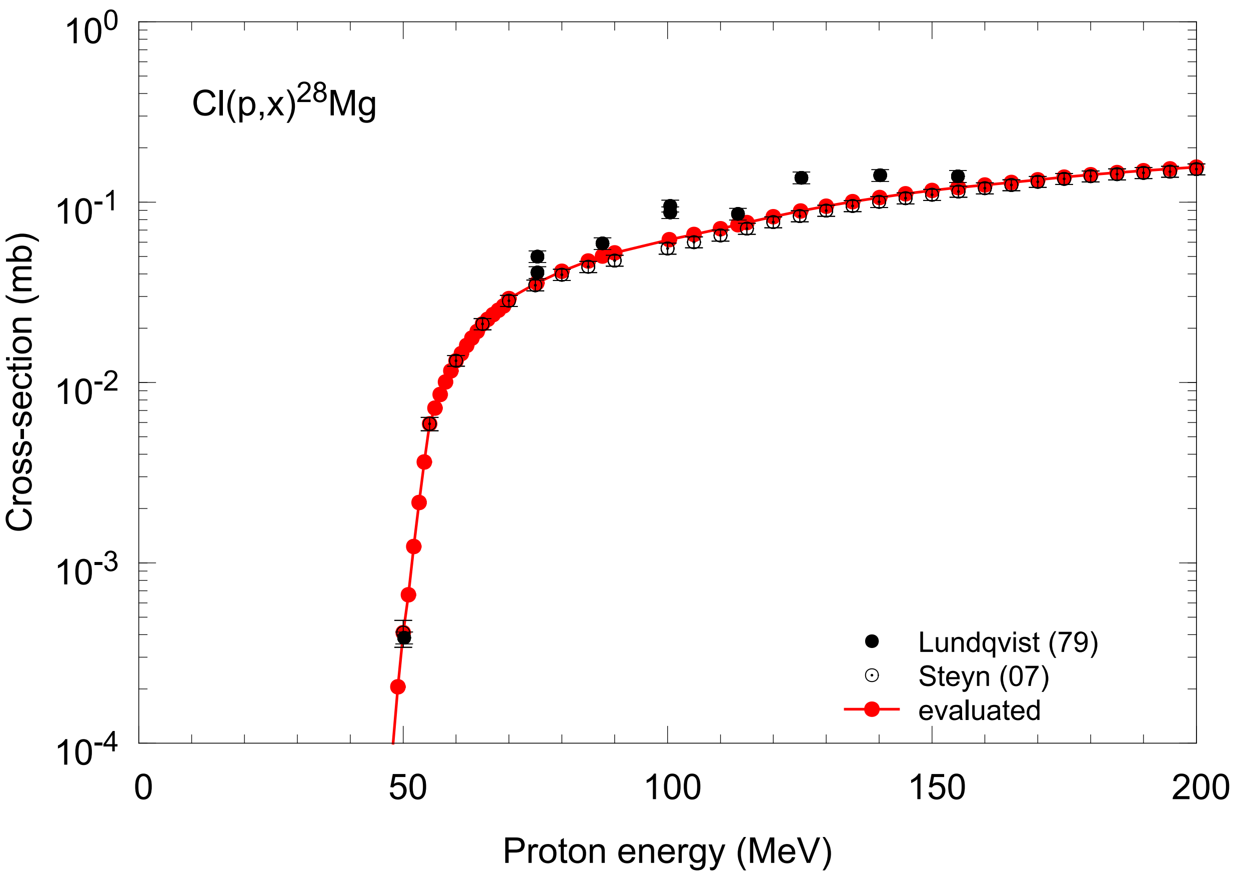

Cl(p,x)28Mg
Cross-section (mb)
Proton energy (MeV)
Lundqvist (79)
Steyn (07)
evaluated

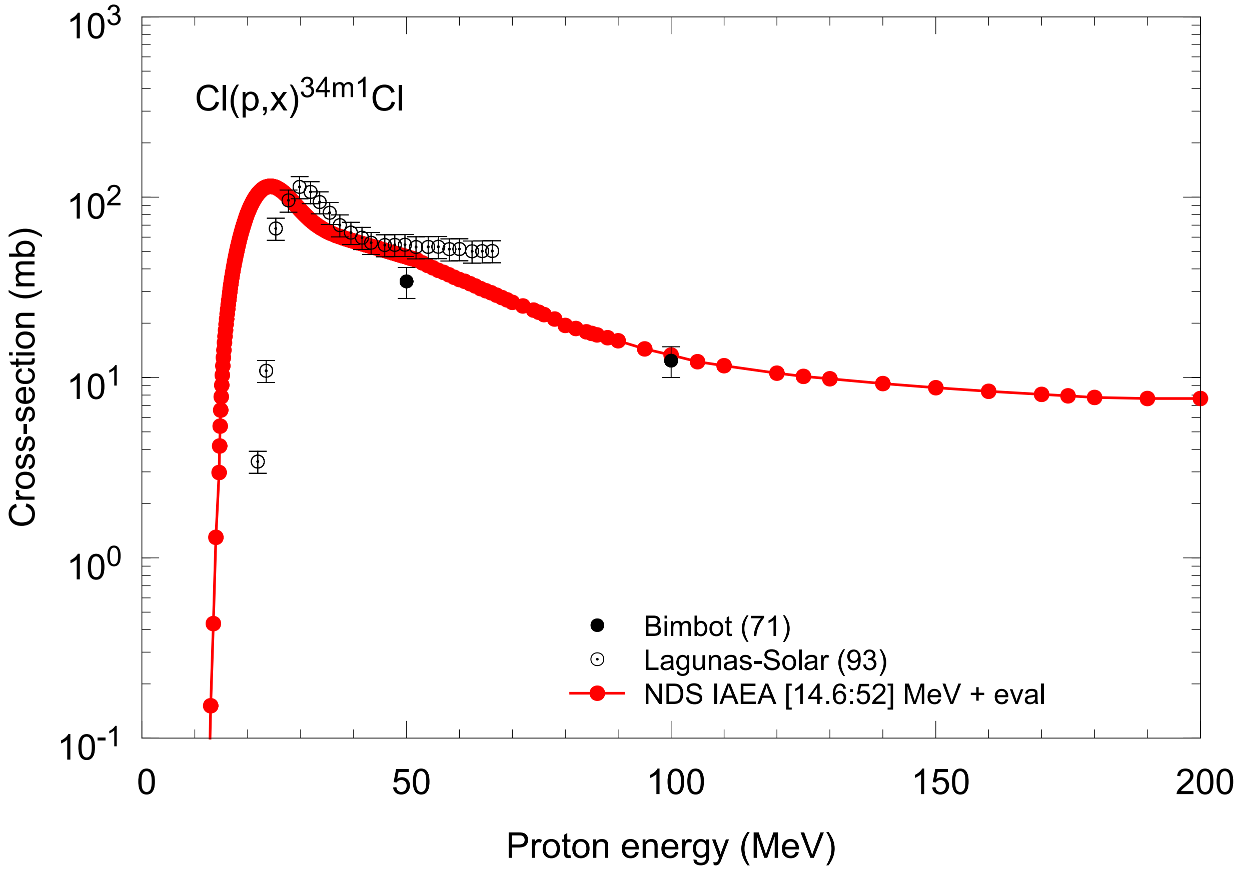

Cl(p,x)34m1Cl
Cross-section (mb)
Proton energy (MeV)
Bimbot (71)
Lagunas-Solar (93)
NDS IAEA [14.6:52] MeV + eval

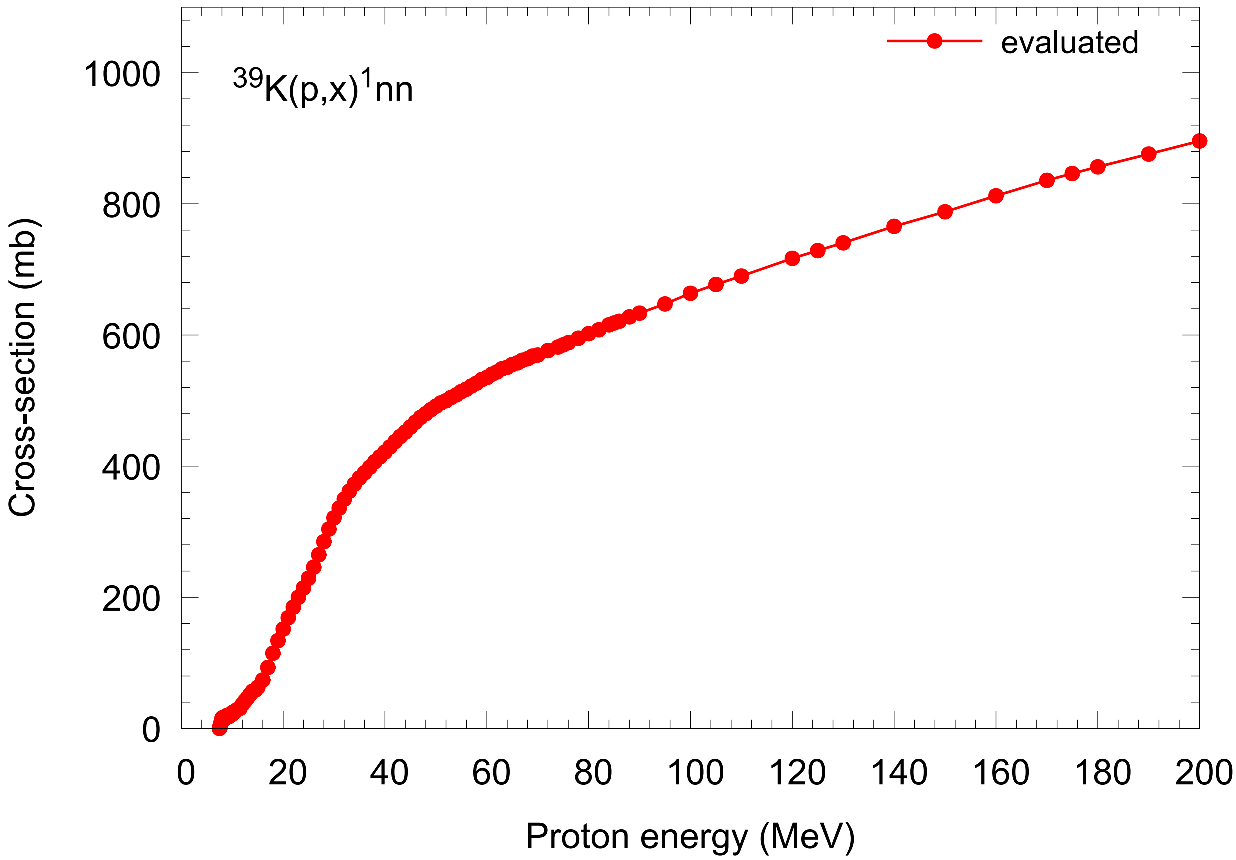

$^{39}K(p,x)^1nn$
evaluated
Cross-section (mb)
Proton energy (MeV)
0
200
400
600
800
1000
0
20
40
60
80
100
120
140
160
180
200

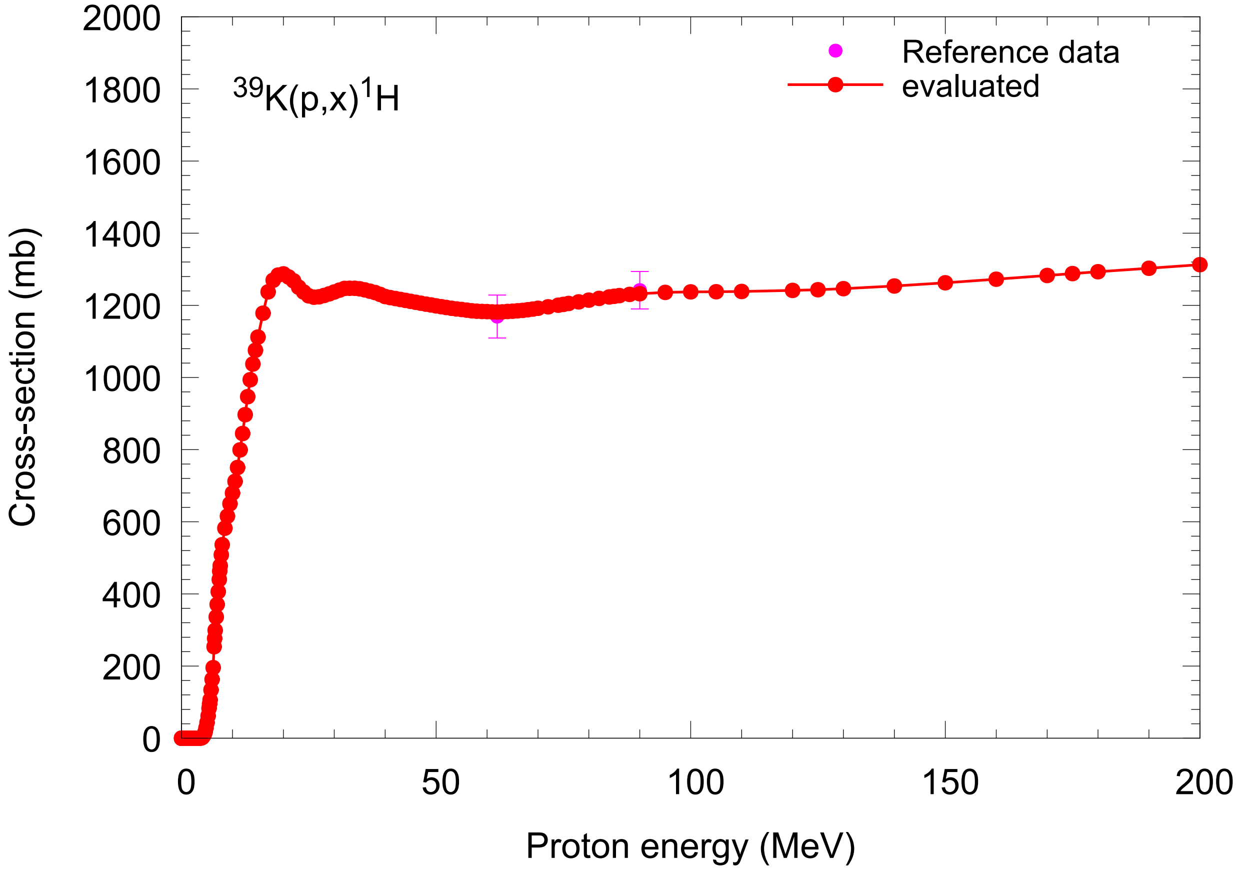

$^{39}K(p,x)^1H$
Reference data
evaluated
Cross-section (mb)
Proton energy (MeV)
0
200
400
600
800
1000
1200
1400
1600
1800
2000
0
50
100
150
200

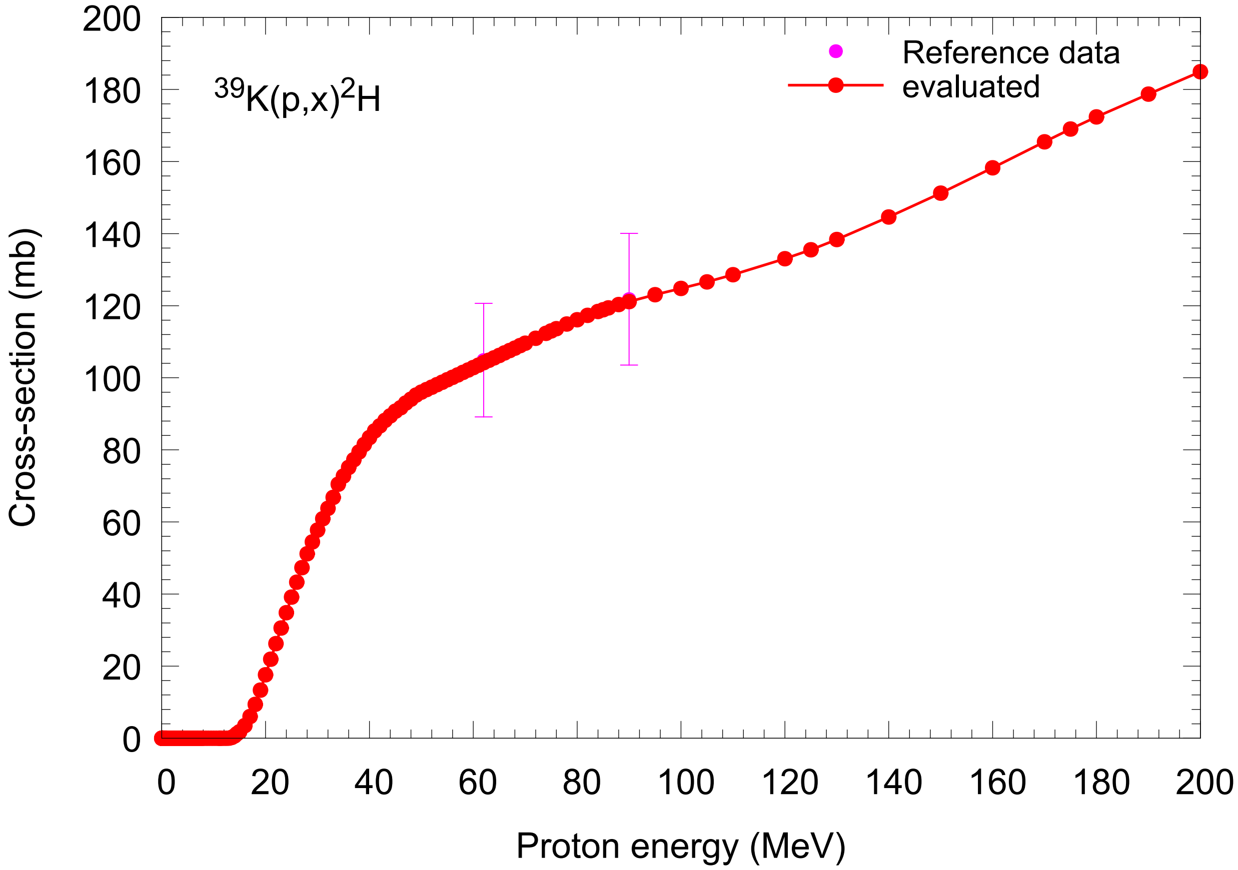

$^{39}K(p,x)^{2}H$
Reference data
evaluated
Cross-section (mb)
Proton energy (MeV)

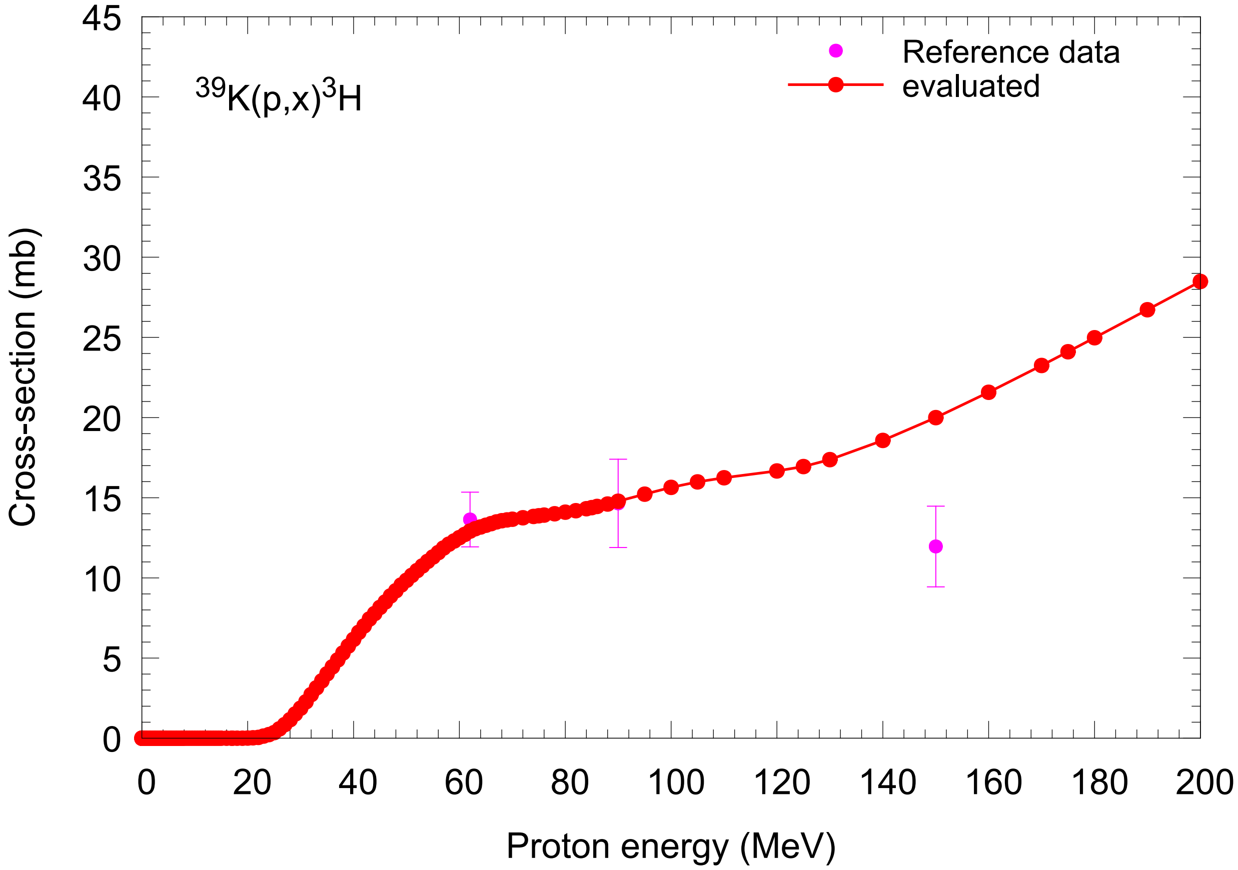

$^{39}K(p,x)^{3}H$
Reference data
evaluated
Cross-section (mb)
Proton energy (MeV)

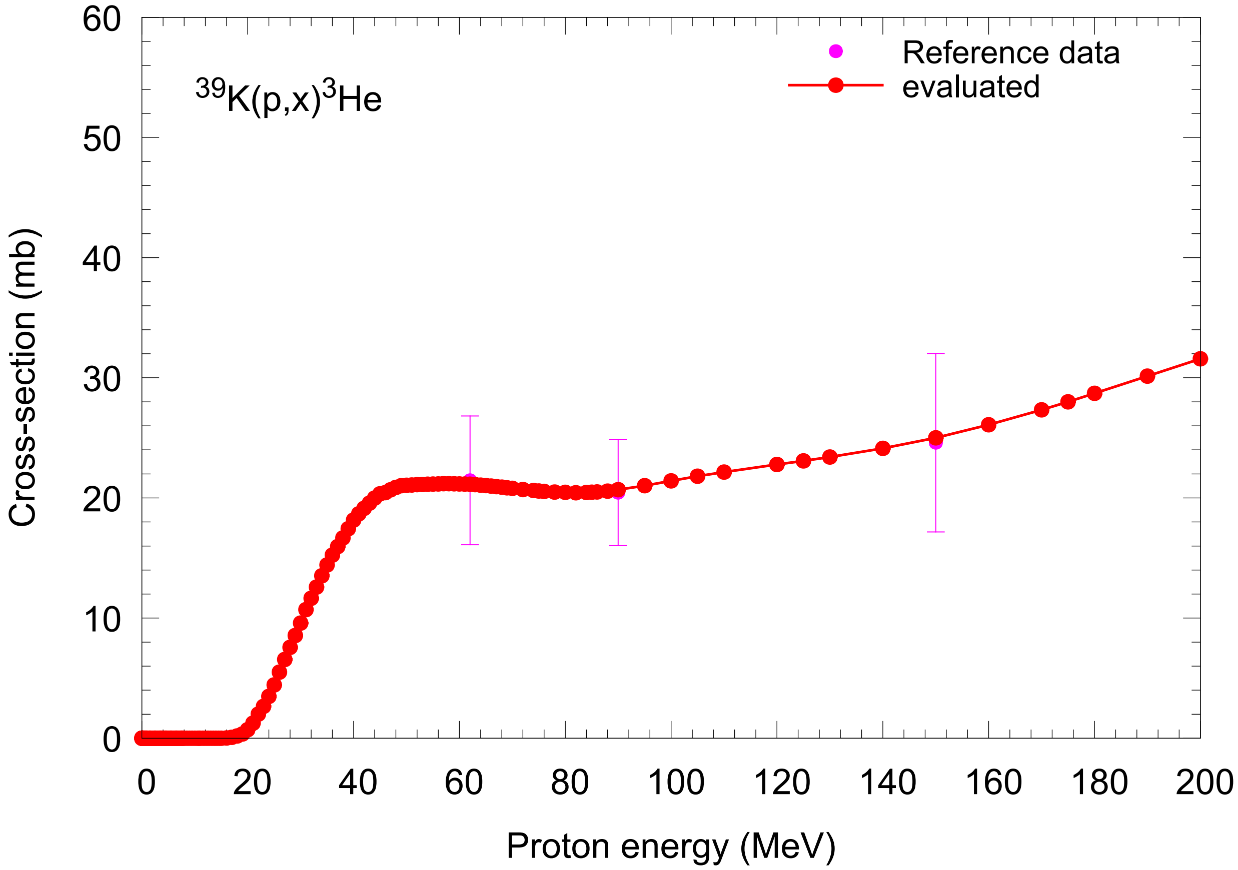

$^{39}K(p,x)^{3}He$
Reference data
evaluated
Cross-section (mb)
Proton energy (MeV)
0
10
20
30
40
50
60
0
20
40
60
80
100
120
140
160
180
200

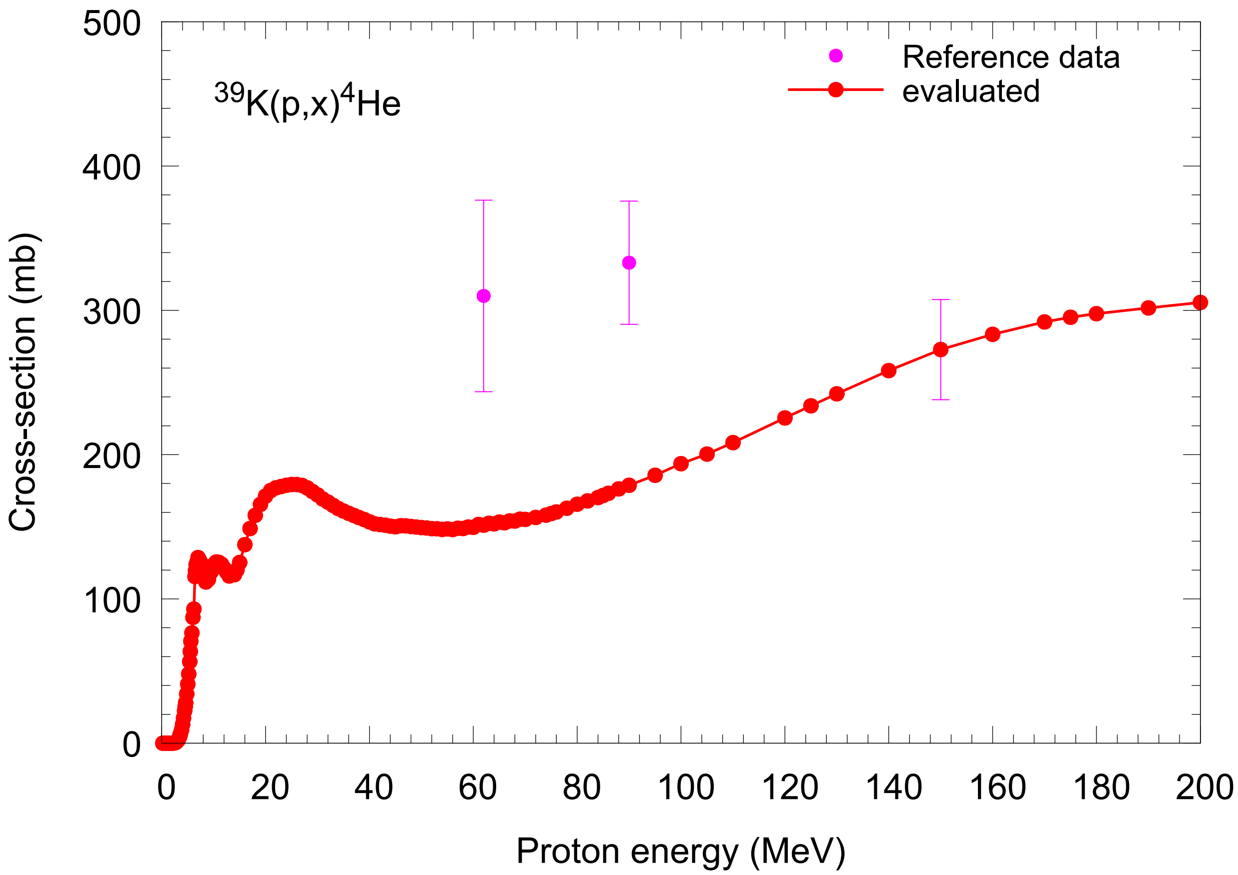

$^{39}K(p,x)^{4}He$
Reference data
evaluated
Cross-section (mb)
Proton energy (MeV)
0
100
200
300
400
500
0
20
40
60
80
100
120
140
160
180
200

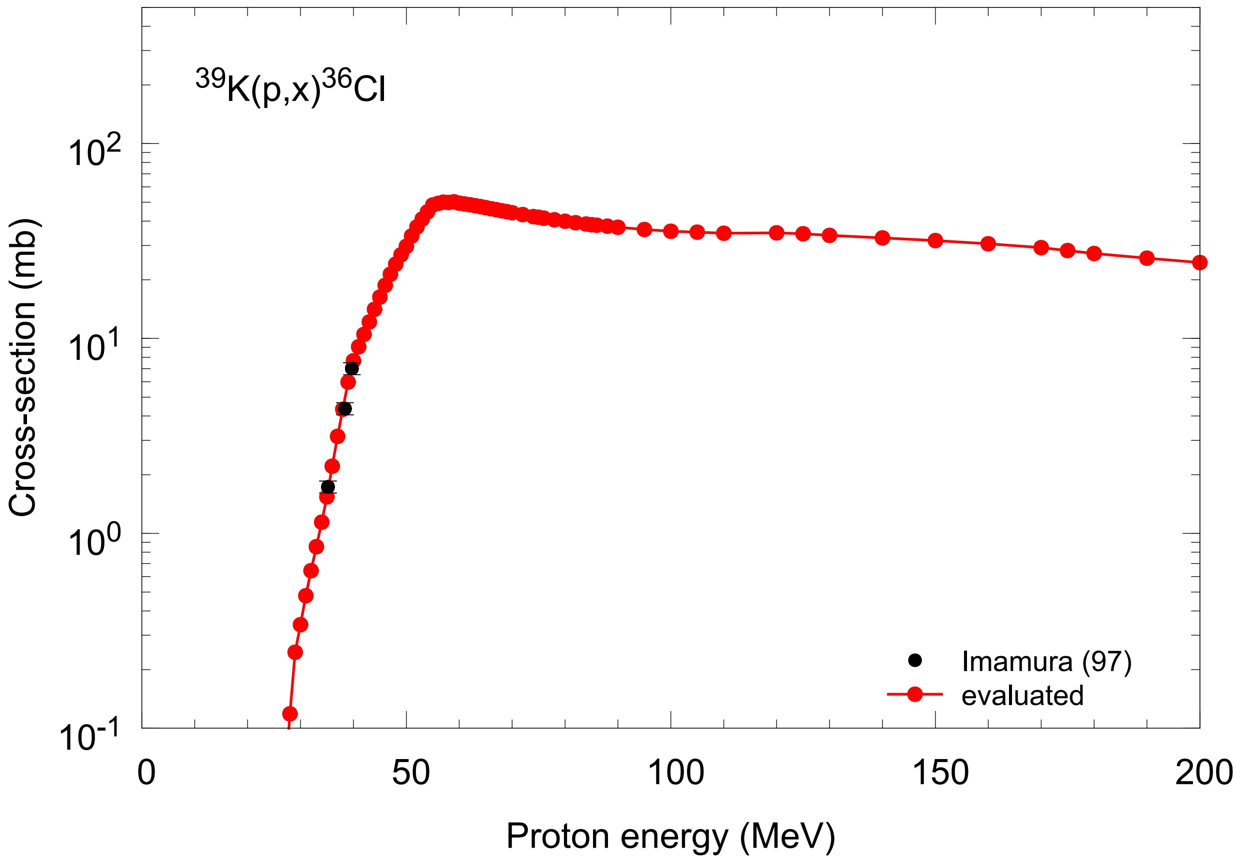

$^{39}K(p,x)^{36}Cl$
Imamura (97)
evaluated
10^{2}
10^{1}
10^{0}
10^{-1}
Cross-section (mb)
0
50
100
150
200
Proton energy (MeV)

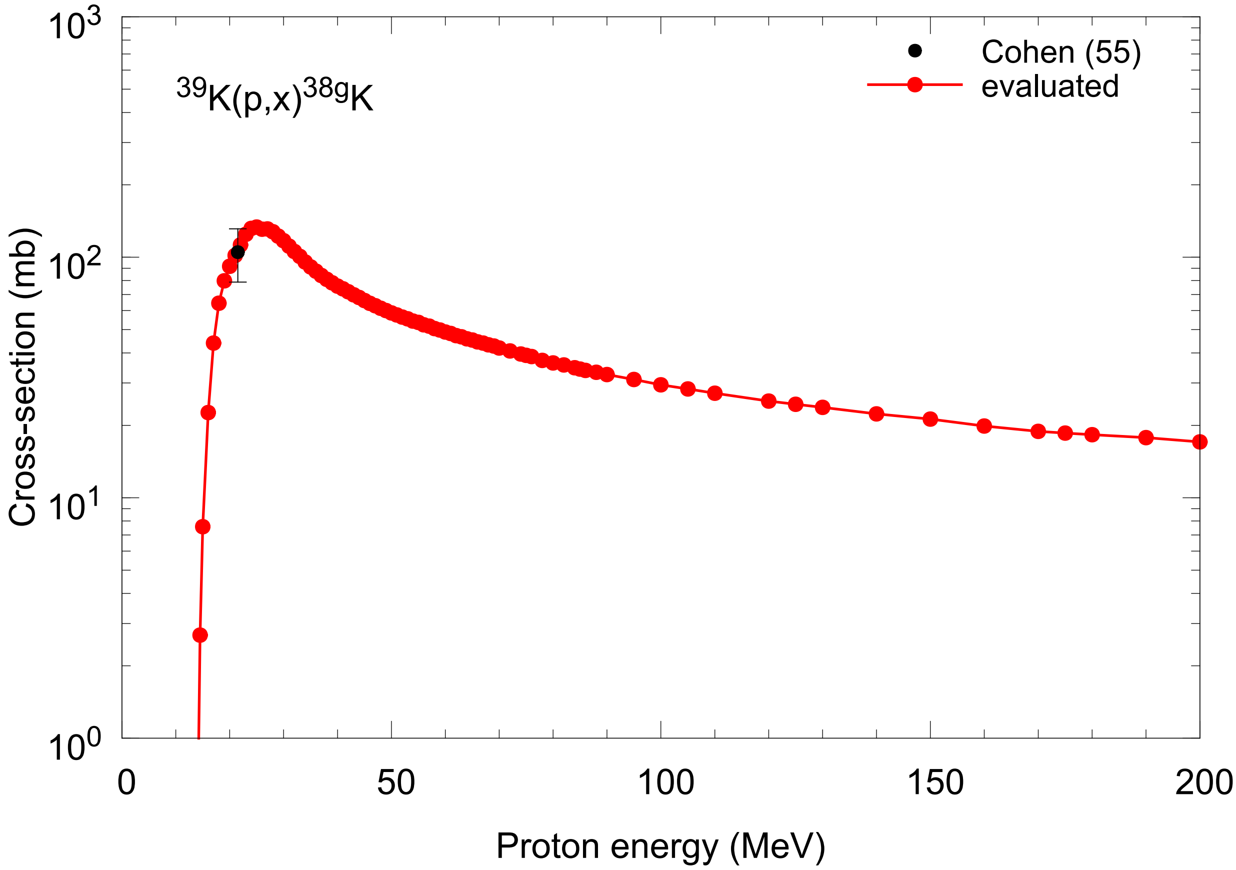

$^{39}K(p,x)^{38g}K$
Cohen (55)
evaluated
10^{3}
10^{2}
10^{1}
10^{0}
Cross-section (mb)
0
50
100
150
200
Proton energy (MeV)

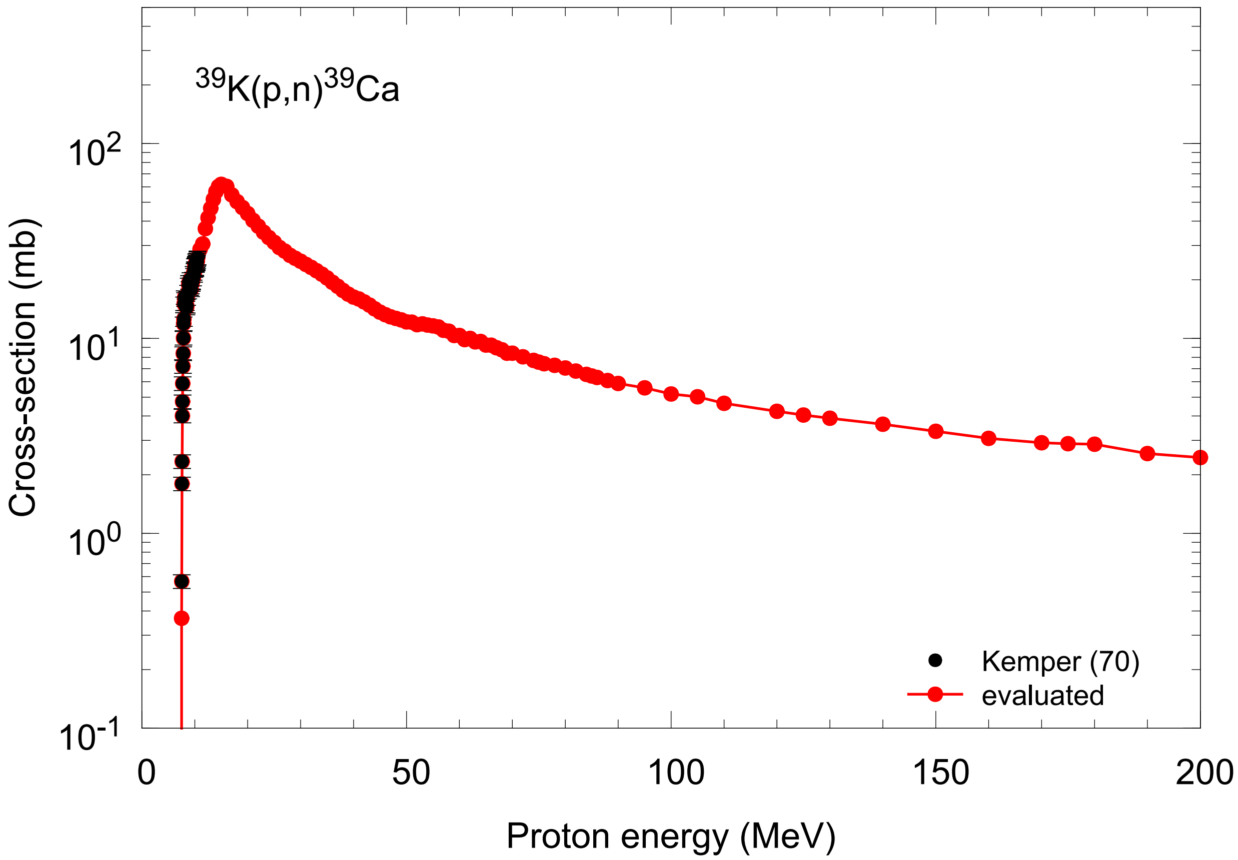

$^{39}K(p,n)^{39}Ca$
10^2
10^1
10^0
10^{-1}
Cross-section (mb)
0
50
100
150
200
Proton energy (MeV)
Kemper (70)
evaluated

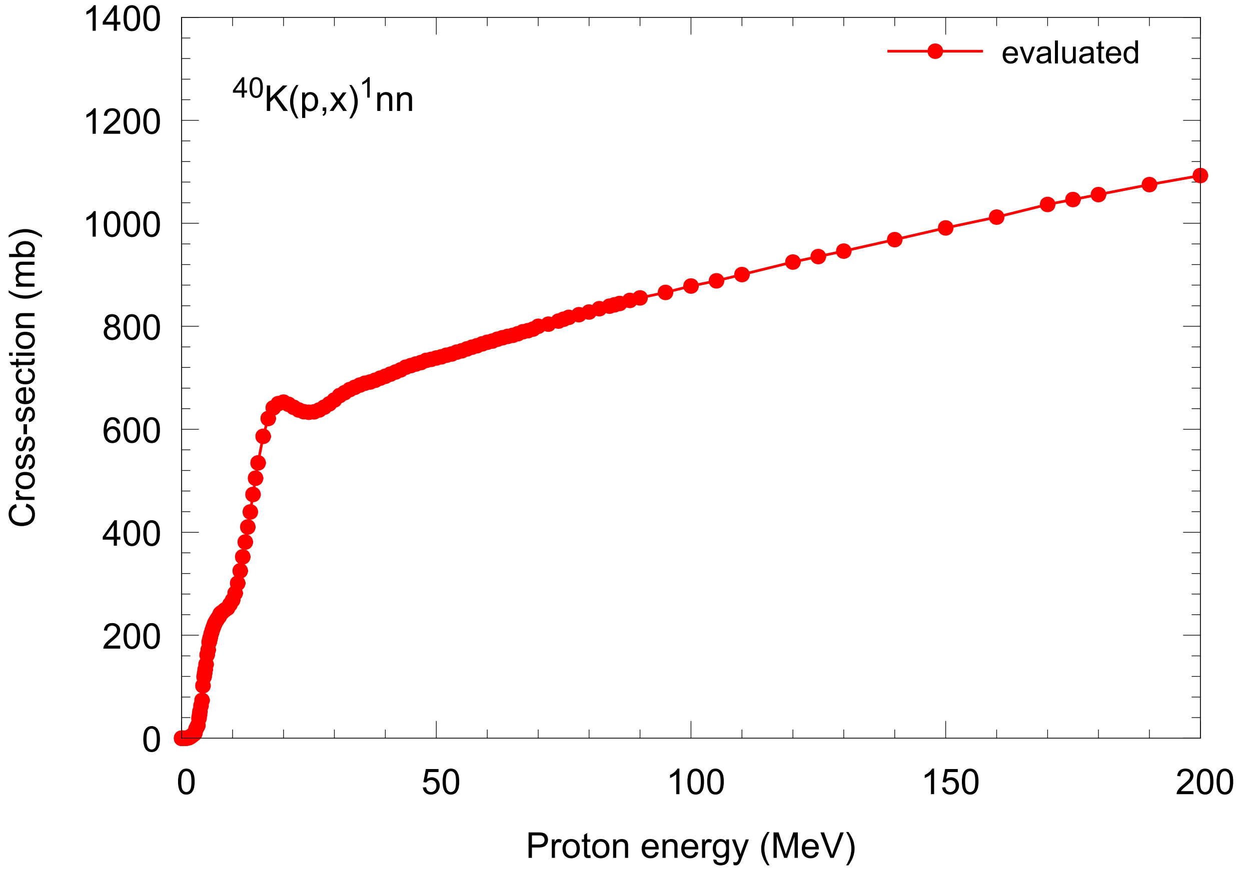

1400
1200
1000
800
600
400
200
0
Cross-section (mb)
0
50
100
150
200
Proton energy (MeV)
evaluated
^{40}K(p,x)^{1}nn

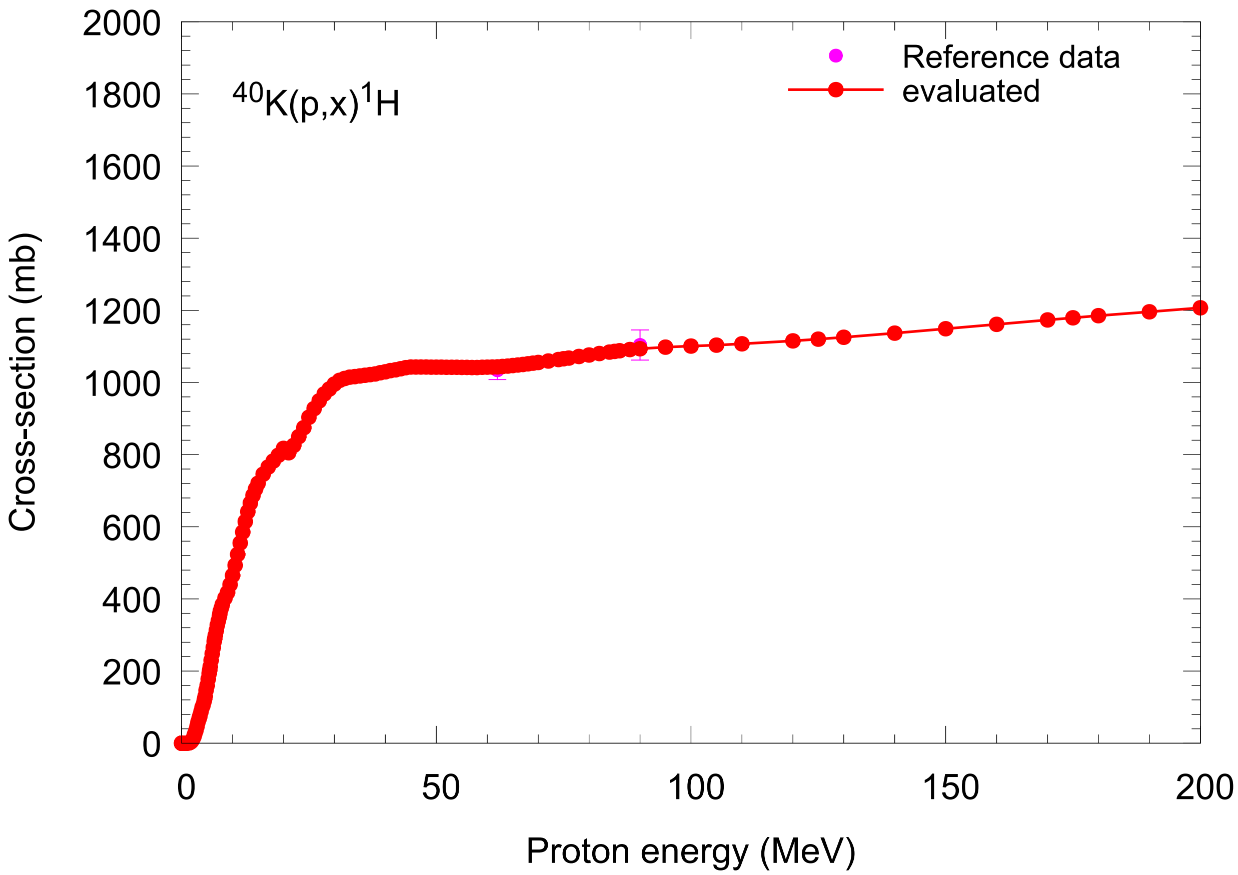

2000
1800
1600
1400
1200
1000
800
600
400
200
0
Cross-section (mb)
0
50
100
150
200
Proton energy (MeV)
Reference data
evaluated
^{40}K(p,x)^{1}H

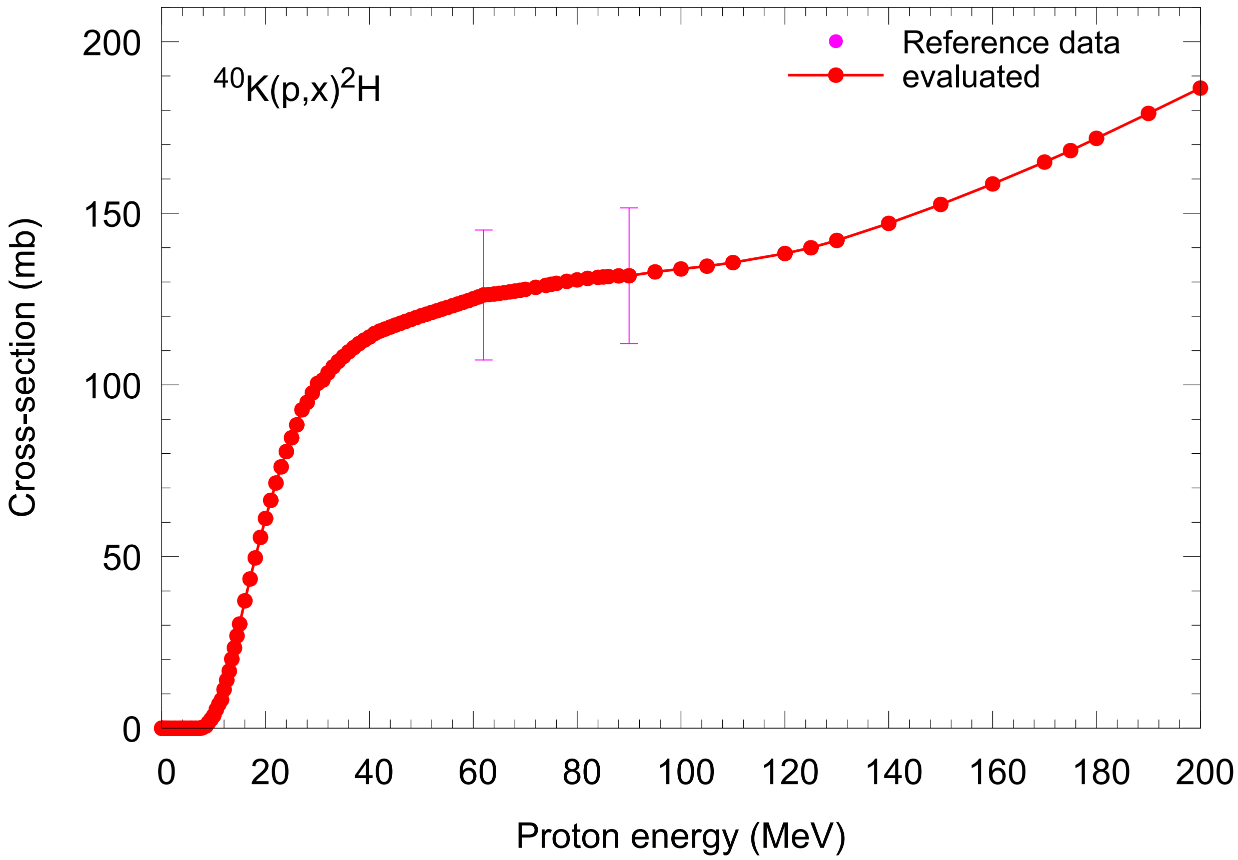

$^{40}K(p,x)^{2}H$
Reference data
evaluated
Cross-section (mb)
Proton energy (MeV)
0
50
100
150
200
0
20
40
60
80
100
120
140
160
180
200

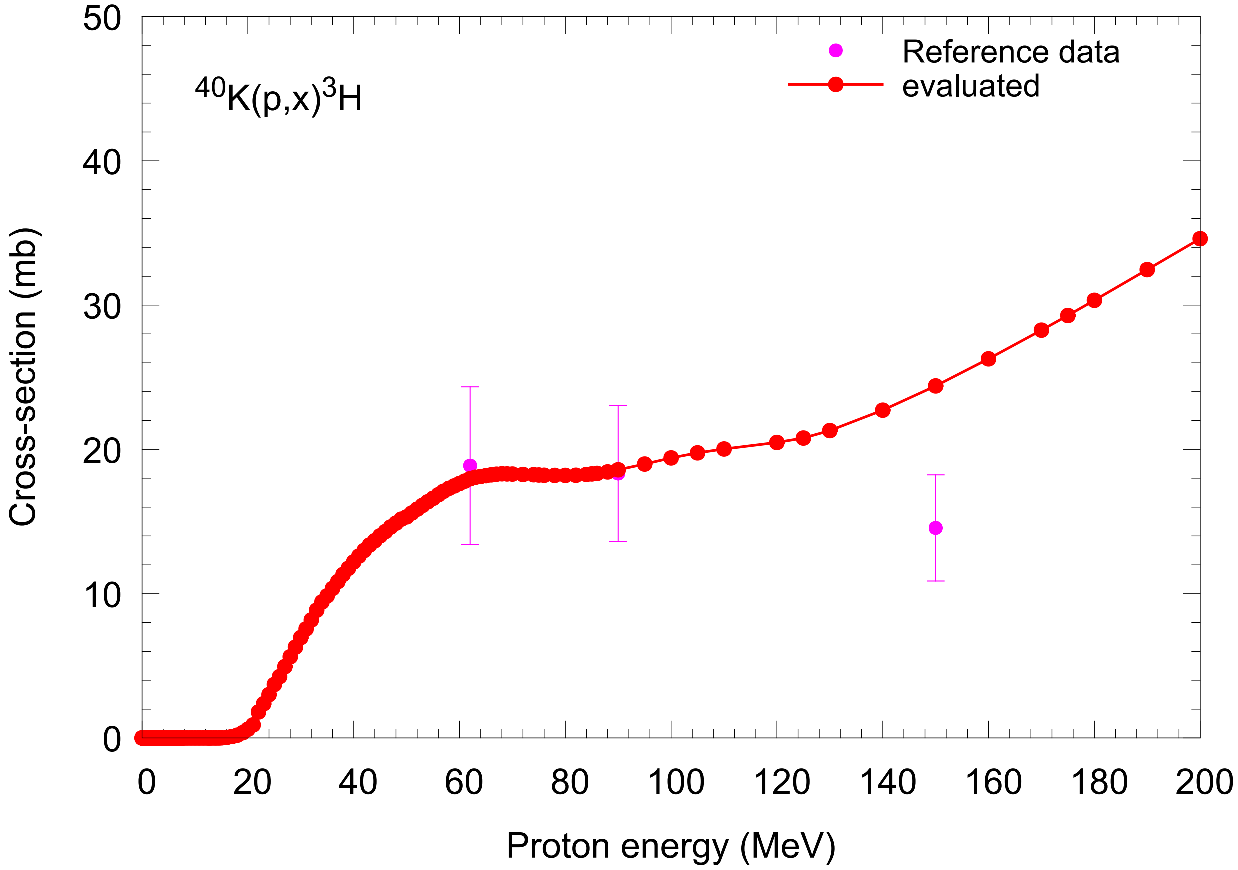

$^{40}K(p,x)^{3}H$
Reference data
evaluated
Cross-section (mb)
Proton energy (MeV)
0
10
20
30
40
50
0
20
40
60
80
100
120
140
160
180
200

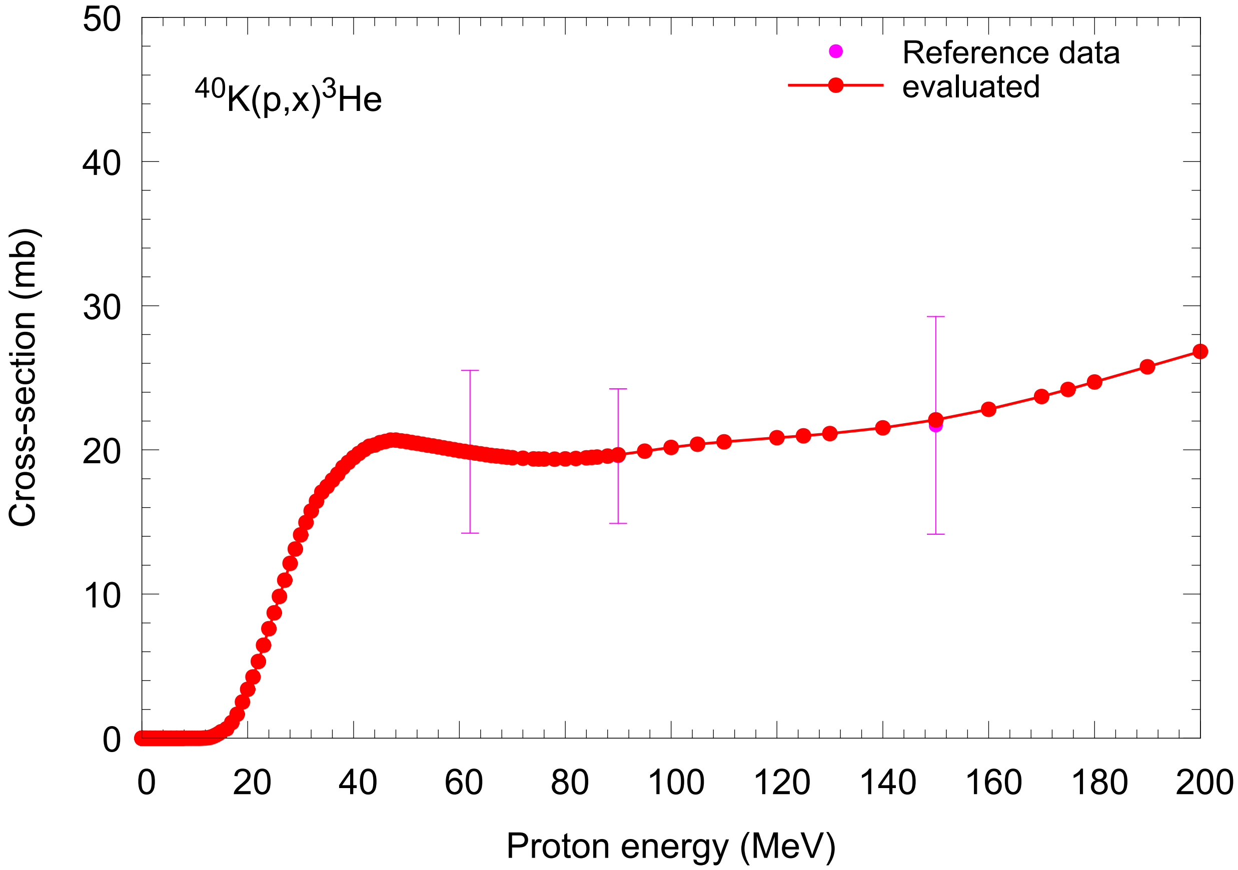

$^{40}K(p,x)^{3}He$
Reference data
evaluated
Cross-section (mb)
Proton energy (MeV)
0
10
20
30
40
50
0
20
40
60
80
100
120
140
160
180
200

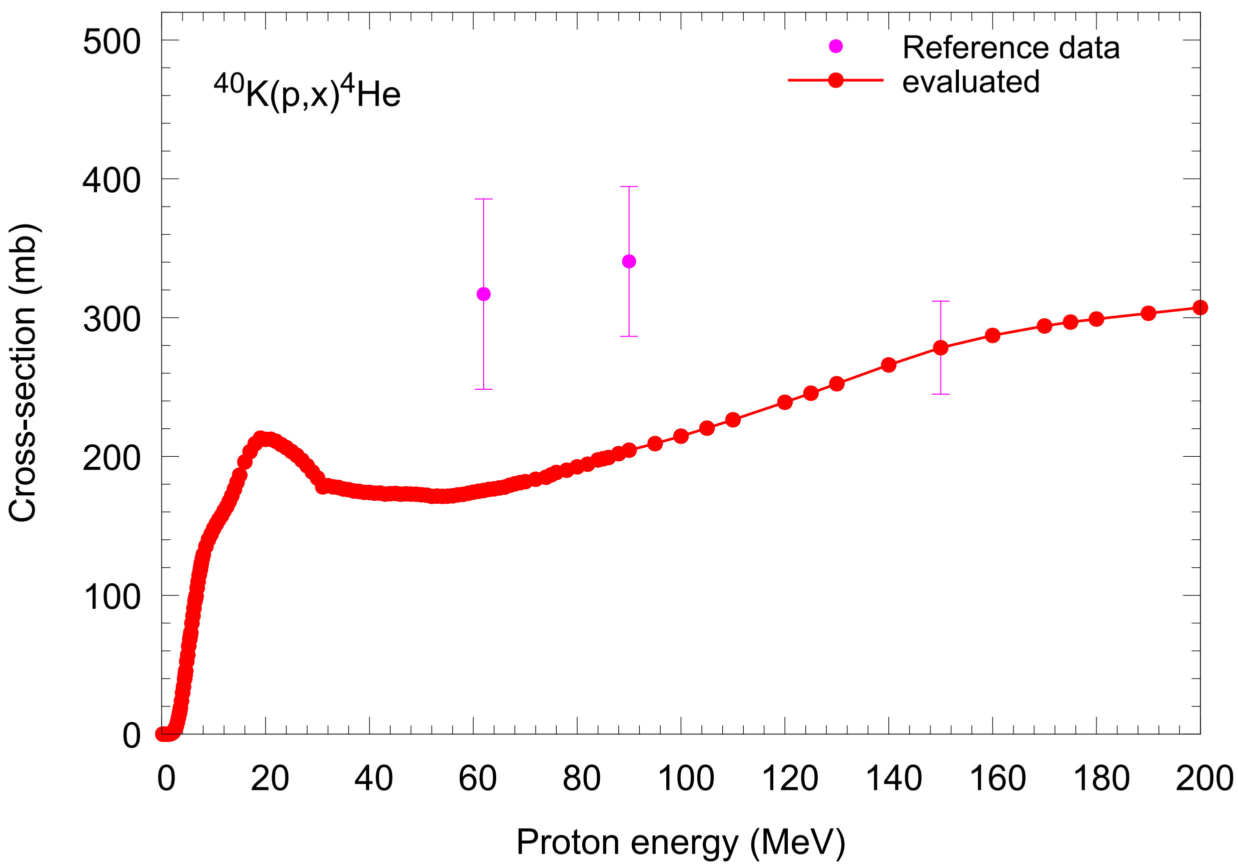

$^{40}K(p,x)^{4}He$
Reference data
evaluated
Cross-section (mb)
Proton energy (MeV)
0
100
200
300
400
500
0
20
40
60
80
100
120
140
160
180
200

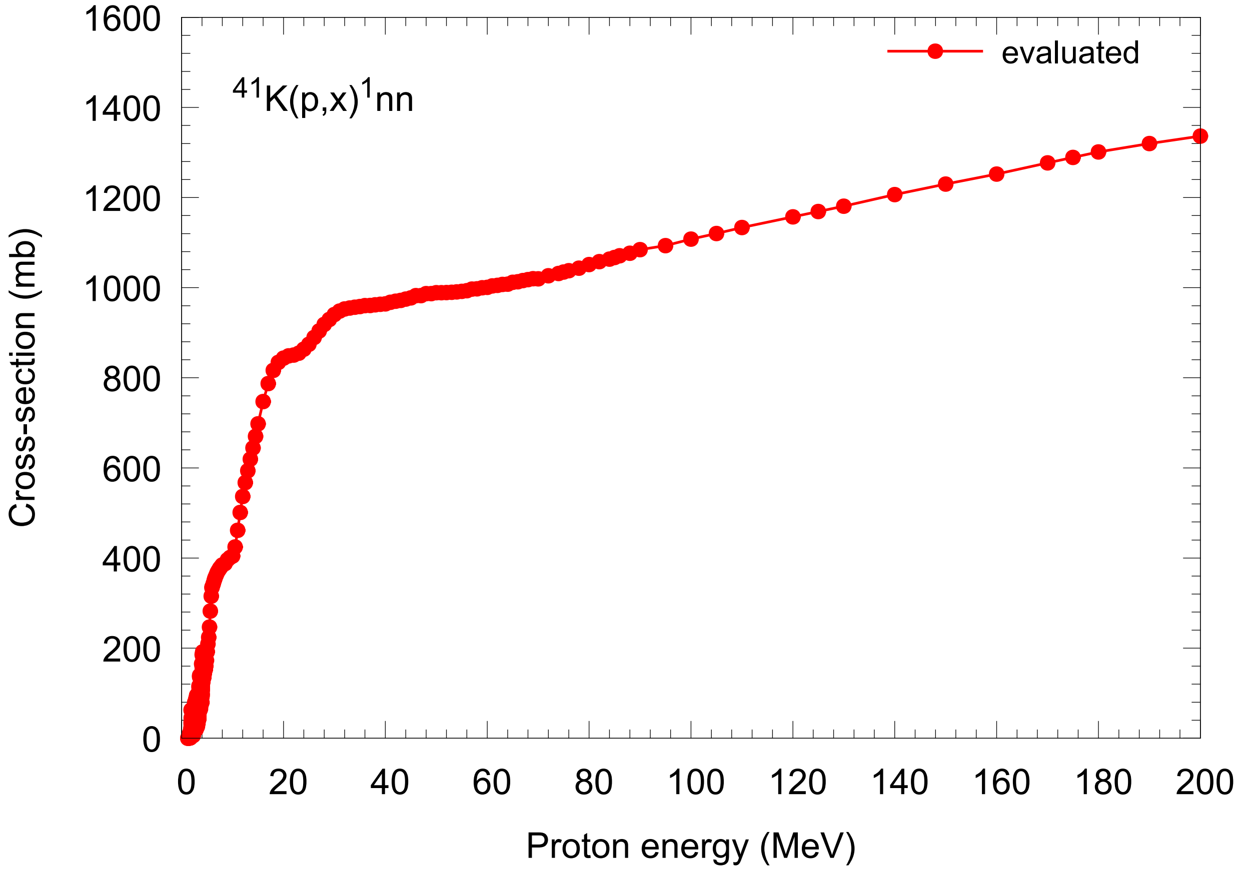

$^{41}K(p,x)^{1}nn$
evaluated
Cross-section (mb)
Proton energy (MeV)

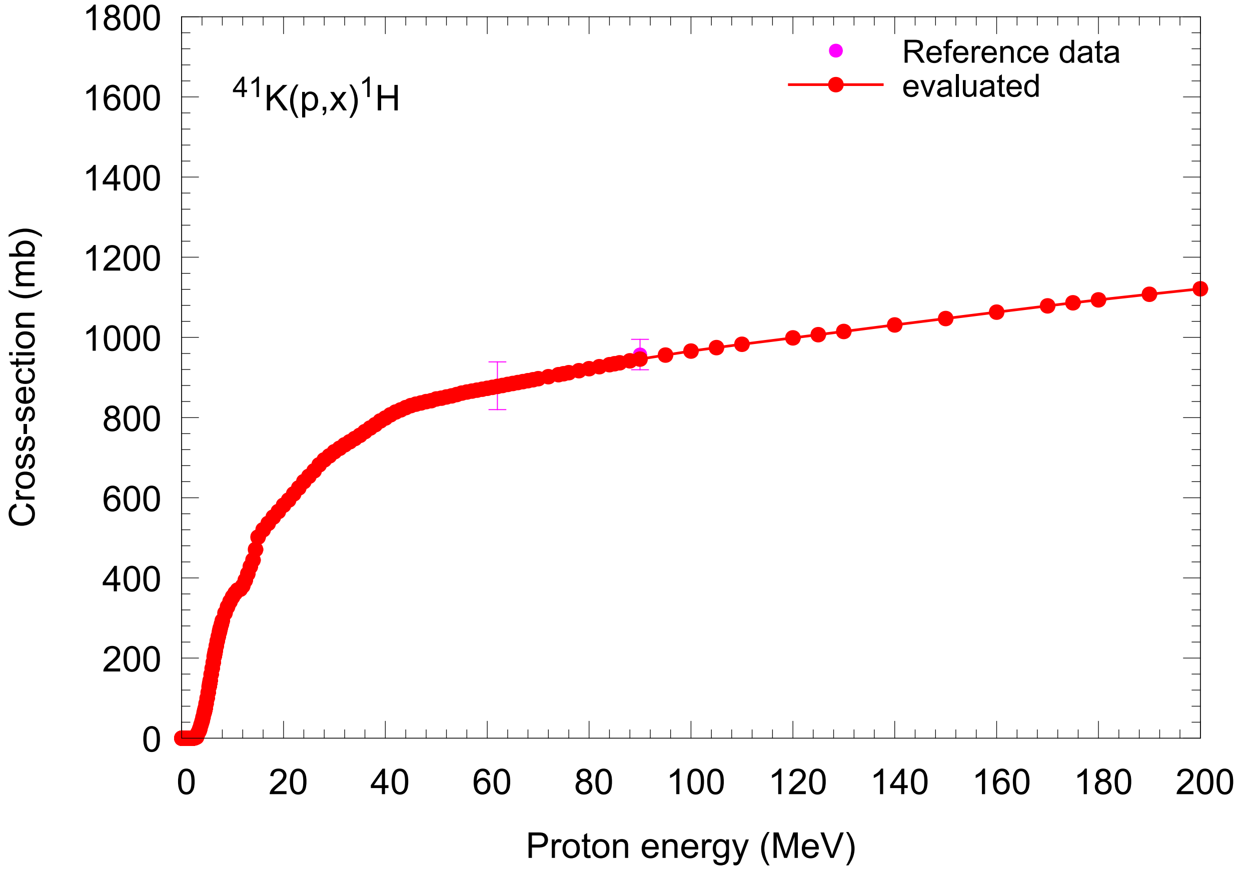

$^{41}K(p,x)^{1}H$
Reference data
evaluated
Cross-section (mb)
Proton energy (MeV)

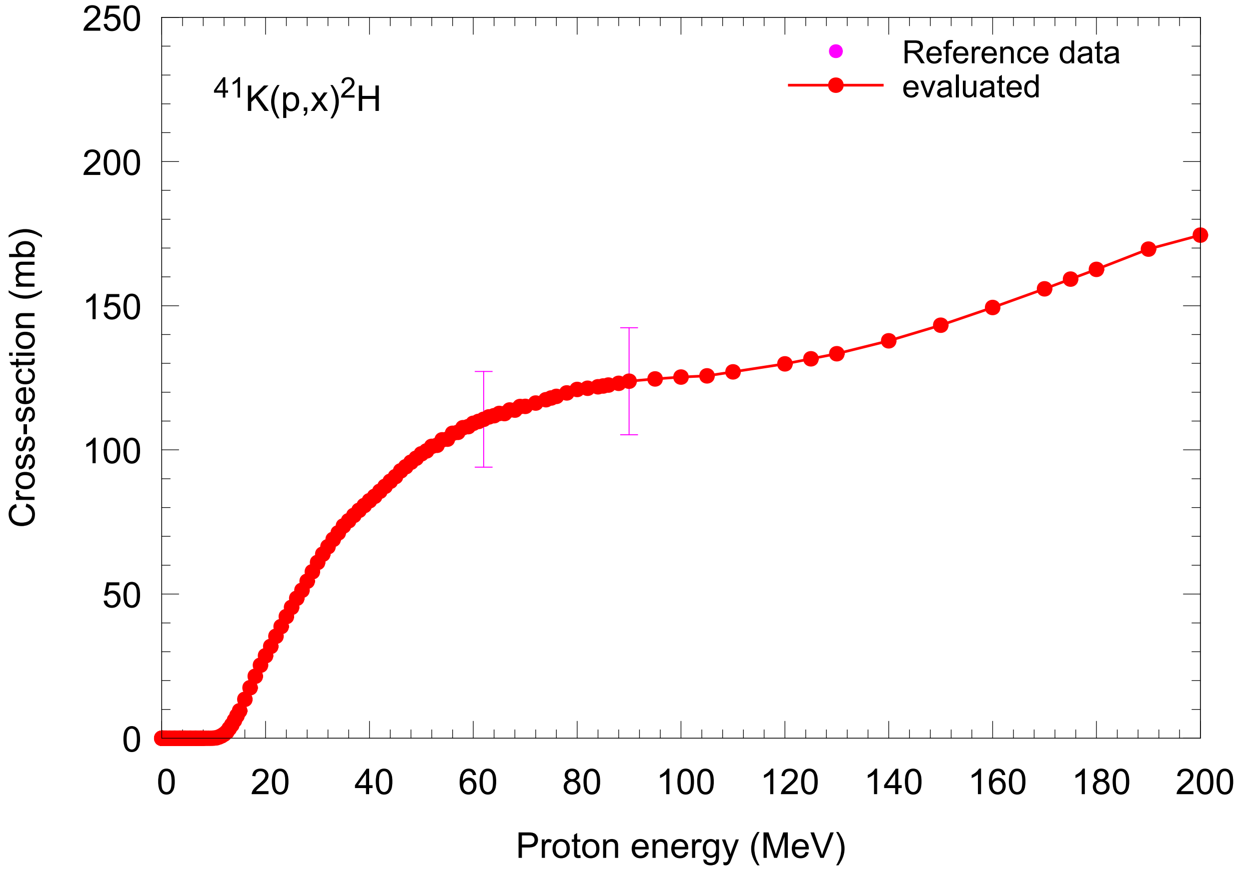

$^{41}K(p,x)^{2}H$
Reference data
evaluated
Cross-section (mb)
Proton energy (MeV)
0
50
100
150
200
250
0
20
40
60
80
100
120
140
160
180
200

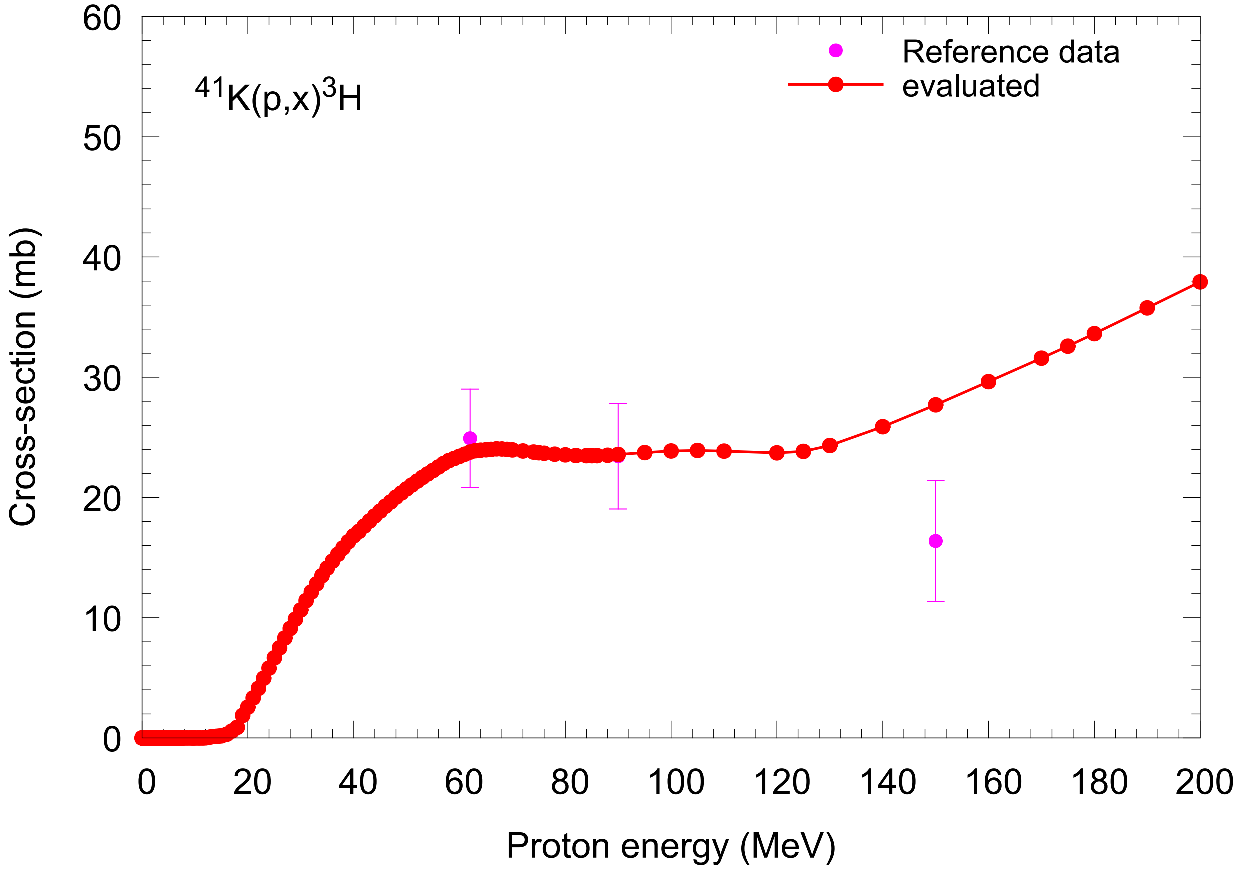

$^{41}K(p,x)^{3}H$
Reference data
evaluated
Cross-section (mb)
Proton energy (MeV)
0
10
20
30
40
50
60
0
20
40
60
80
100
120
140
160
180
200

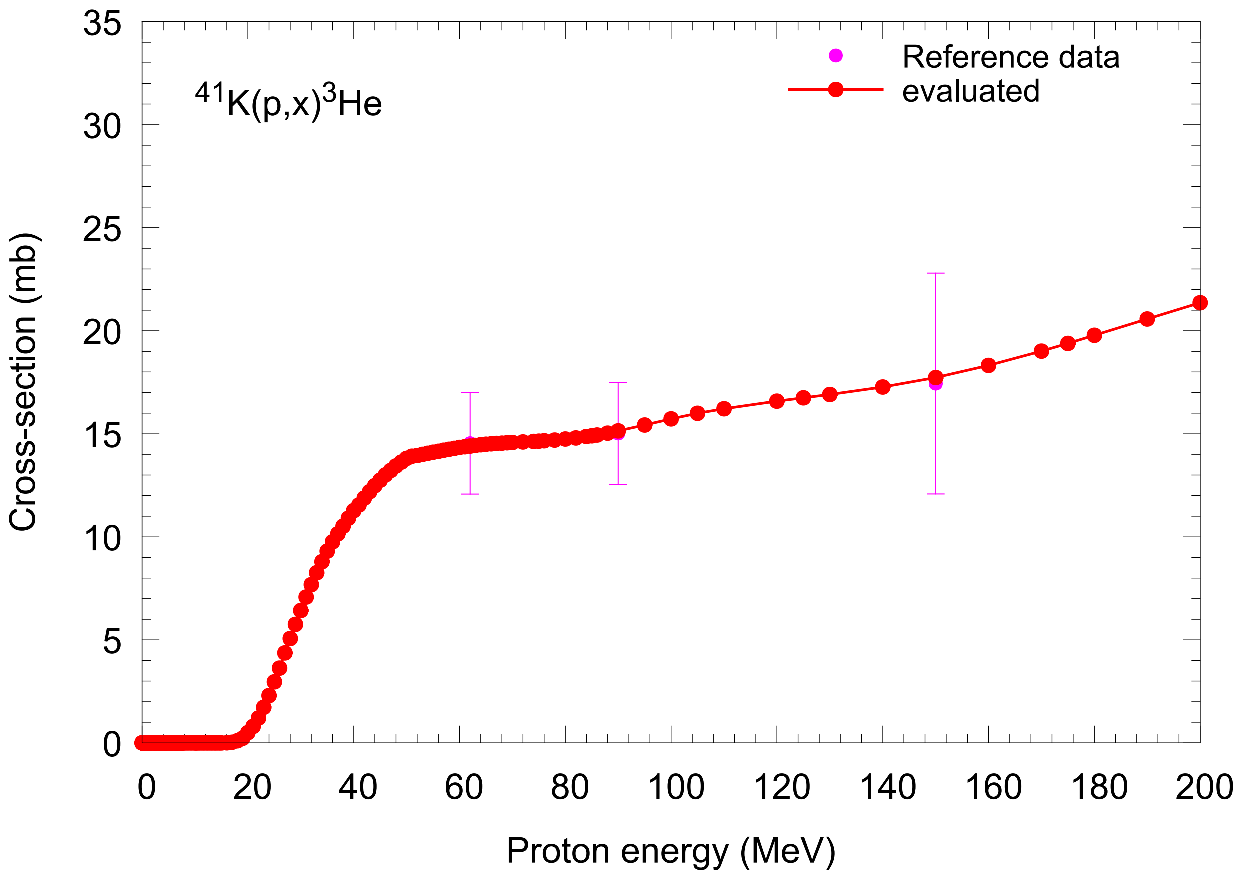

$^{41}K(p,x)^{3}He$
Reference data
evaluated
Cross-section (mb)
Proton energy (MeV)
0
5
10
15
20
25
30
35
0
20
40
60
80
100
120
140
160
180
200

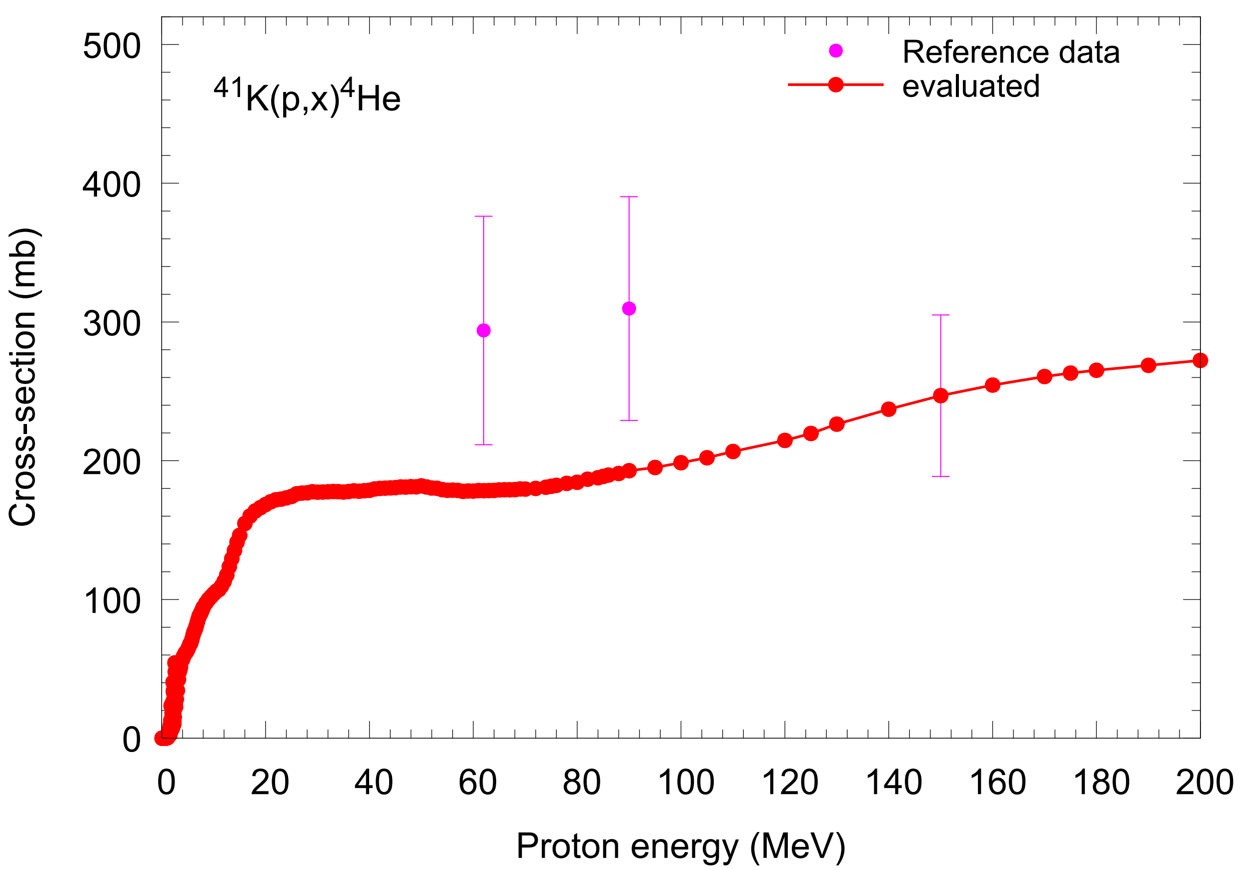

$^{41}K(p,x)^{4}He$
Reference data
evaluated
Cross-section (mb)
Proton energy (MeV)
0
100
200
300
400
500
0
20
40
60
80
100
120
140
160
180
200

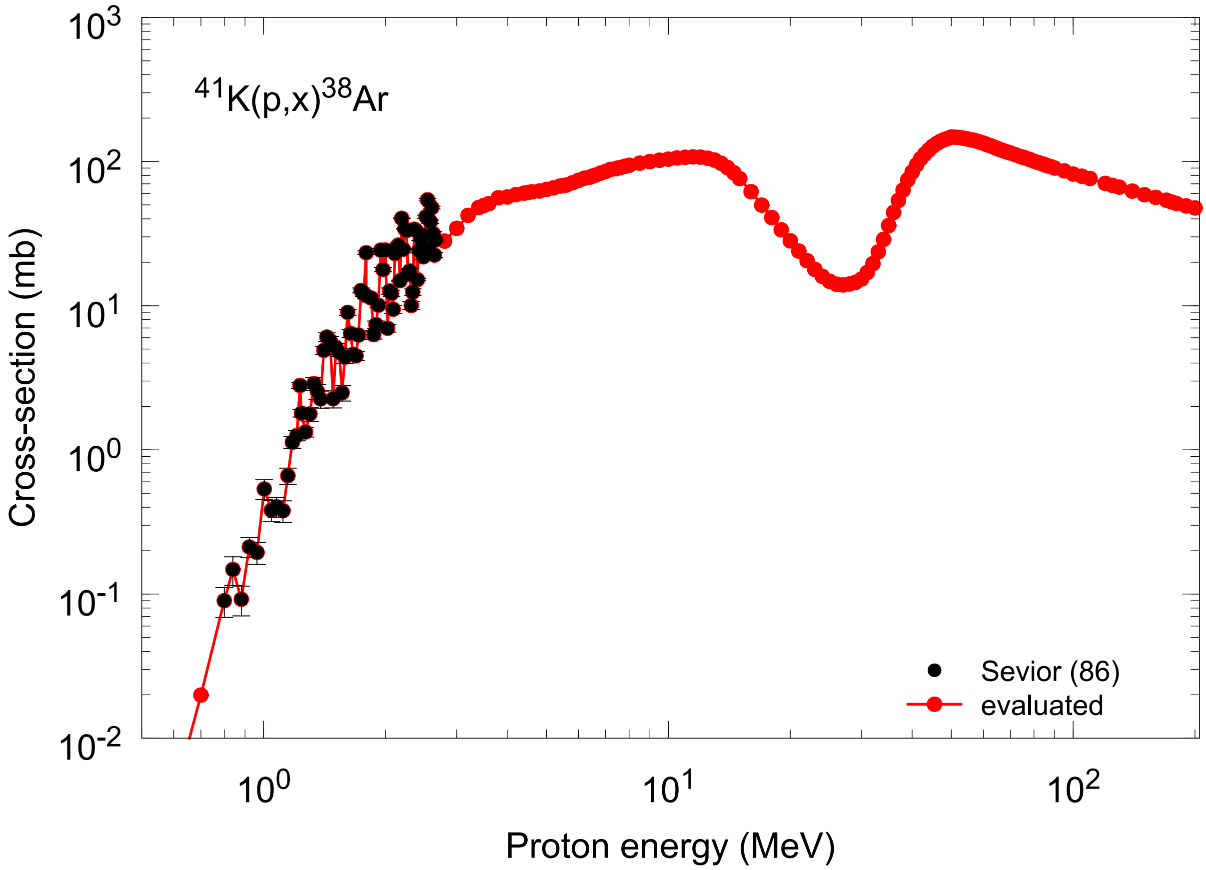

$^{41}K(p,x)^{38}Ar$
Cross-section (mb)
Proton energy (MeV)
Sevior (86)
evaluated

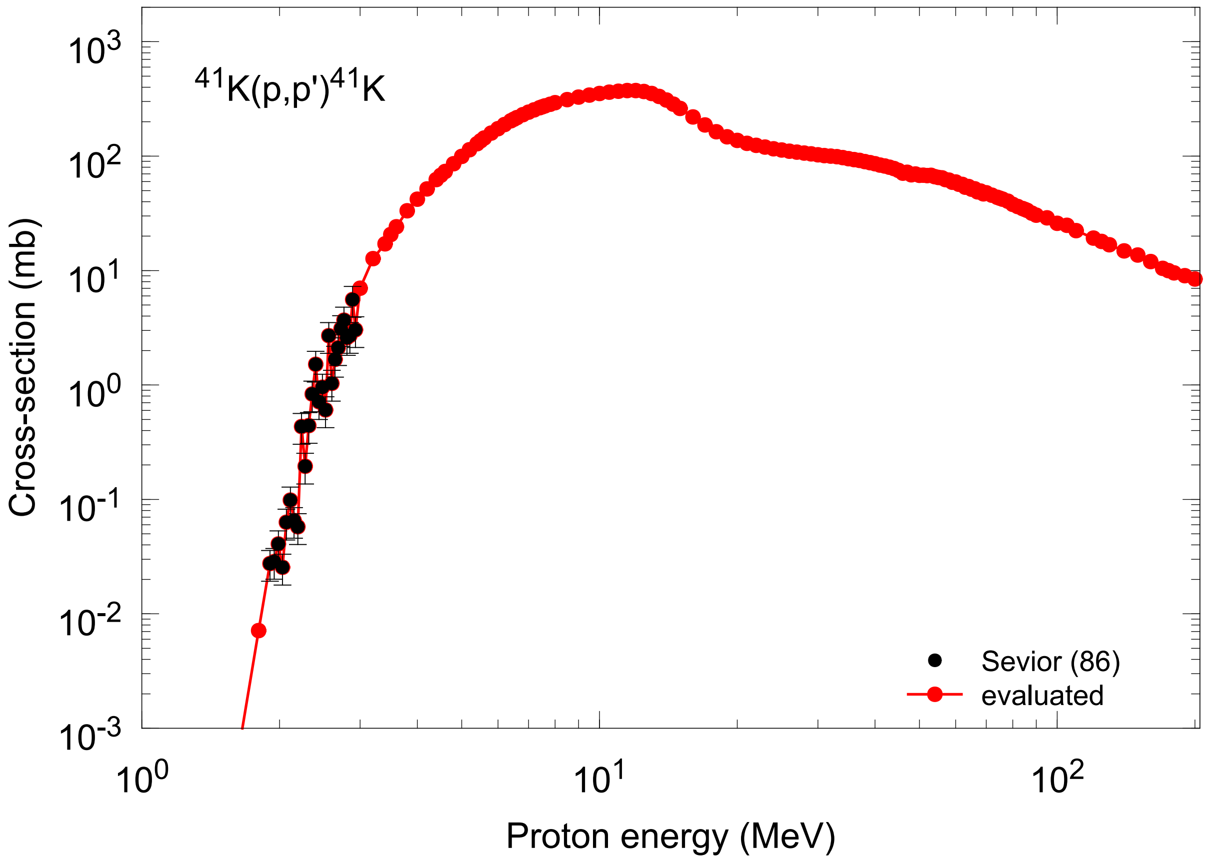

$^{41}K(p,p')^{41}K$
Cross-section (mb)
Proton energy (MeV)
Sevior (86)
evaluated

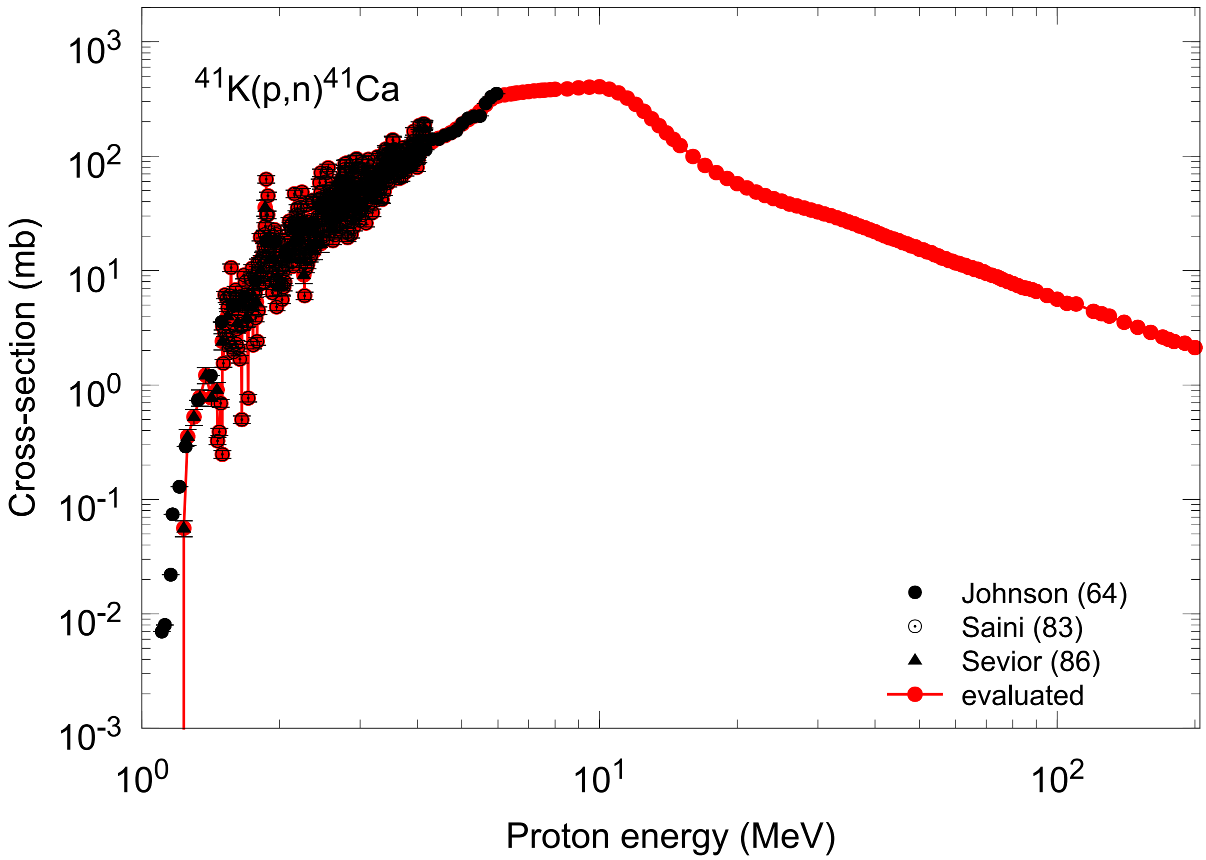
$^{41}K(p,n)^{41}Ca$
Johnson (64)
Saini (83)
Sevior (86)
evaluated
Cross-section (mb)
Proton energy (MeV)

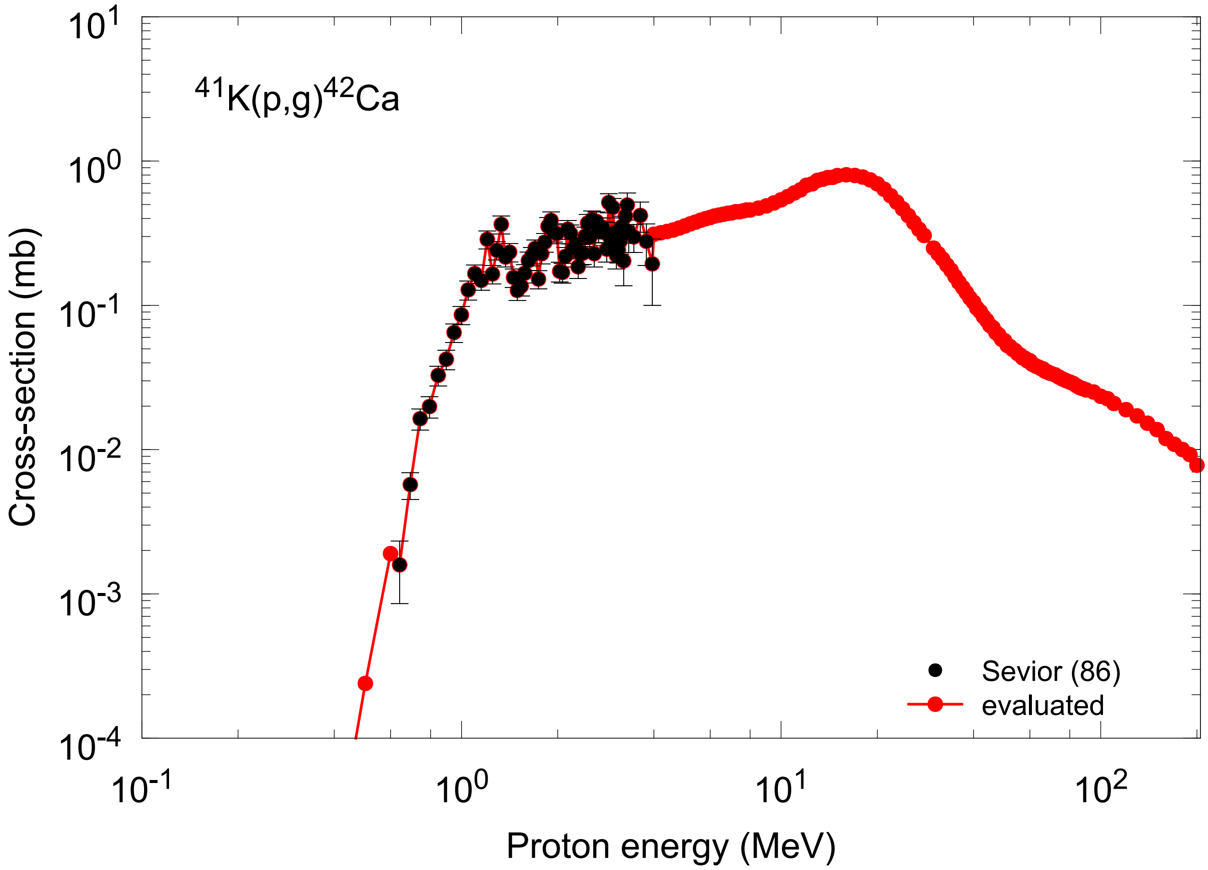
$^{41}K(p,g)^{42}Ca$
Sevior (86)
evaluated
Cross-section (mb)
Proton energy (MeV)

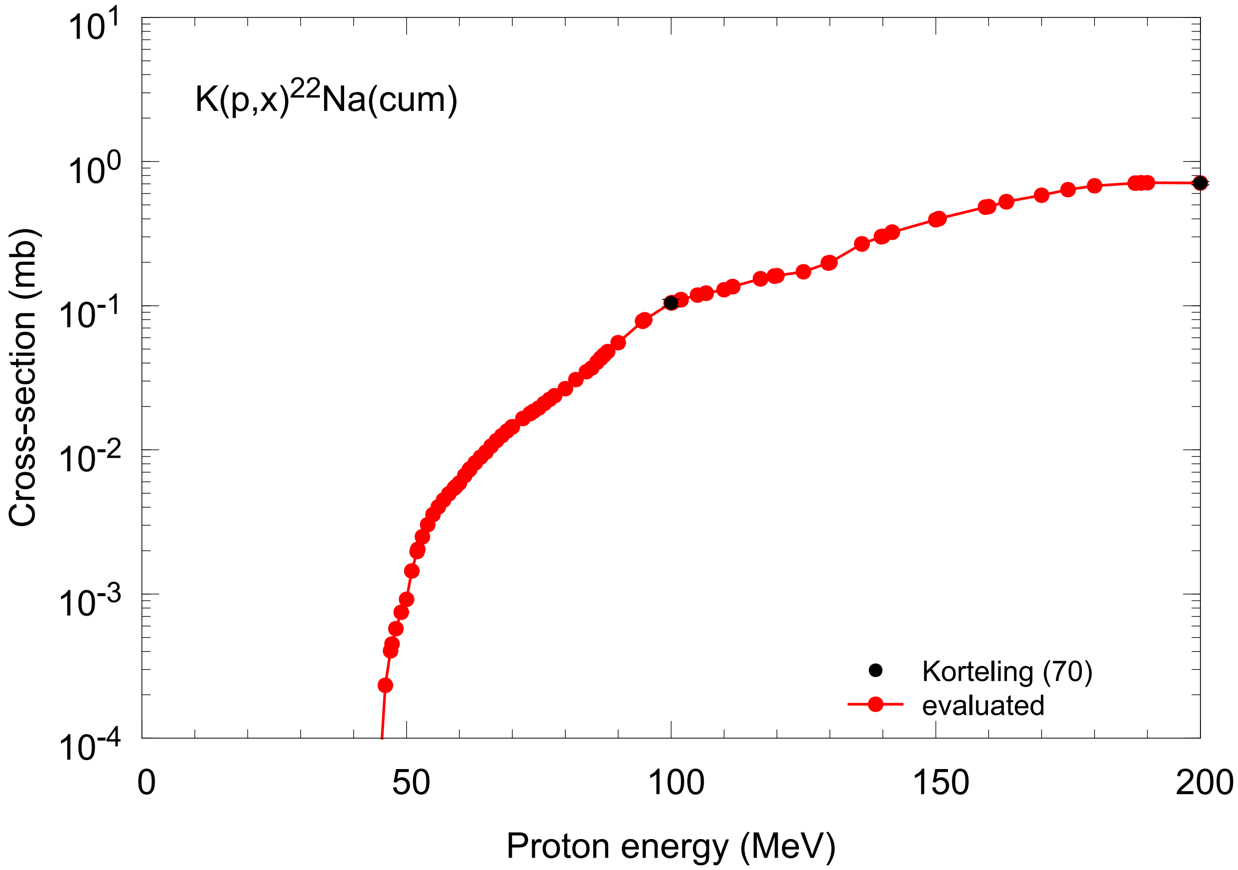

K(p,x)^{22}Na(cum)
Cross-section (mb)
Proton energy (MeV)
Korteling (70)
evaluated

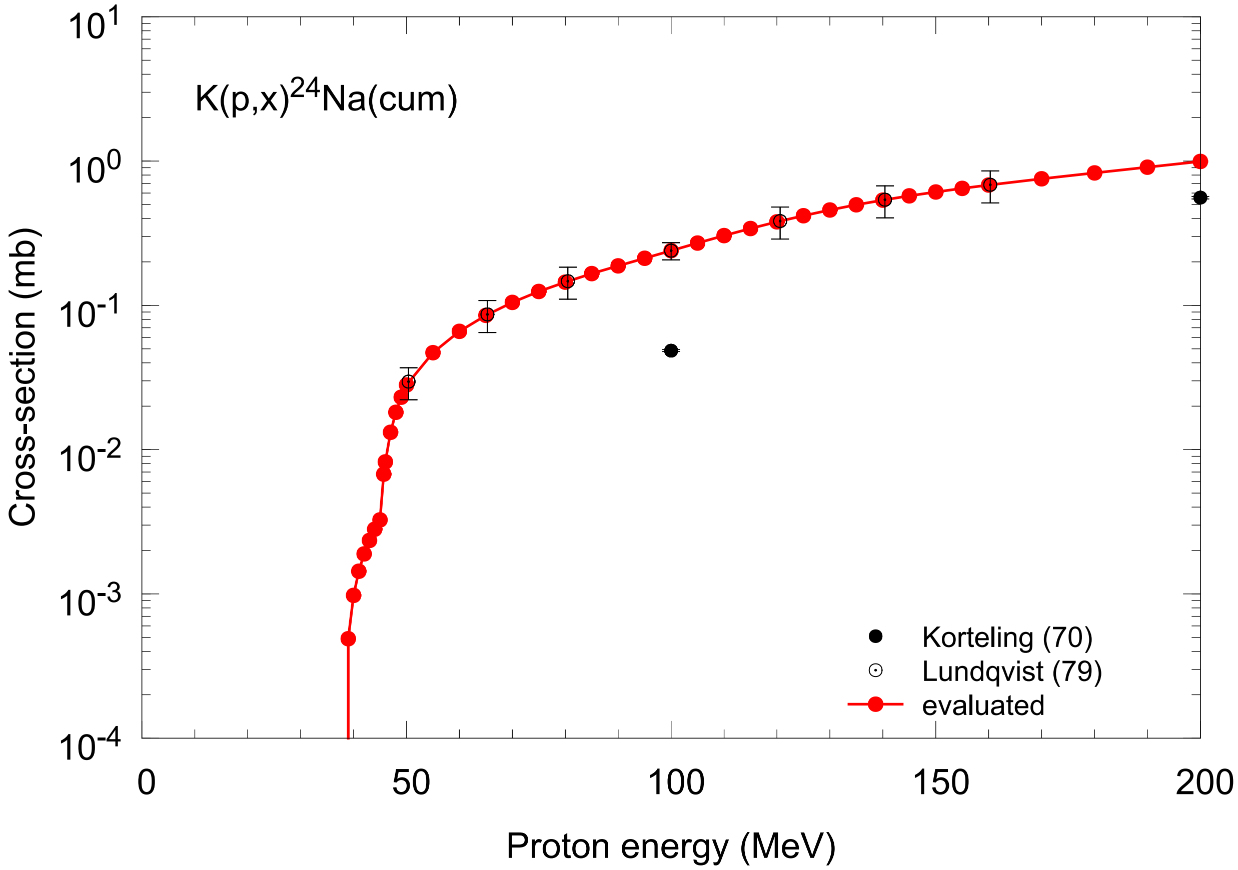

K(p,x)^{24}Na(cum)
Cross-section (mb)
Proton energy (MeV)
Korteling (70)
Lundqvist (79)
evaluated

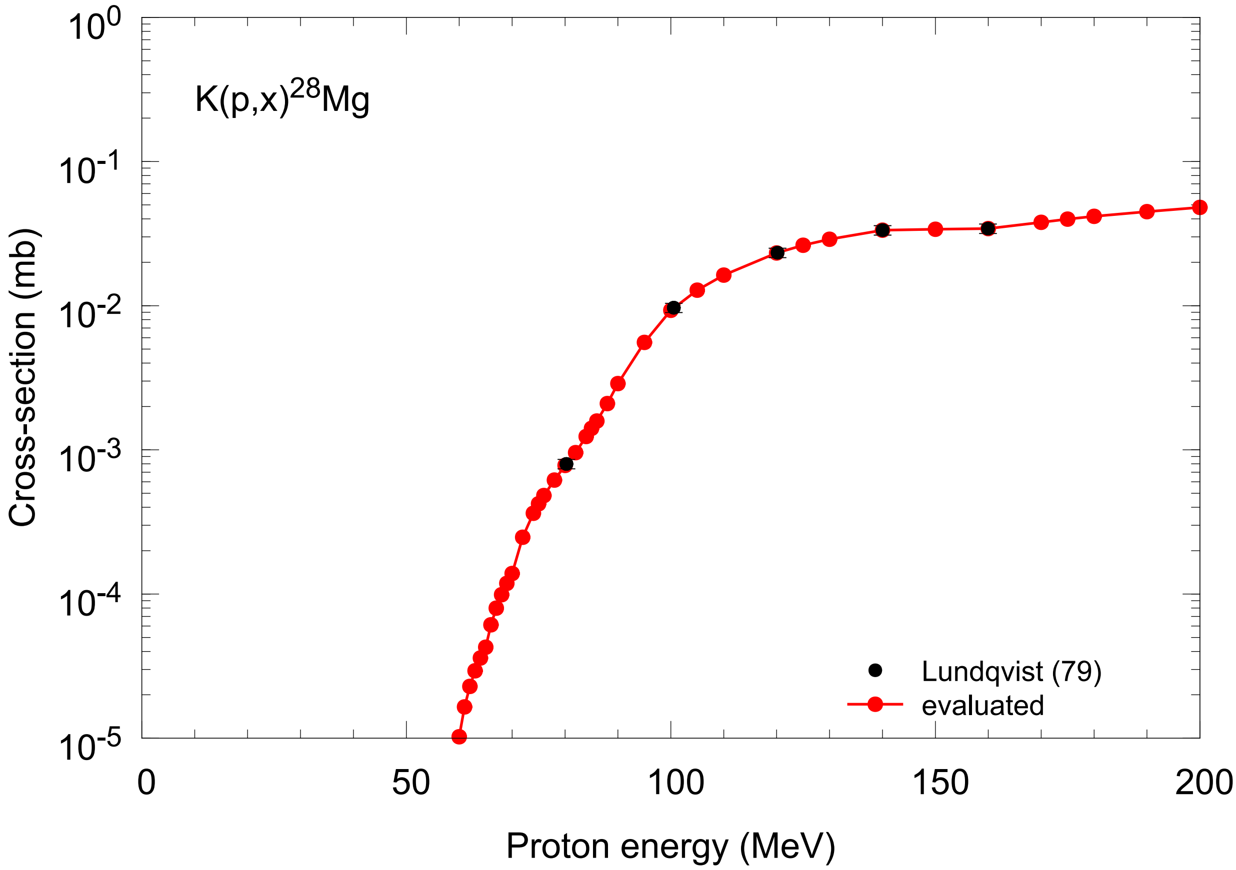

K(p,x)^{28}Mg
Cross-section (mb)
Proton energy (MeV)
Lundqvist (79)
evaluated

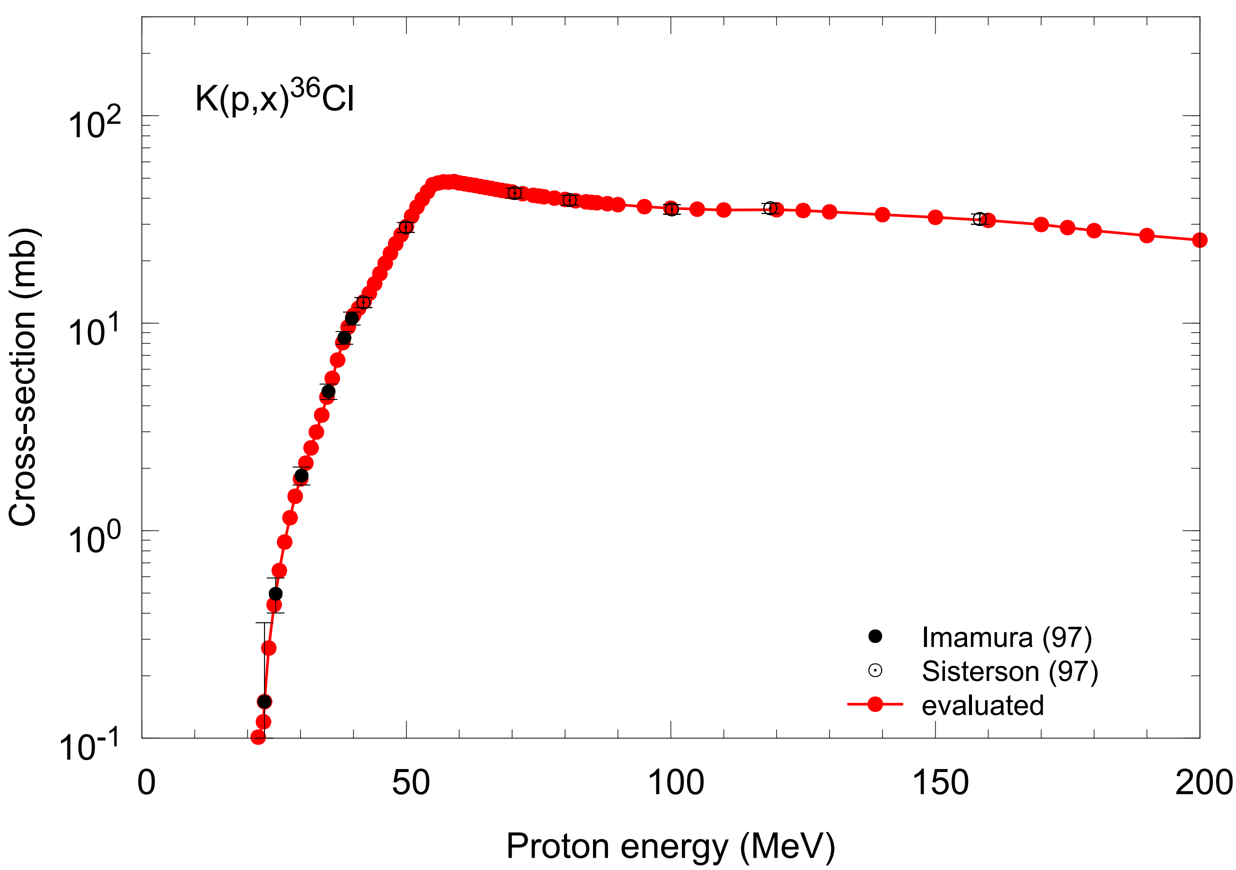

K(p,x)^{36}Cl
Cross-section (mb)
Proton energy (MeV)
Imamura (97)
Sisterson (97)
evaluated

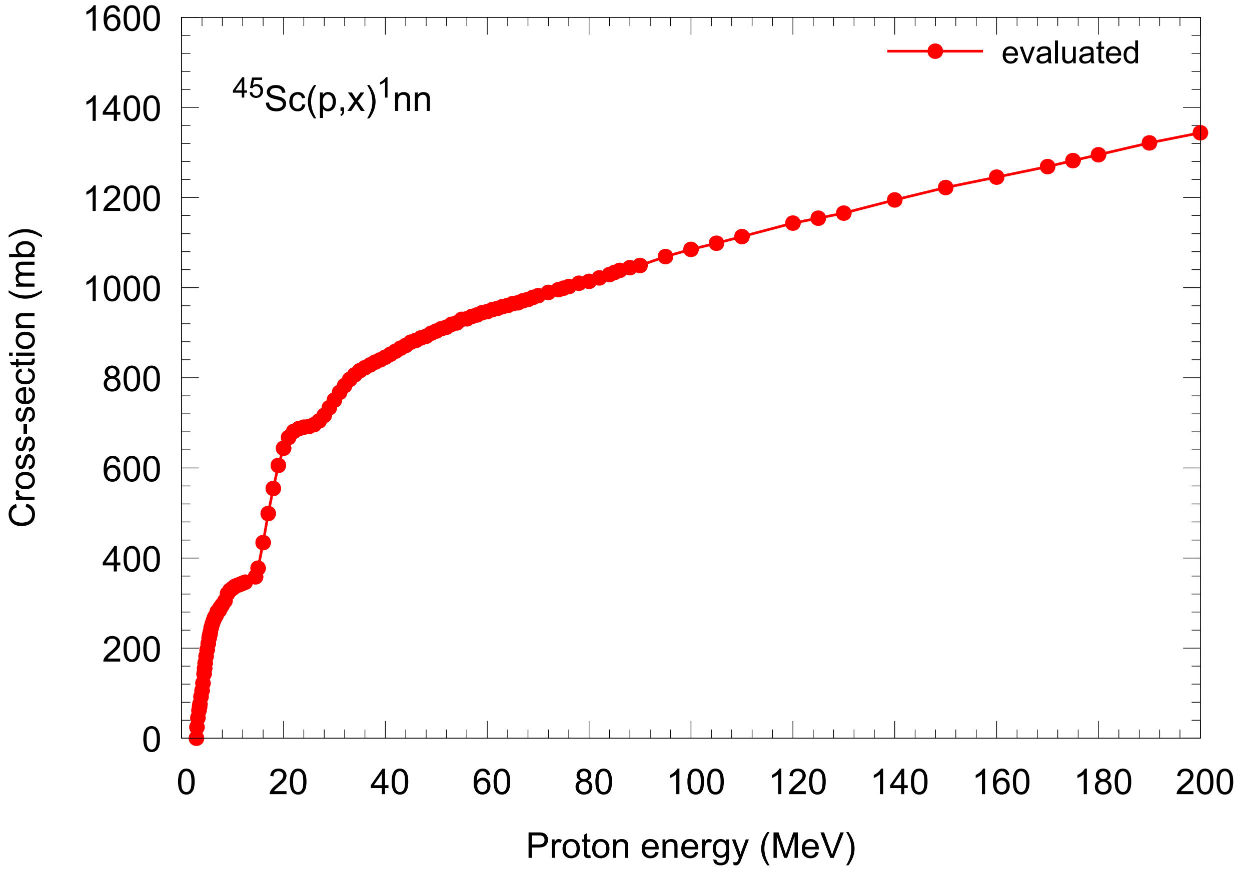

$^{45}Sc(p,x)^{1}nn$
evaluated
Cross-section (mb)
Proton energy (MeV)
0
200
400
600
800
1000
1200
1400
1600
0
20
40
60
80
100
120
140
160
180
200

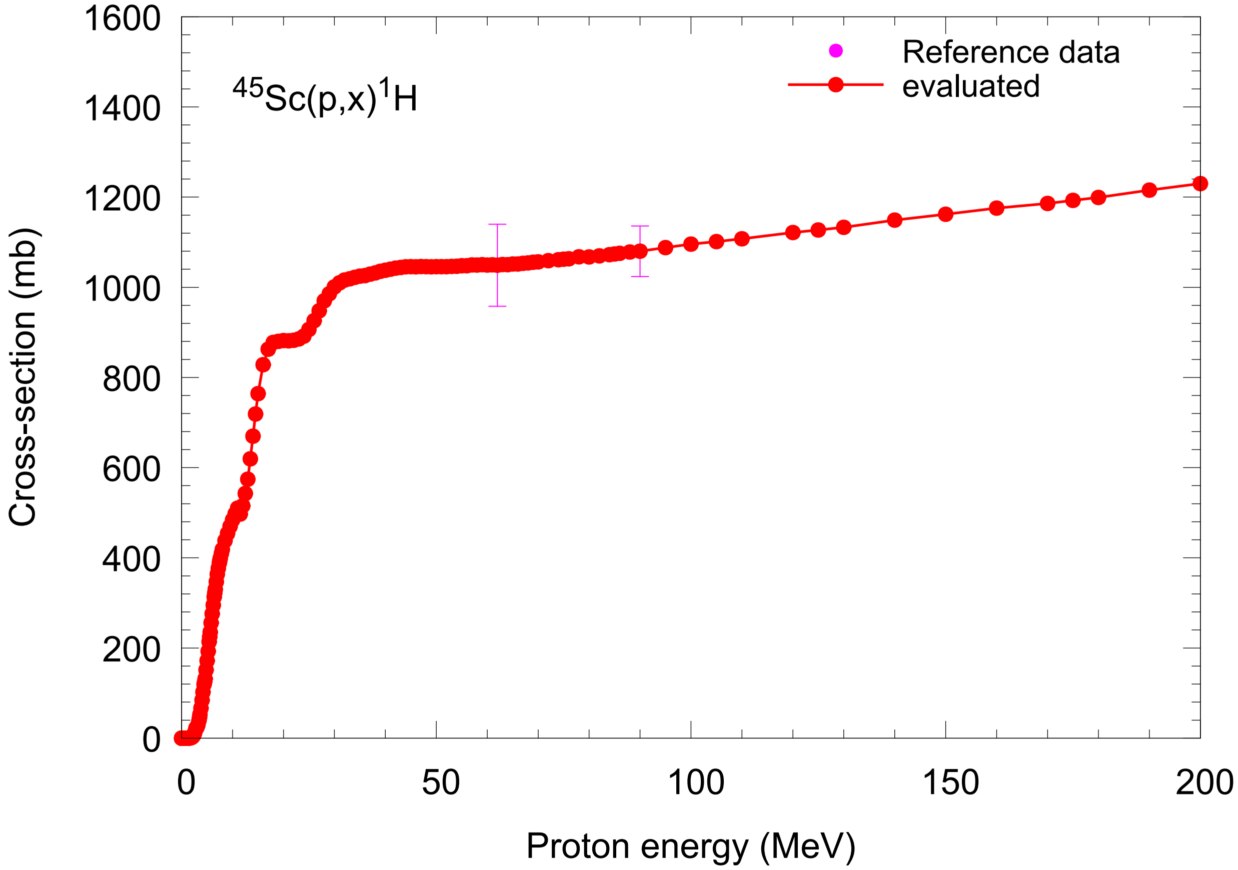

$^{45}Sc(p,x)^{1}H$
Reference data
evaluated
Cross-section (mb)
Proton energy (MeV)
0
200
400
600
800
1000
1200
1400
1600
0
50
100
150
200

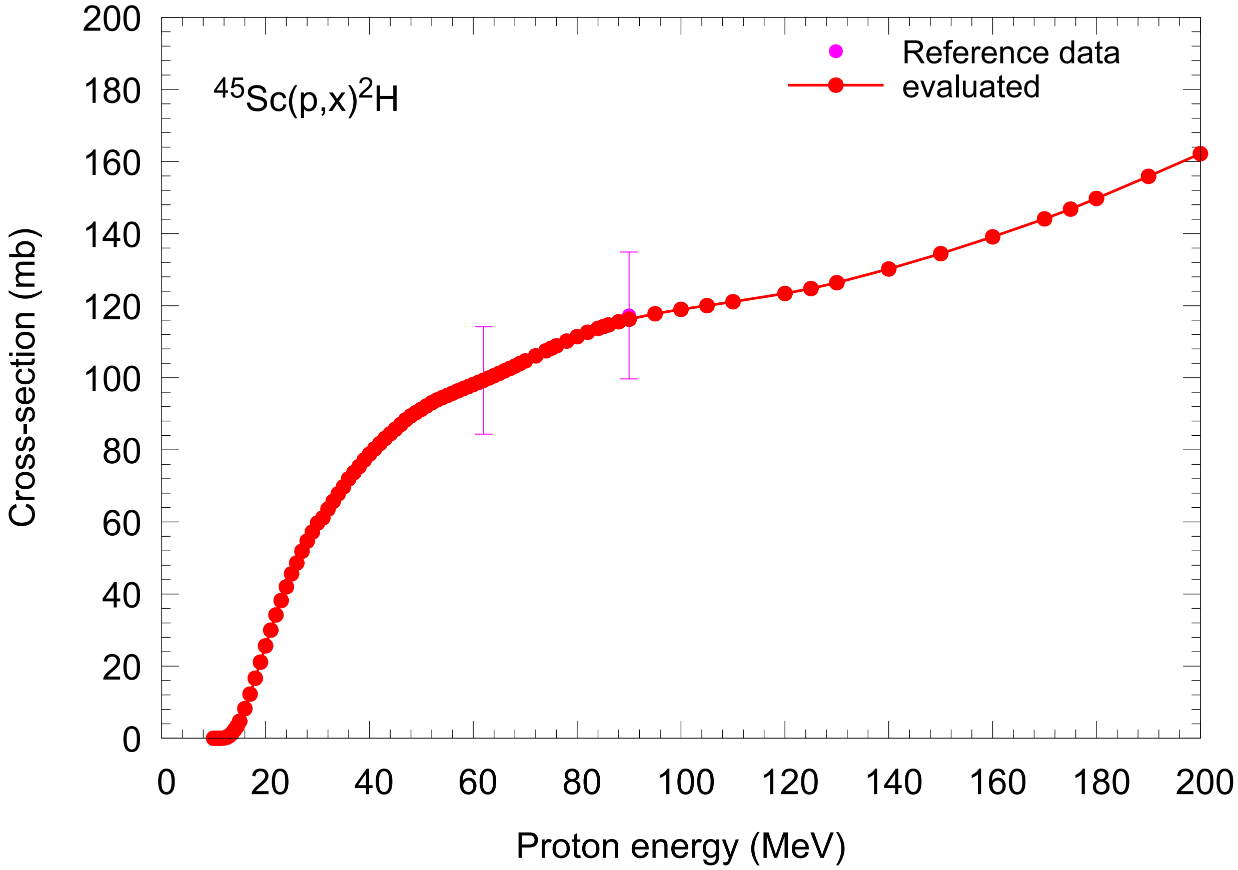

$^{45}Sc(p,x)^{2}H$
Reference data
evaluated
Cross-section (mb)
Proton energy (MeV)
0
20
40
60
80
100
120
140
160
180
200

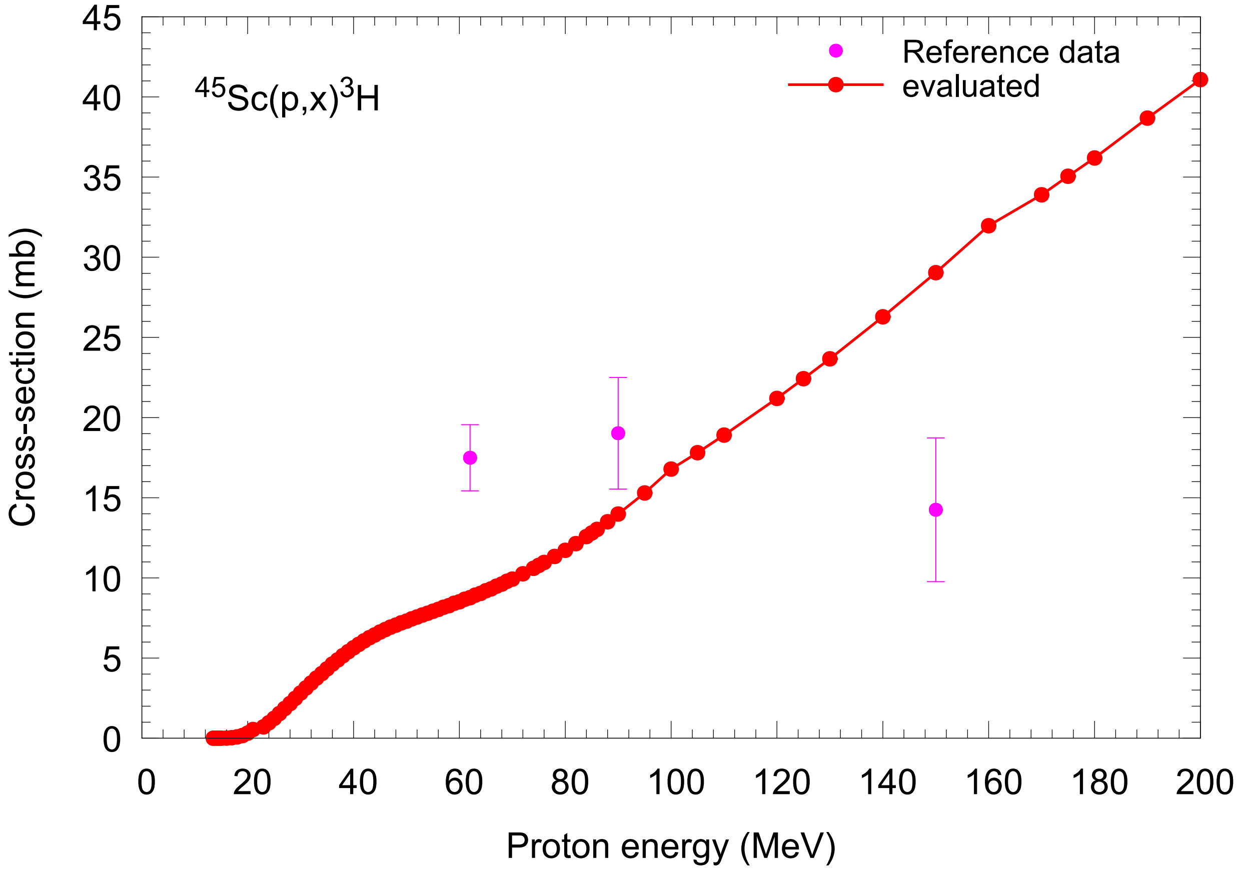

$^{45}Sc(p,x)^{3}H$
Reference data
evaluated
Cross-section (mb)
Proton energy (MeV)
0
5
10
15
20
25
30
35
40
45
0
20
40
60
80
100
120
140
160
180
200

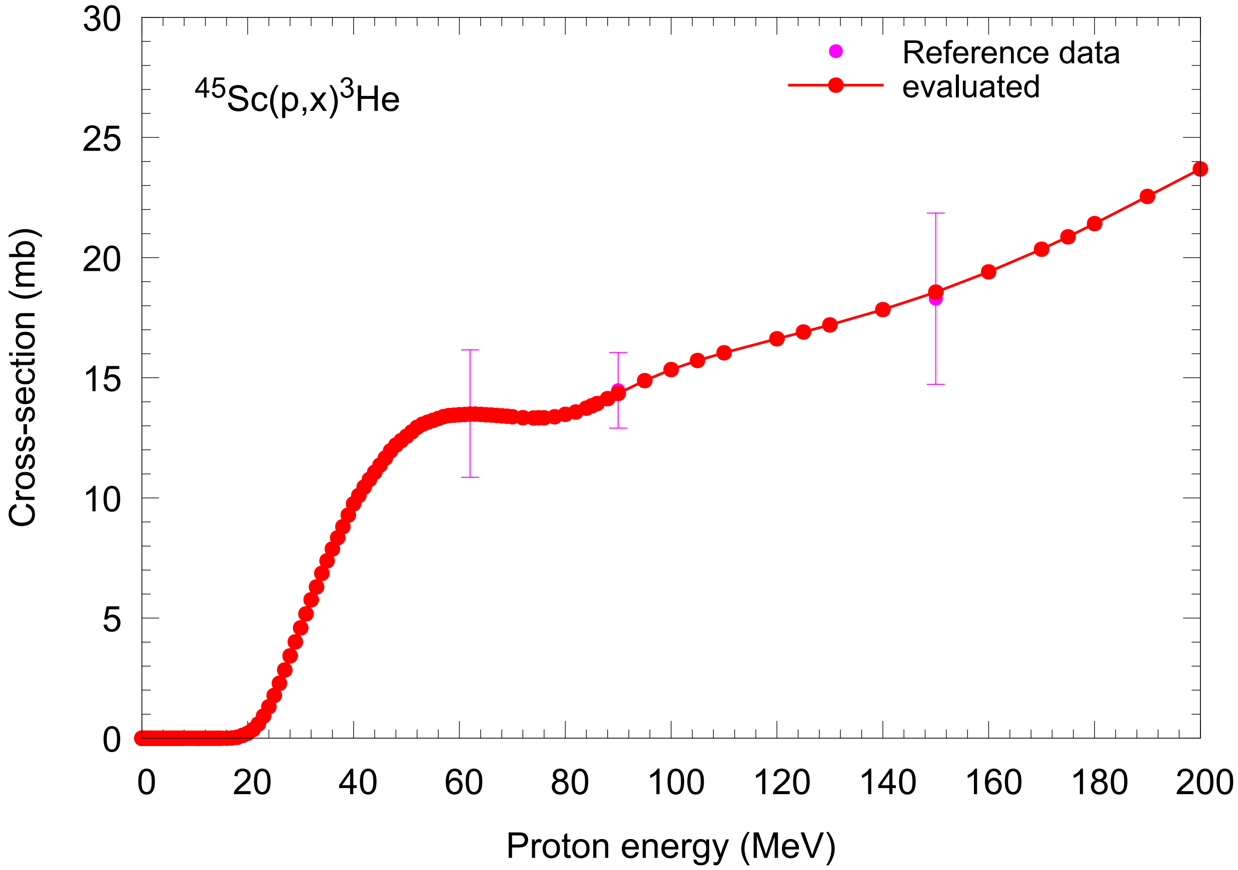
$^{45}Sc(p,x)^{3}He$
Reference data
evaluated
Cross-section (mb)
Proton energy (MeV)
0
5
10
15
20
25
30
0
20
40
60
80
100
120
140
160
180
200

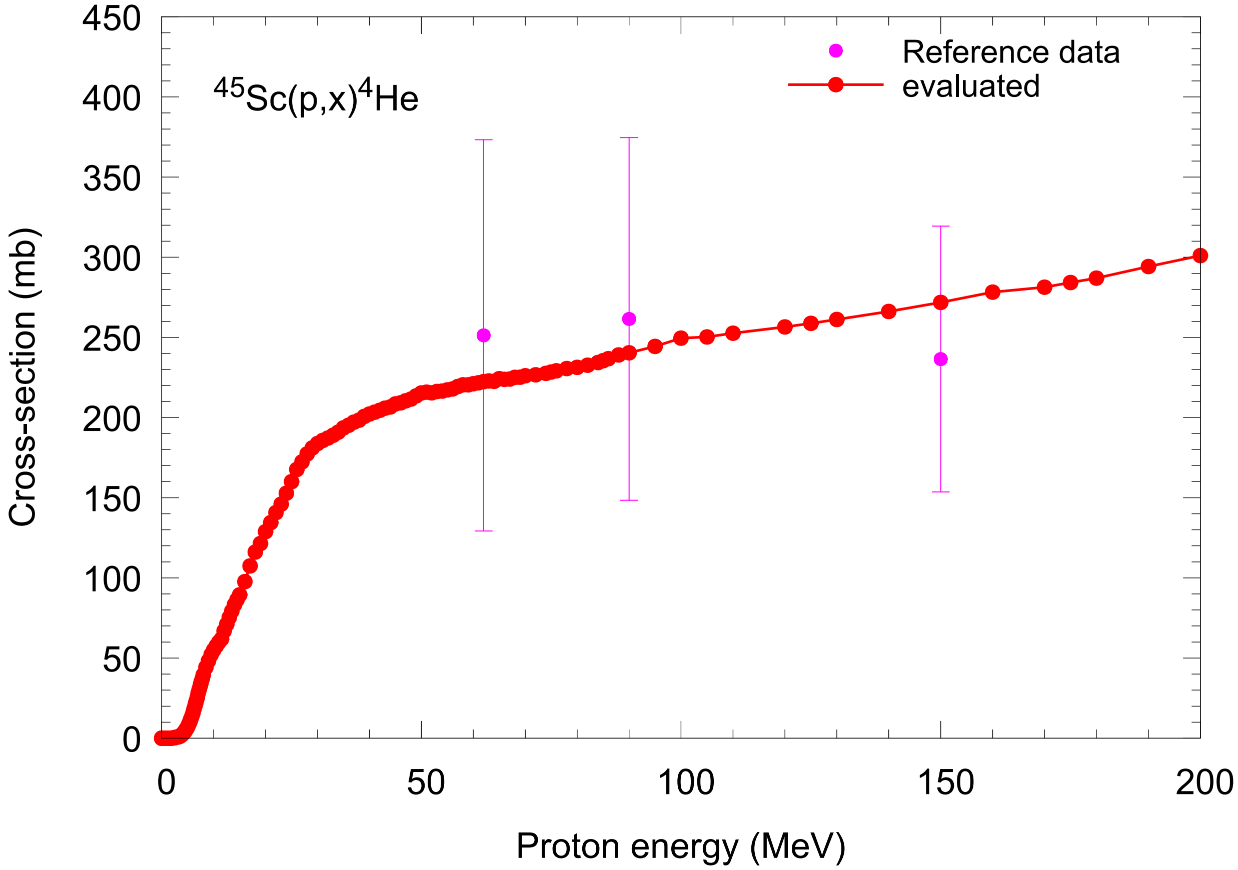
$^{45}Sc(p,x)^{4}He$
Reference data
evaluated
Cross-section (mb)
Proton energy (MeV)
0
50
100
150
200
250
300
350
400
450
0
50
100
150
200

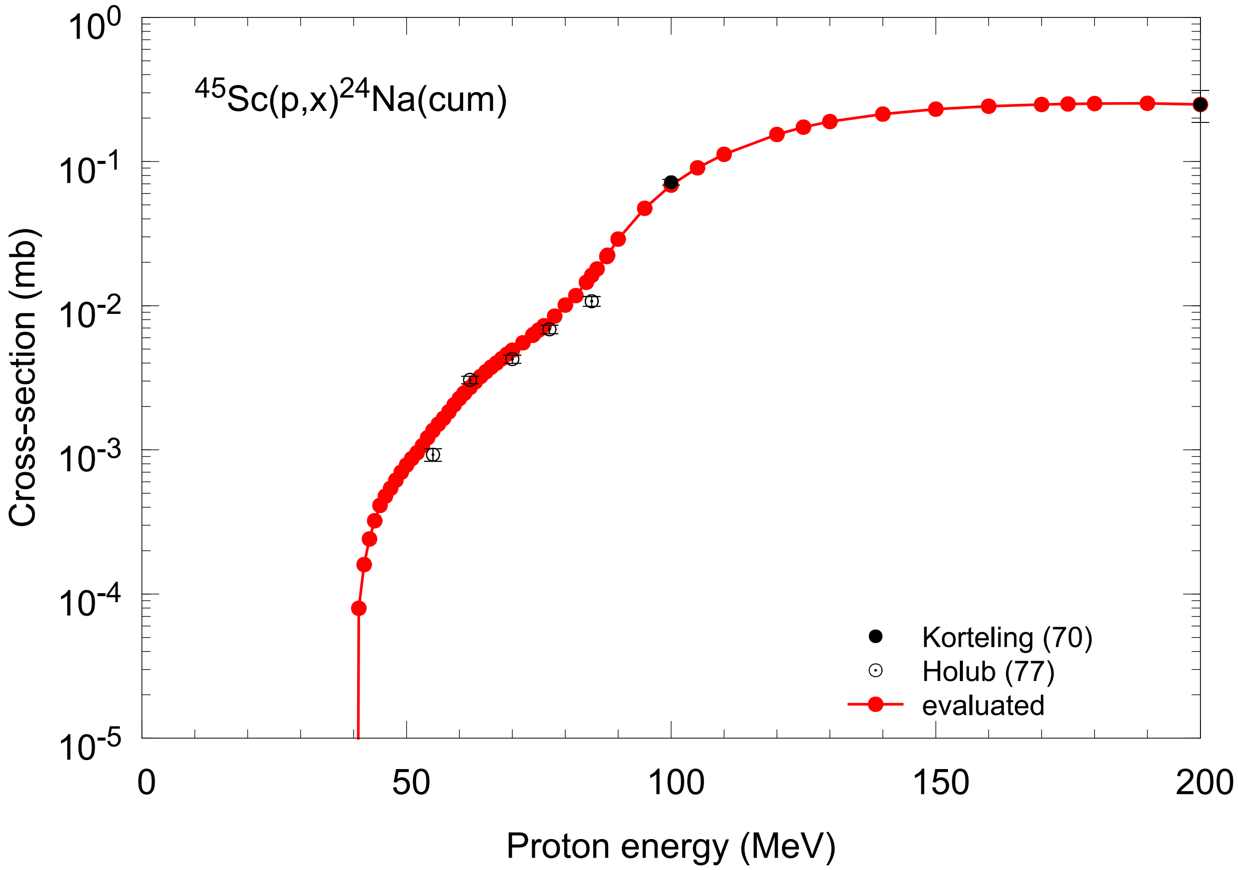

$^{45}Sc(p,x)^{24}Na(cum)$
Cross-section (mb)
Proton energy (MeV)
Korteling (70)
Holub (77)
evaluated

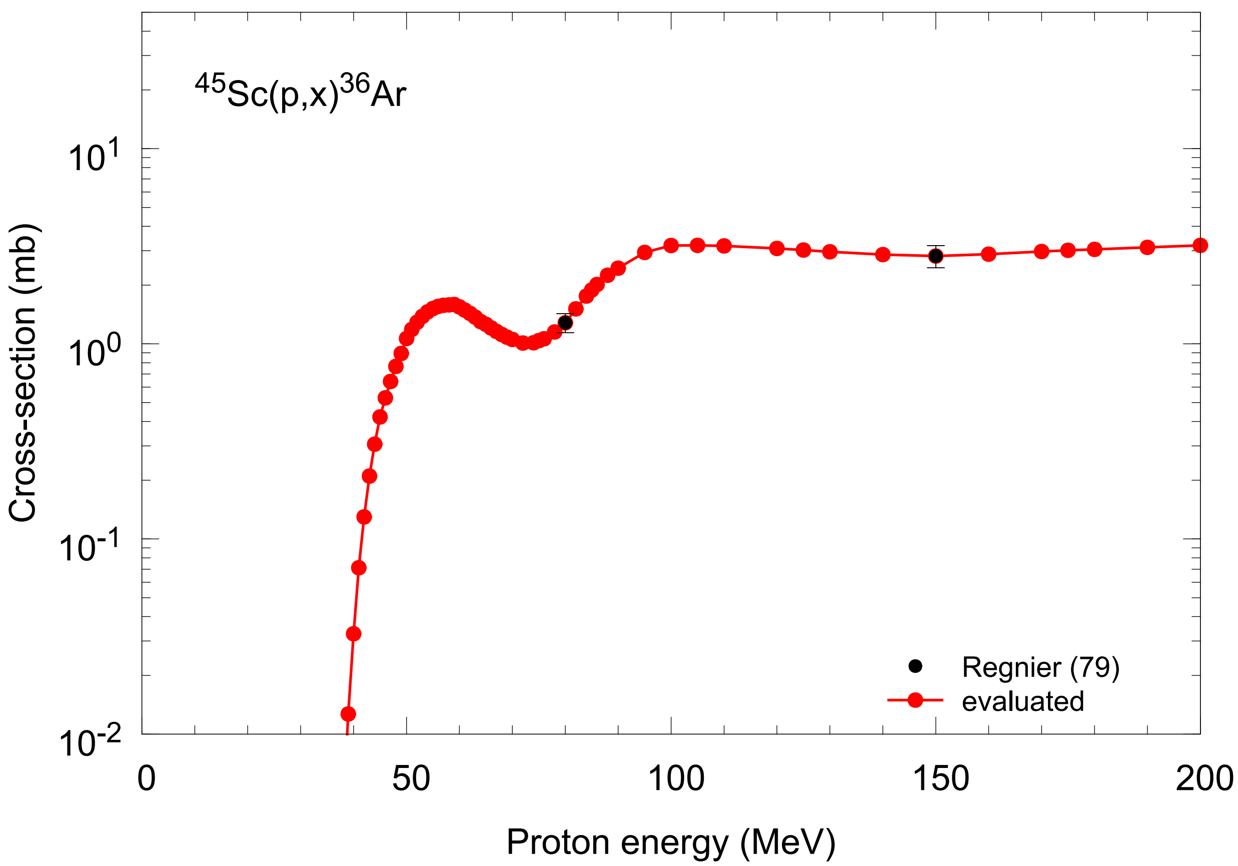

$^{45}Sc(p,x)^{36}Ar$
Cross-section (mb)
Proton energy (MeV)
Regnier (79)
evaluated

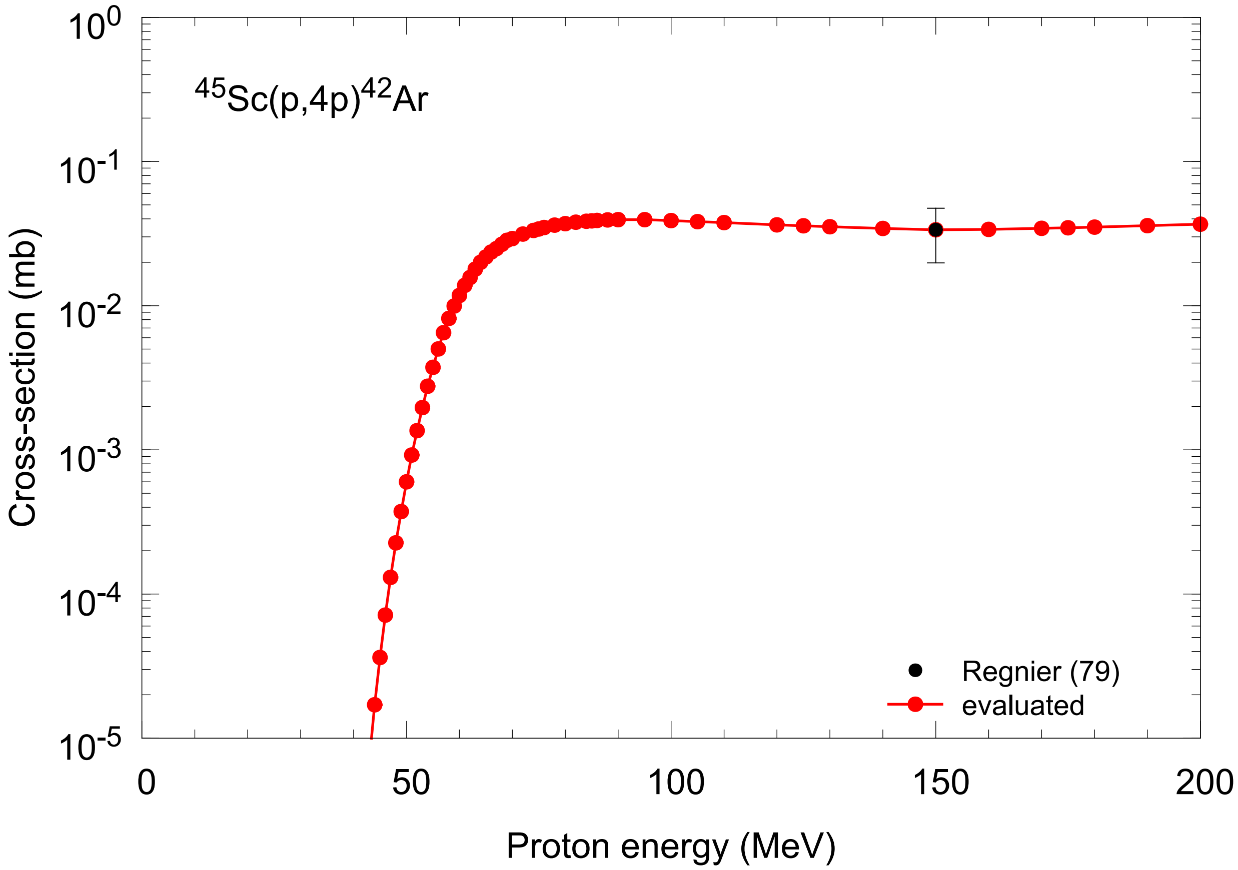
$^{45}Sc(p,4p)^{42}Ar$
Cross-section (mb)
10^{0}
10^{-1}
10^{-2}
10^{-3}
10^{-4}
10^{-5}
0
50
100
150
200
Proton energy (MeV)
Regnier (79)
evaluated

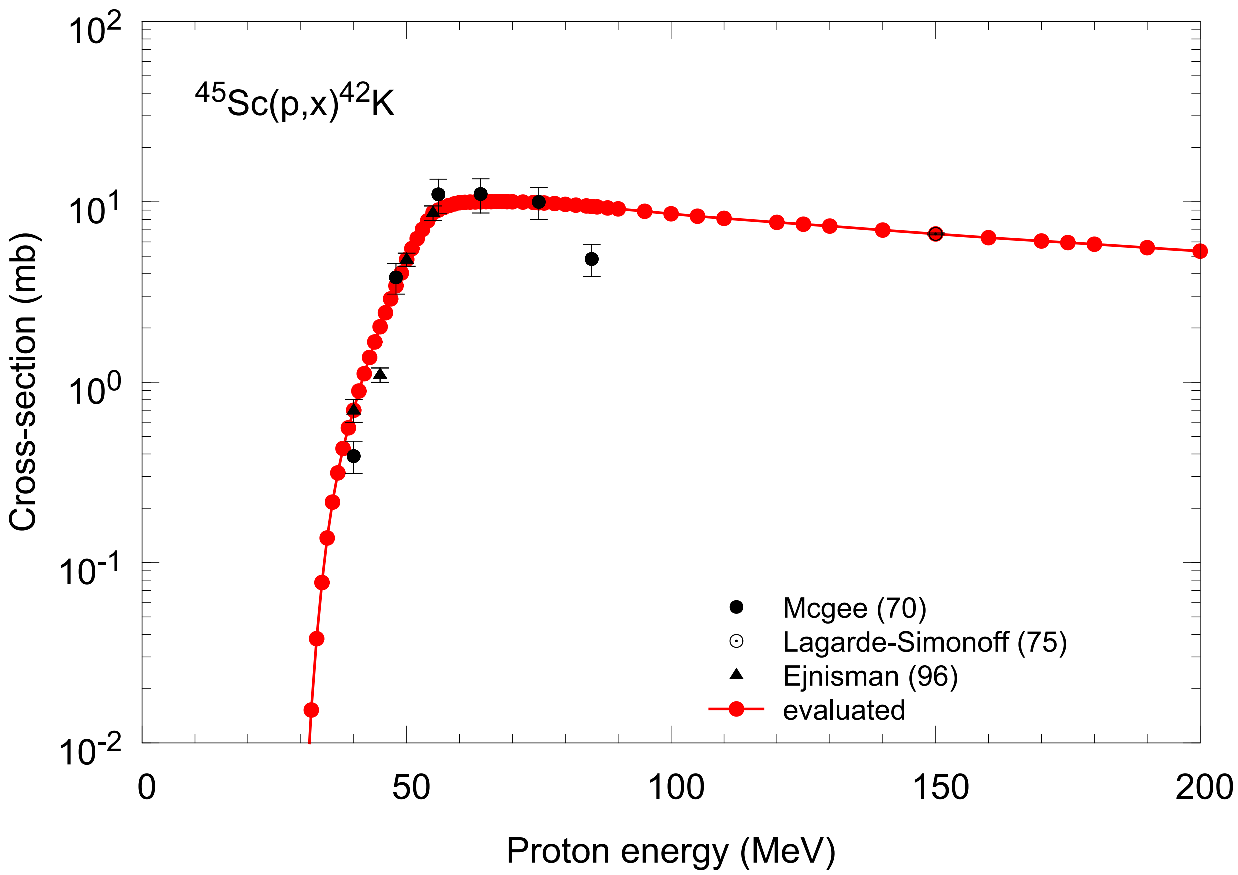
$^{45}Sc(p,x)^{42}K$
Cross-section (mb)
10^{2}
10^{1}
10^{0}
10^{-1}
10^{-2}
0
50
100
150
200
Proton energy (MeV)
Mcgee (70)
Lagarde-Simonoff (75)
Ejnisman (96)
evaluated

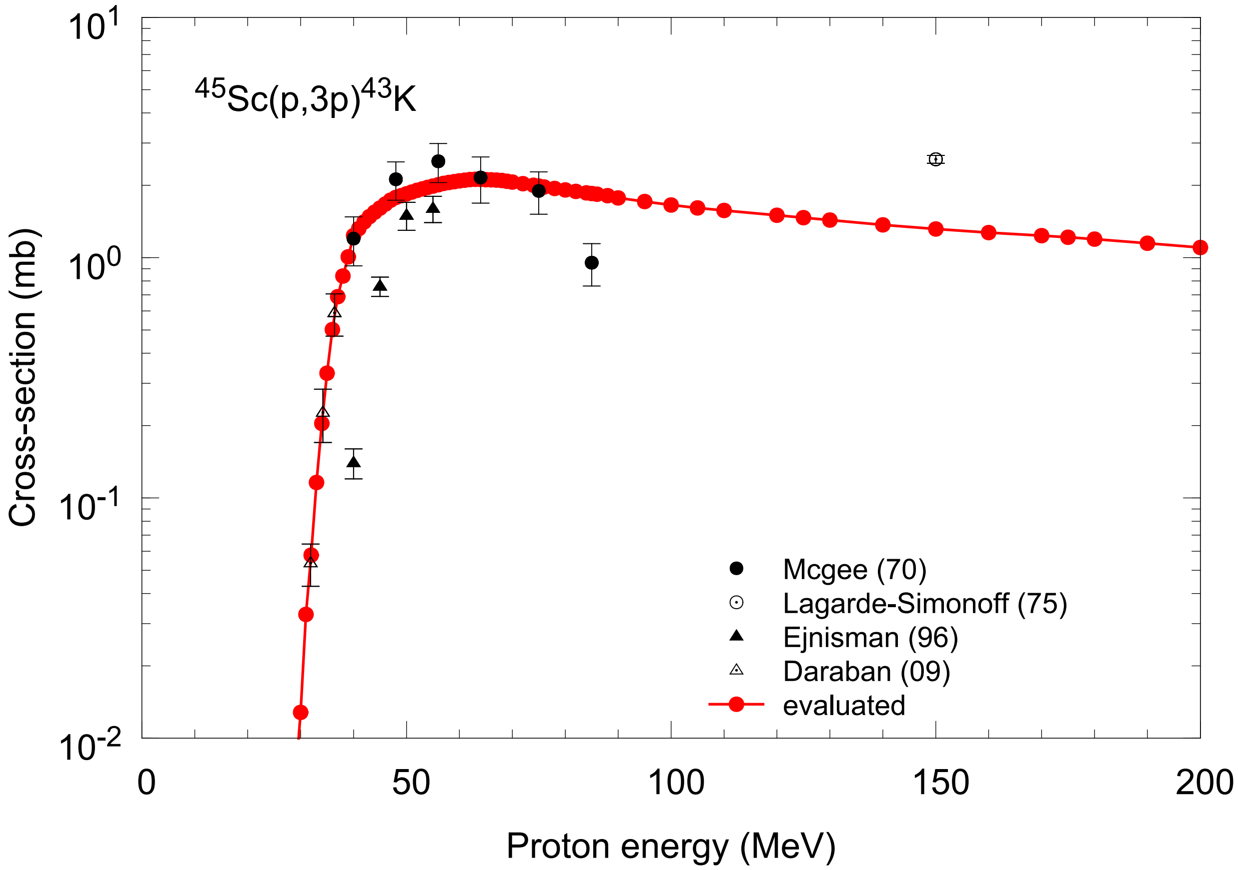

45Sc(p,3p)43K
Cross-section (mb)
Proton energy (MeV)
Mcgee (70)
Lagarde-Simonoff (75)
Ejnisman (96)
Daraban (09)
evaluated

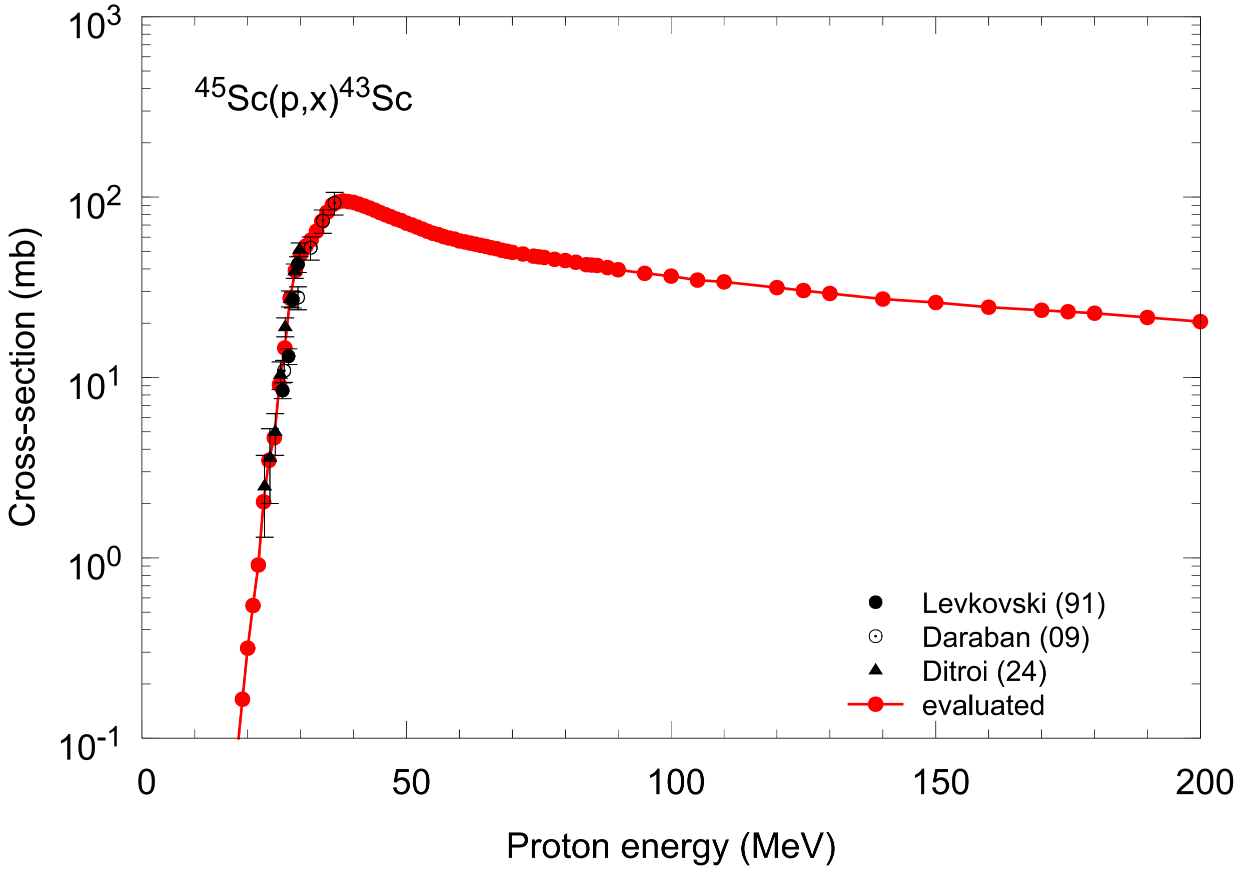

45Sc(p,x)43Sc
Cross-section (mb)
Proton energy (MeV)
Levkovski (91)
Daraban (09)
Ditroi (24)
evaluated

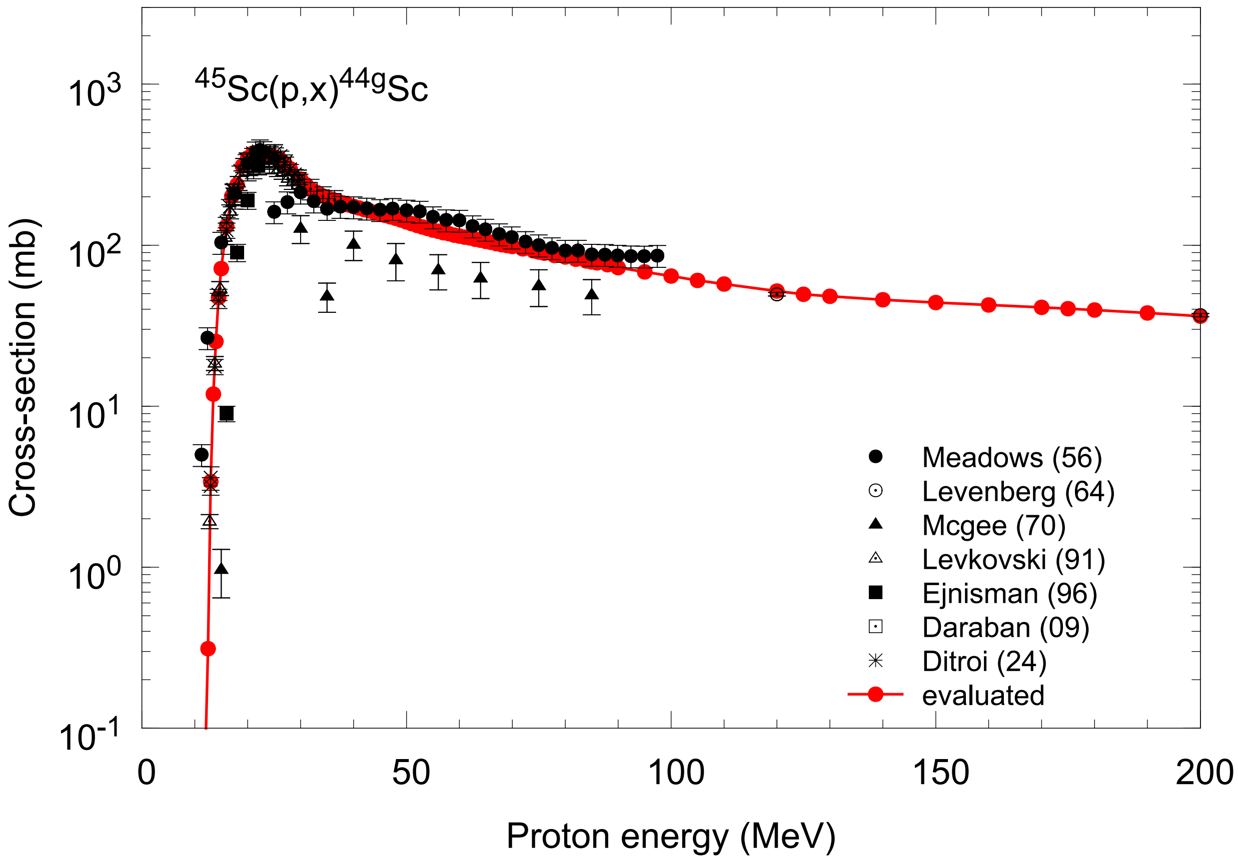

$^{45}Sc(p,x)^{44g}Sc$
Cross-section (mb)
Proton energy (MeV)
Meadows (56)
Levenberg (64)
Mcgee (70)
Levkovski (91)
Ejnisman (96)
Daraban (09)
Ditroi (24)
evaluated

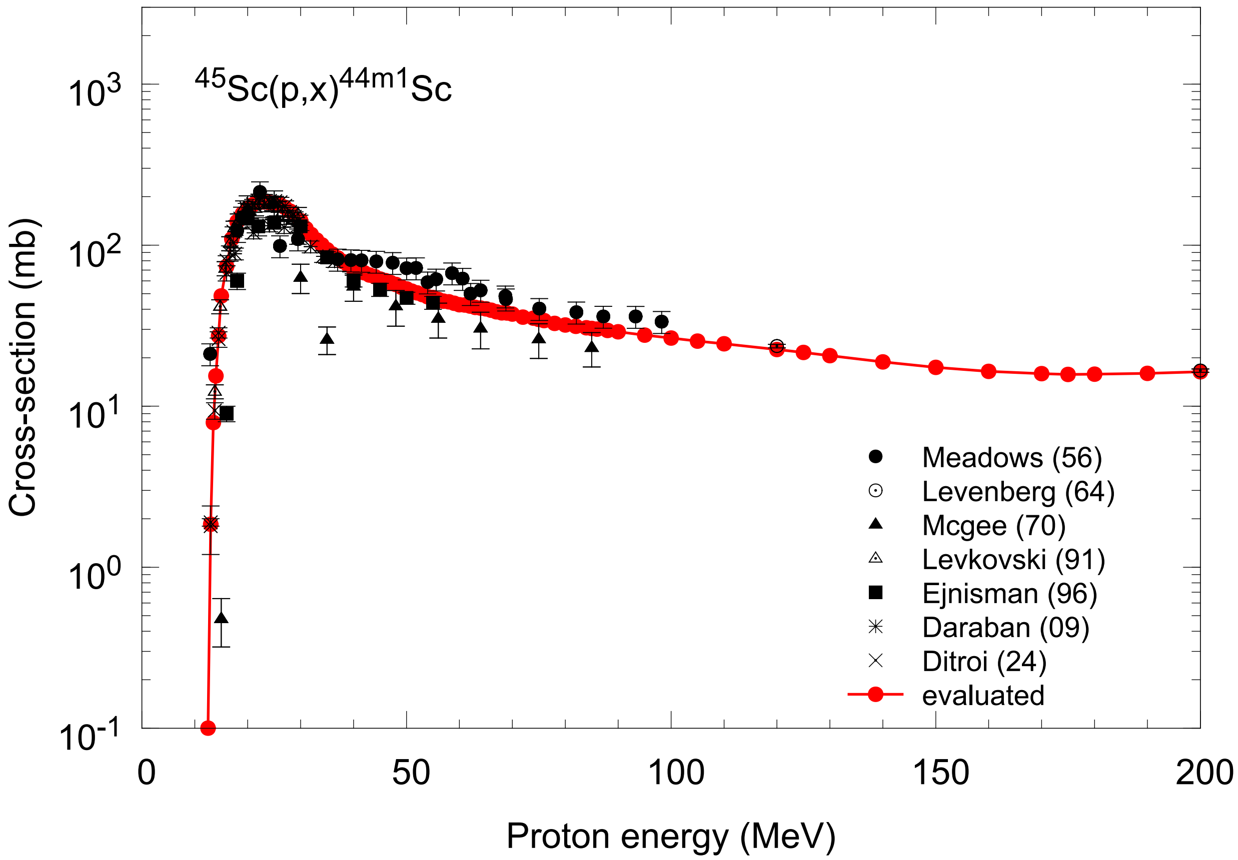

$^{45}Sc(p,x)^{44m1}Sc$
Cross-section (mb)
Proton energy (MeV)
Meadows (56)
Levenberg (64)
Mcgee (70)
Levkovski (91)
Ejnisman (96)
Daraban (09)
Ditroi (24)
evaluated

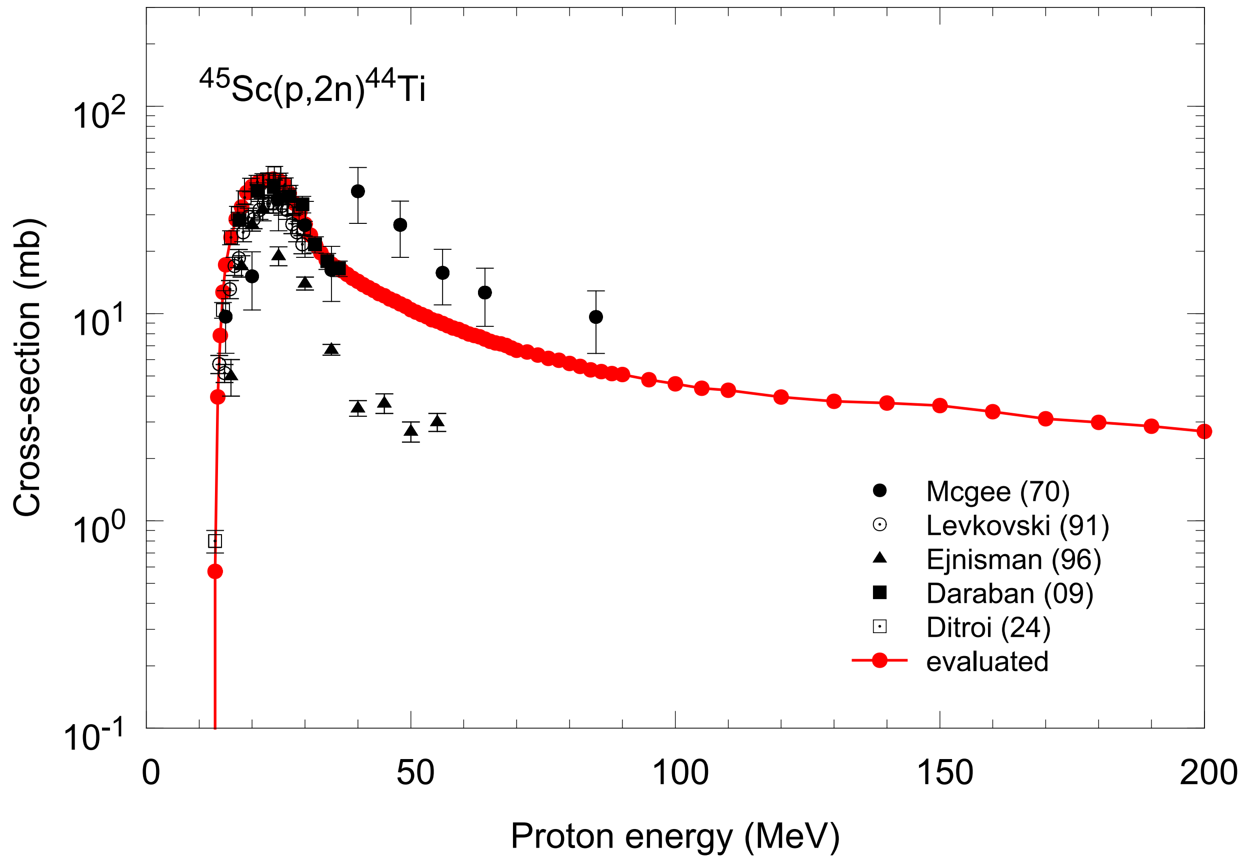

$^{45}Sc(p,2n)^{44}Ti$
Cross-section (mb)
10^2
10^1
10^0
10^{-1}
0
50
100
150
200
Proton energy (MeV)
Mcgee (70)
Levkovski (91)
Ejnisman (96)
Daraban (09)
Ditroi (24)
evaluated

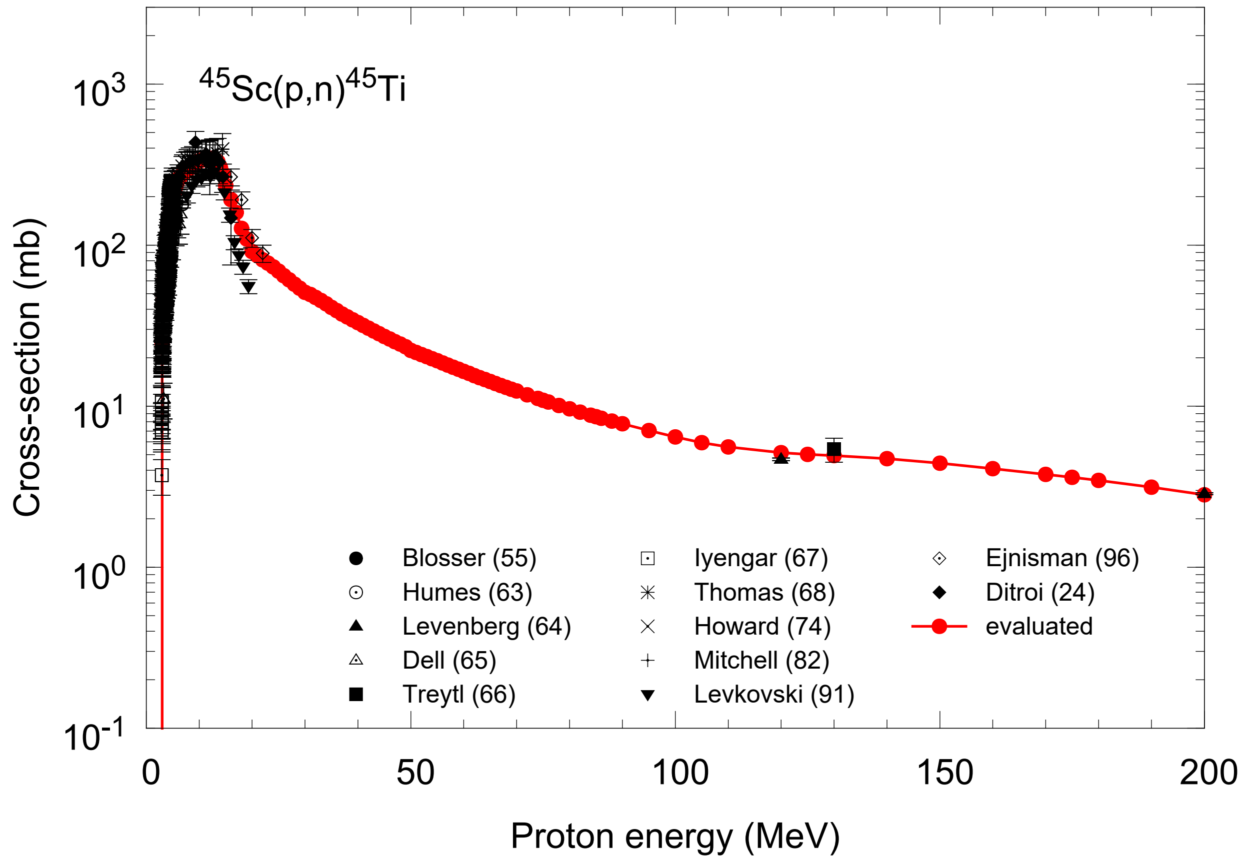

$^{45}Sc(p,n)^{45}Ti$
Cross-section (mb)
10^3
10^2
10^1
10^0
10^{-1}
0
50
100
150
200
Proton energy (MeV)
Blosser (55)
Humes (63)
Levenberg (64)
Dell (65)
Treytl (66)
Iyengar (67)
Thomas (68)
Howard (74)
Mitchell (82)
Levkovski (91)
Ejnisman (96)
Ditroi (24)
evaluated

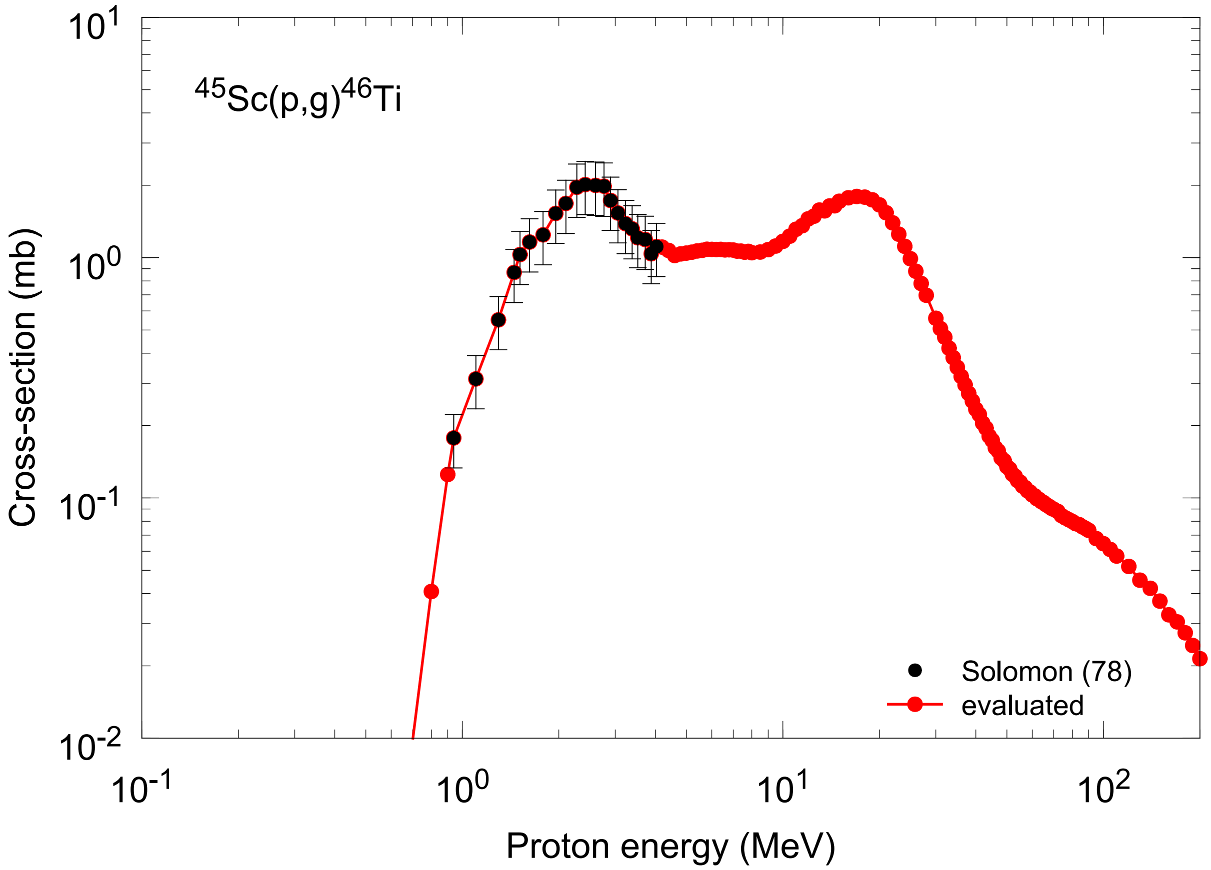

$^{45}Sc(p,g)^{46}Ti$
Cross-section (mb)
10^{1}
10^{0}
10^{-1}
10^{-2}
10^{-1}
10^{0}
10^{1}
10^{2}
Proton energy (MeV)
Solomon (78)
evaluated

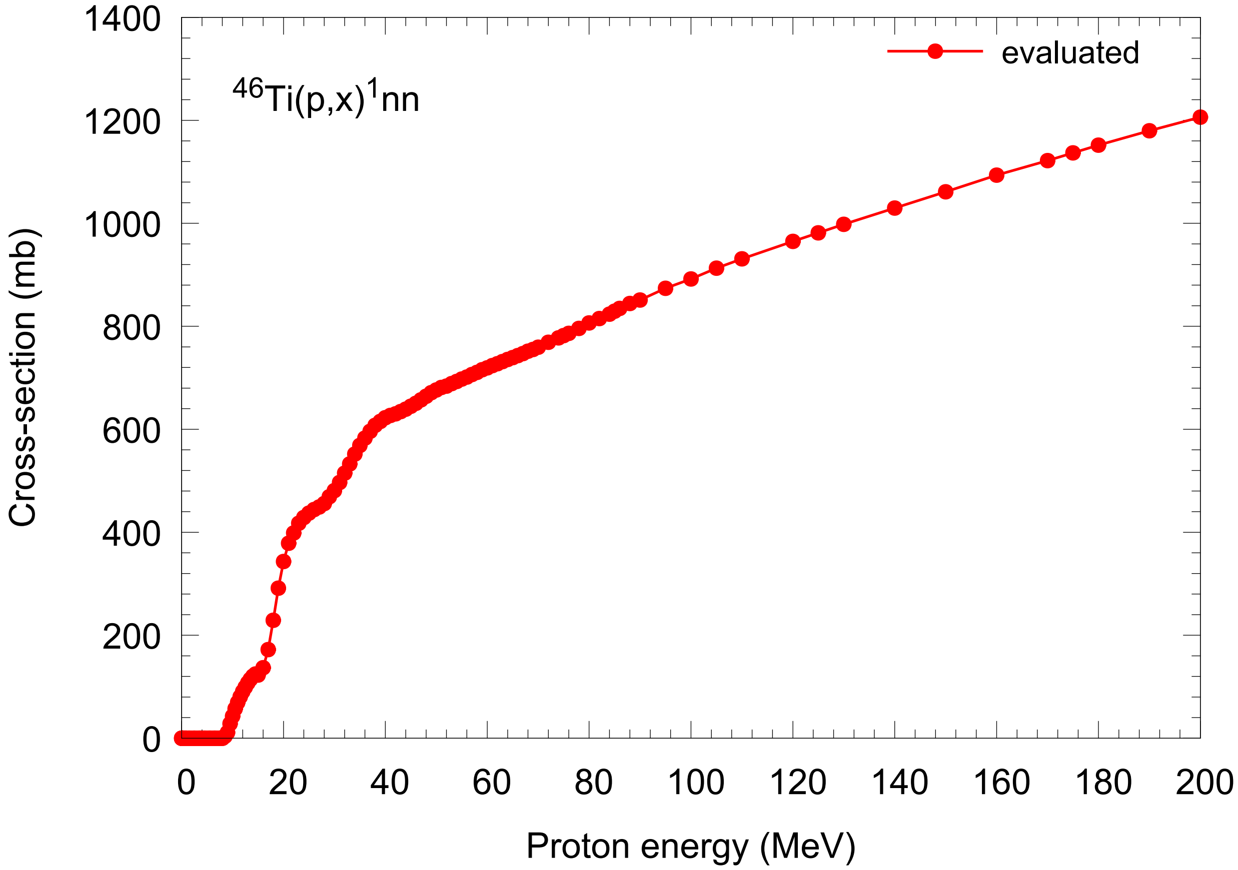

evaluated
$^{46}Ti(p,x)^1nn$
Cross-section (mb)
Proton energy (MeV)
0
200
400
600
800
1000
1200
1400
0
20
40
60
80
100
120
140
160
180
200

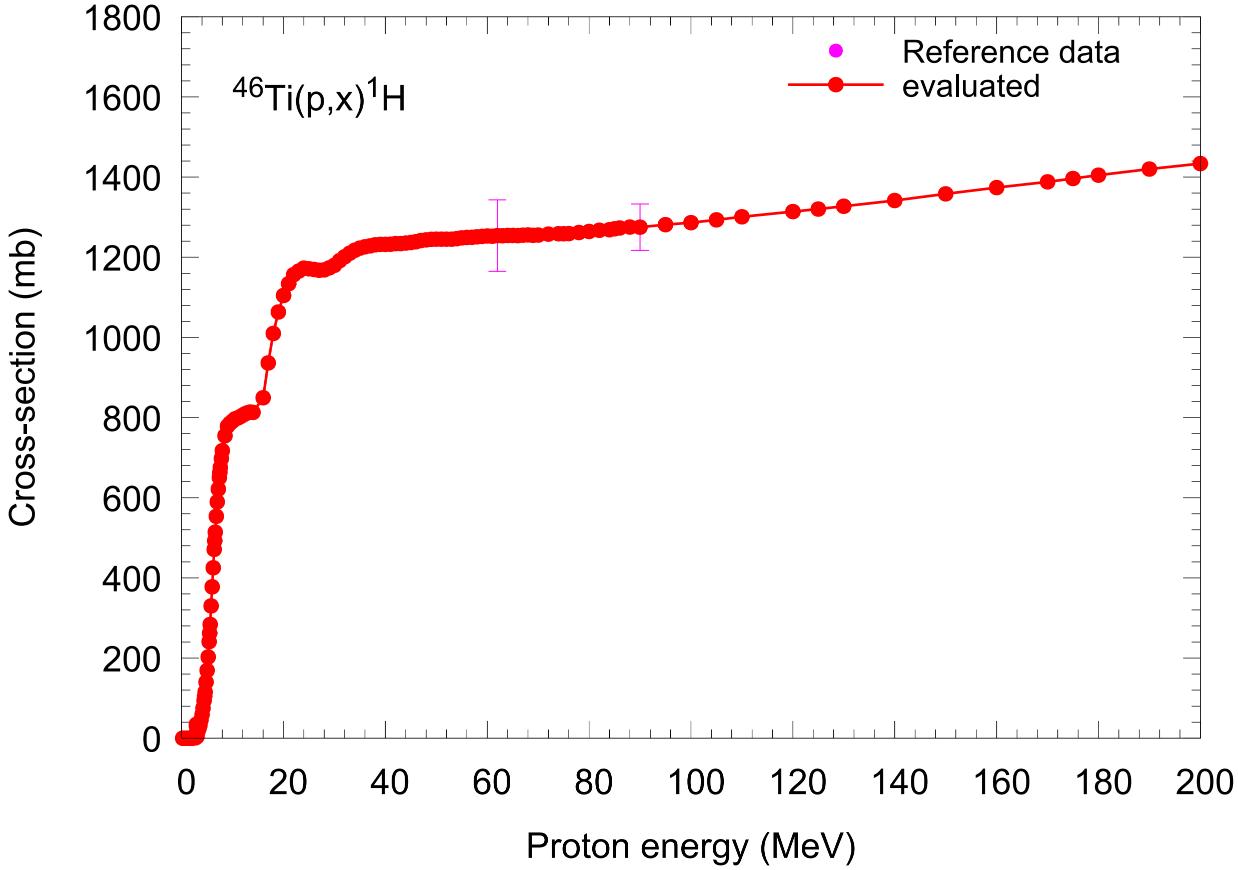

Reference data
evaluated
$^{46}Ti(p,x)^1H$
Cross-section (mb)
Proton energy (MeV)
0
200
400
600
800
1000
1200
1400
1600
1800
0
20
40
60
80
100
120
140
160
180
200

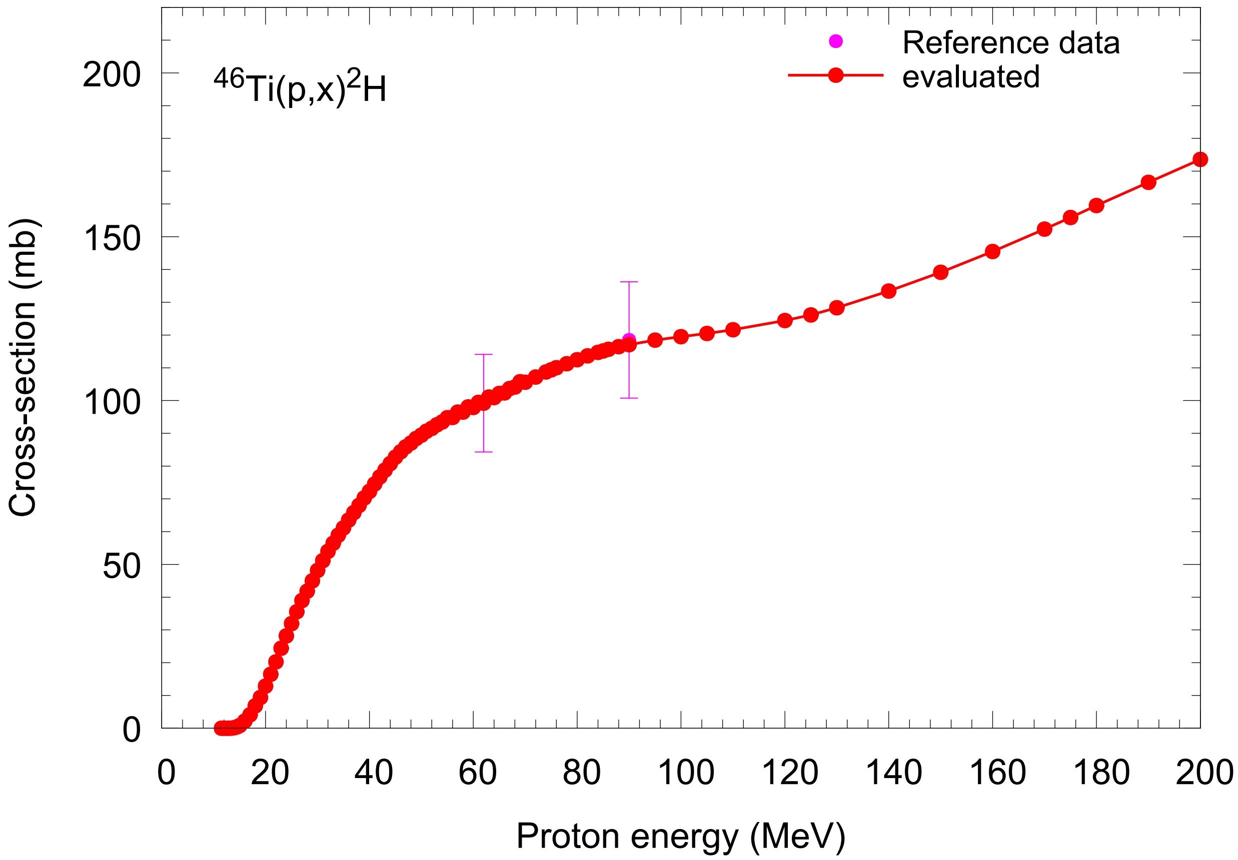

$^{46}Ti(p,x)^{2}H$
Reference data
evaluated
Cross-section (mb)
Proton energy (MeV)
0
50
100
150
200
0
20
40
60
80
100
120
140
160
180
200

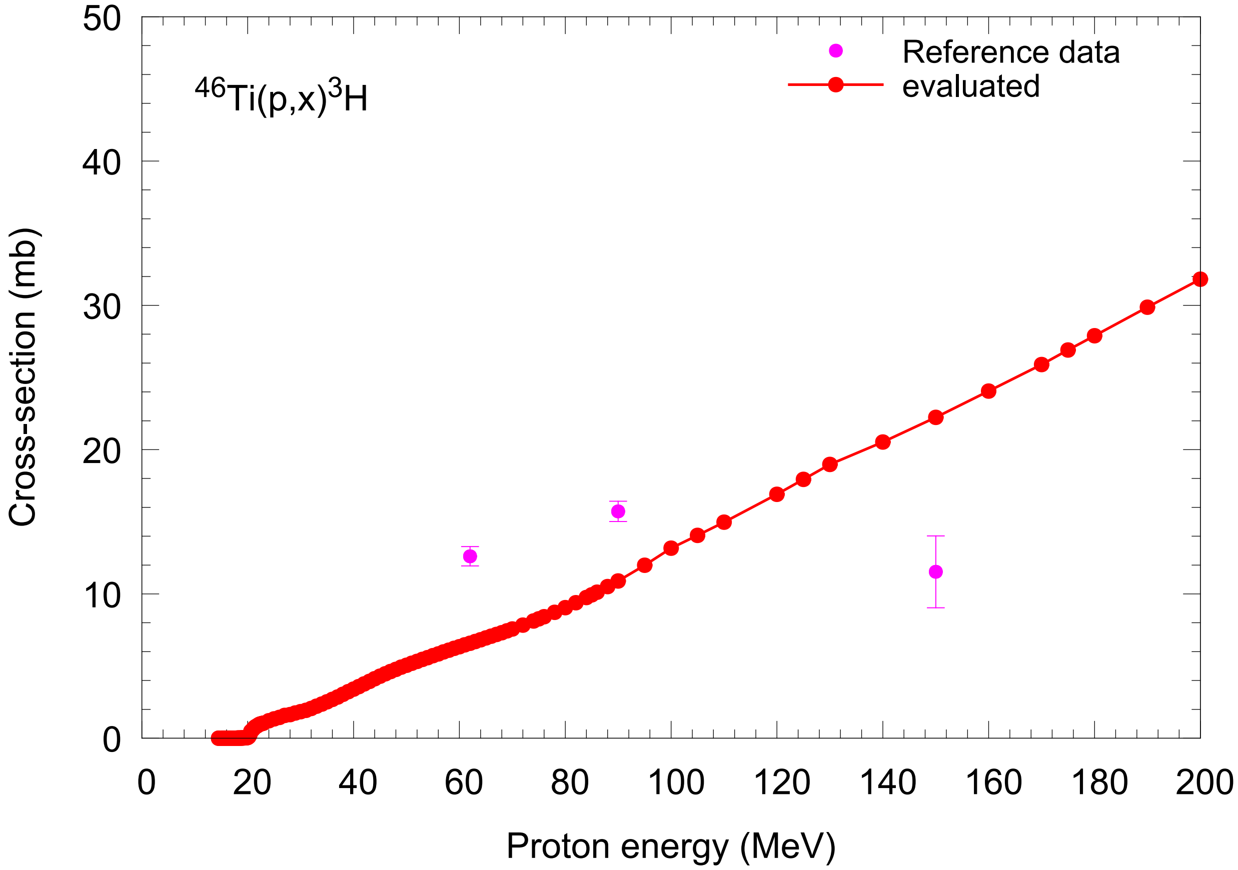

$^{46}Ti(p,x)^{3}H$
Reference data
evaluated
Cross-section (mb)
Proton energy (MeV)
0
10
20
30
40
50
0
20
40
60
80
100
120
140
160
180
200

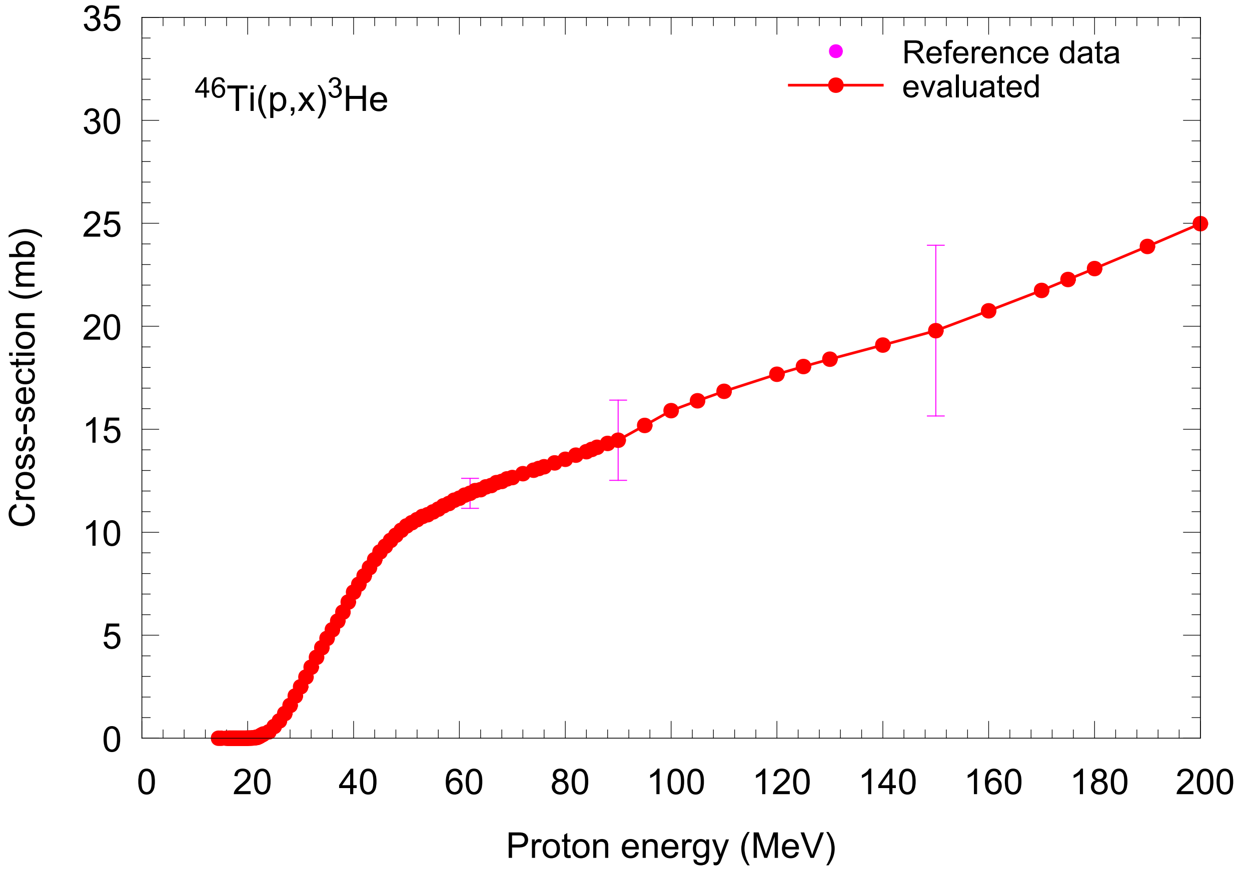

$^{46}Ti(p,x)^{3}He$
Reference data
evaluated
Cross-section (mb)
Proton energy (MeV)
0
5
10
15
20
25
30
35
0
20
40
60
80
100
120
140
160
180
200

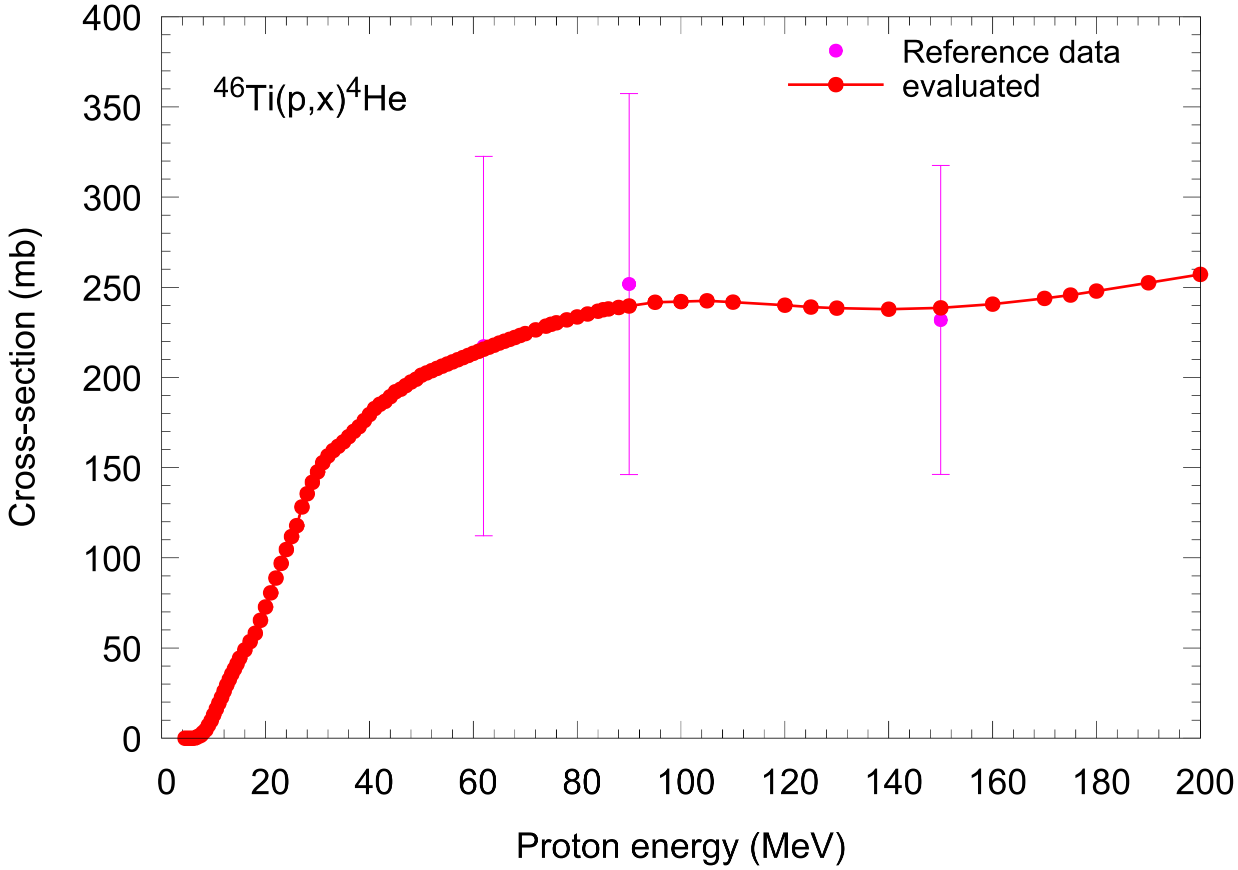

$^{46}Ti(p,x)^{4}He$
Reference data
evaluated
Cross-section (mb)
Proton energy (MeV)
0
50
100
150
200
250
300
350
400
0
20
40
60
80
100
120
140
160
180
200

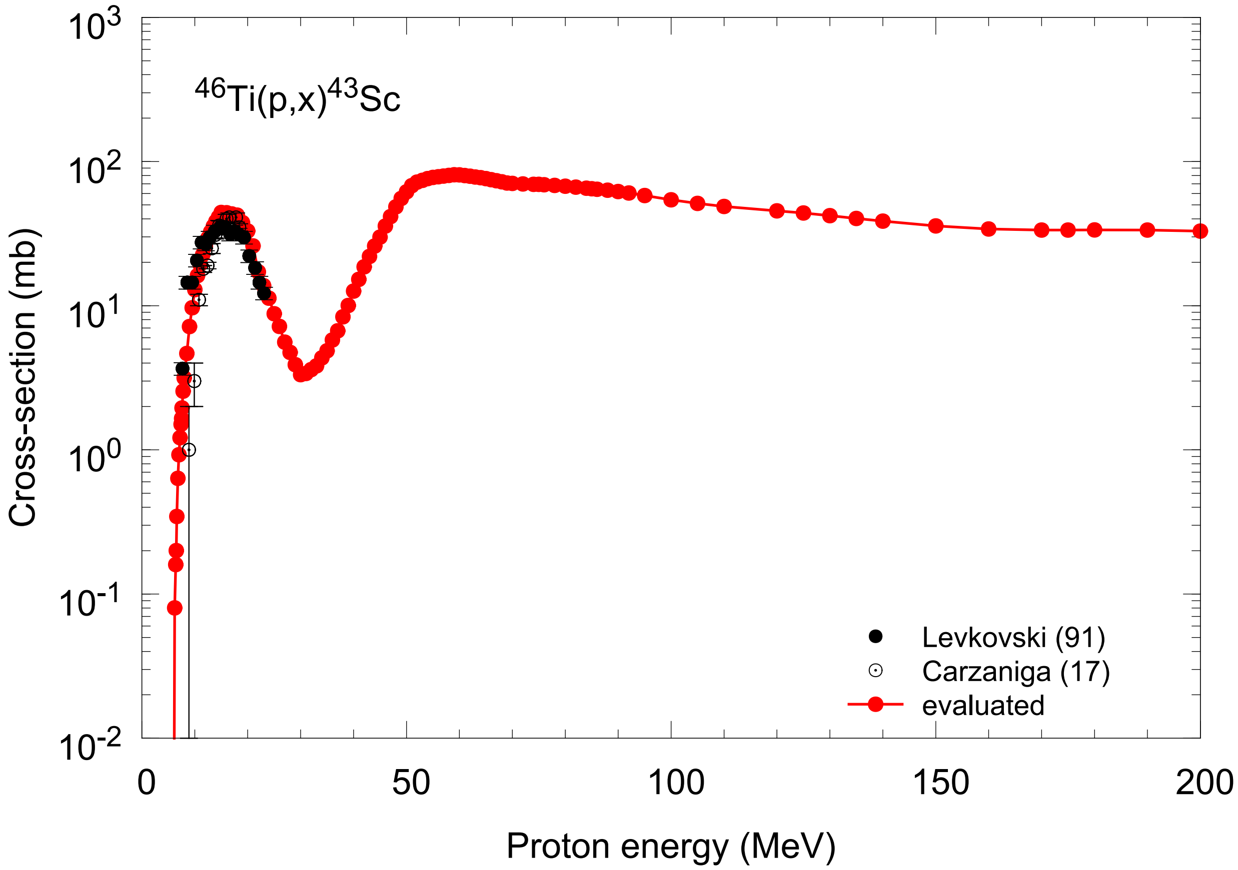

$^{46}Ti(p,x)^{43}Sc$
Levkovski (91)
Carzaniga (17)
evaluated
Cross-section (mb)
Proton energy (MeV)

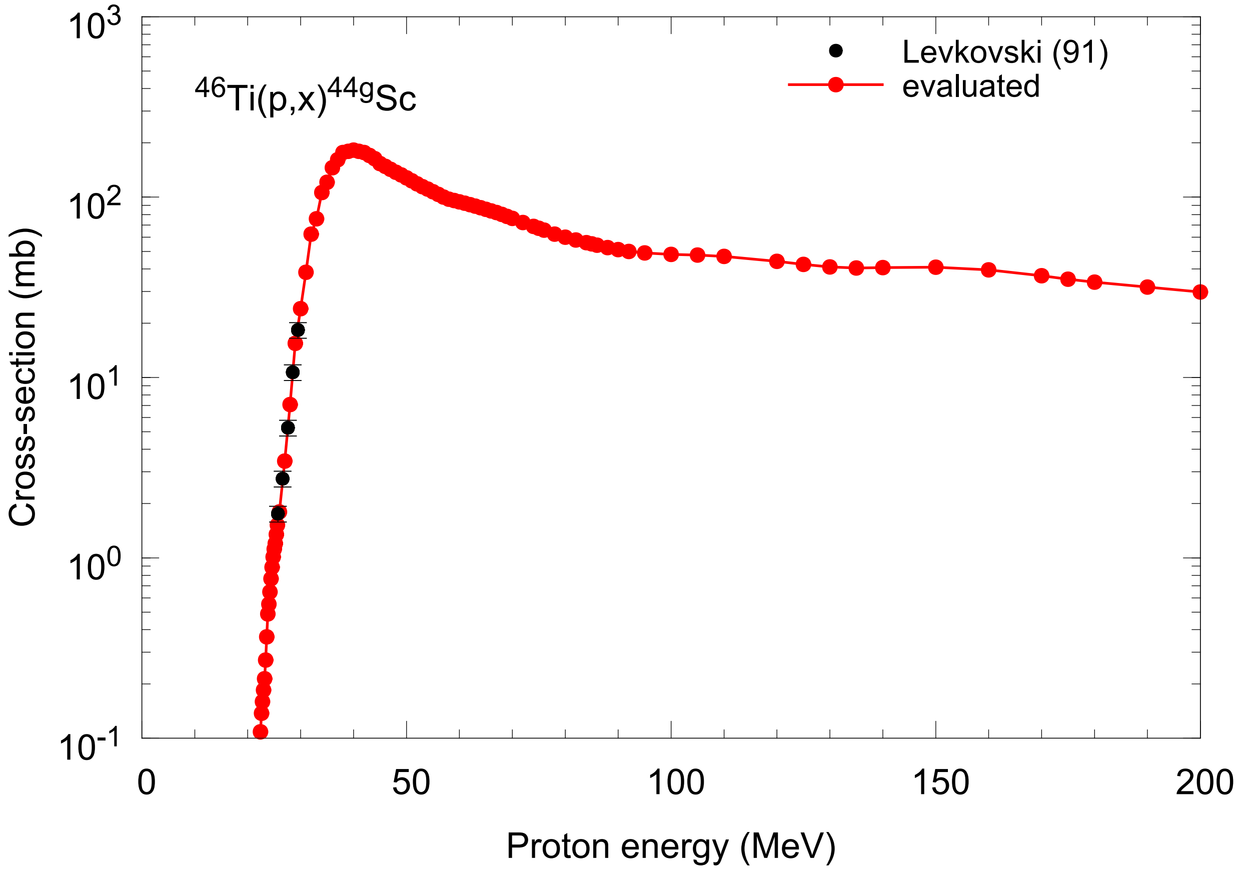

$^{46}Ti(p,x)^{44g}Sc$
Levkovski (91)
evaluated
Cross-section (mb)
Proton energy (MeV)

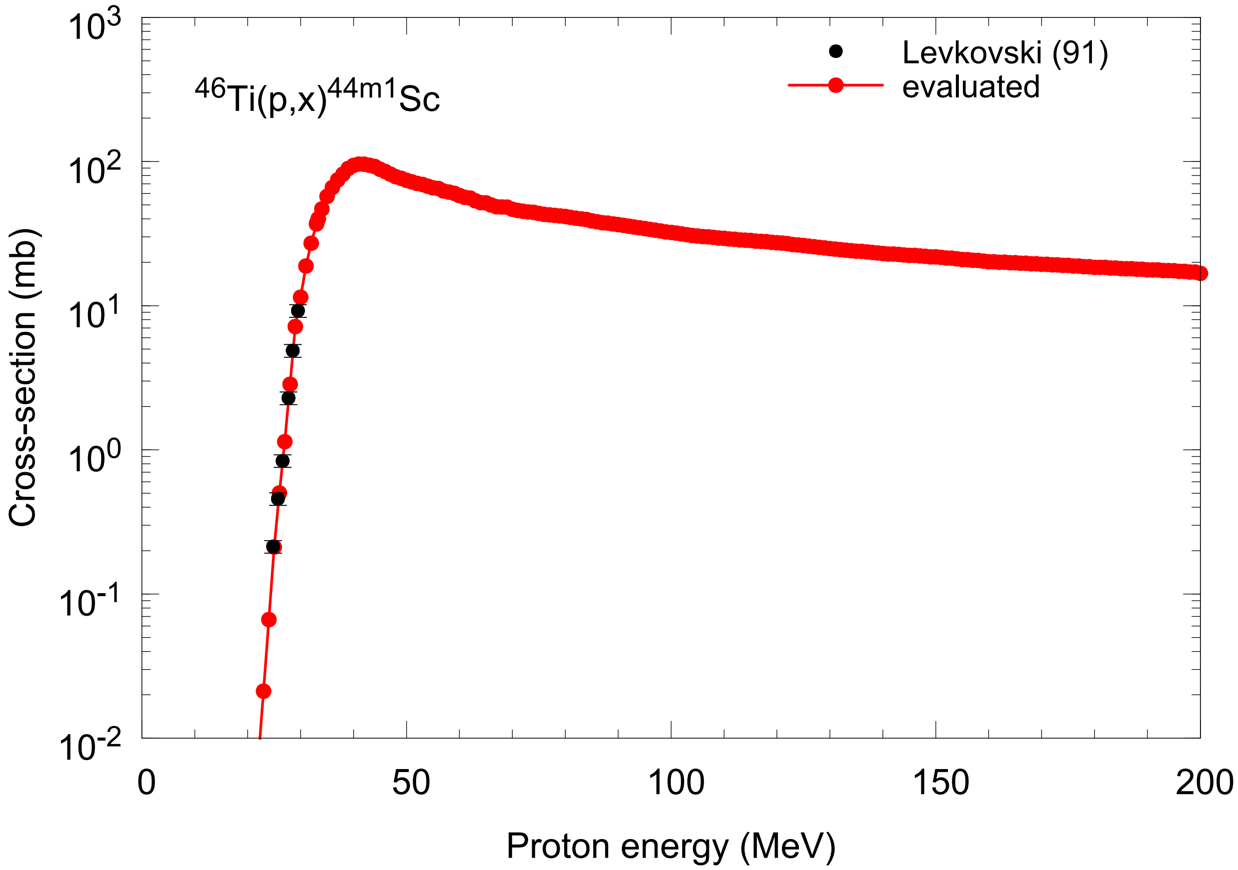

10^3
10^2
10^1
10^0
10^{-1}
10^{-2}
Cross-section (mb)
$^{46}Ti(p,x)^{44m1}Sc$
Levkovski (91)
evaluated
0
50
100
150
200
Proton energy (MeV)

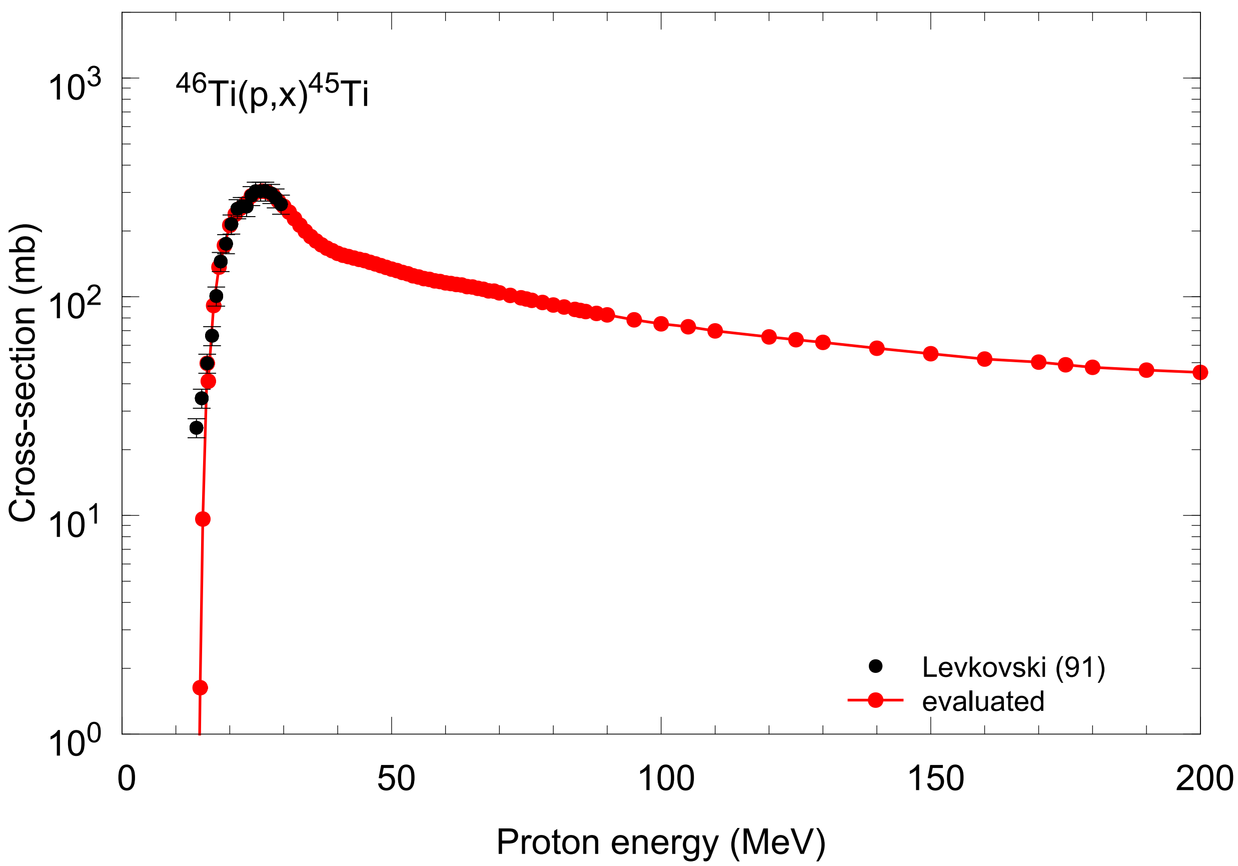

10^3
10^2
10^1
10^0
Cross-section (mb)
$^{46}Ti(p,x)^{45}Ti$
Levkovski (91)
evaluated
0
50
100
150
200
Proton energy (MeV)

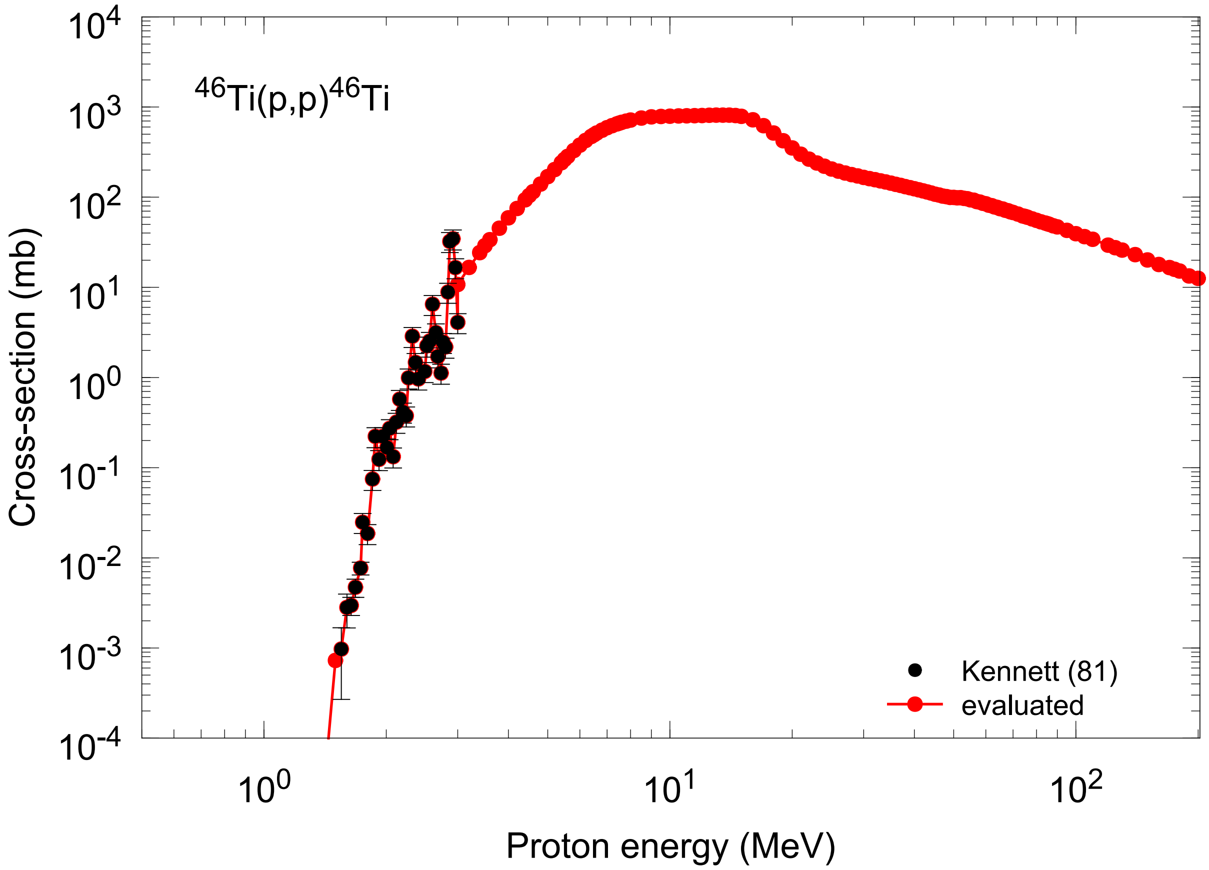

^{46}Ti(p,p)^{46}Ti
Cross-section (mb)
Proton energy (MeV)
Kennett (81)
evaluated

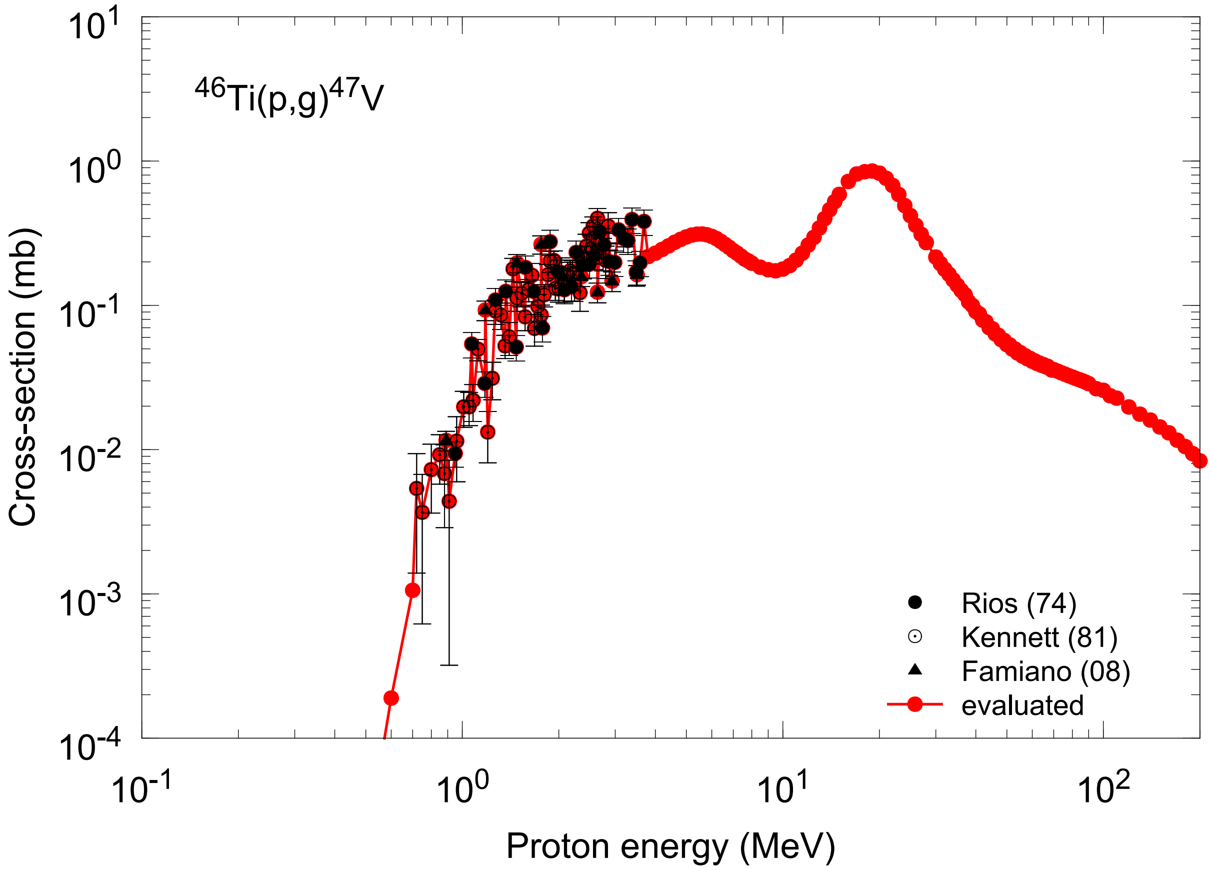

^{46}Ti(p,g)^{47}V
Cross-section (mb)
Proton energy (MeV)
Rios (74)
Kennett (81)
Famiano (08)
evaluated

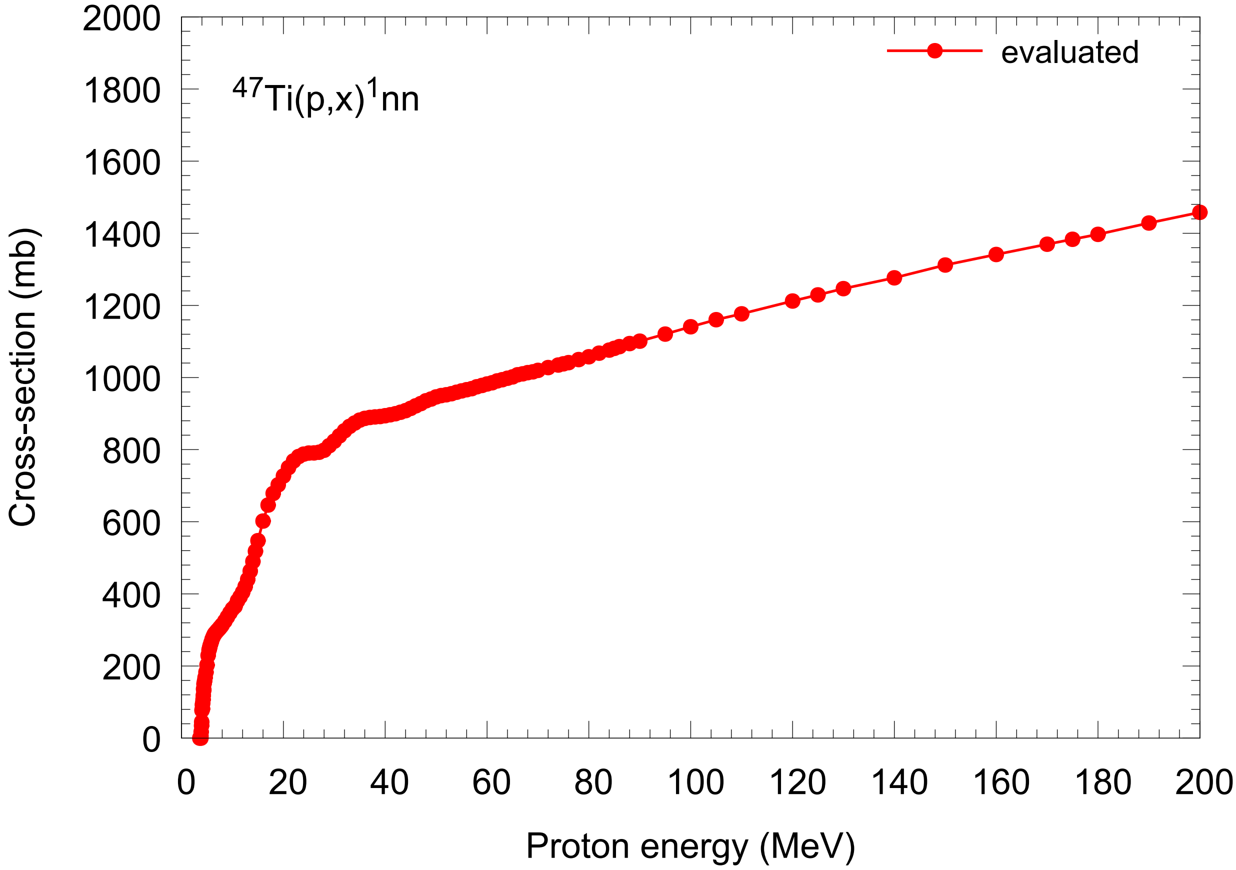

$^{47}Ti(p,x)^1nn$
evaluated
Cross-section (mb)
Proton energy (MeV)
0
200
400
600
800
1000
1200
1400
1600
1800
2000
0
20
40
60
80
100
120
140
160
180
200

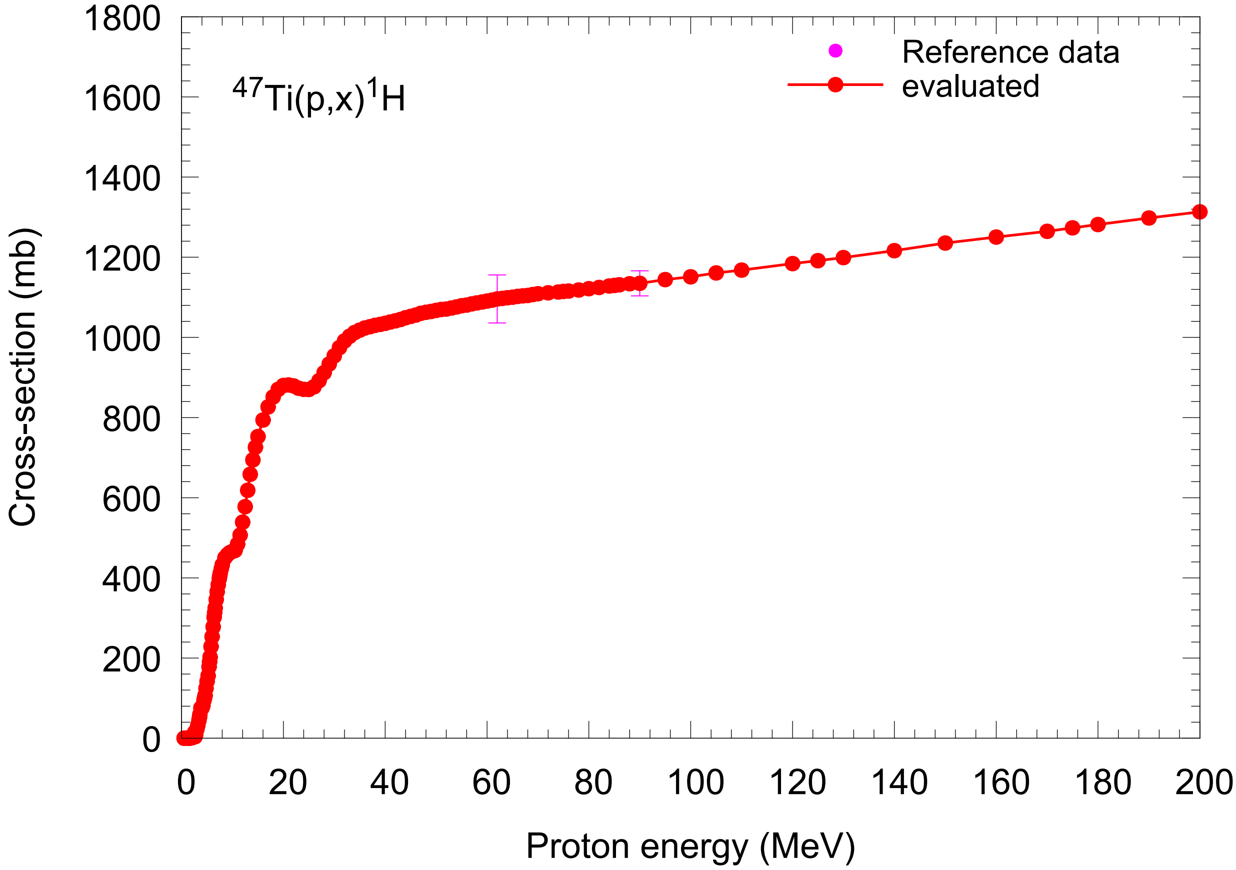

$^{47}Ti(p,x)^1H$
Reference data
evaluated
Cross-section (mb)
Proton energy (MeV)
0
200
400
600
800
1000
1200
1400
1600
1800
0
20
40
60
80
100
120
140
160
180
200

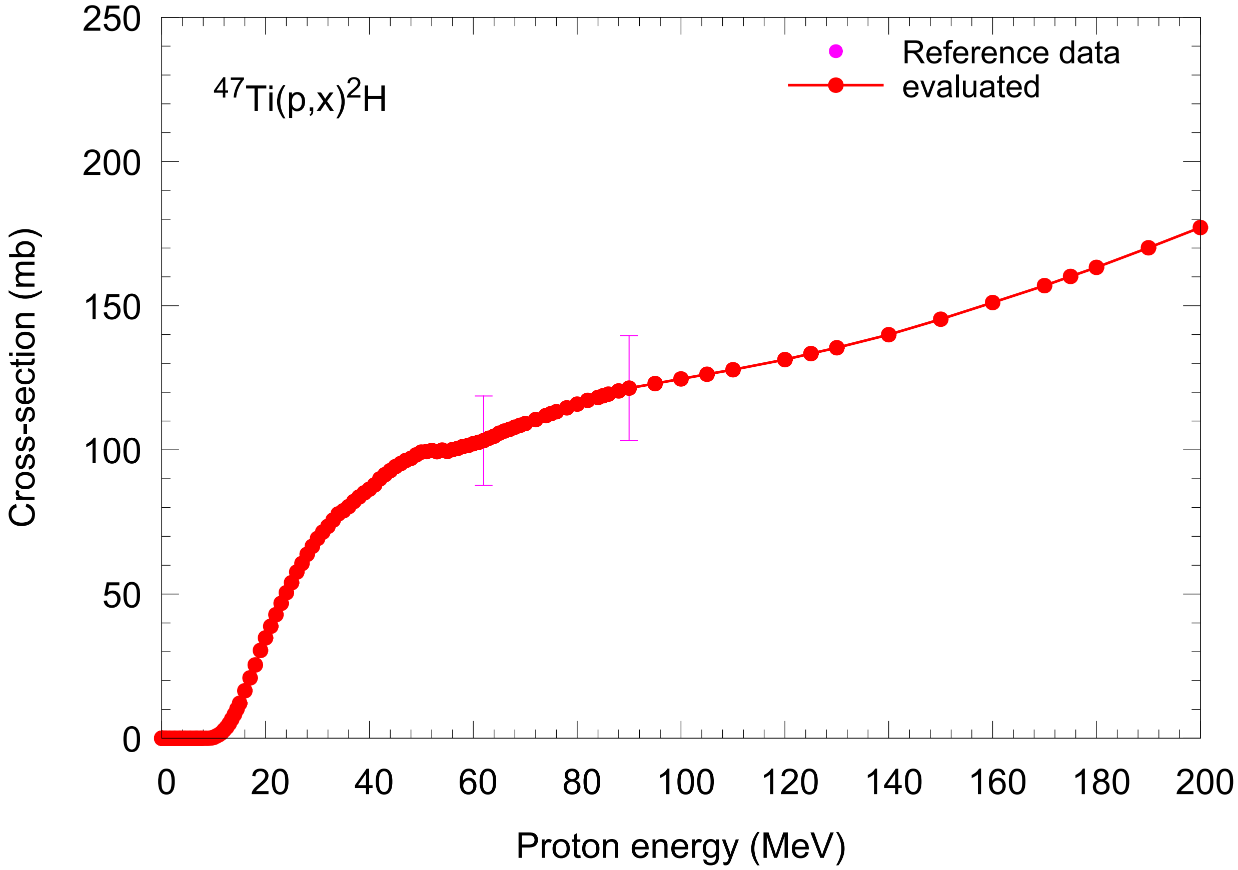

$^{47}Ti(p,x)^{2}H$
Reference data
evaluated
Cross-section (mb)
Proton energy (MeV)
0
50
100
150
200
250
0
20
40
60
80
100
120
140
160
180
200

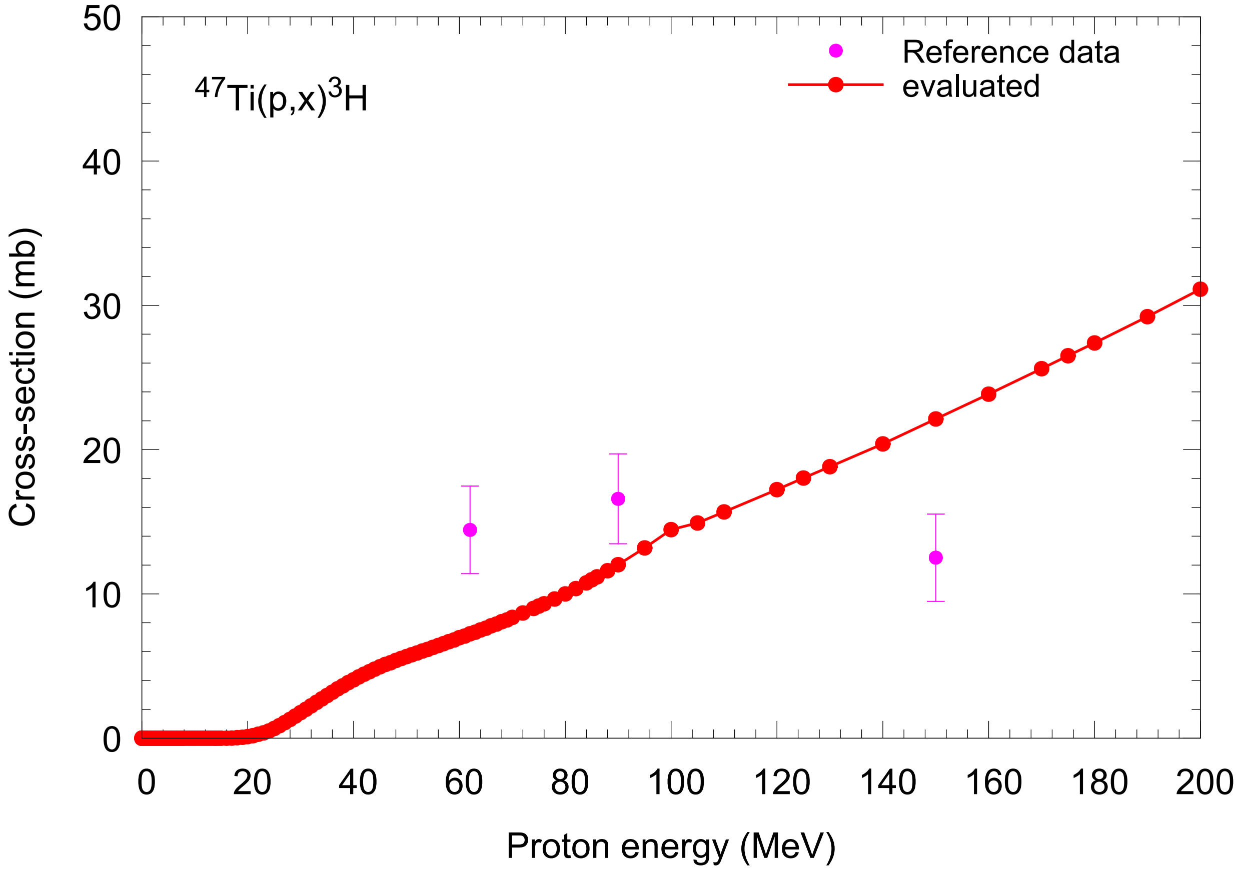

$^{47}Ti(p,x)^{3}H$
Reference data
evaluated
Cross-section (mb)
Proton energy (MeV)
0
10
20
30
40
50
0
20
40
60
80
100
120
140
160
180
200

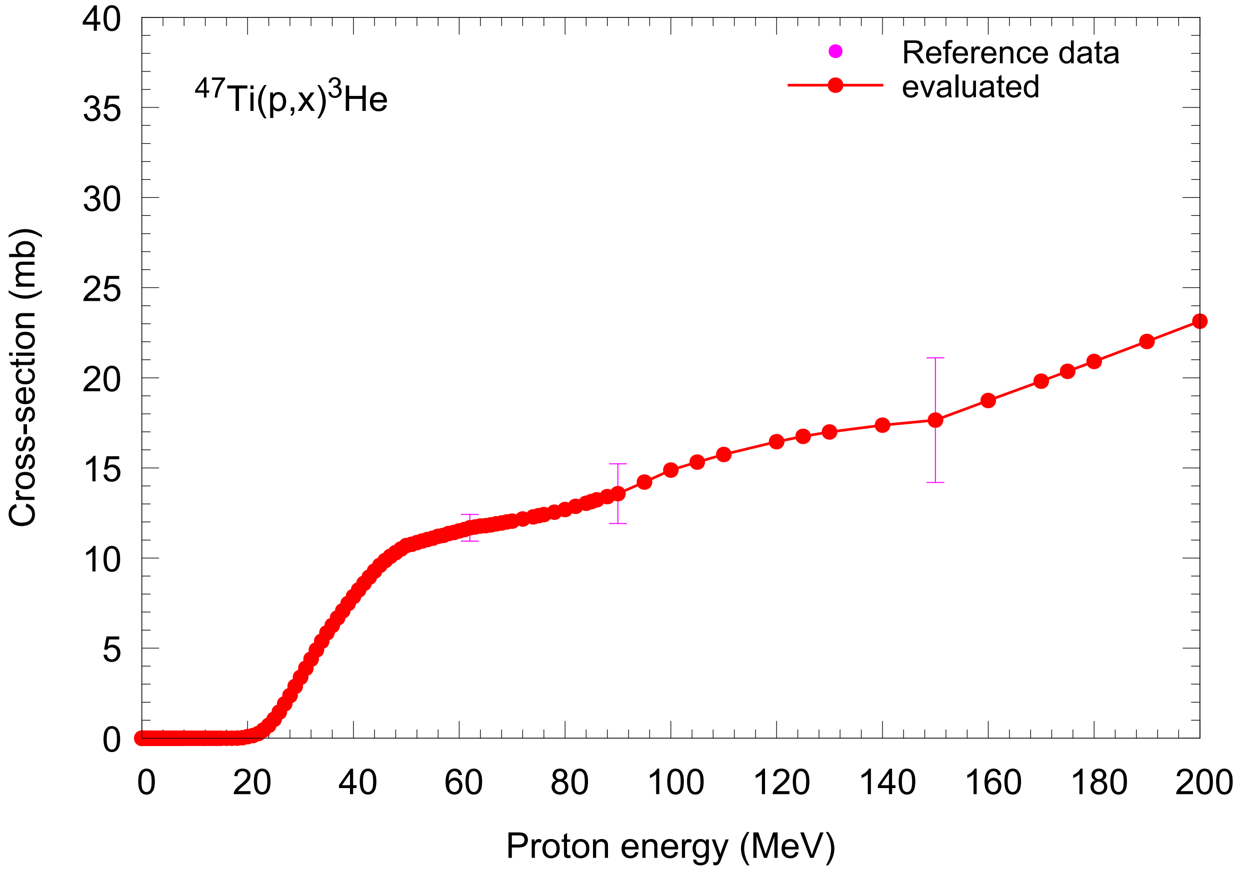

$^{47}Ti(p,x)^{3}He$
Reference data
evaluated
Cross-section (mb)
Proton energy (MeV)
0
5
10
15
20
25
30
35
40
0
20
40
60
80
100
120
140
160
180
200

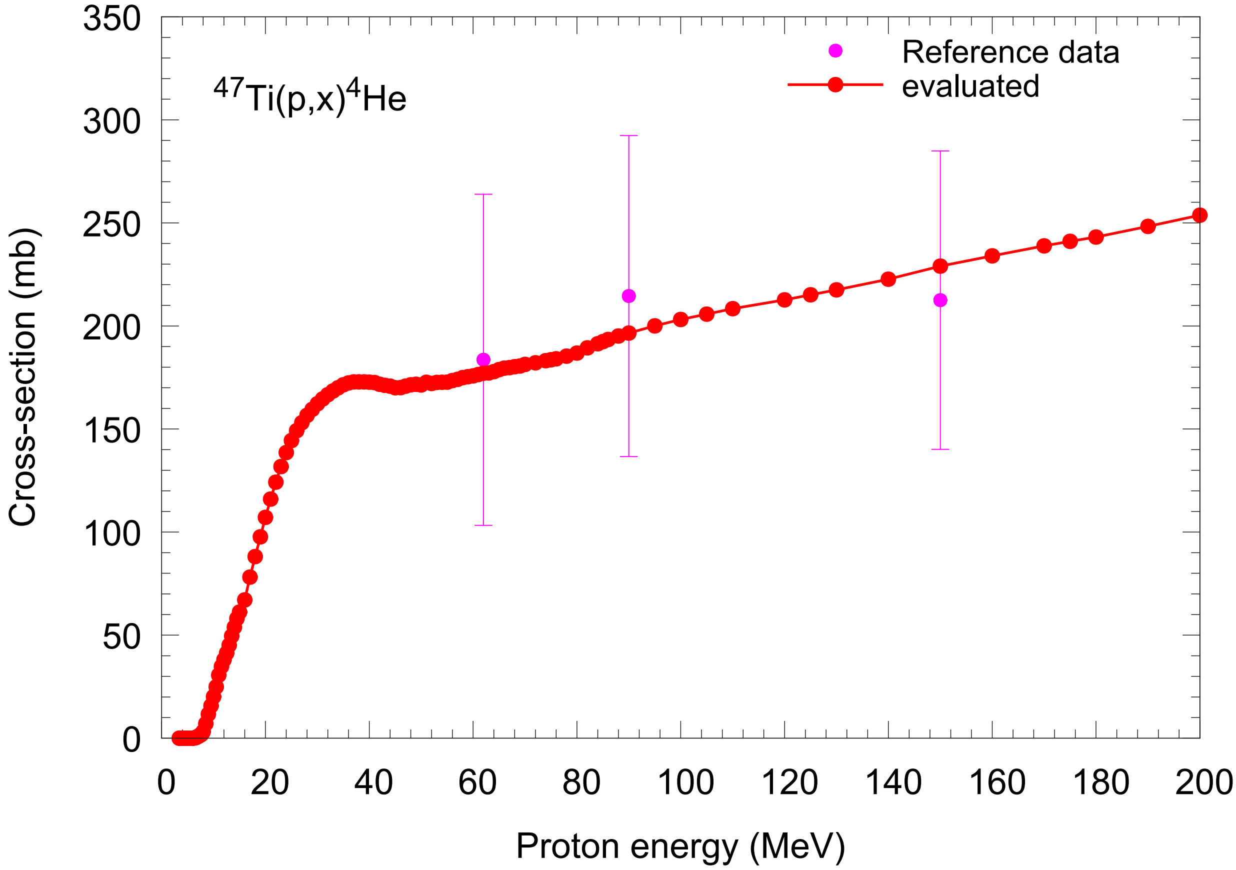

$^{47}Ti(p,x)^{4}He$
Reference data
evaluated
Cross-section (mb)
Proton energy (MeV)
0
50
100
150
200
250
300
350
0
20
40
60
80
100
120
140
160
180
200

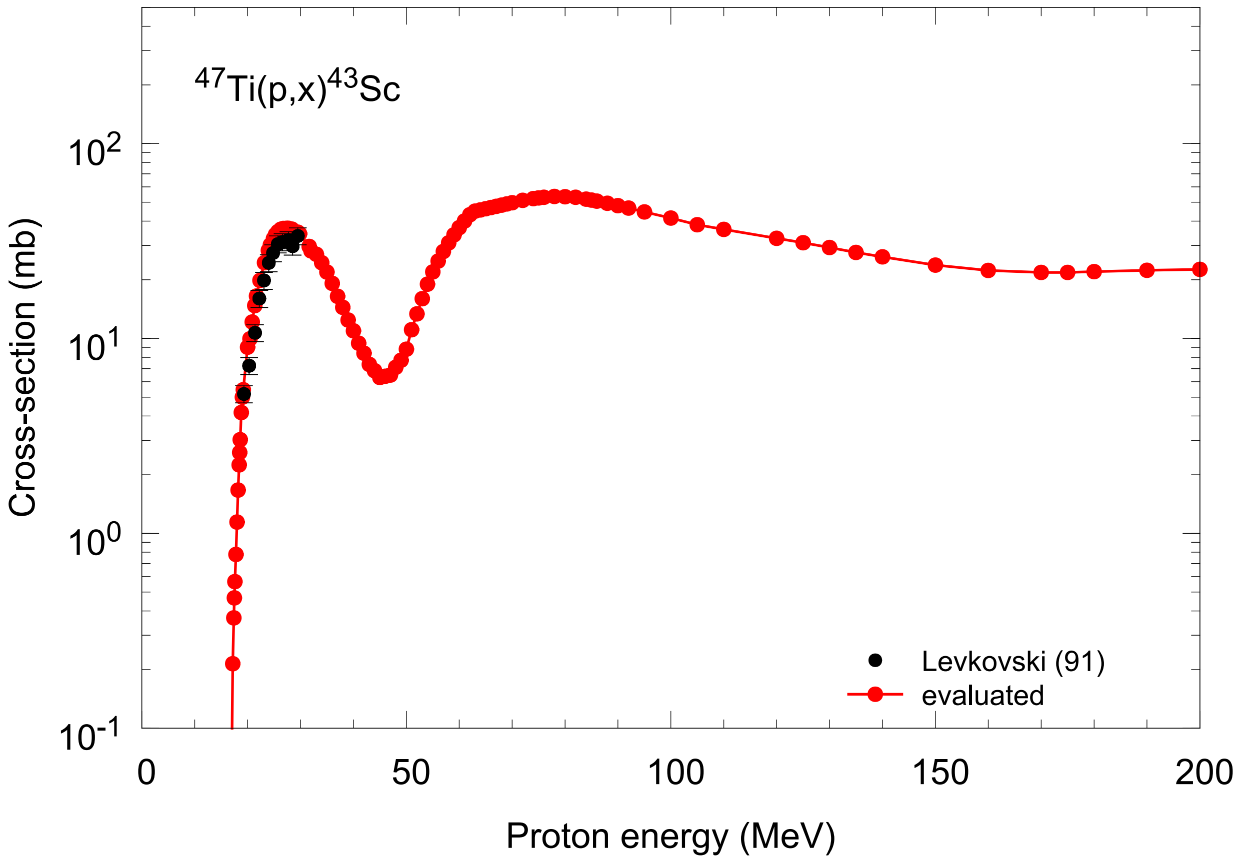

$^{47}Ti(p,x)^{43}Sc$
Cross-section (mb)
10^2
10^1
10^0
10^{-1}
0
50
100
150
200
Proton energy (MeV)
Levkovski (91)
evaluated

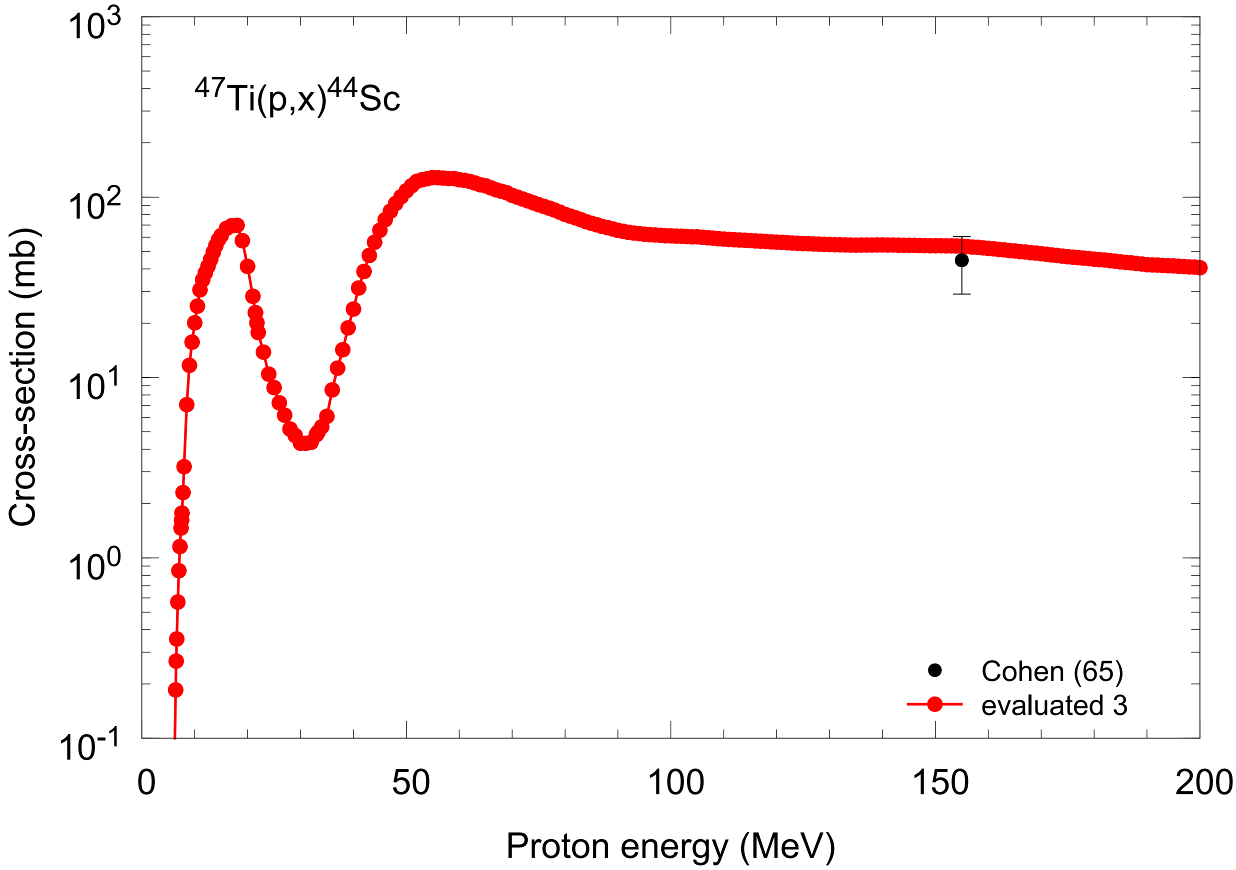

$^{47}Ti(p,x)^{44}Sc$
Cross-section (mb)
10^3
10^2
10^1
10^0
10^{-1}
0
50
100
150
200
Proton energy (MeV)
Cohen (65)
evaluated 3

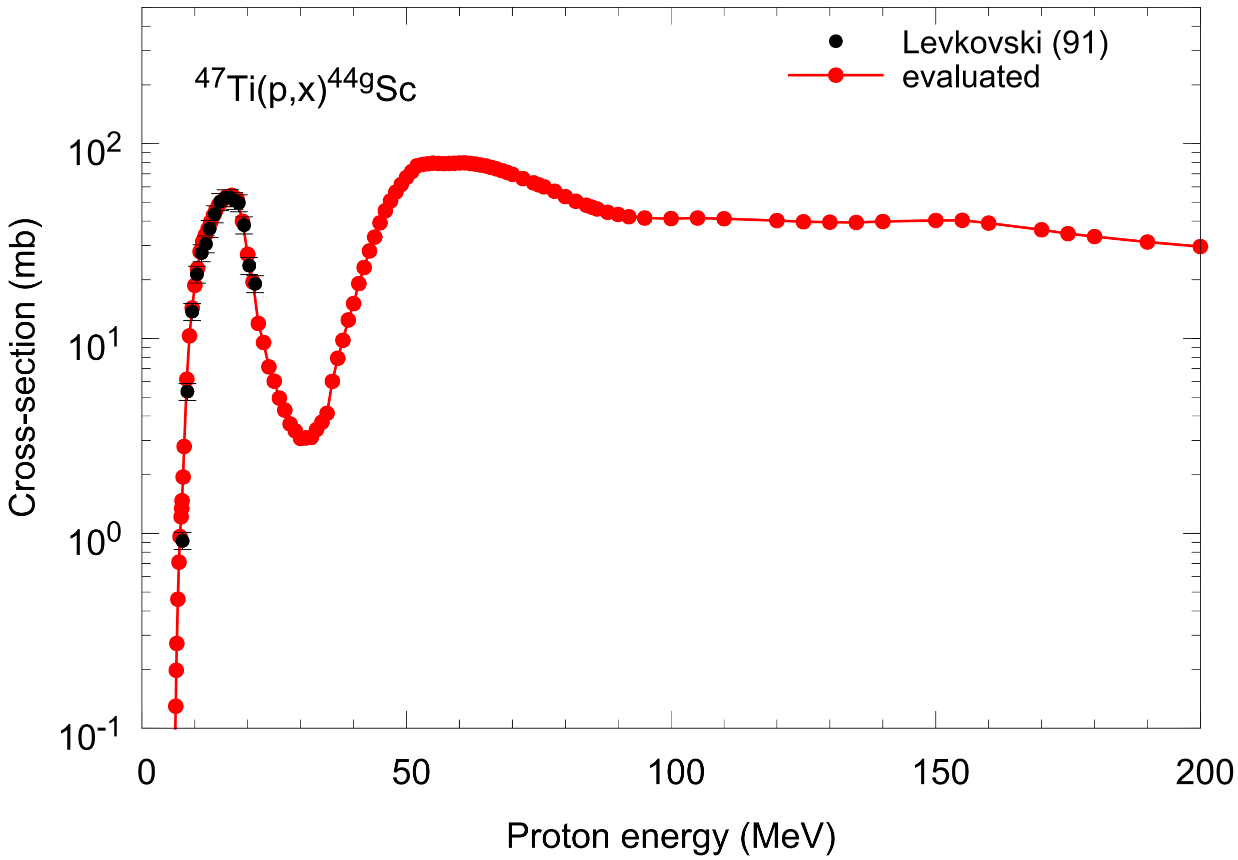

$^{47}Ti(p,x)^{44g}Sc$
Levkovski (91)
evaluated
Cross-section (mb)
Proton energy (MeV)

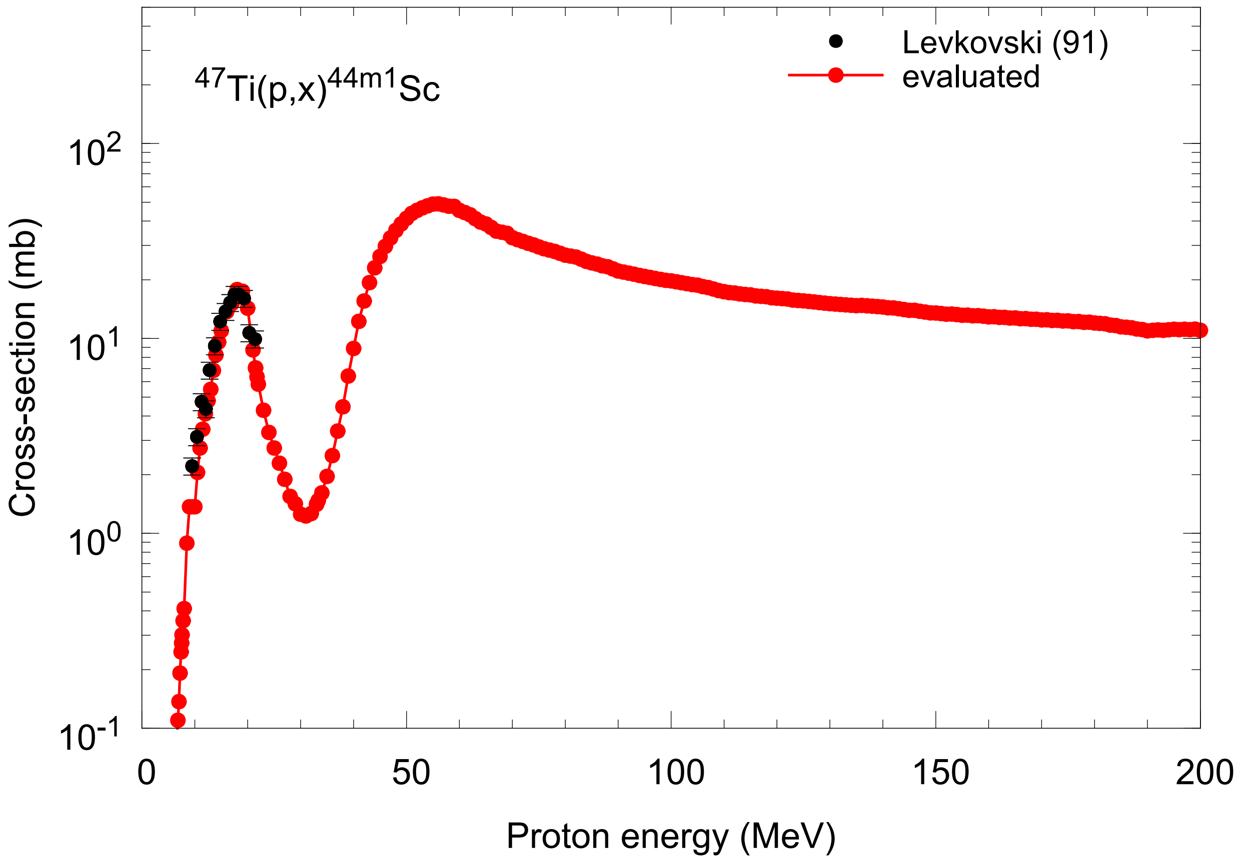

$^{47}Ti(p,x)^{44m1}Sc$
Levkovski (91)
evaluated
Cross-section (mb)
Proton energy (MeV)

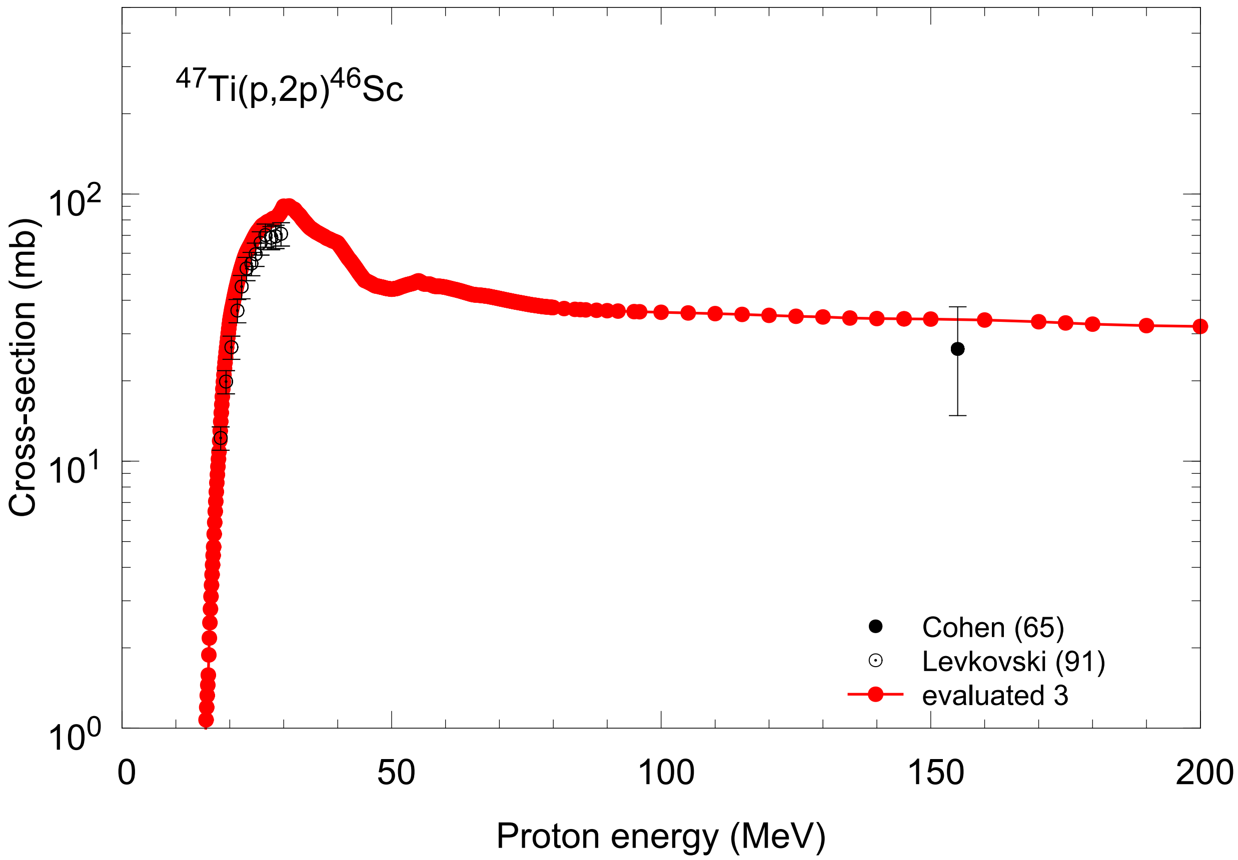

$^{47}Ti(p,2p)^{46}Sc$
Cross-section (mb)
10^2
10^1
10^0
0
50
100
150
200
Proton energy (MeV)
Cohen (65)
Levkovski (91)
evaluated 3

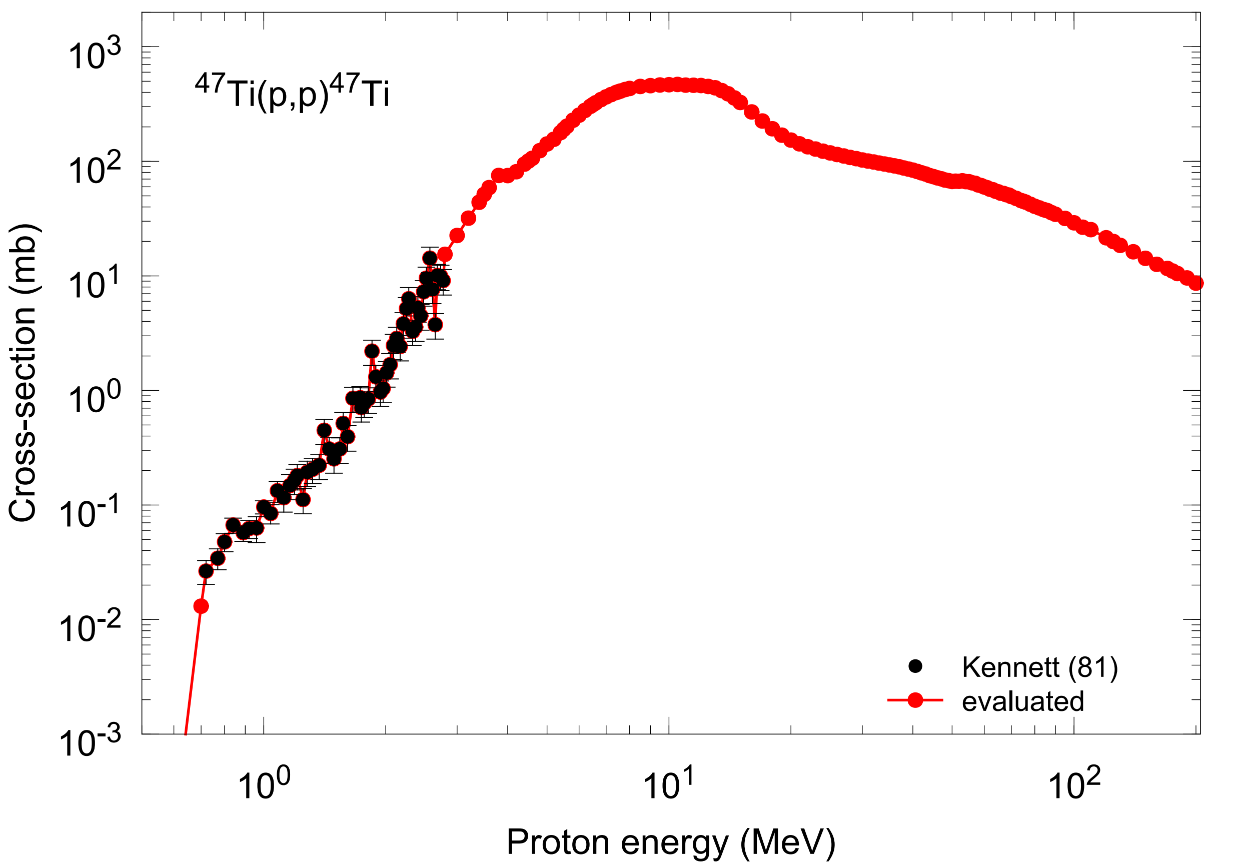

$^{47}Ti(p,p)^{47}Ti$
Cross-section (mb)
10^3
10^2
10^1
10^0
10^{-1}
10^{-2}
10^{-3}
10^0
10^1
10^2
Proton energy (MeV)
Kennett (81)
evaluated

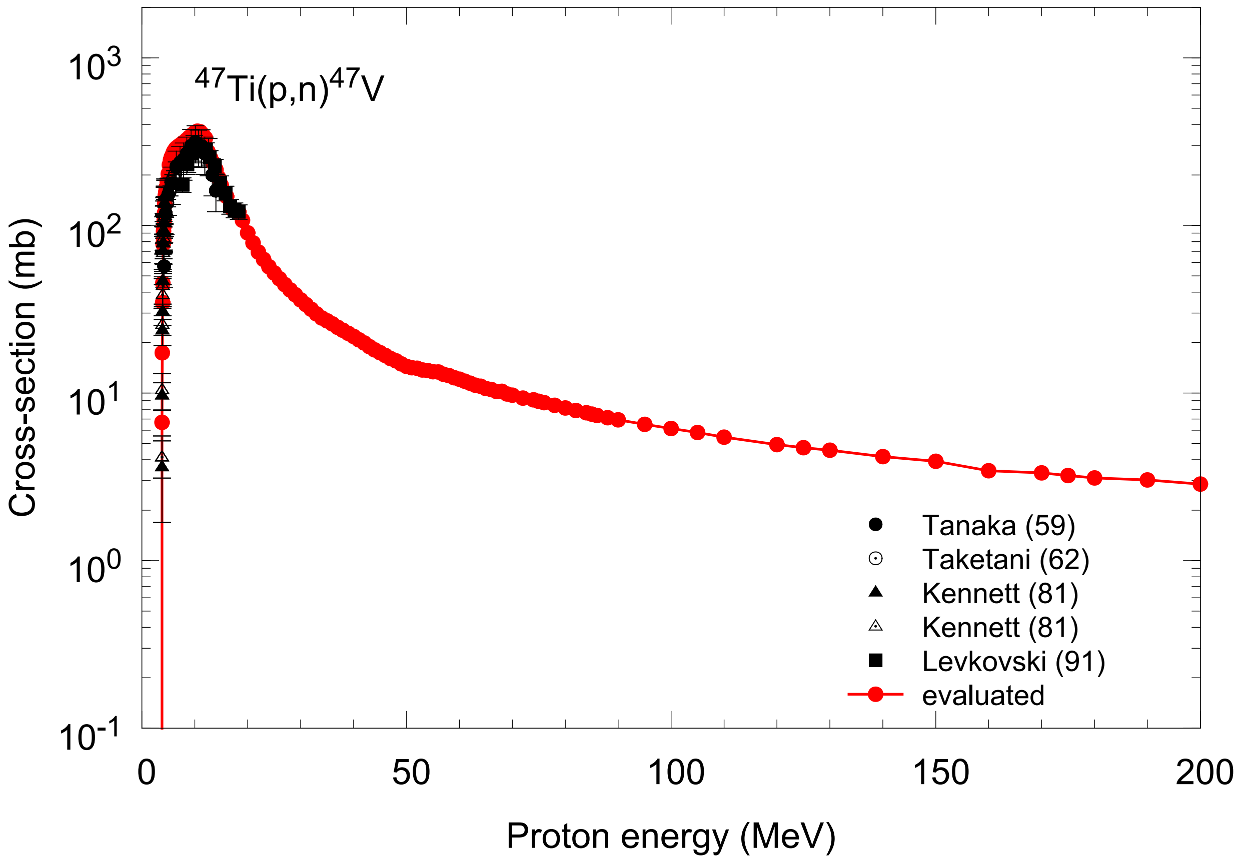

$^{47}Ti(p,n)^{47}V$
Cross-section (mb)
Proton energy (MeV)
Tanaka (59)
Taketani (62)
Kennett (81)
Kennett (81)
Levkovski (91)
evaluated

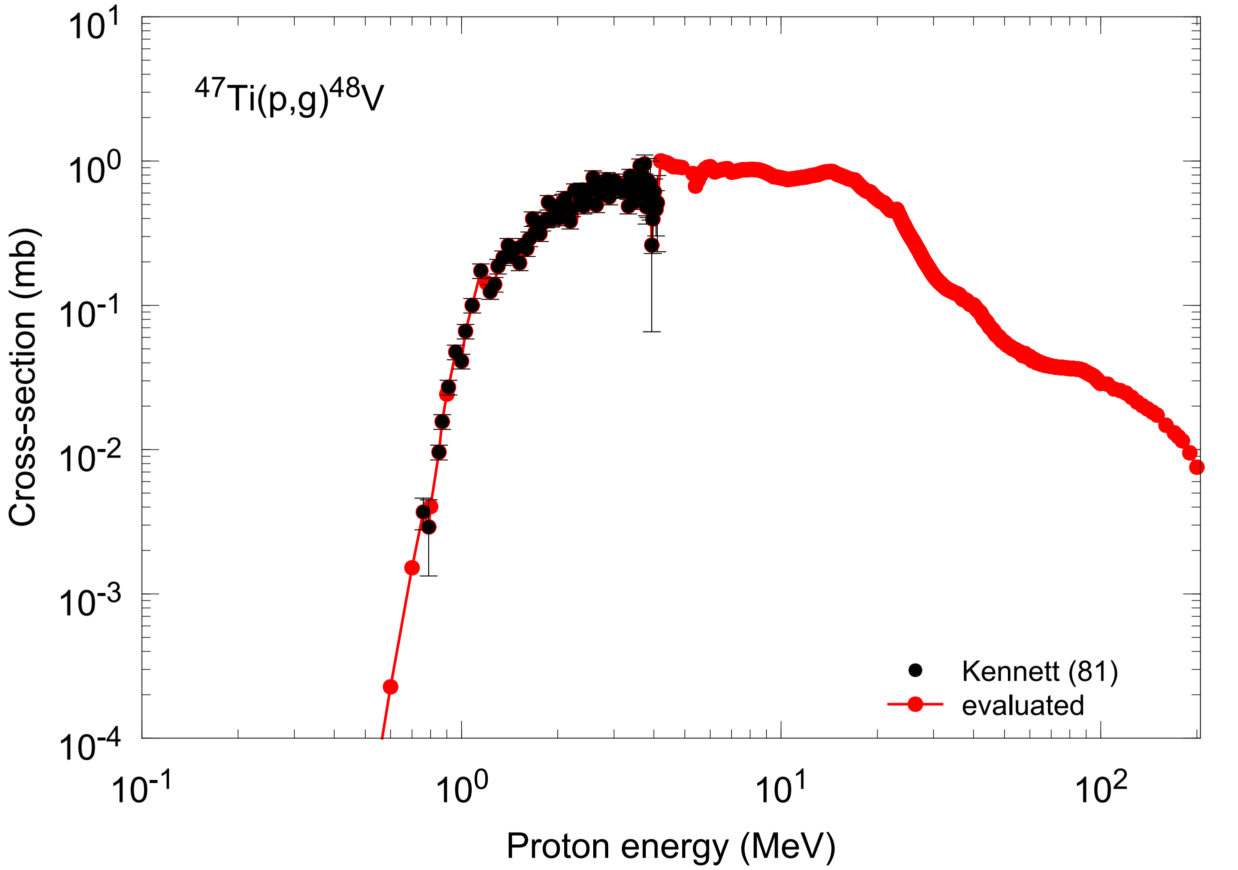

$^{47}Ti(p,g)^{48}V$
Cross-section (mb)
Proton energy (MeV)
Kennett (81)
evaluated

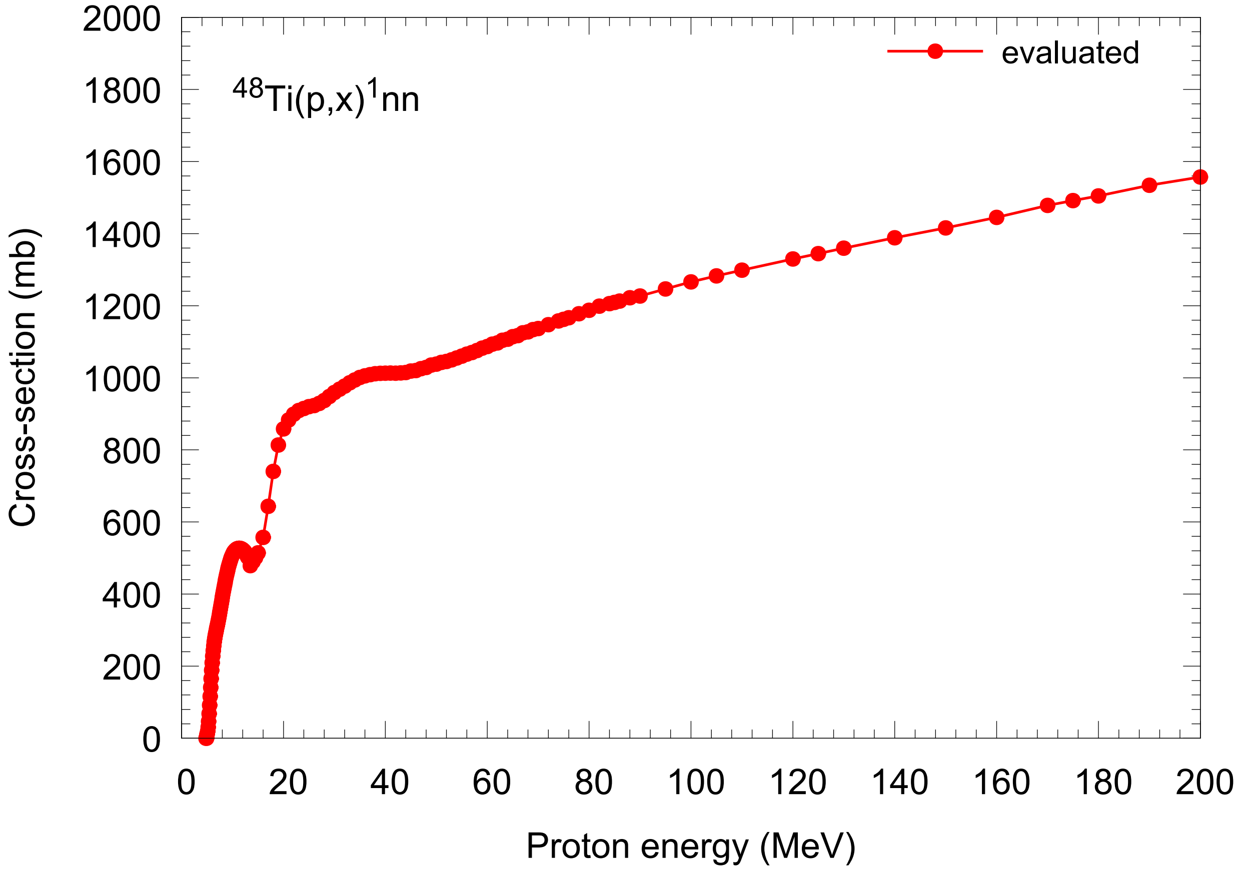

evaluated
^{48}Ti(p,x)^{1}nn
Cross-section (mb)
Proton energy (MeV)

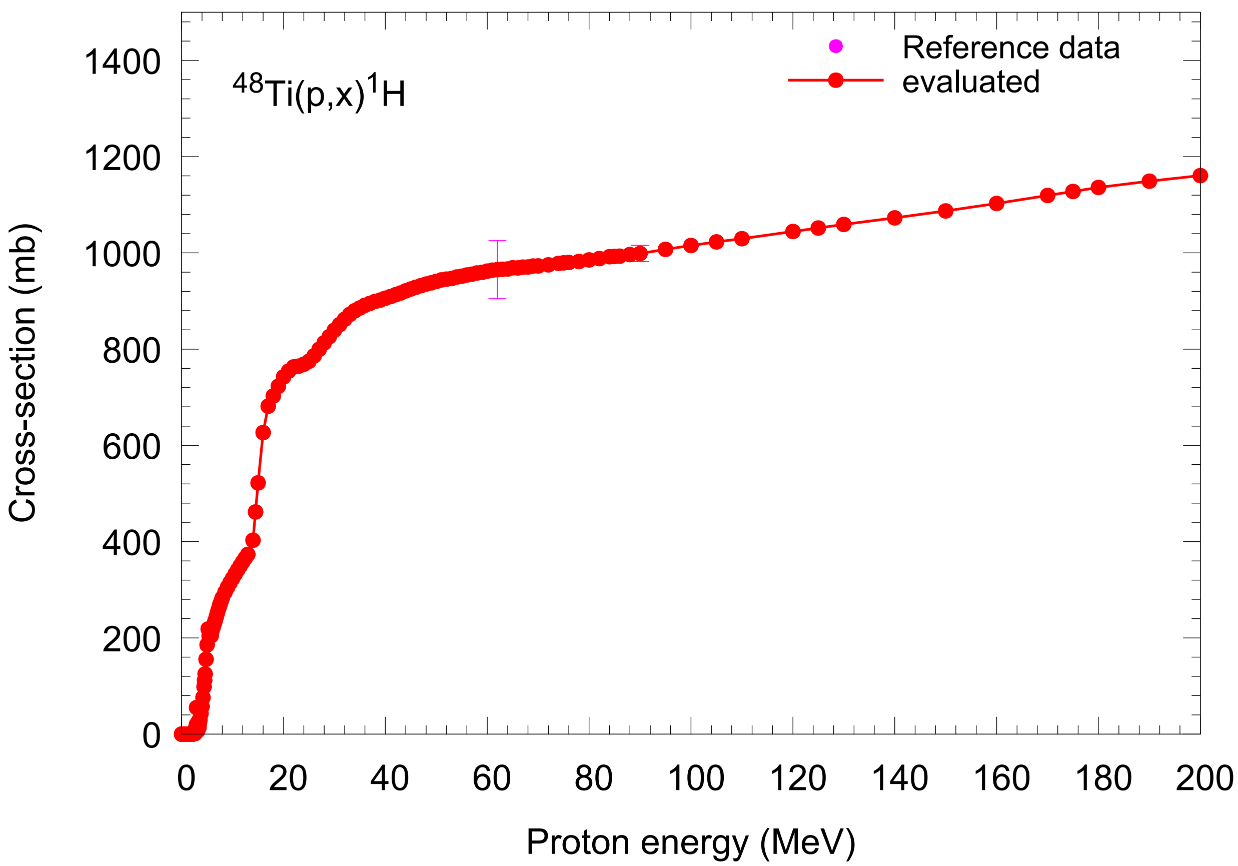

Reference data
evaluated
^{48}Ti(p,x)^{1}H
Cross-section (mb)
Proton energy (MeV)

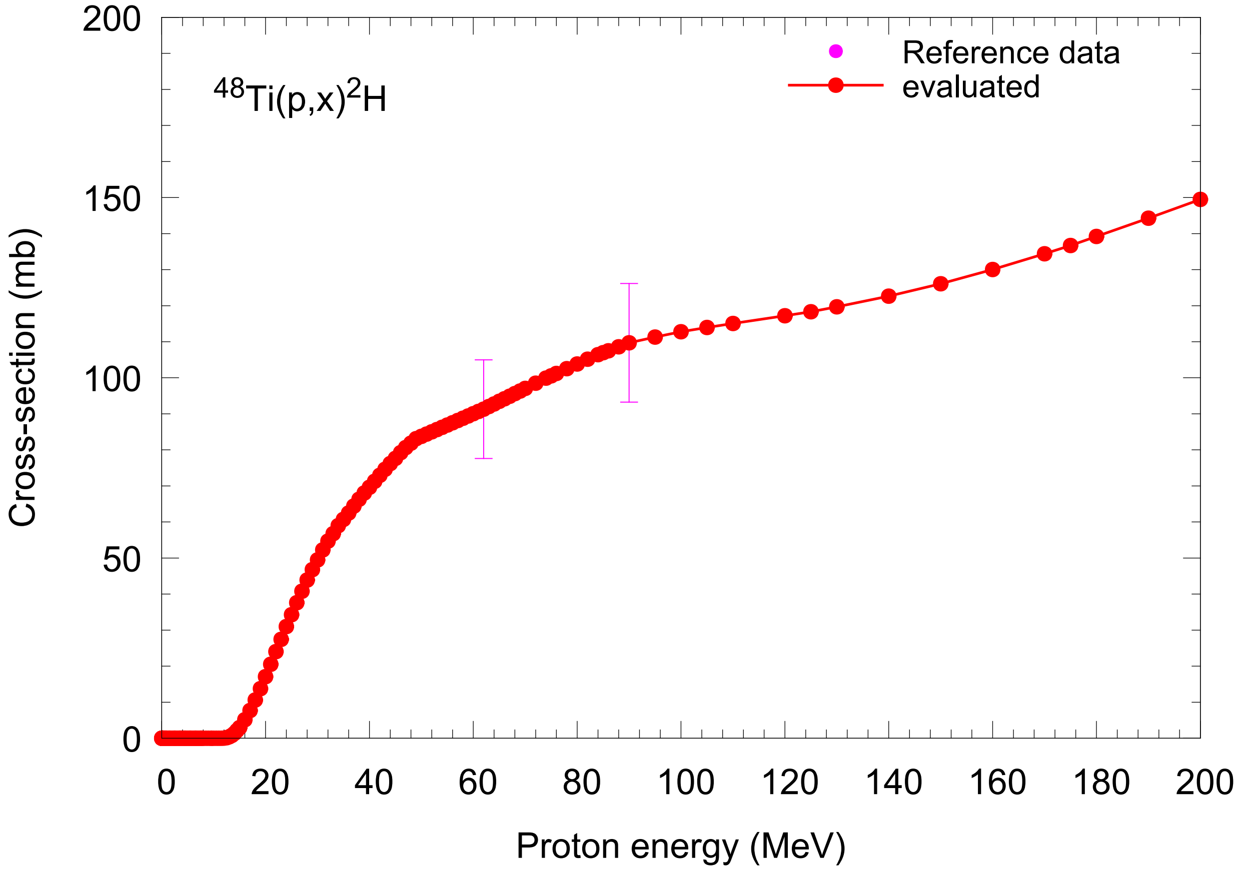

$^{48}Ti(p,x)^{2}H$
Reference data
evaluated
Cross-section (mb)
Proton energy (MeV)

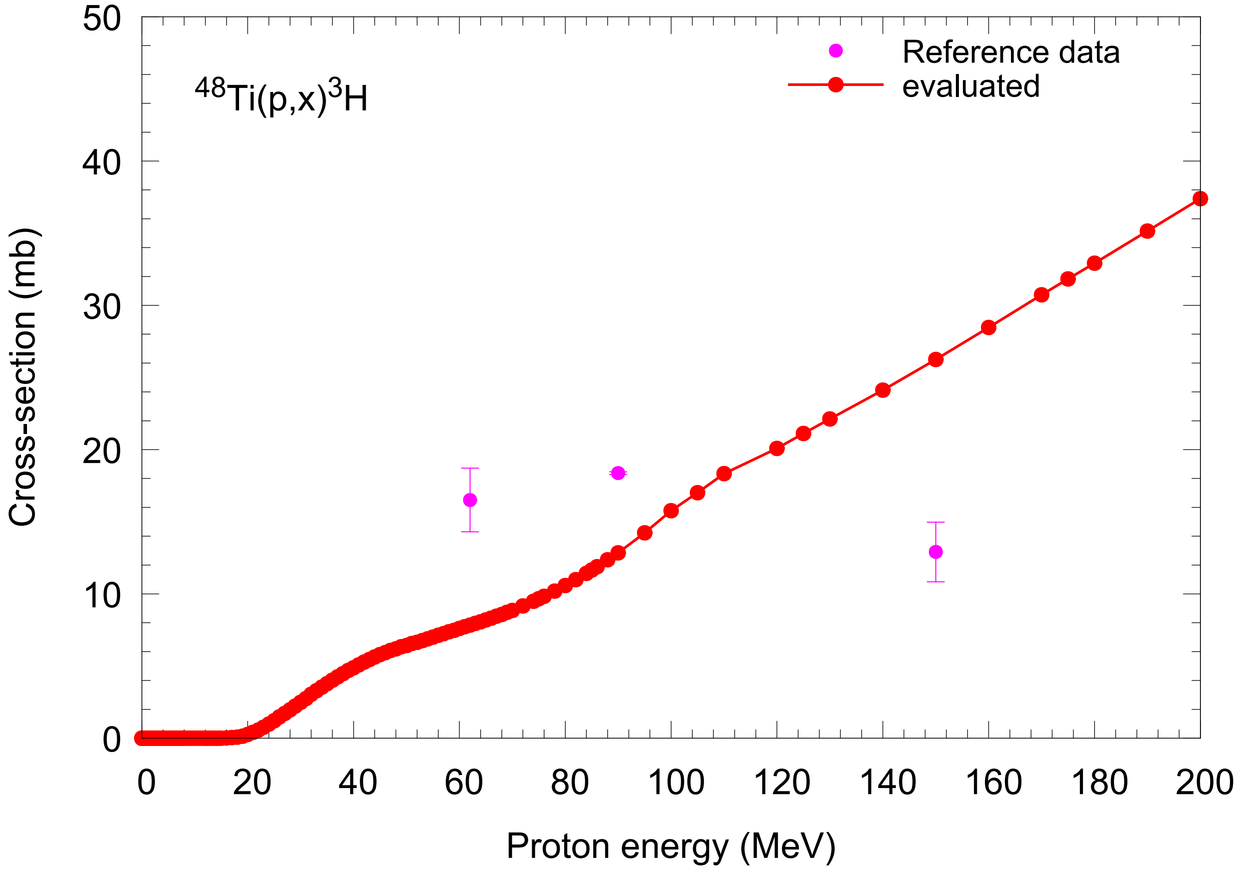

$^{48}Ti(p,x)^{3}H$
Reference data
evaluated
Cross-section (mb)
Proton energy (MeV)

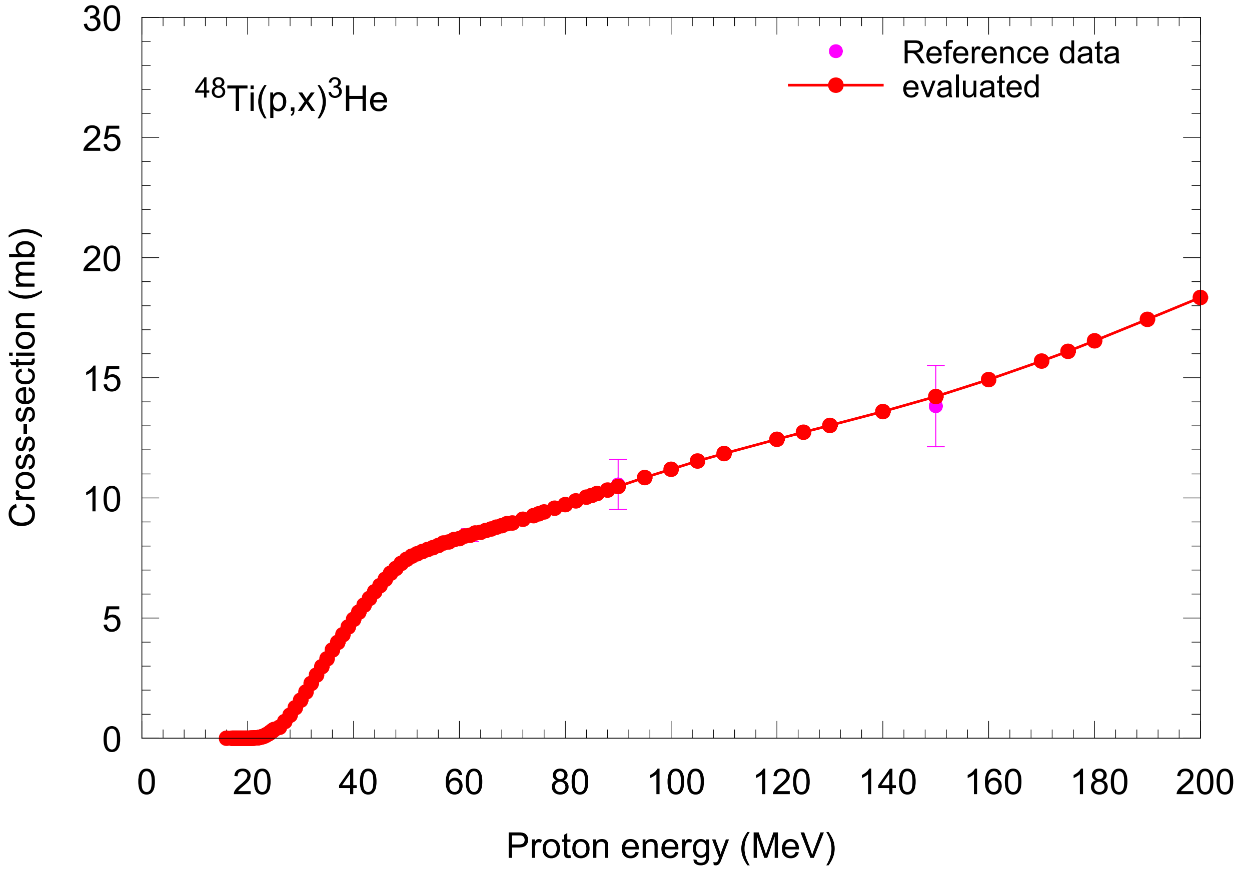

$^{48}Ti(p,x)^{3}He$
Reference data
evaluated
Cross-section (mb)
Proton energy (MeV)
0
5
10
15
20
25
30
0
20
40
60
80
100
120
140
160
180
200

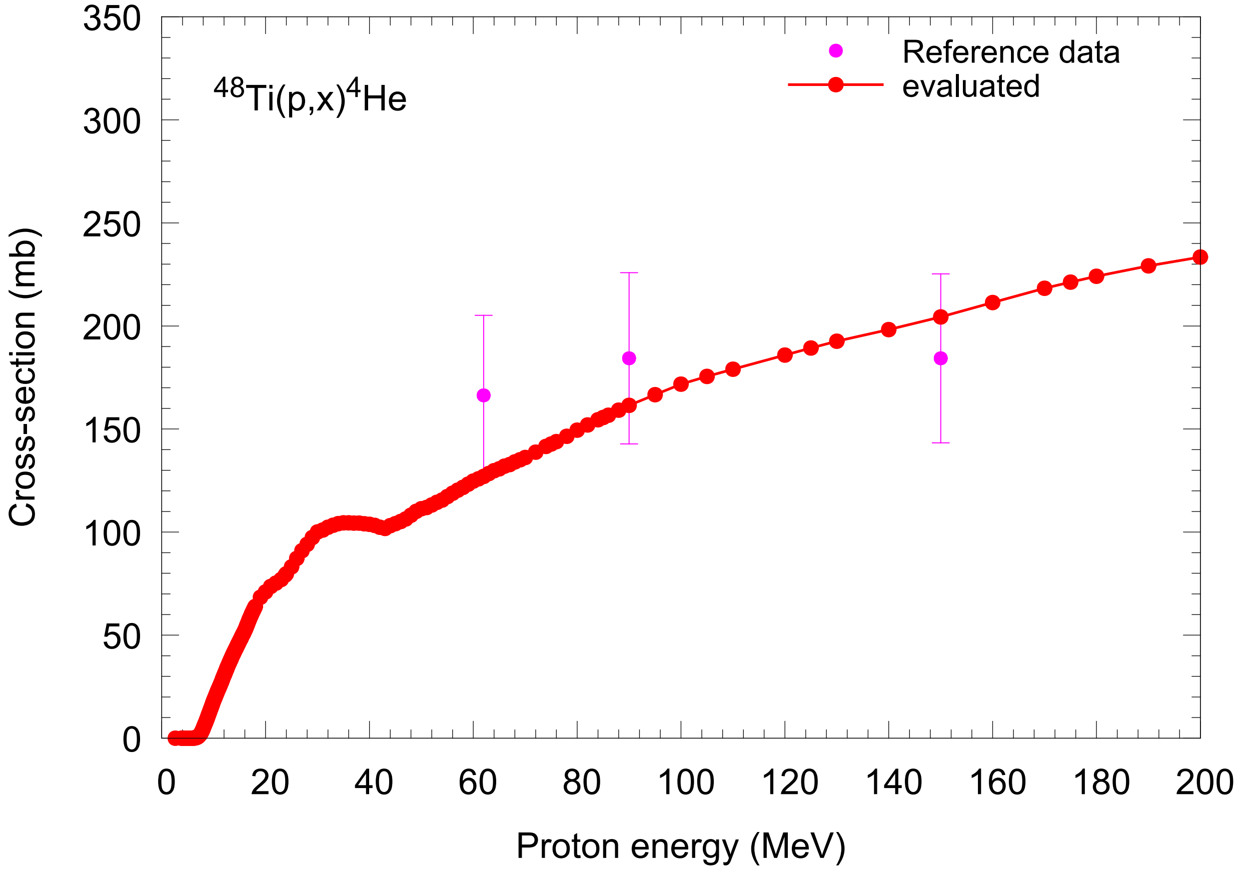

$^{48}Ti(p,x)^{4}He$
Reference data
evaluated
Cross-section (mb)
Proton energy (MeV)
0
50
100
150
200
250
300
350
0
20
40
60
80
100
120
140
160
180
200

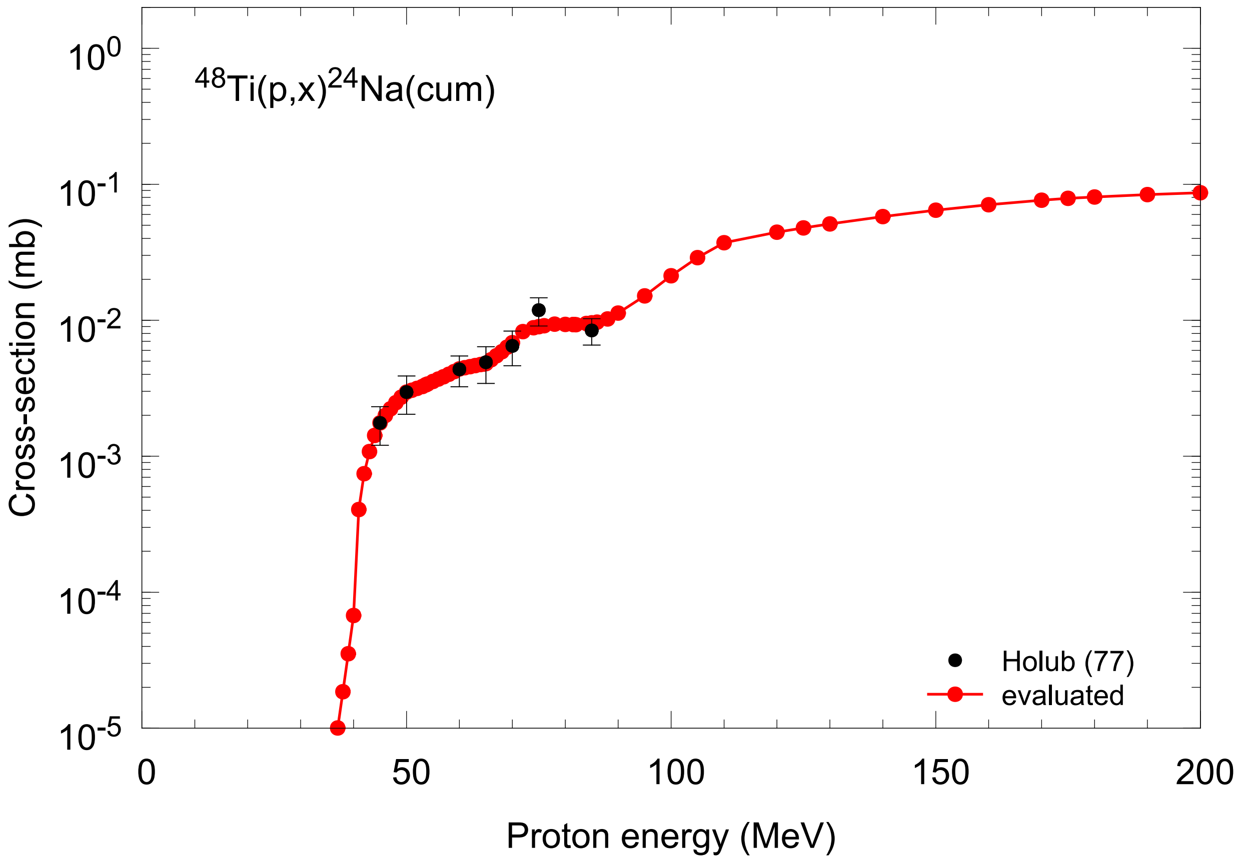

$^{48}Ti(p,x)^{24}Na(cum)$
Holub (77)
evaluated
Cross-section (mb)
Proton energy (MeV)

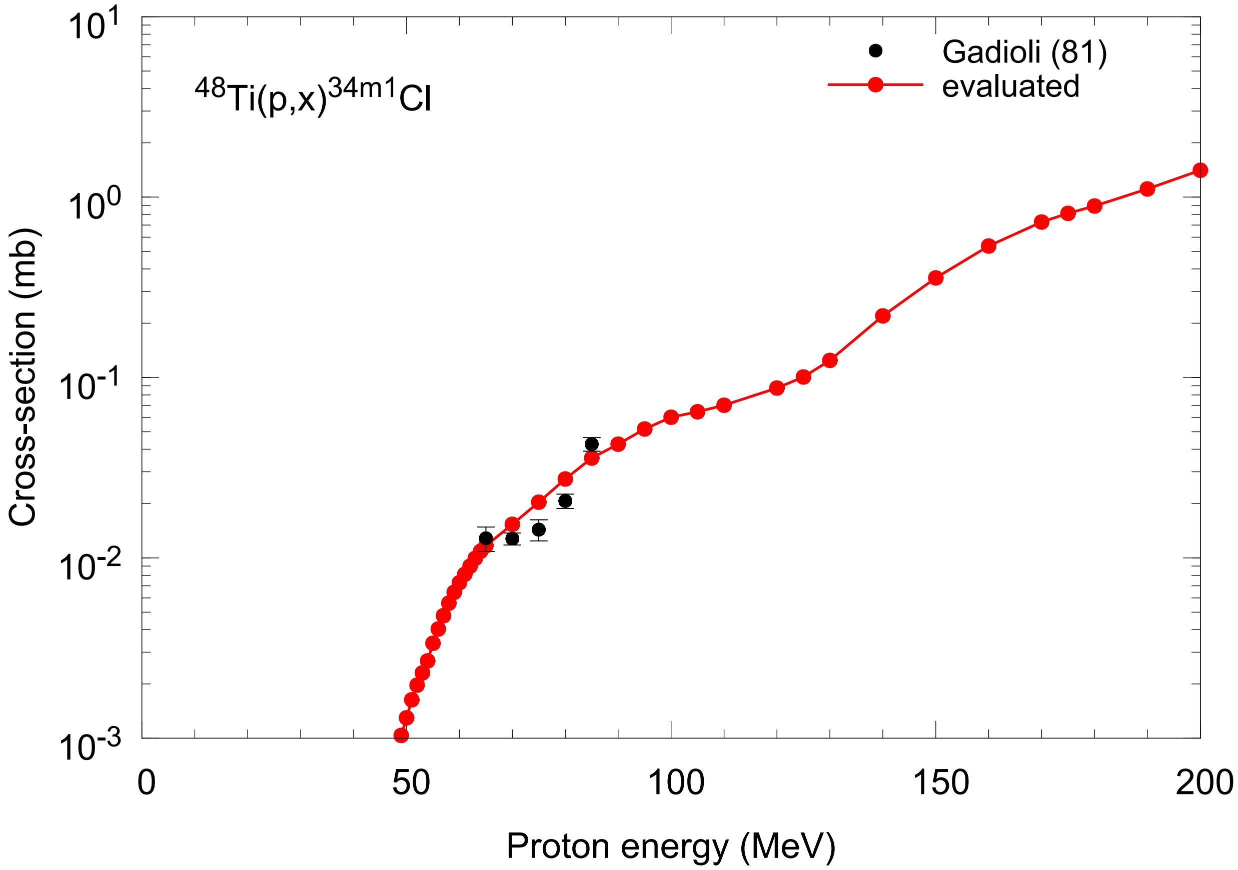

$^{48}Ti(p,x)^{34m1}Cl$
Gadioli (81)
evaluated
Cross-section (mb)
Proton energy (MeV)

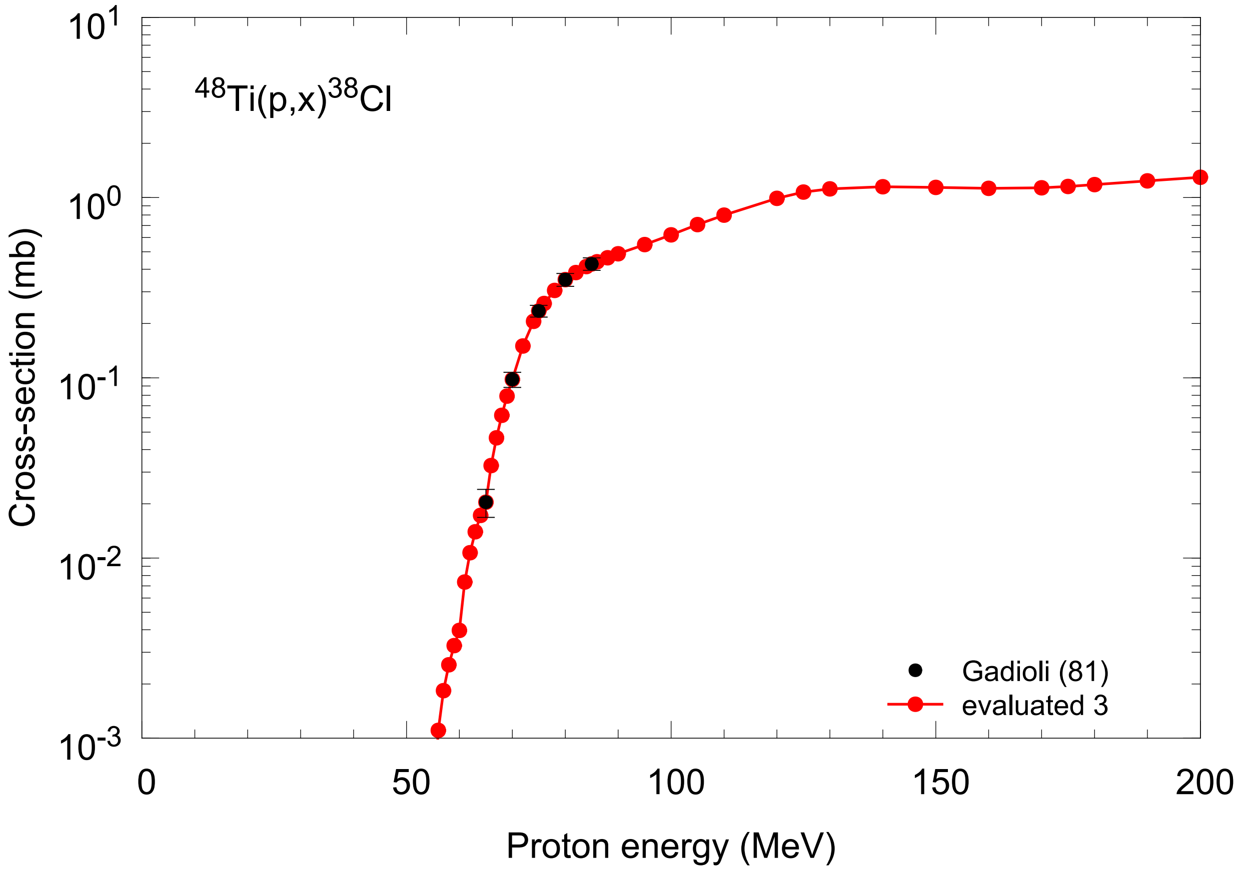
$^{48}Ti(p,x)^{38}Cl$
Cross-section (mb)
Proton energy (MeV)
Gadioli (81)
evaluated 3
10^1
10^0
10^-1
10^-2
10^-3
0
50
100
150
200

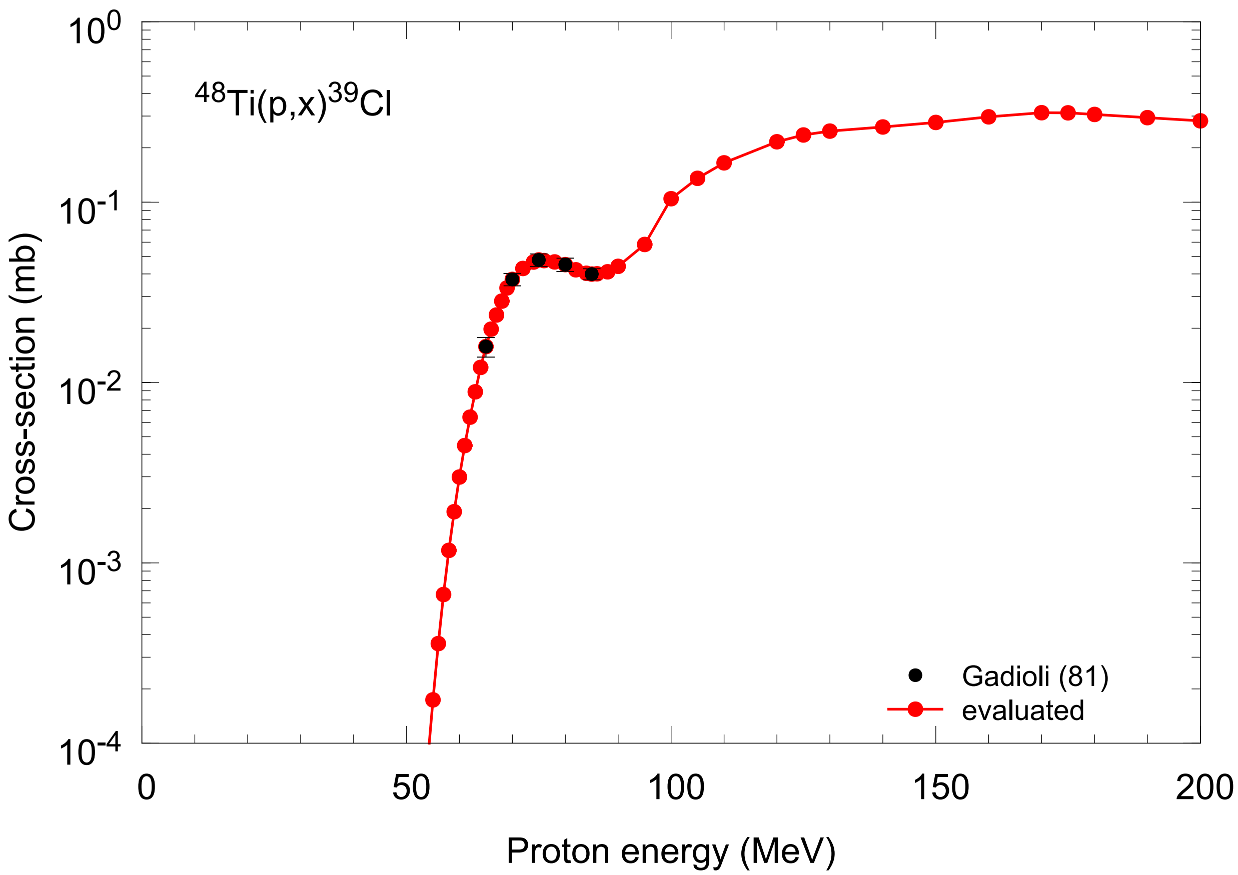
$^{48}Ti(p,x)^{39}Cl$
Cross-section (mb)
Proton energy (MeV)
Gadioli (81)
evaluated
10^0
10^-1
10^-2
10^-3
10^-4
0
50
100
150
200

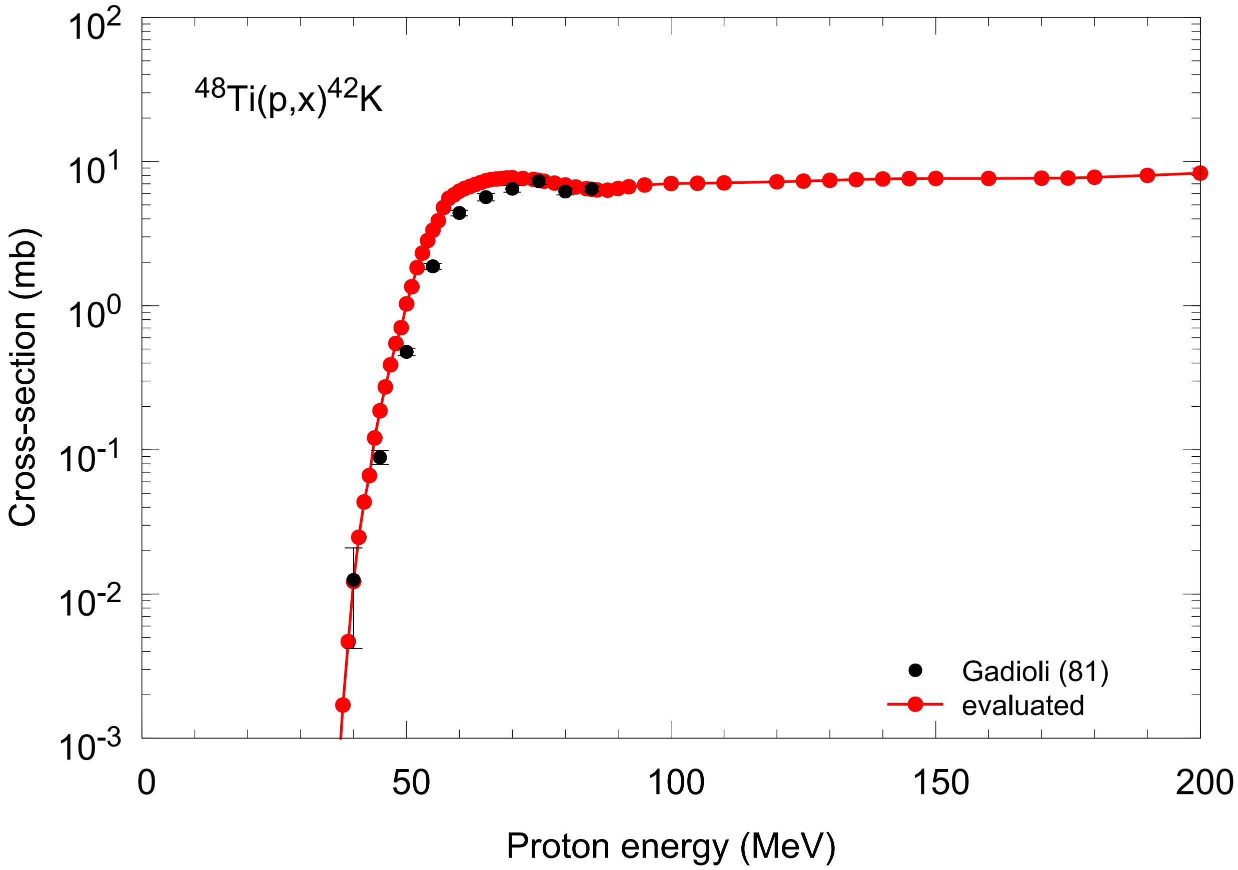

$^{48}Ti(p,x)^{42}K$
Cross-section (mb)
Proton energy (MeV)
Gadioli (81)
evaluated

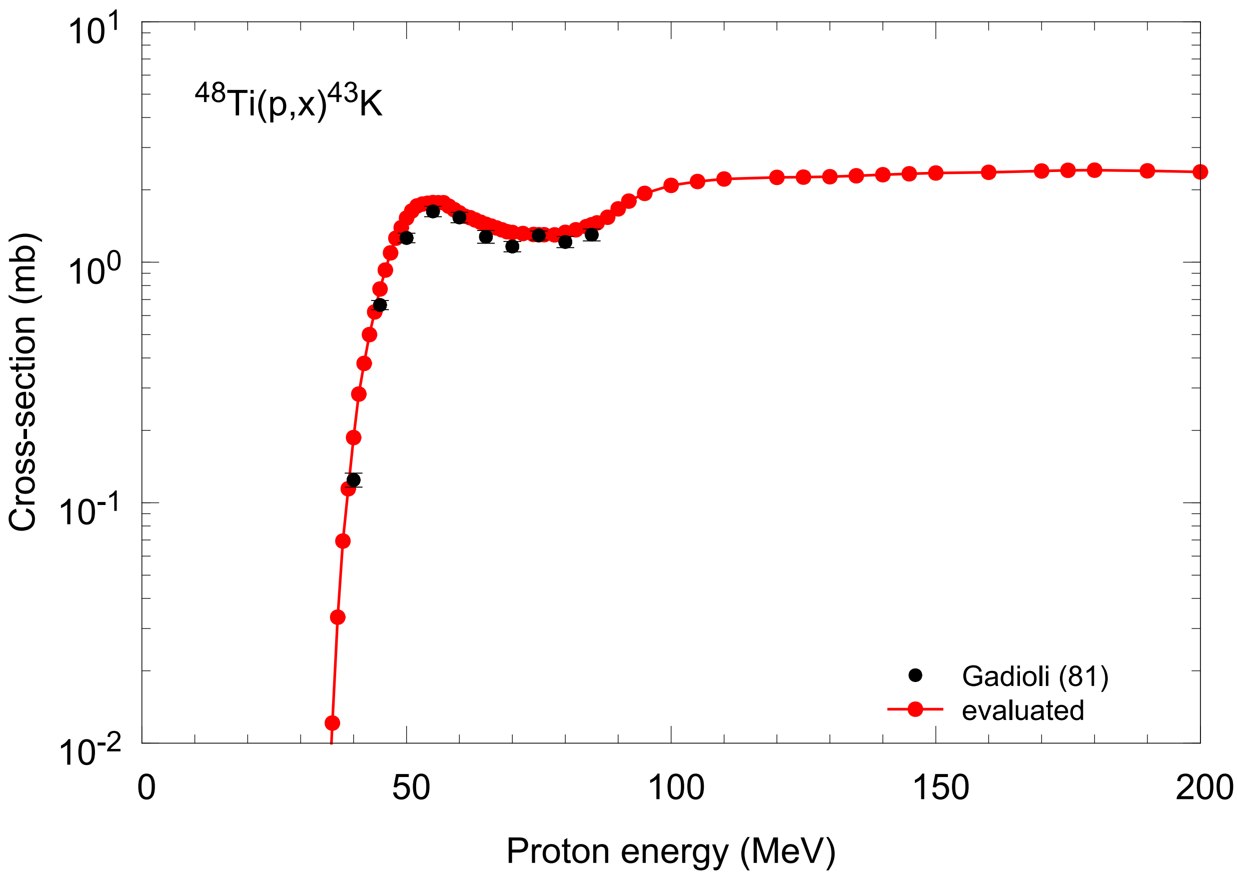

$^{48}Ti(p,x)^{43}K$
Cross-section (mb)
Proton energy (MeV)
Gadioli (81)
evaluated

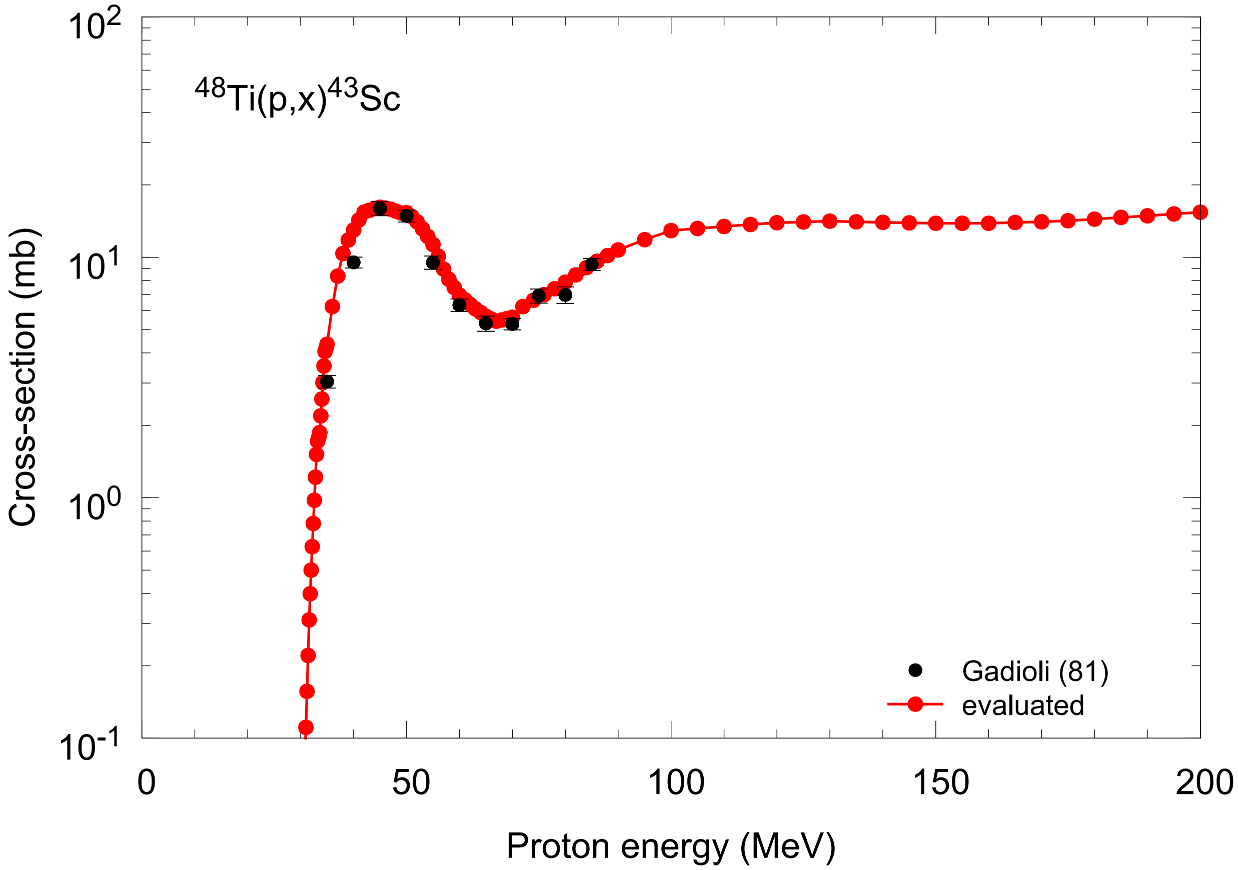

$^{48}Ti(p,x)^{43}Sc$
Cross-section (mb)
Proton energy (MeV)
Gadioli (81)
evaluated
10^{2}
10^{1}
10^{0}
10^{-1}
0
50
100
150
200

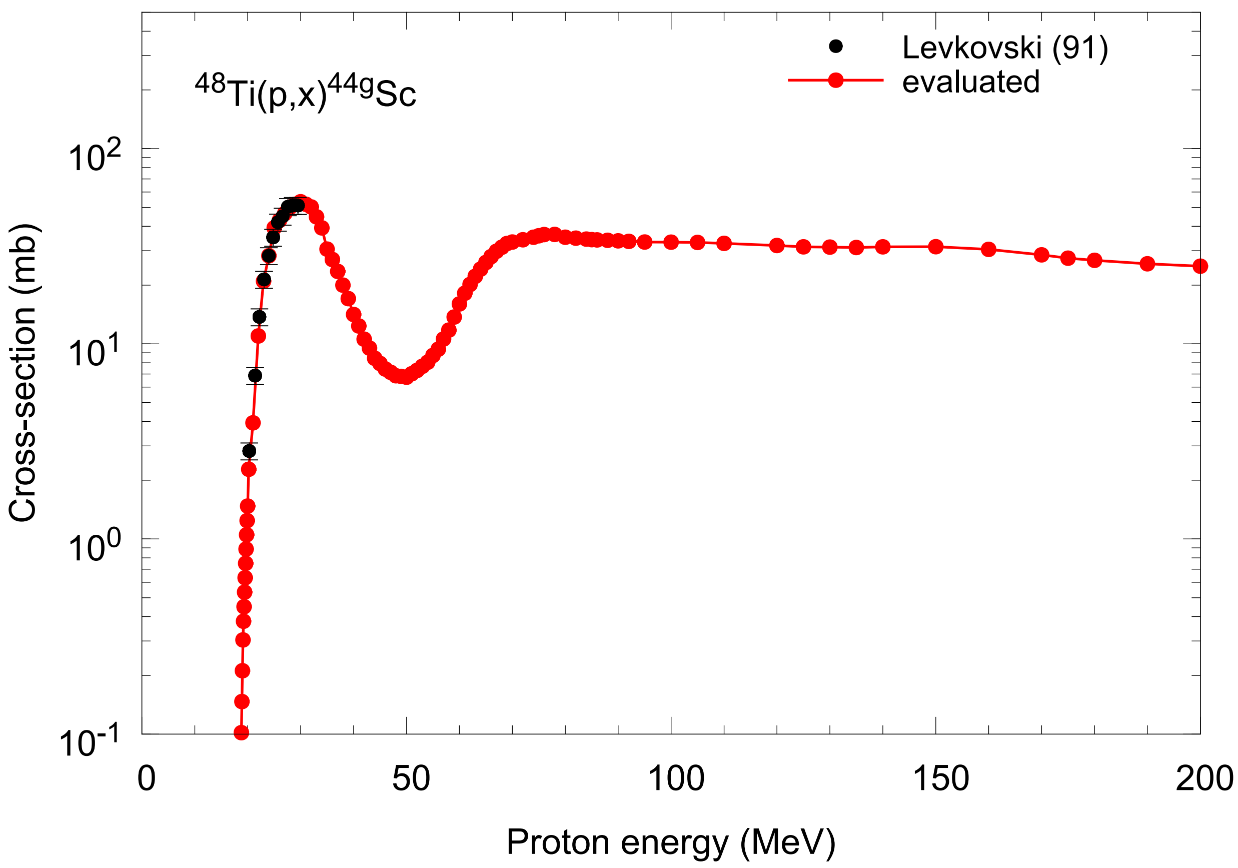

$^{48}Ti(p,x)^{44g}Sc$
Cross-section (mb)
Proton energy (MeV)
Levkovski (91)
evaluated
10^{2}
10^{1}
10^{0}
10^{-1}
0
50
100
150
200

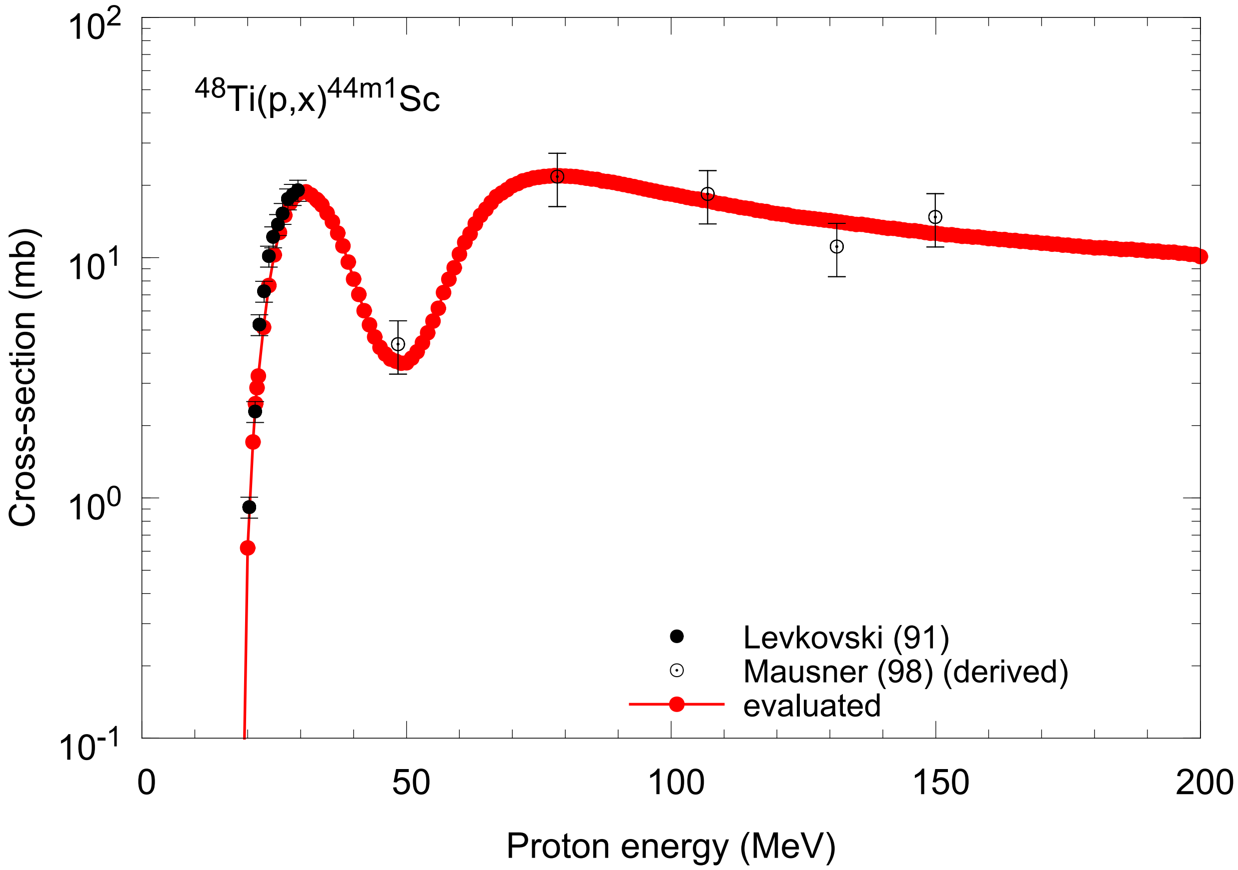

$^{48}Ti(p,x)^{44m1}Sc$
Cross-section (mb)
10^{2}
10^{1}
10^{0}
10^{-1}
0
50
100
150
200
Proton energy (MeV)
Levkovski (91)
Mausner (98) (derived)
evaluated

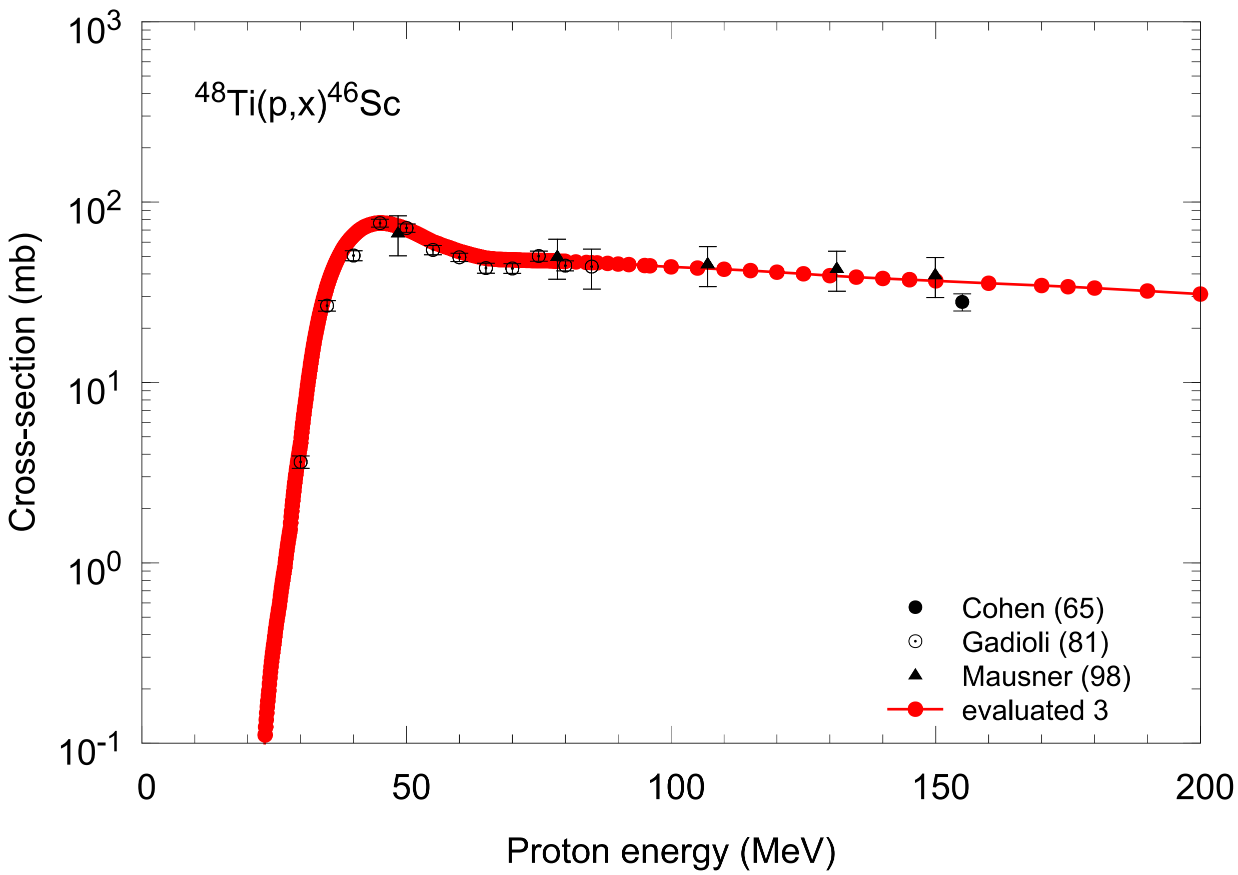

$^{48}Ti(p,x)^{46}Sc$
Cross-section (mb)
10^{3}
10^{2}
10^{1}
10^{0}
10^{-1}
0
50
100
150
200
Proton energy (MeV)
Cohen (65)
Gadioli (81)
Mausner (98)
evaluated 3

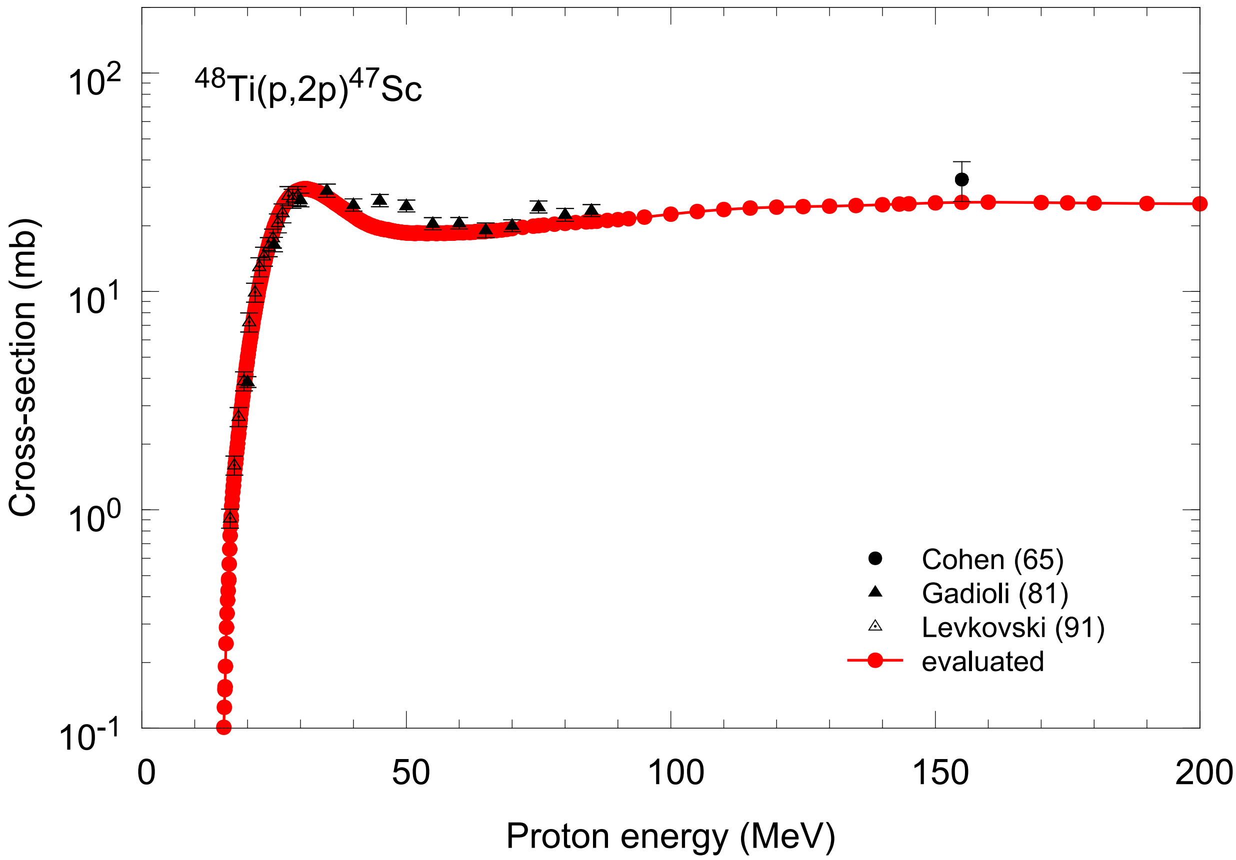

48Ti(p,2p)47Sc
Cohen (65)
Gadioli (81)
Levkovski (91)
evaluated
Cross-section (mb)
Proton energy (MeV)

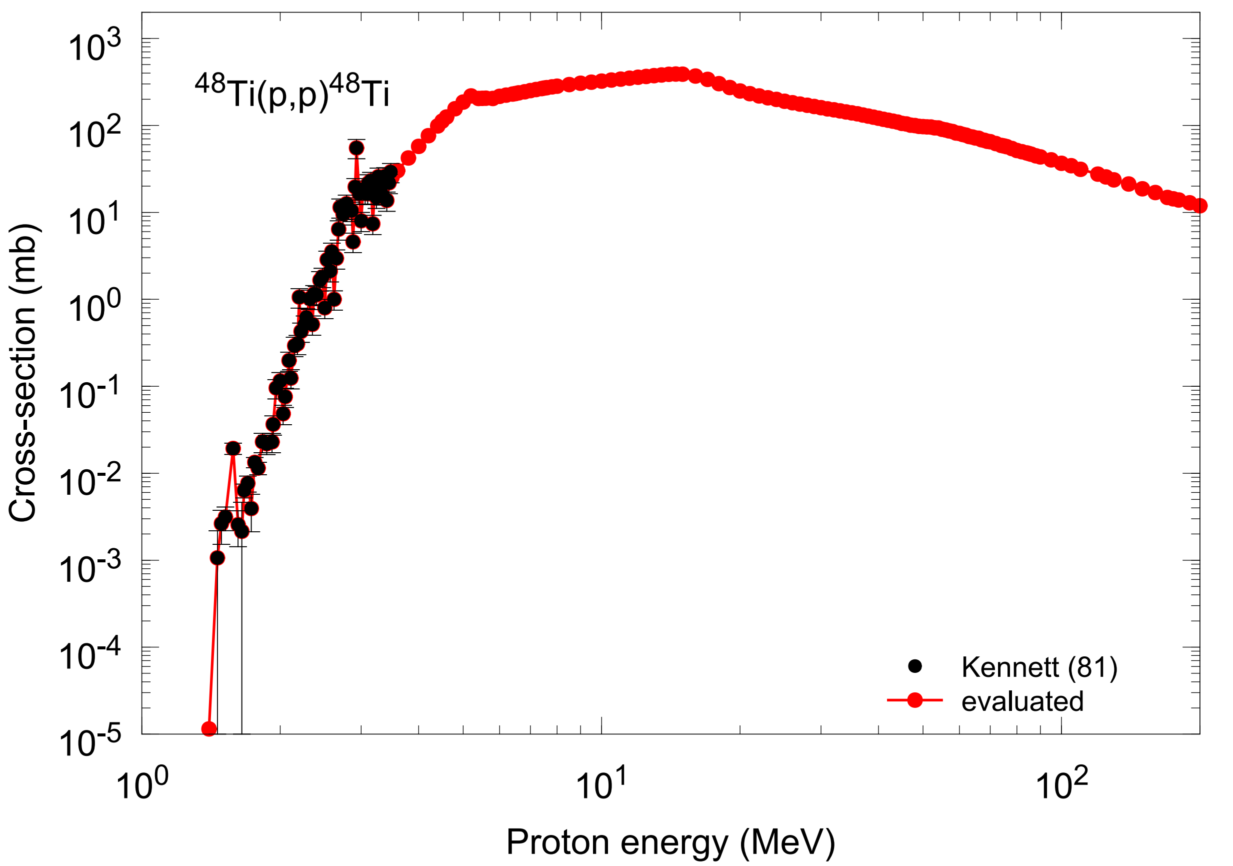

48Ti(p,p)48Ti
Kennett (81)
evaluated
Cross-section (mb)
Proton energy (MeV)

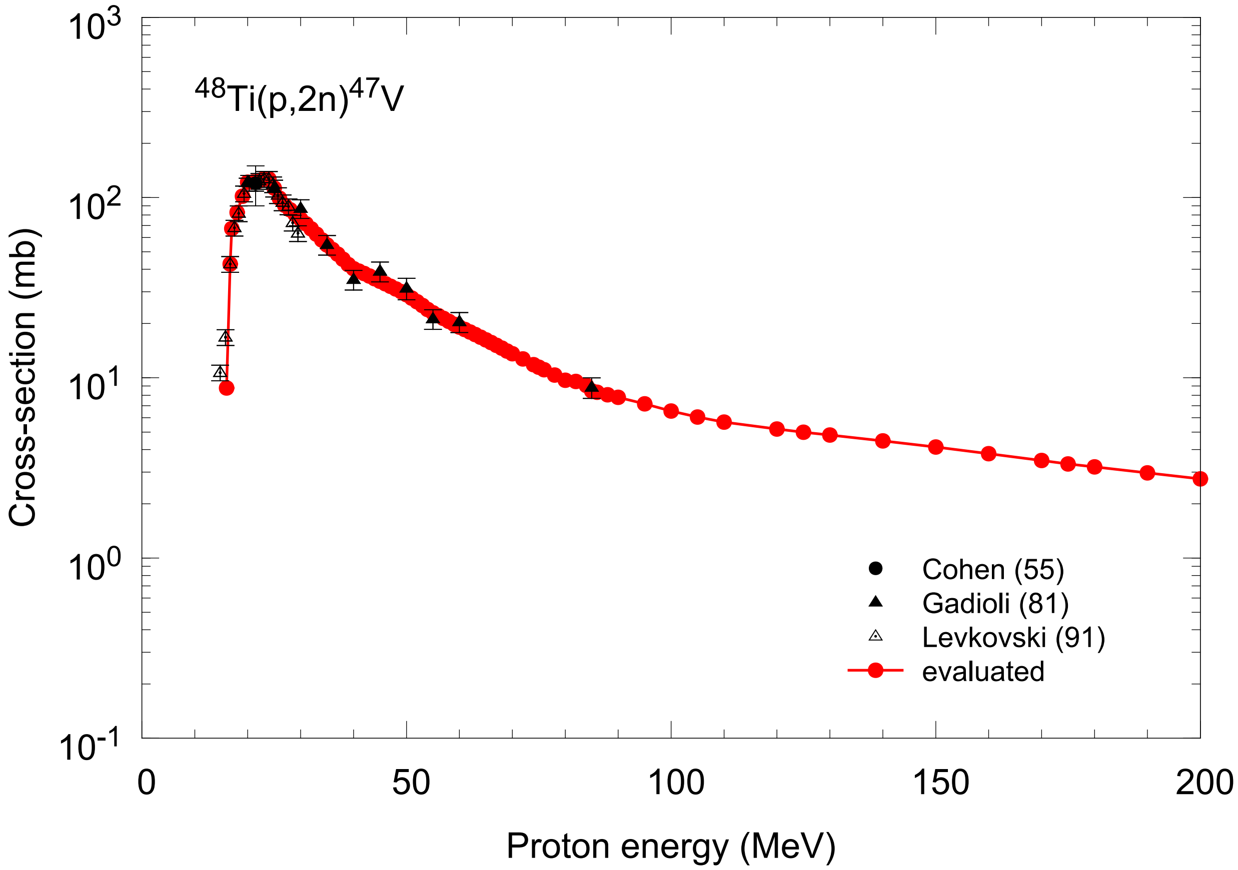
$^{48}Ti(p,2n)^{47}V$
Cross-section (mb)
Proton energy (MeV)
Cohen (55)
Gadioli (81)
Levkovski (91)
evaluated

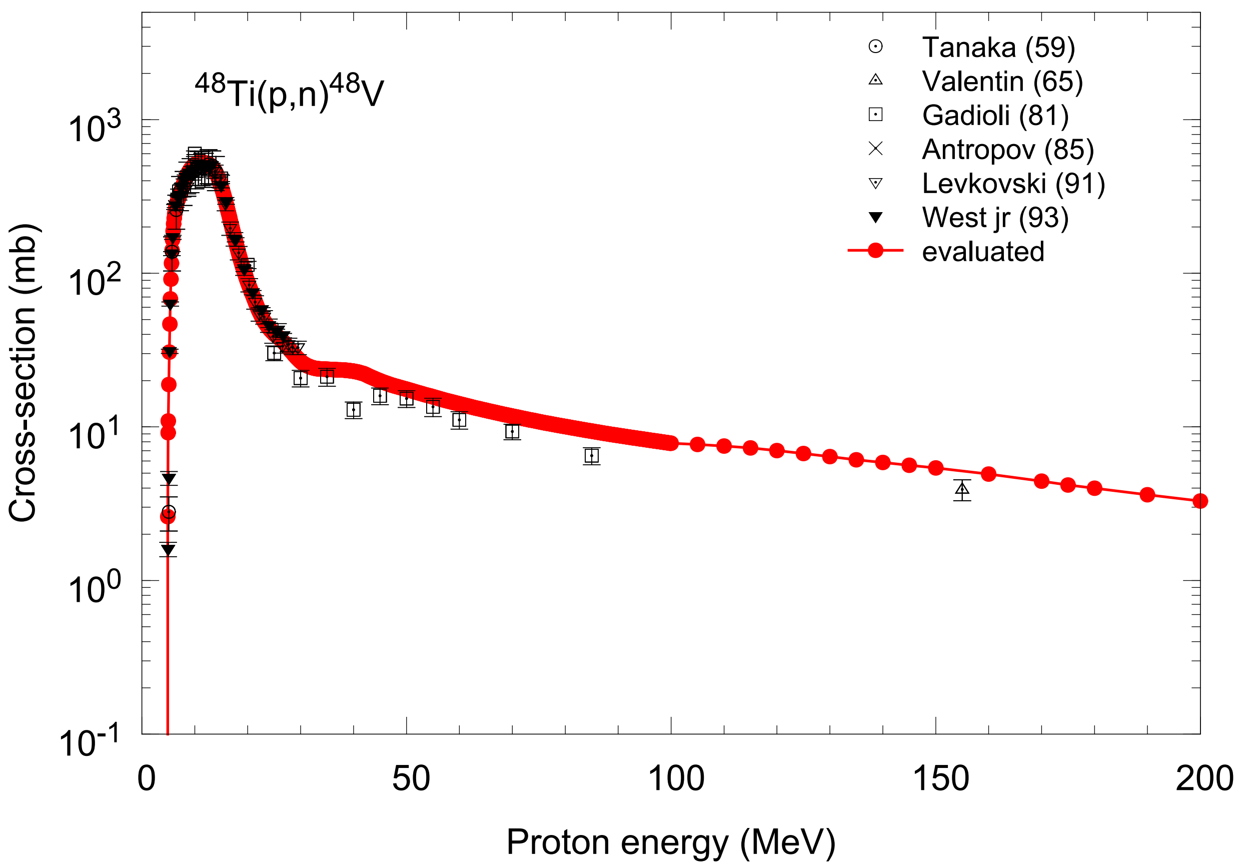
$^{48}Ti(p,n)^{48}V$
Cross-section (mb)
Proton energy (MeV)
Tanaka (59)
Valentin (65)
Gadioli (81)
Antropov (85)
Levkovski (91)
West jr (93)
evaluated

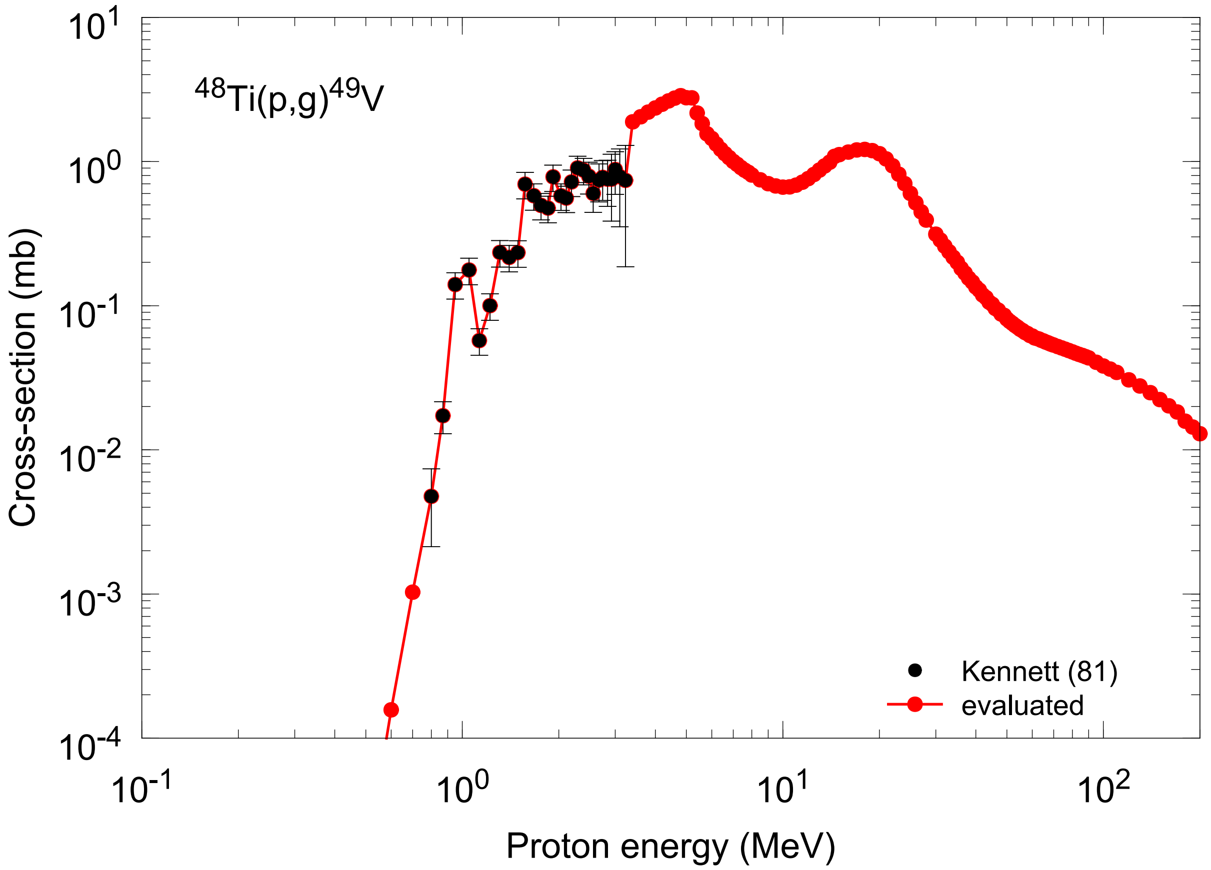

^{48}Ti(p,g)^{49}V
Cross-section (mb)
Proton energy (MeV)
Kennett (81)
evaluated
10^{1}
10^{0}
10^{-1}
10^{-2}
10^{-3}
10^{-4}
10^{-1}
10^{0}
10^{1}
10^{2}

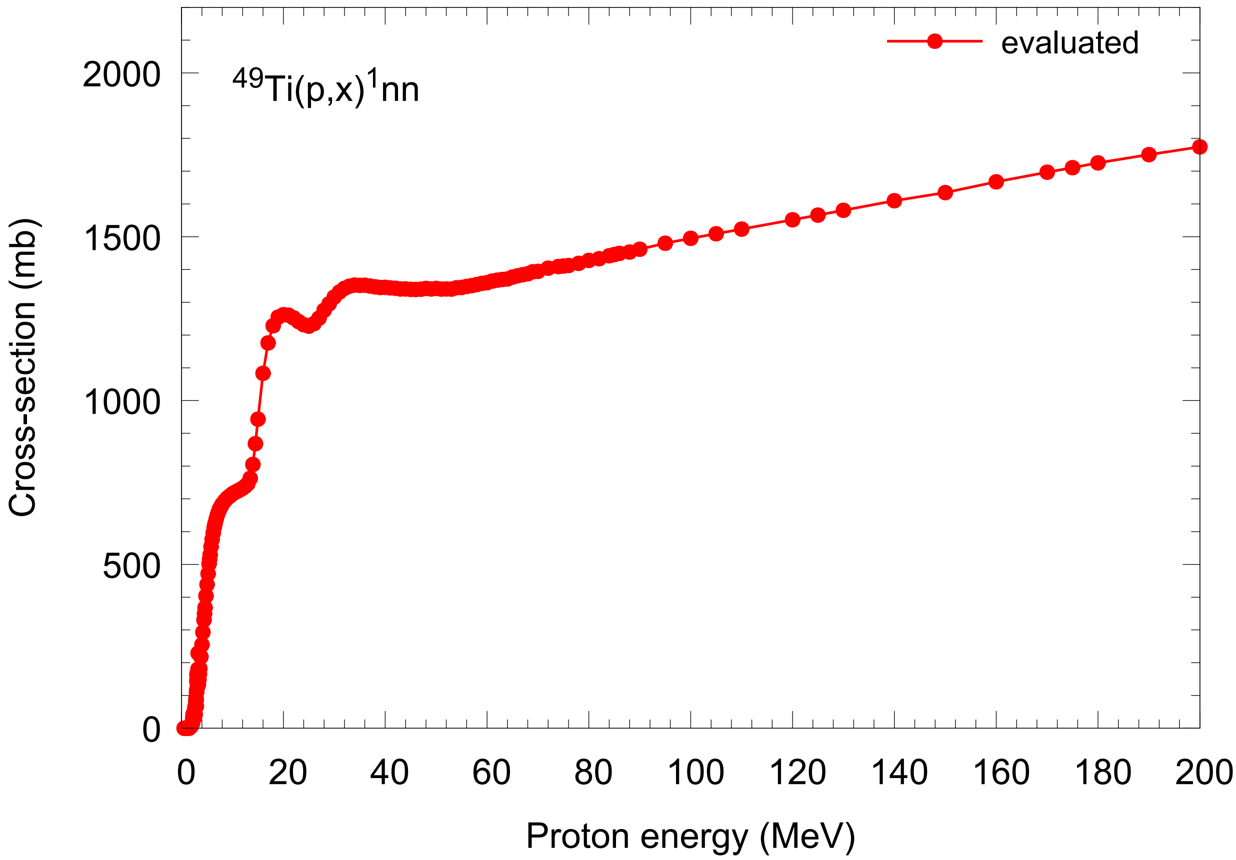

$^{49}Ti(p,x)^{1}nn$
evaluated
Cross-section (mb)
Proton energy (MeV)
0
500
1000
1500
2000
0
20
40
60
80
100
120
140
160
180
200

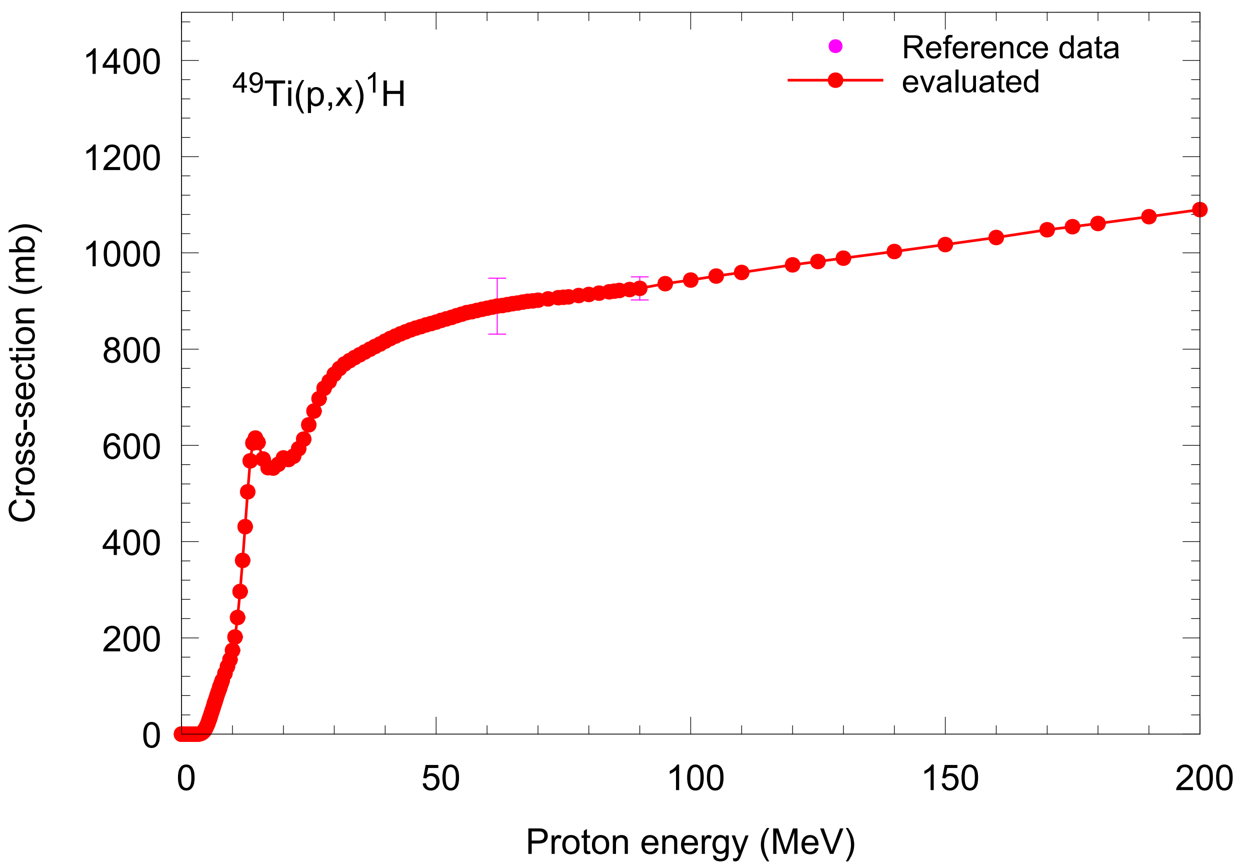

$^{49}Ti(p,x)^{1}H$
Reference data
evaluated
Cross-section (mb)
Proton energy (MeV)
0
200
400
600
800
1000
1200
1400
0
50
100
150
200

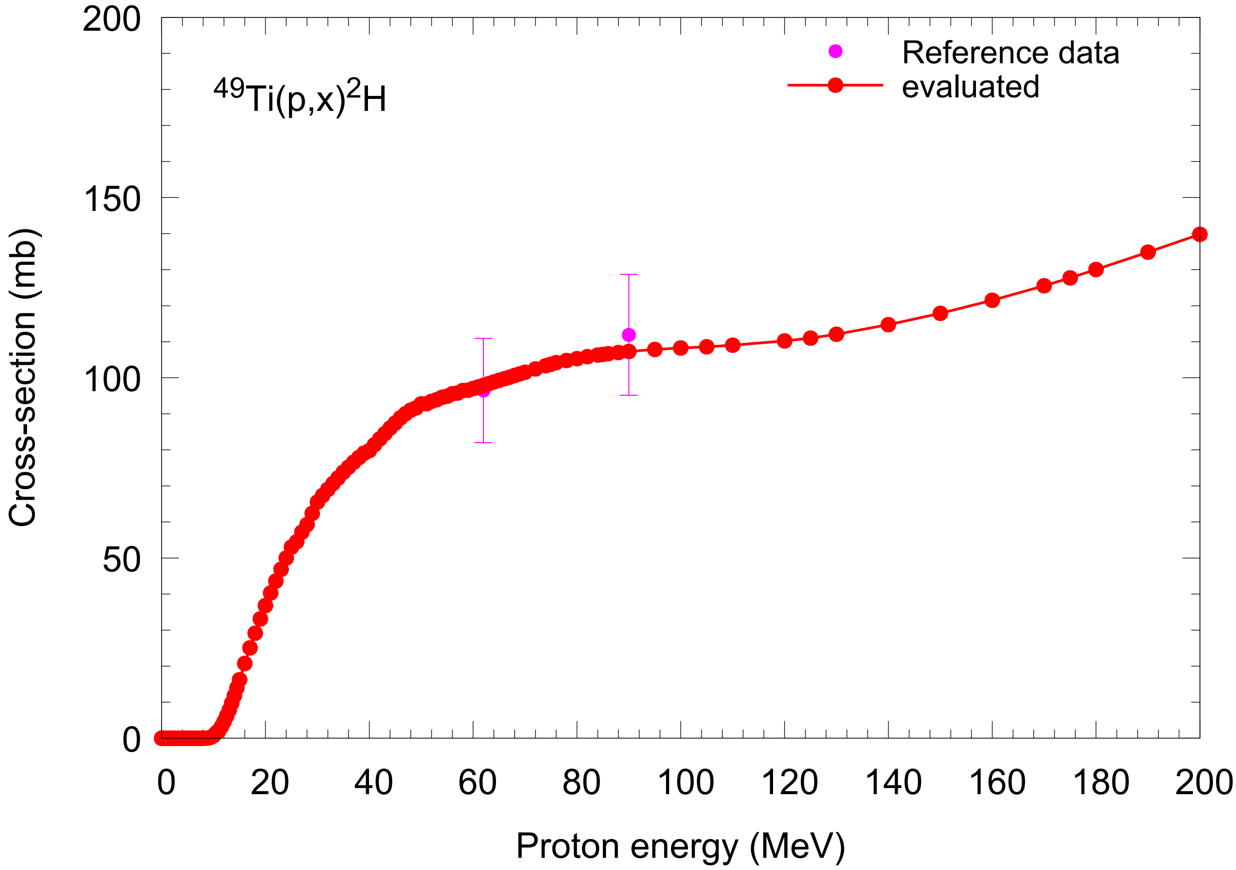

$^{49}Ti(p,x)^{2}H$
Reference data
evaluated
Cross-section (mb)
Proton energy (MeV)
0
50
100
150
200
0
20
40
60
80
100
120
140
160
180
200

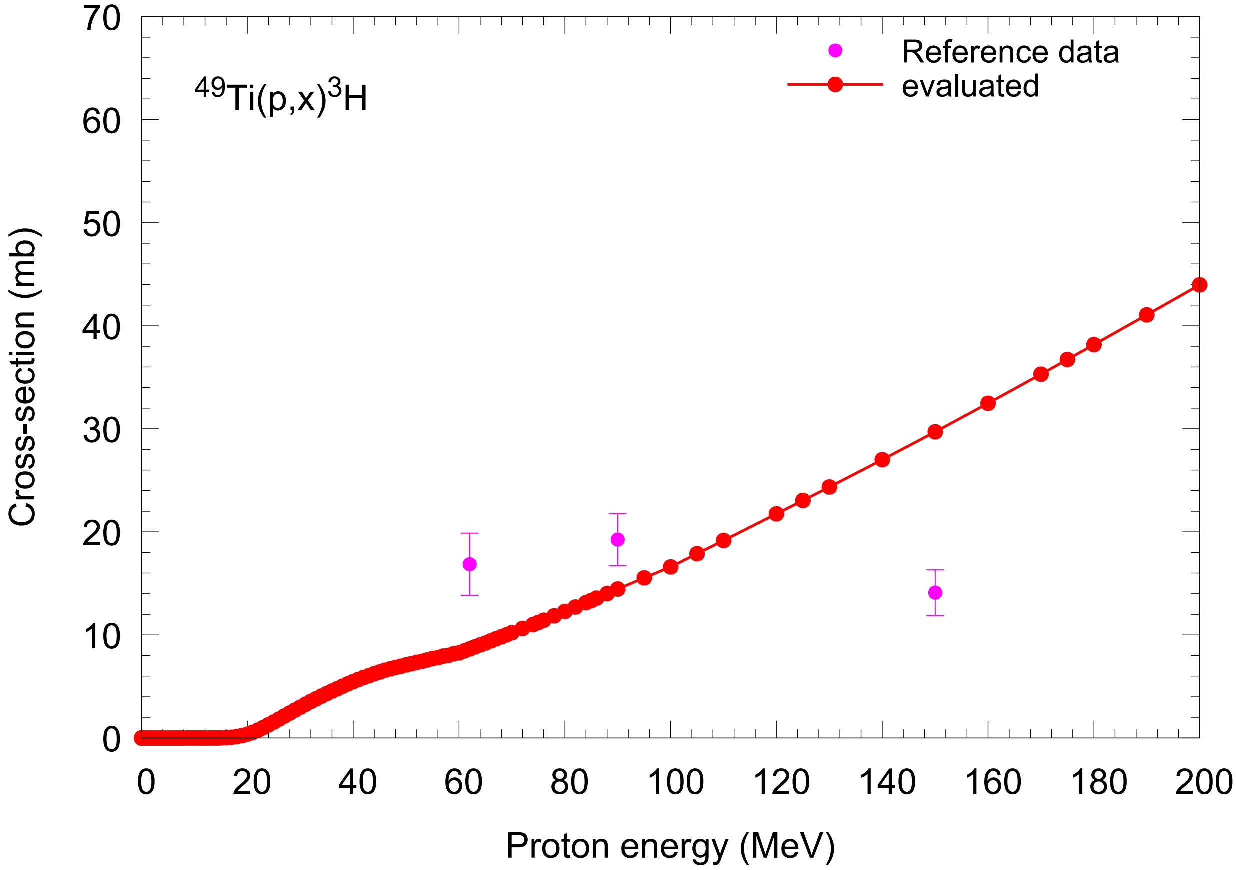

$^{49}Ti(p,x)^{3}H$
Reference data
evaluated
Cross-section (mb)
Proton energy (MeV)
0
10
20
30
40
50
60
70
0
20
40
60
80
100
120
140
160
180
200

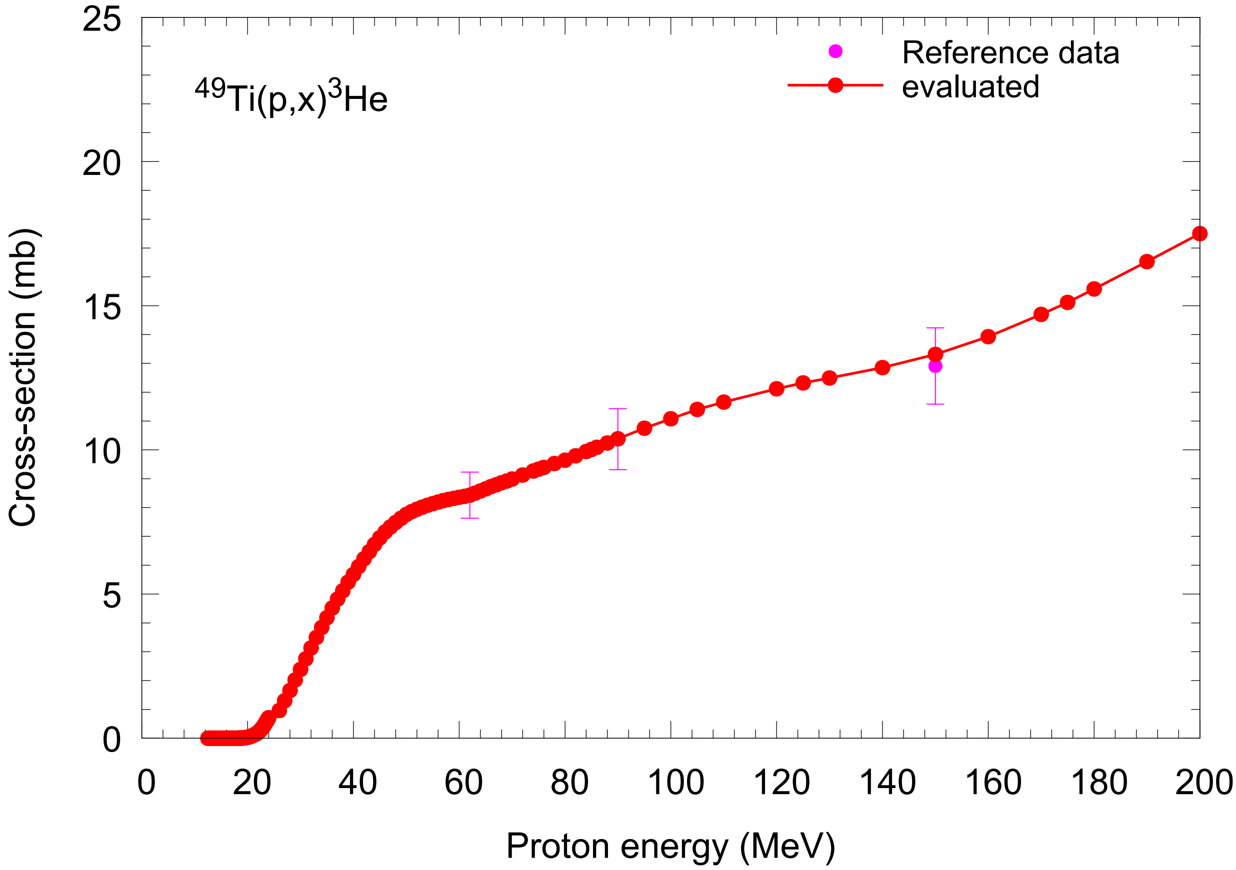

$^{49}Ti(p,x)^{3}He$
Reference data
evaluated
Cross-section (mb)
Proton energy (MeV)
0
5
10
15
20
25
0
20
40
60
80
100
120
140
160
180
200

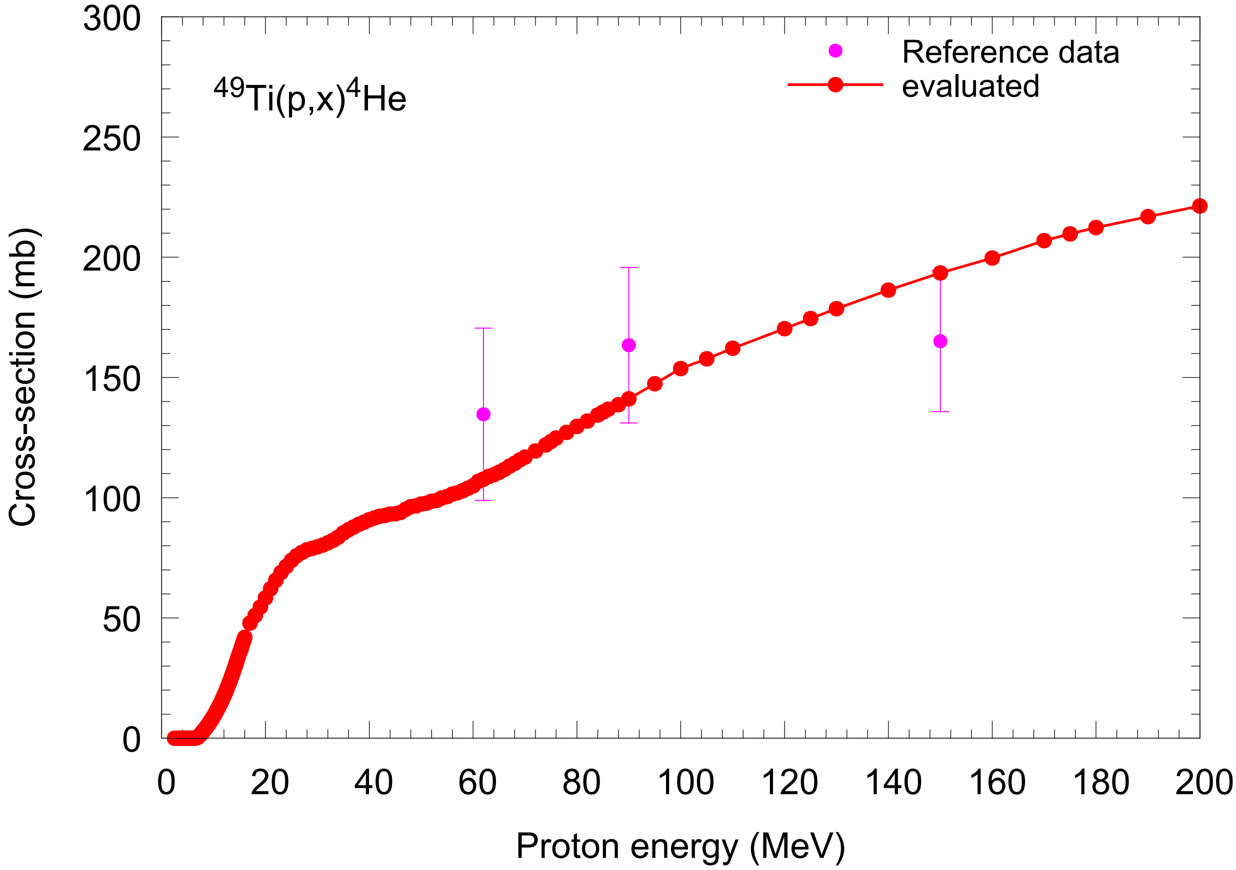

$^{49}Ti(p,x)^{4}He$
Reference data
evaluated
Cross-section (mb)
Proton energy (MeV)
0
50
100
150
200
250
300
0
20
40
60
80
100
120
140
160
180
200

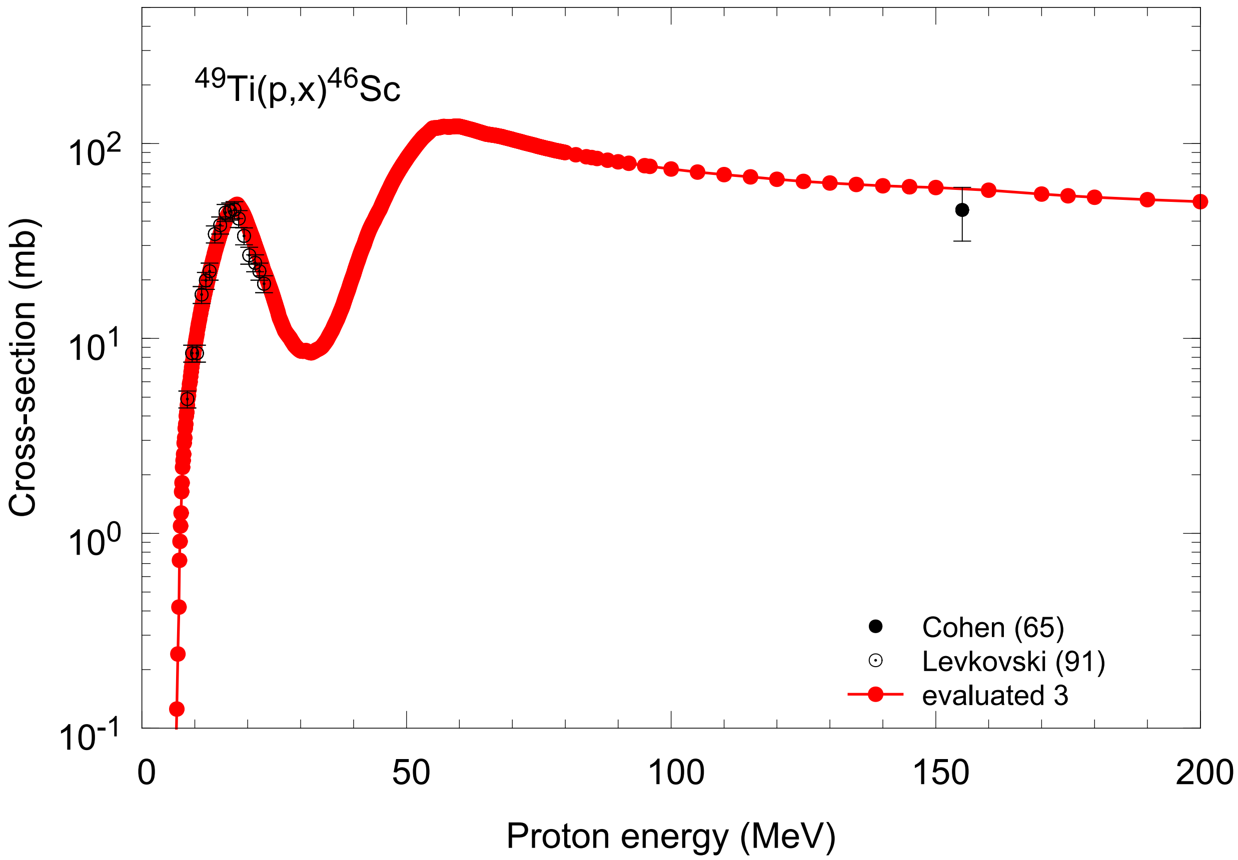

$^{49}Ti(p,x)^{46}Sc$
Cross-section (mb)
10^{-1}
10^{0}
10^{1}
10^{2}
0
50
100
150
200
Proton energy (MeV)
Cohen (65)
Levkovski (91)
evaluated 3

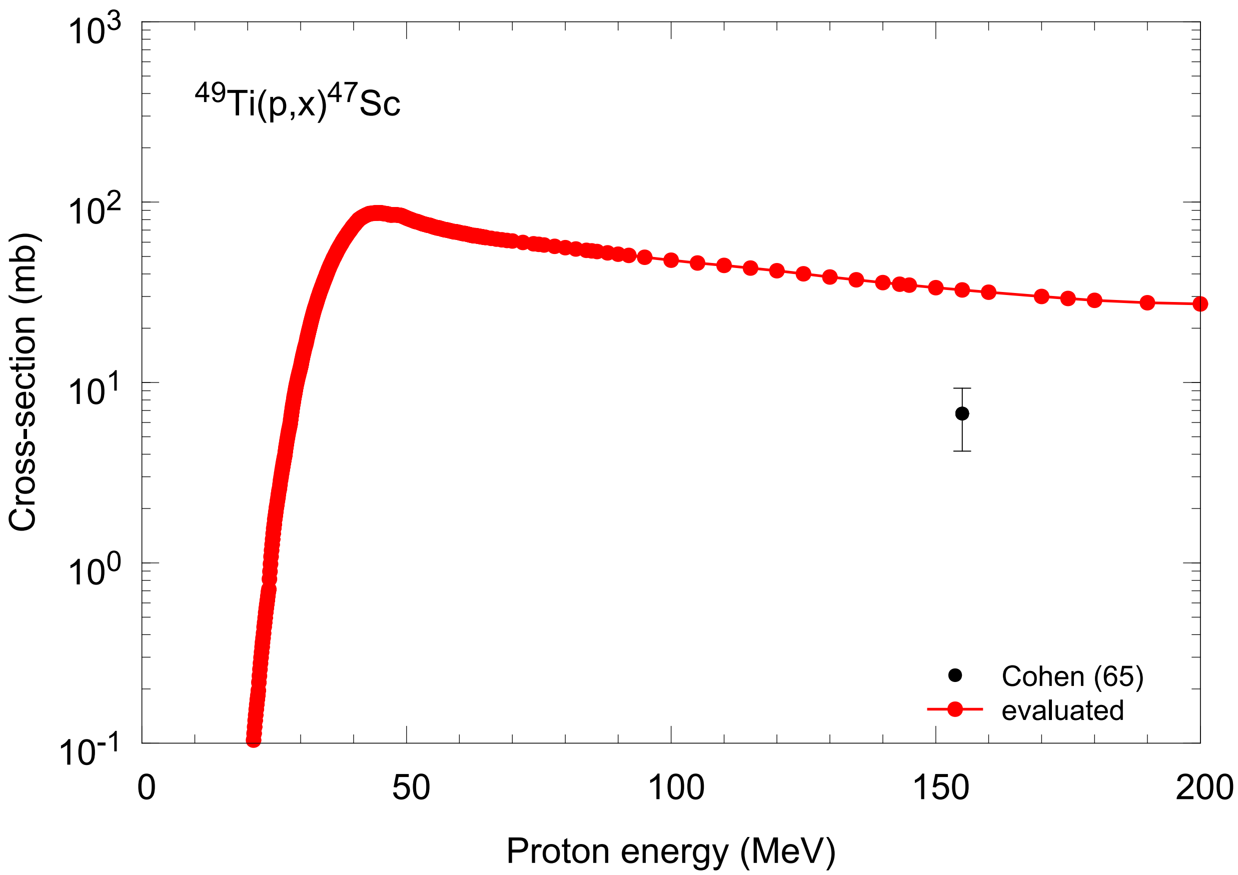

$^{49}Ti(p,x)^{47}Sc$
Cross-section (mb)
10^{-1}
10^{0}
10^{1}
10^{2}
10^{3}
0
50
100
150
200
Proton energy (MeV)
Cohen (65)
evaluated

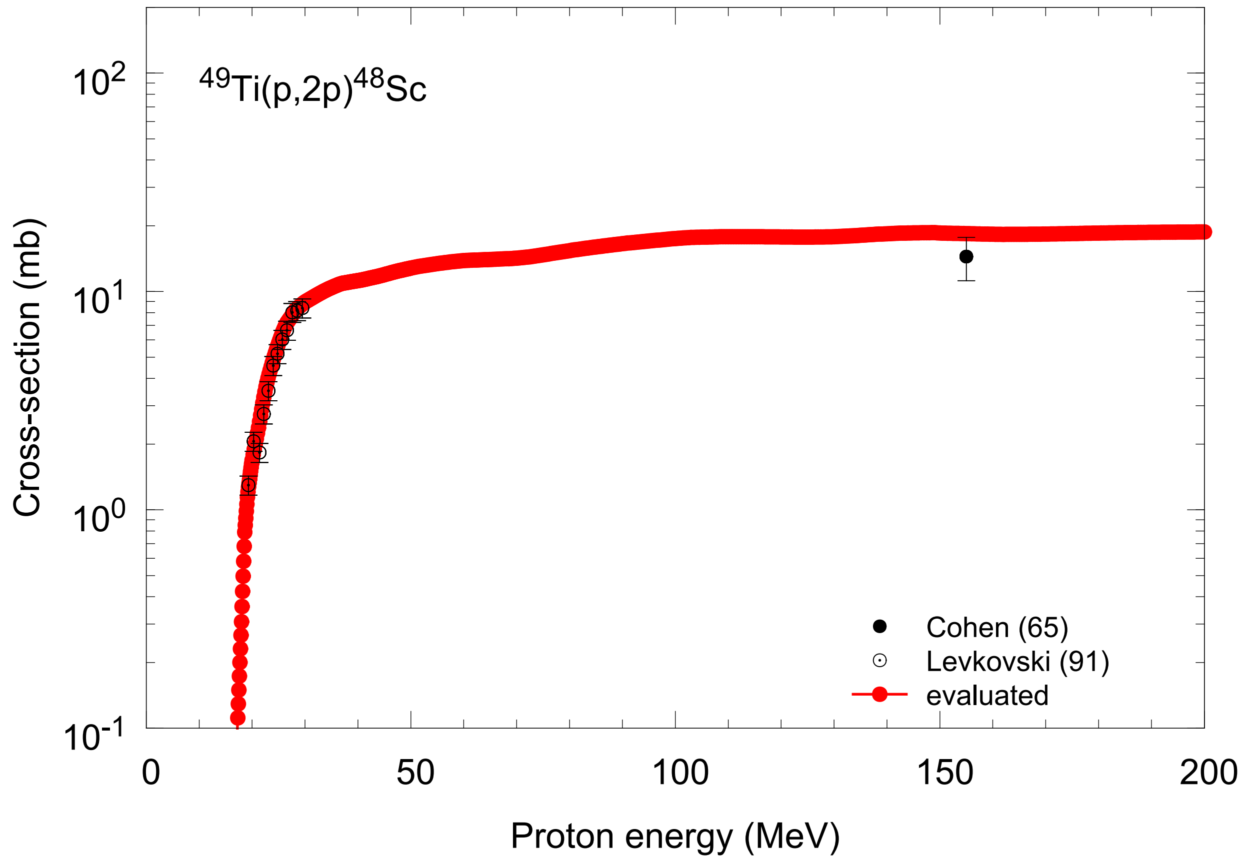
$^{49}Ti(p,2p)^{48}Sc$
Cross-section (mb)
Proton energy (MeV)
Cohen (65)
Levkovski (91)
evaluated

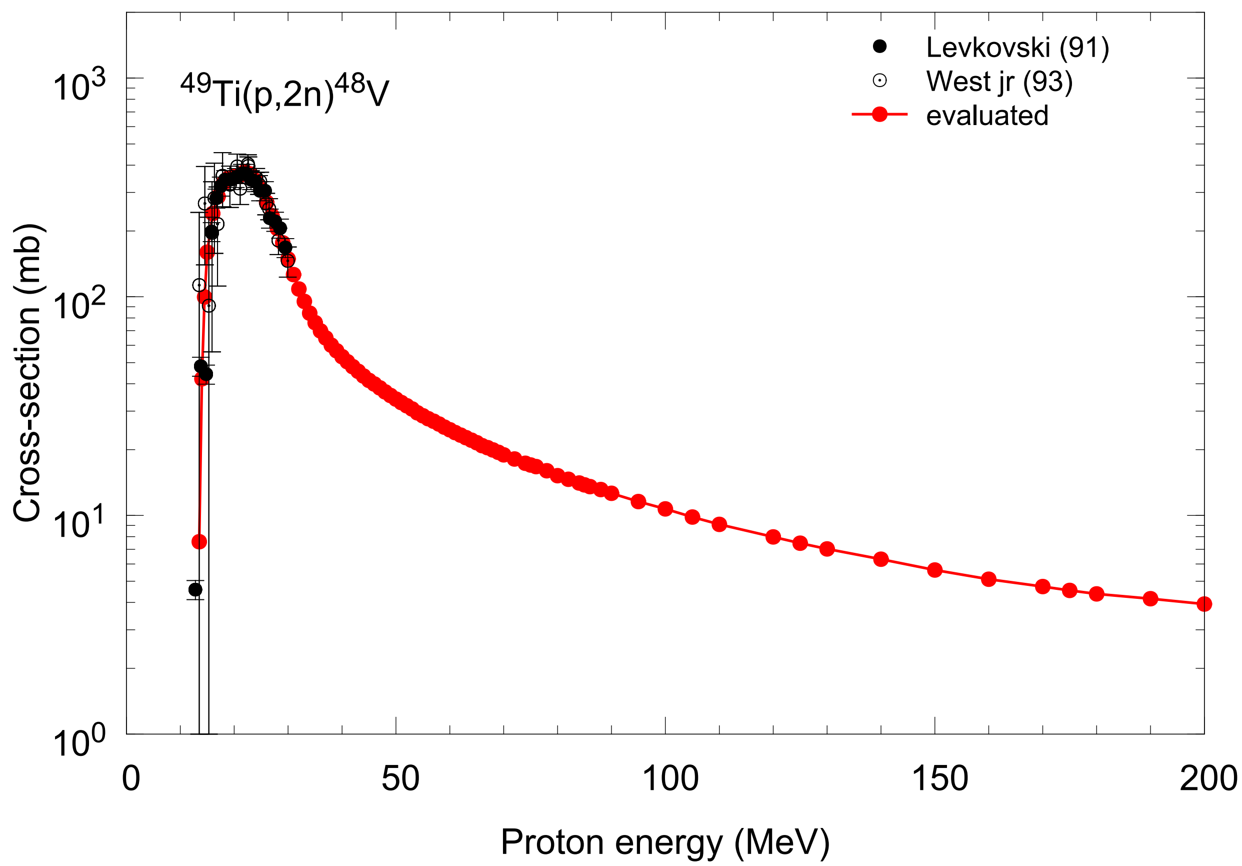
$^{49}Ti(p,2n)^{48}V$
Cross-section (mb)
Proton energy (MeV)
Levkovski (91)
West jr (93)
evaluated

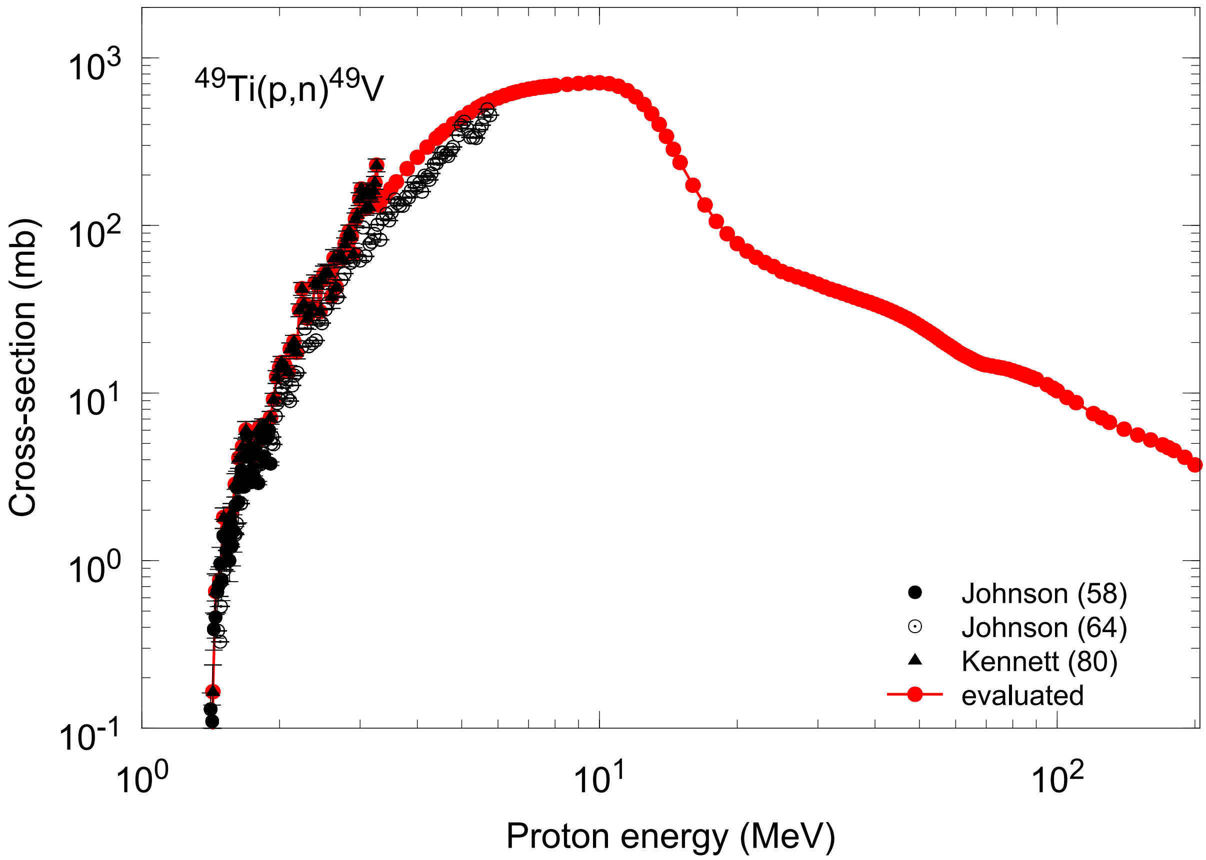
$^{49}Ti(p,n)^{49}V$
Cross-section (mb)
Proton energy (MeV)
Johnson (58)
Johnson (64)
Kennett (80)
evaluated

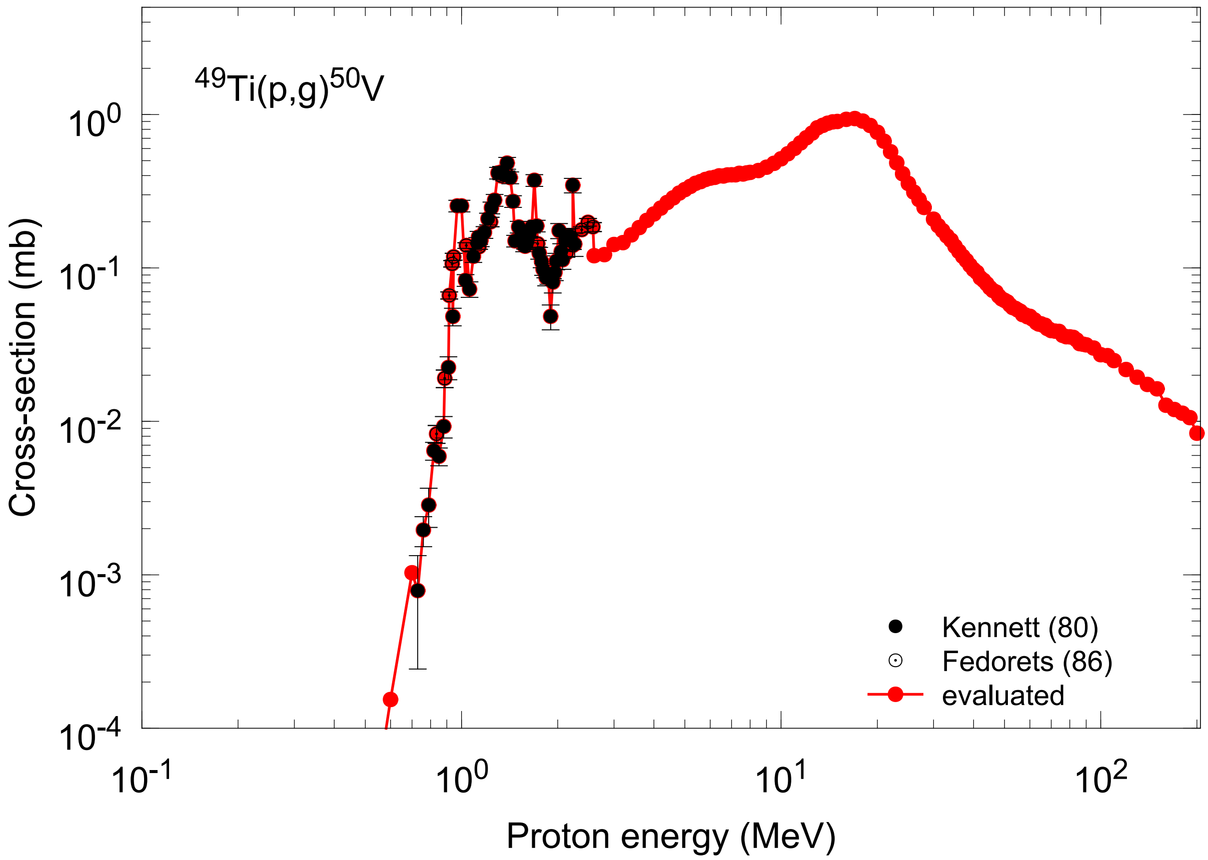
$^{49}Ti(p,g)^{50}V$
Cross-section (mb)
Proton energy (MeV)
Kennett (80)
Fedorets (86)
evaluated

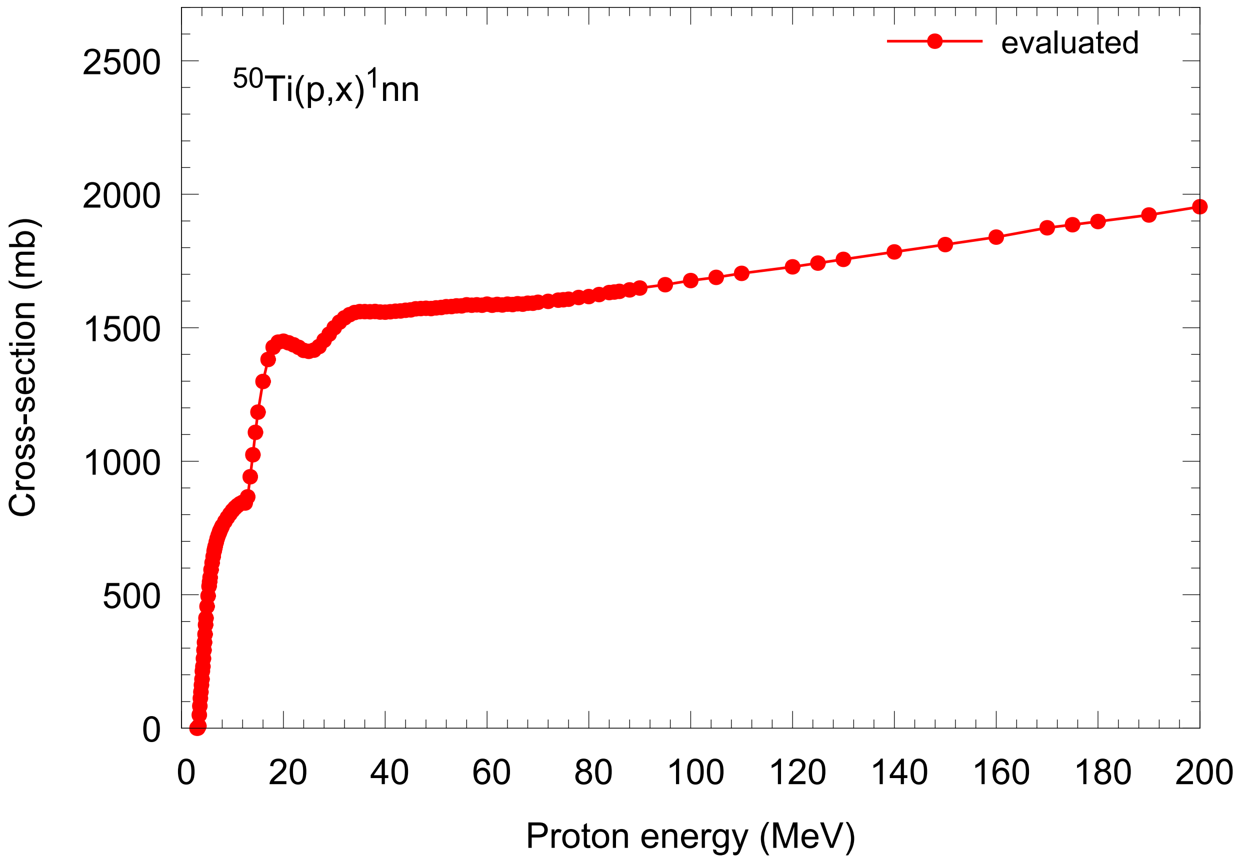

^{50}Ti(p,x)^{1}nn
evaluated
2500
2000
1500
1000
500
0
0
20
40
60
80
100
120
140
160
180
200
Cross-section (mb)
Proton energy (MeV)

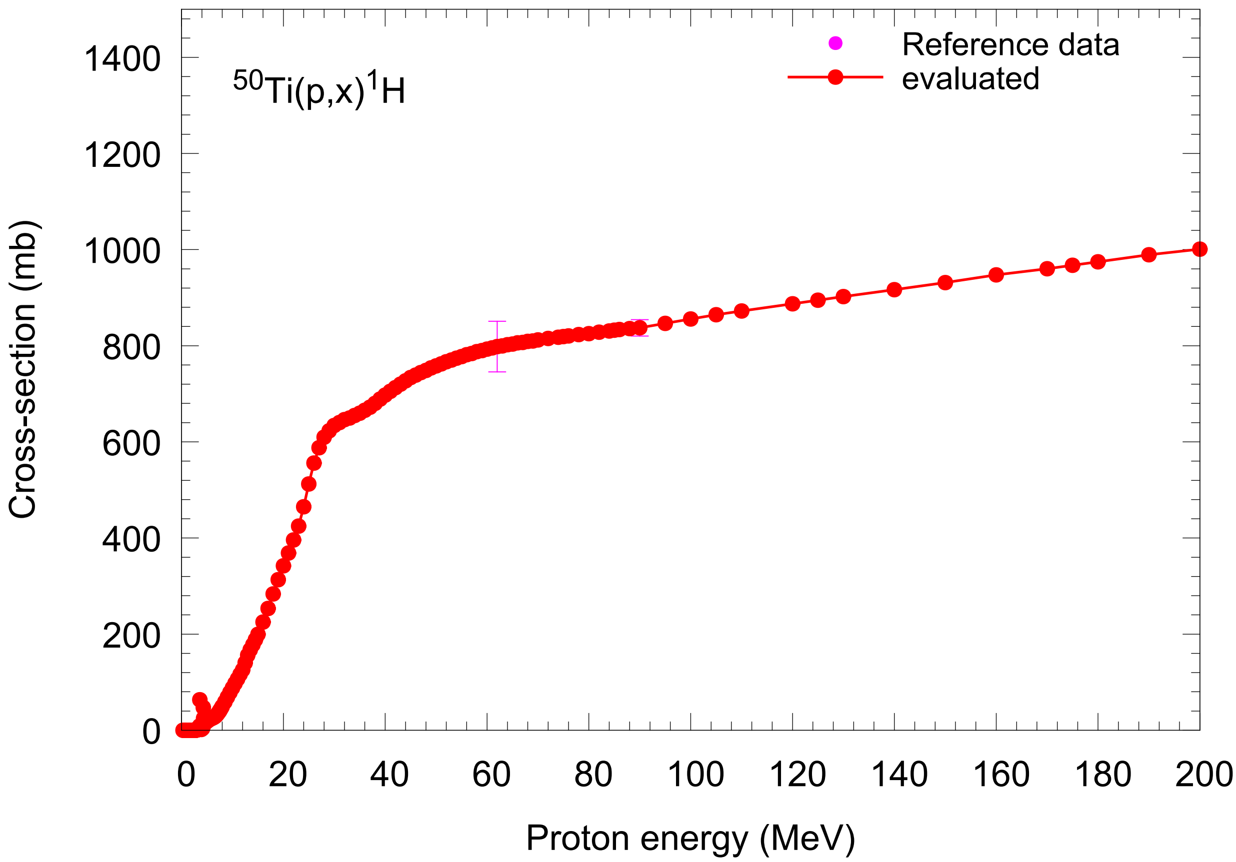

^{50}Ti(p,x)^{1}H
Reference data
evaluated
1400
1200
1000
800
600
400
200
0
0
20
40
60
80
100
120
140
160
180
200
Cross-section (mb)
Proton energy (MeV)

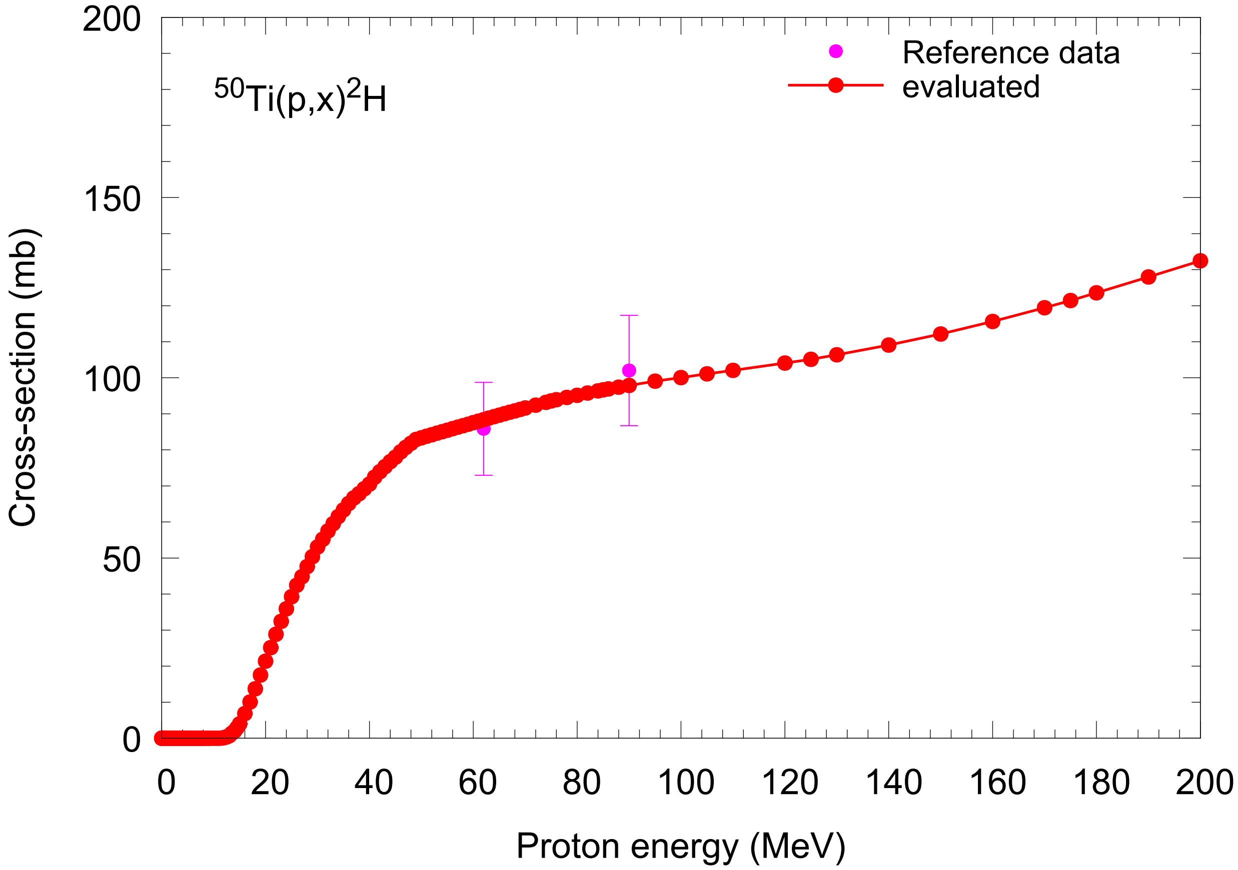

$^{50}Ti(p,x)^{2}H$
Reference data
evaluated
Cross-section (mb)
Proton energy (MeV)
0
50
100
150
200
0
20
40
60
80
100
120
140
160
180
200

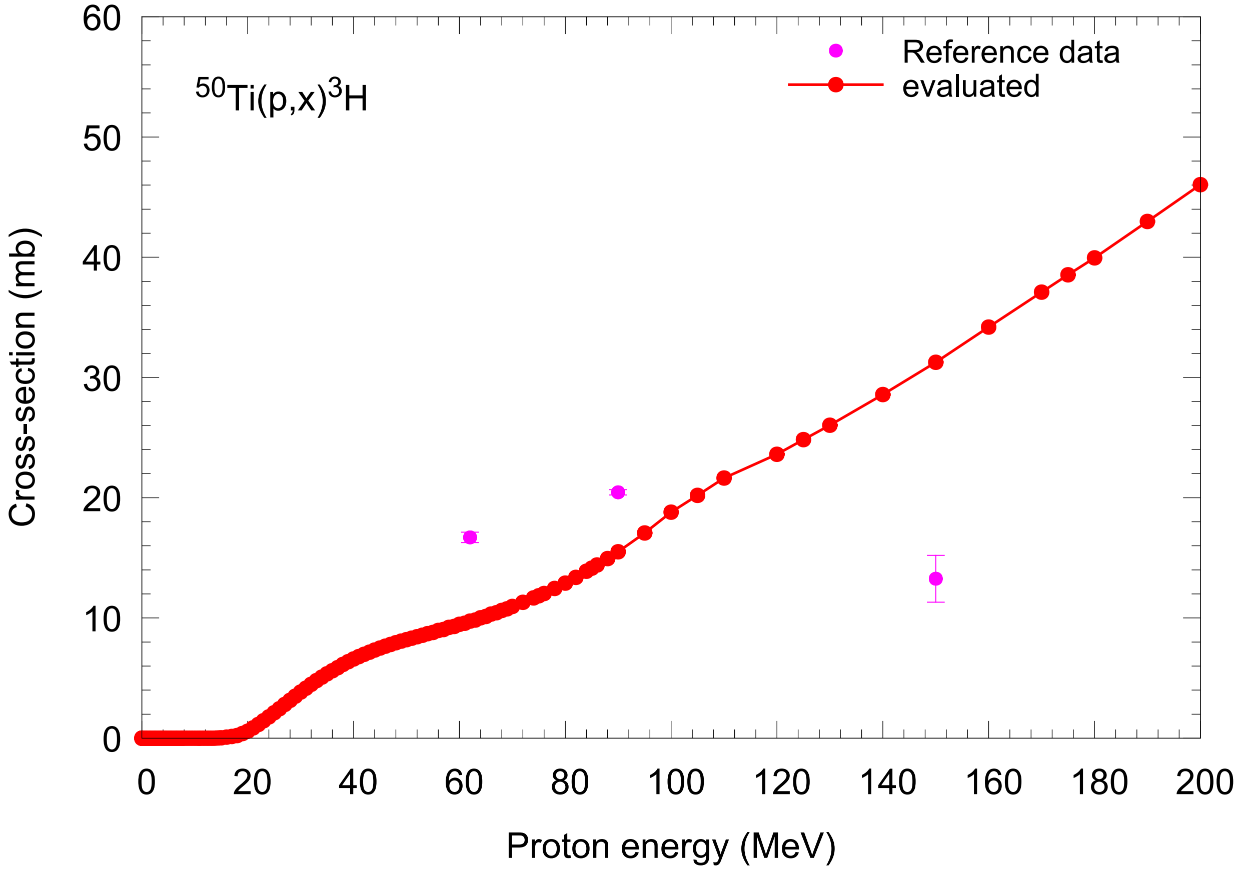

$^{50}Ti(p,x)^{3}H$
Reference data
evaluated
Cross-section (mb)
Proton energy (MeV)
0
10
20
30
40
50
60
0
20
40
60
80
100
120
140
160
180
200

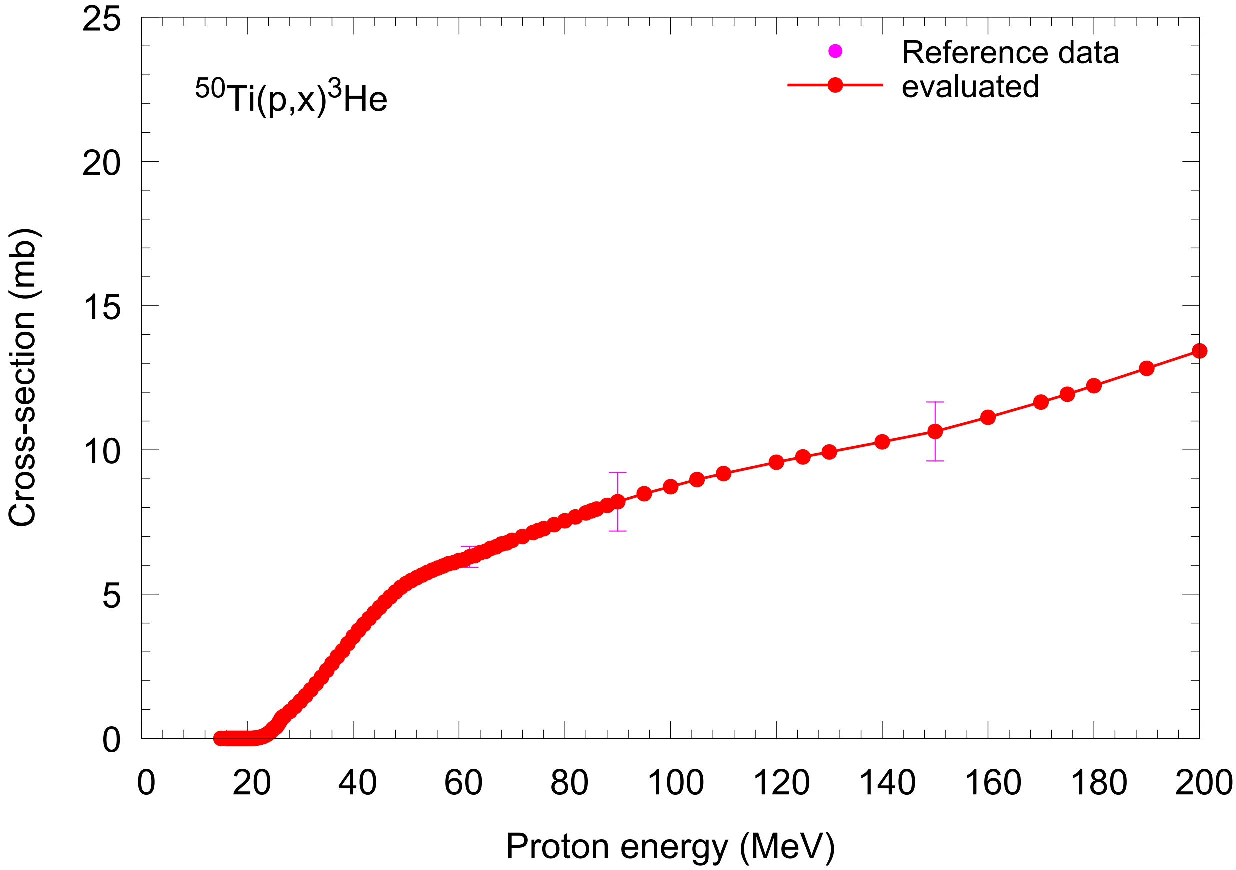

$^{50}Ti(p,x)^{3}He$
Reference data
evaluated
Cross-section (mb)
Proton energy (MeV)

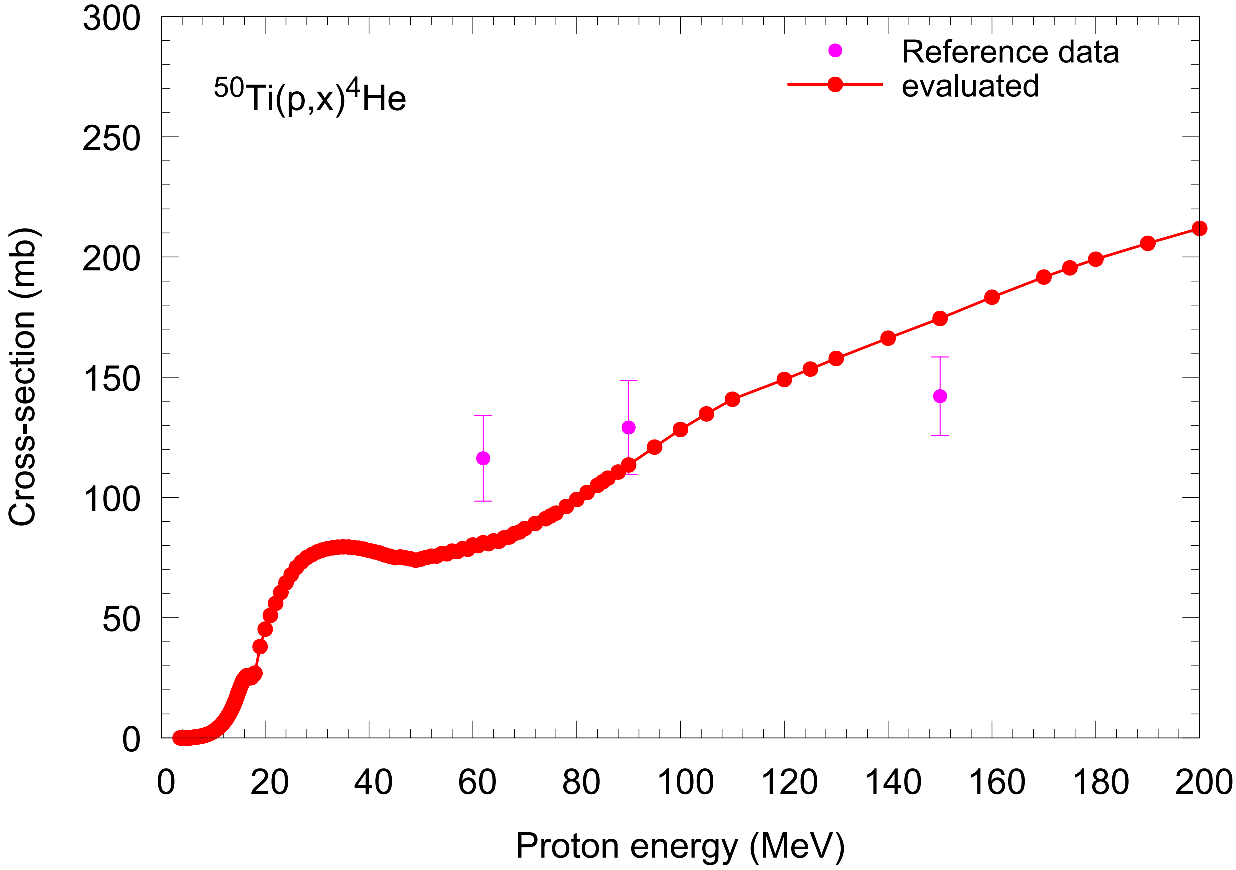

$^{50}Ti(p,x)^{4}He$
Reference data
evaluated
Cross-section (mb)
Proton energy (MeV)

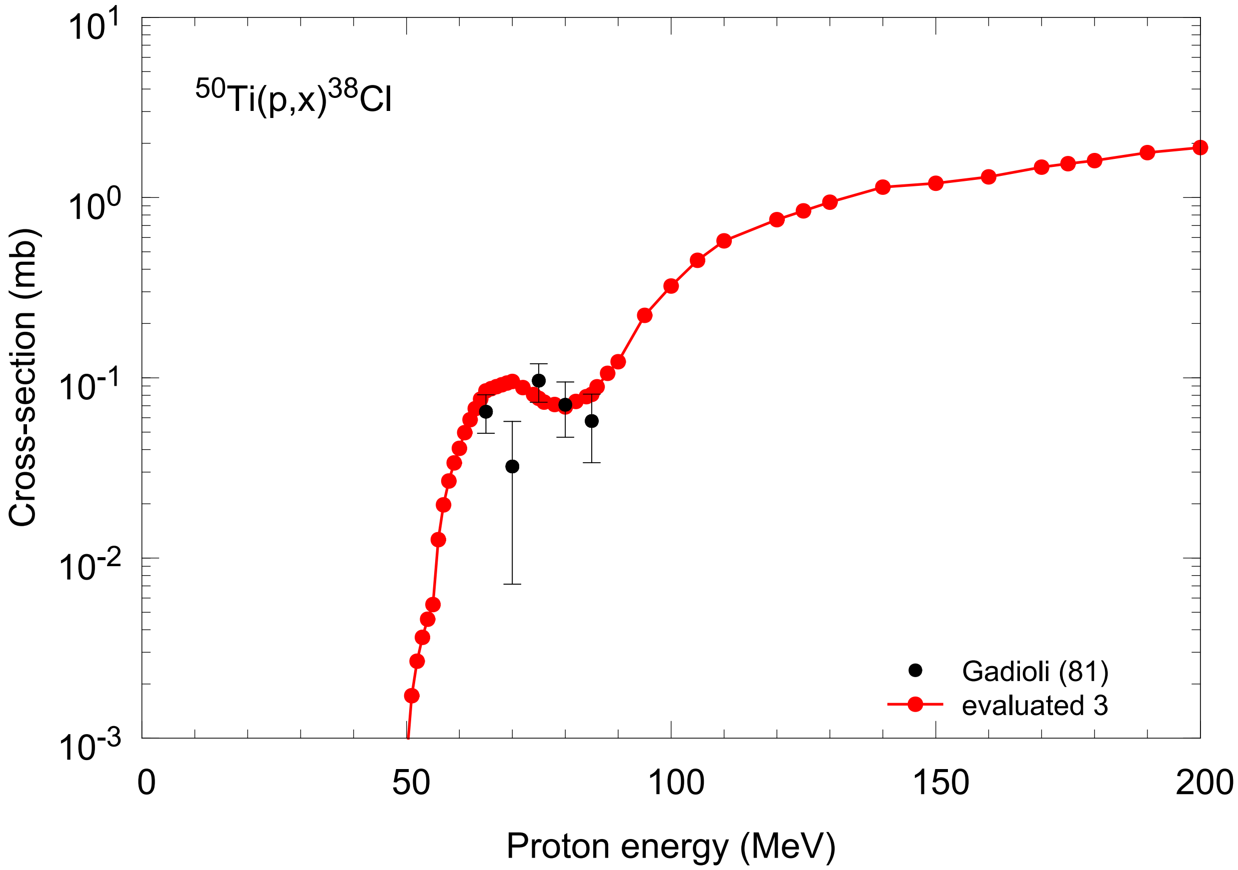
$^{50}Ti(p,x)^{38}Cl$
Cross-section (mb)
Proton energy (MeV)
Gadioli (81)
evaluated 3

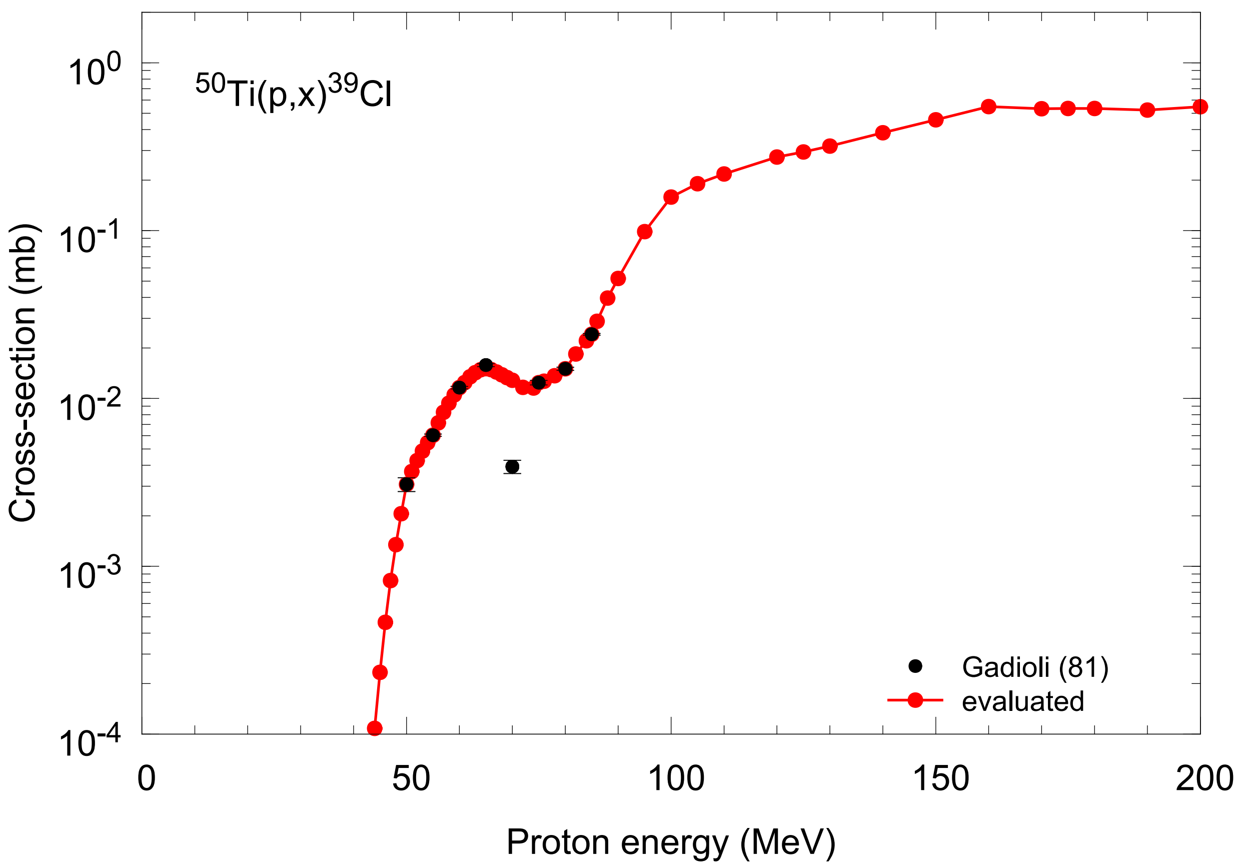
$^{50}Ti(p,x)^{39}Cl$
Cross-section (mb)
Proton energy (MeV)
Gadioli (81)
evaluated

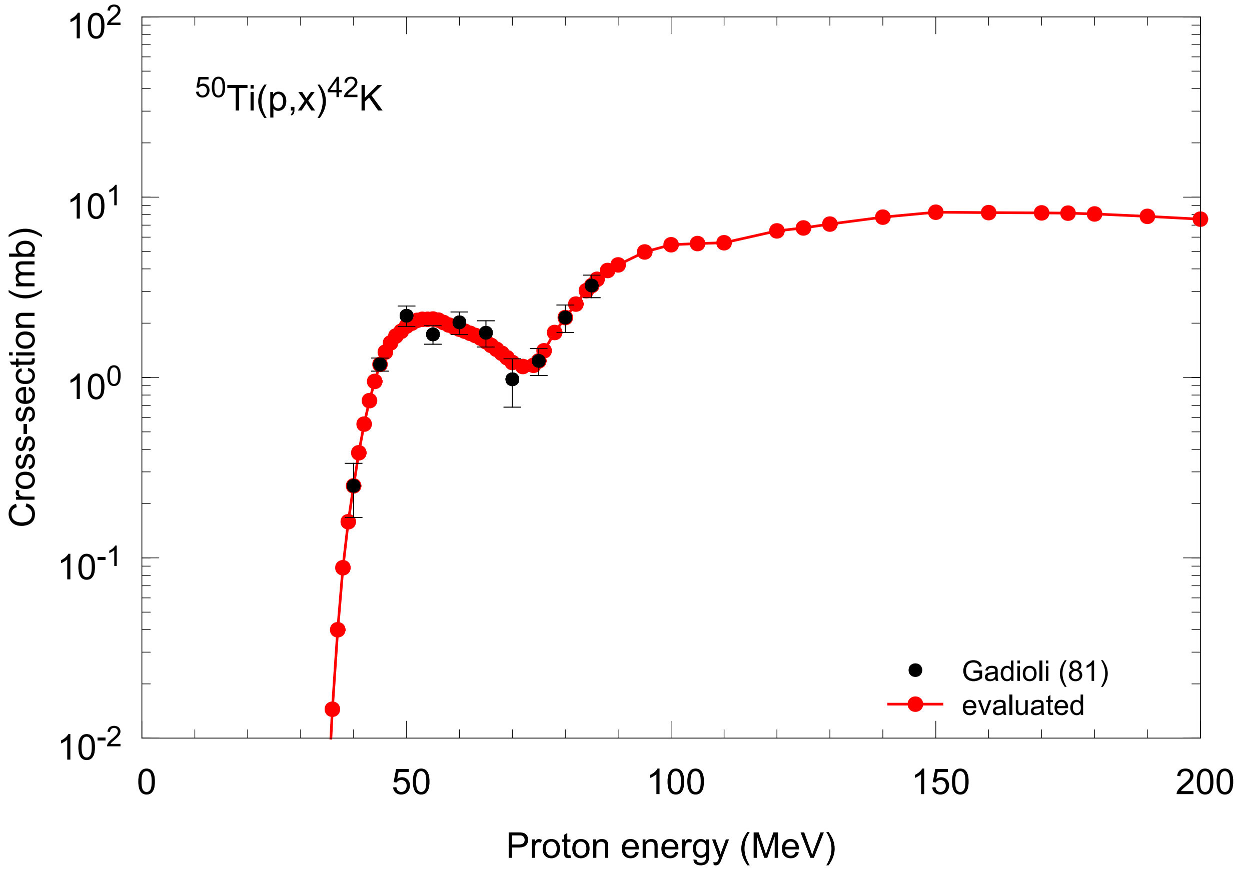

10^2
10^1
10^0
10^{-1}
10^{-2}
$^{50}Ti(p,x)^{42}K$
Cross-section (mb)
Gadioli (81)
evaluated
0
50
100
150
200
Proton energy (MeV)

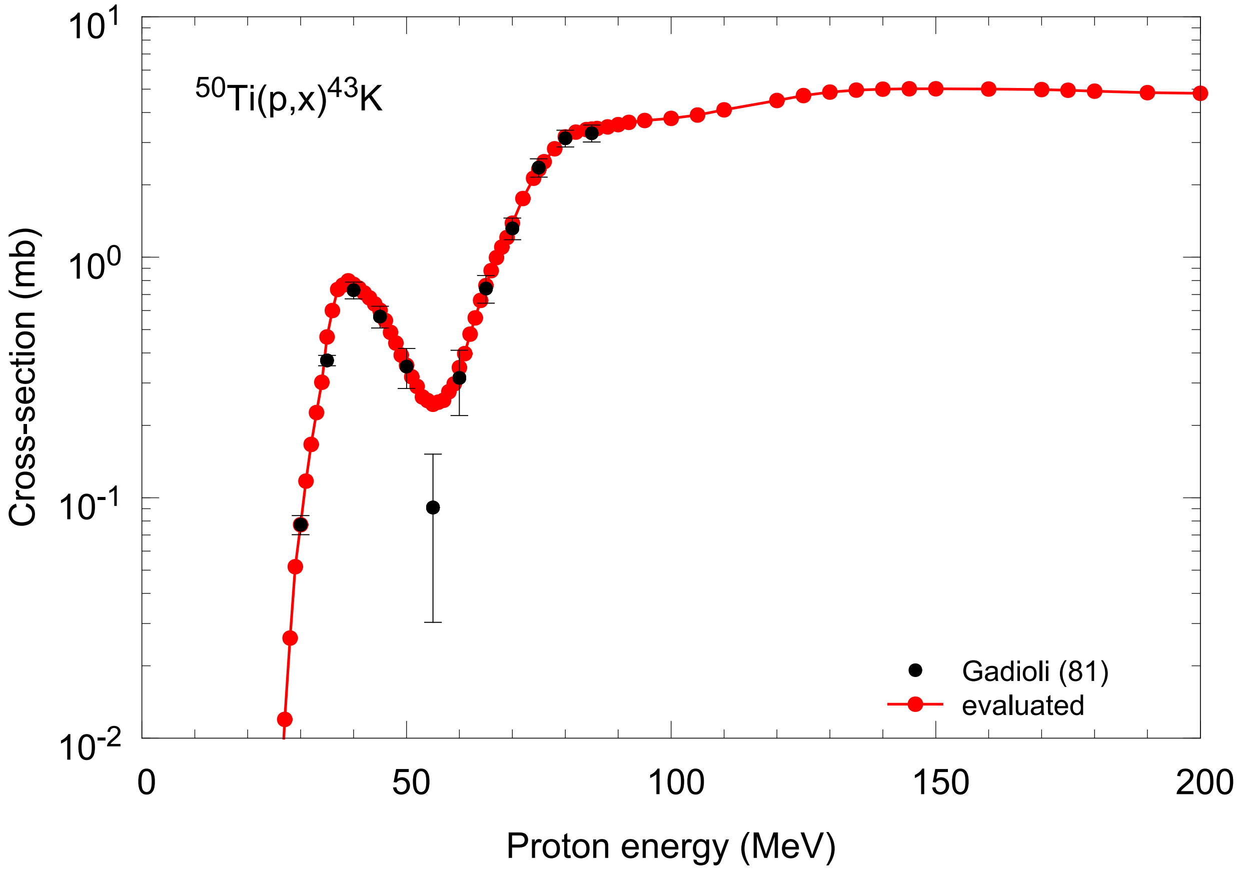

10^1
10^0
10^{-1}
10^{-2}
$^{50}Ti(p,x)^{43}K$
Cross-section (mb)
Gadioli (81)
evaluated
0
50
100
150
200
Proton energy (MeV)

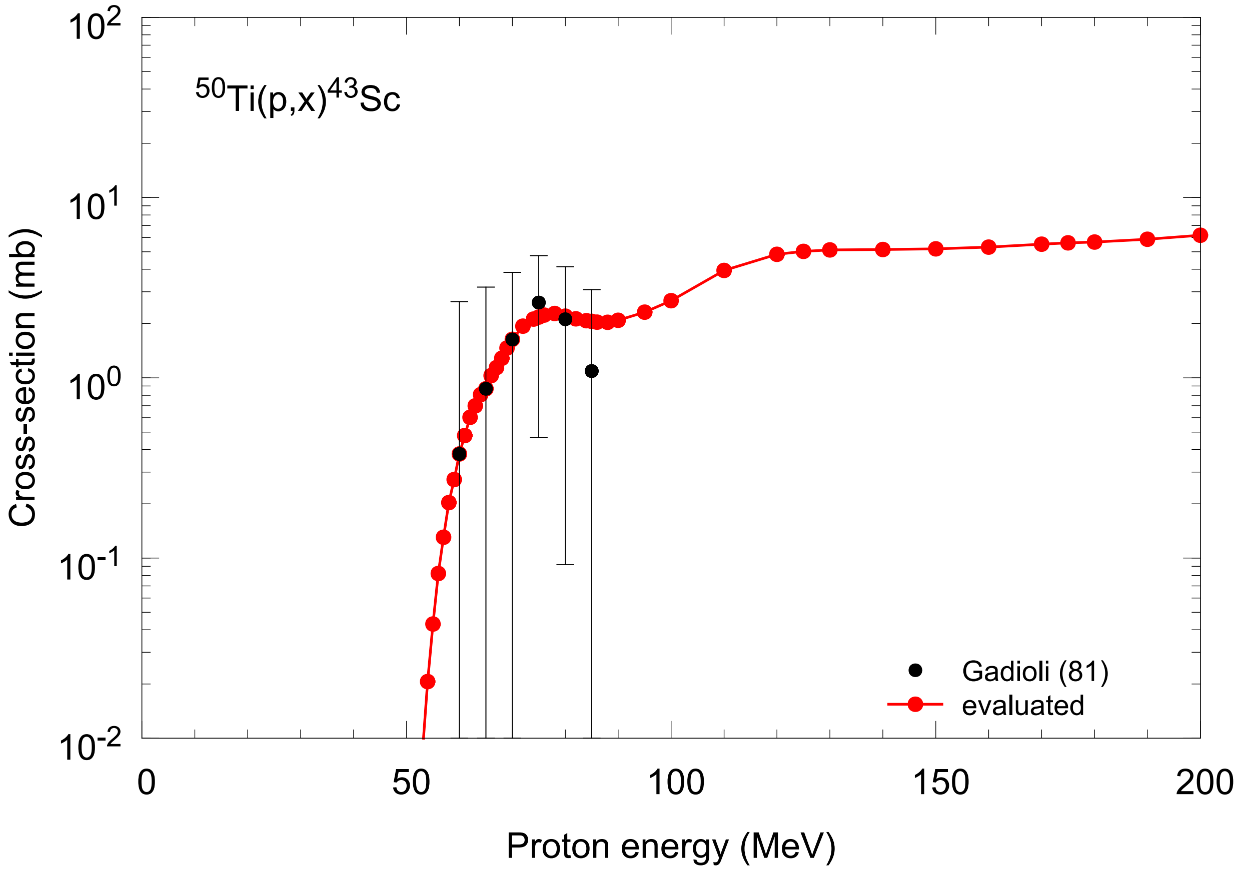

$^{50}Ti(p,x)^{43}Sc$
Gadioli (81)
evaluated
Cross-section (mb)
Proton energy (MeV)

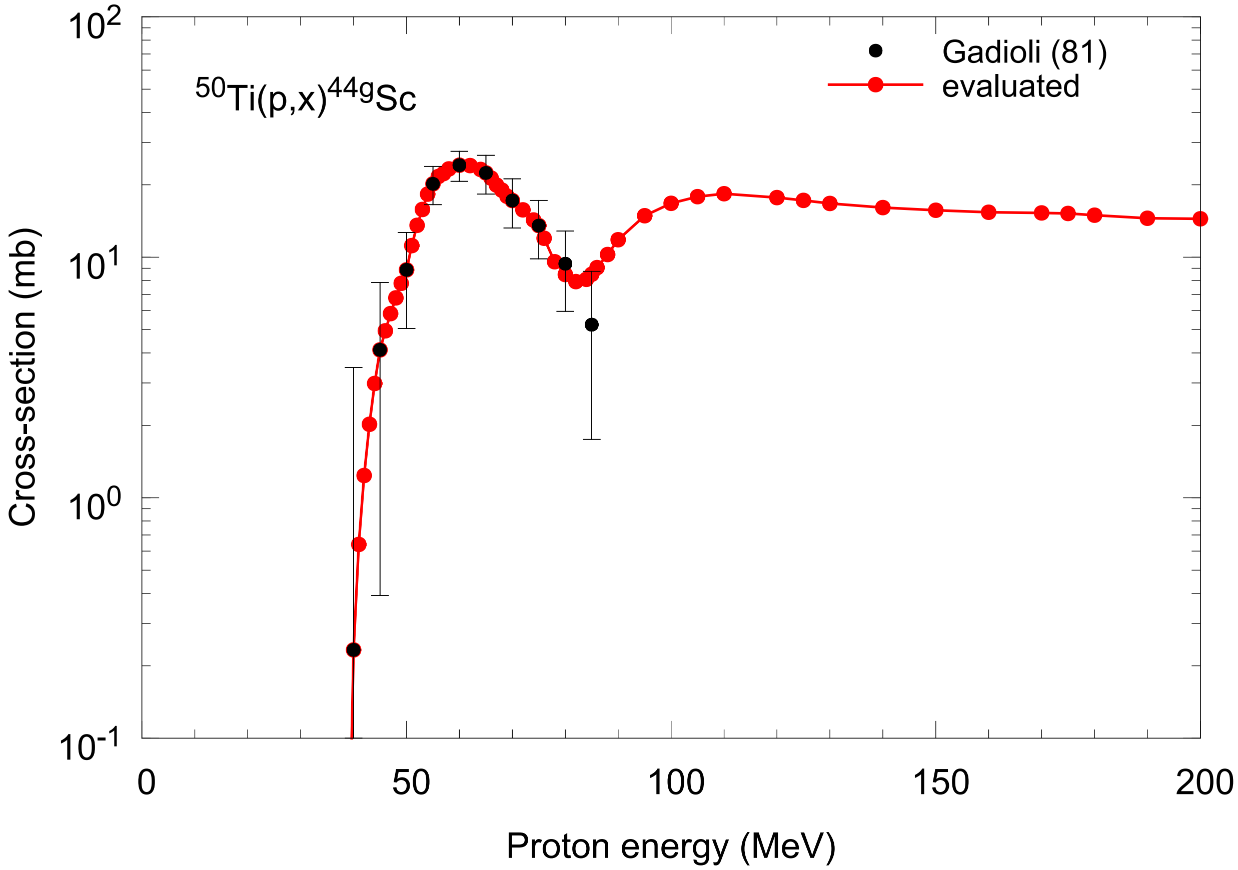

$^{50}Ti(p,x)^{44g}Sc$
Gadioli (81)
evaluated
Cross-section (mb)
Proton energy (MeV)

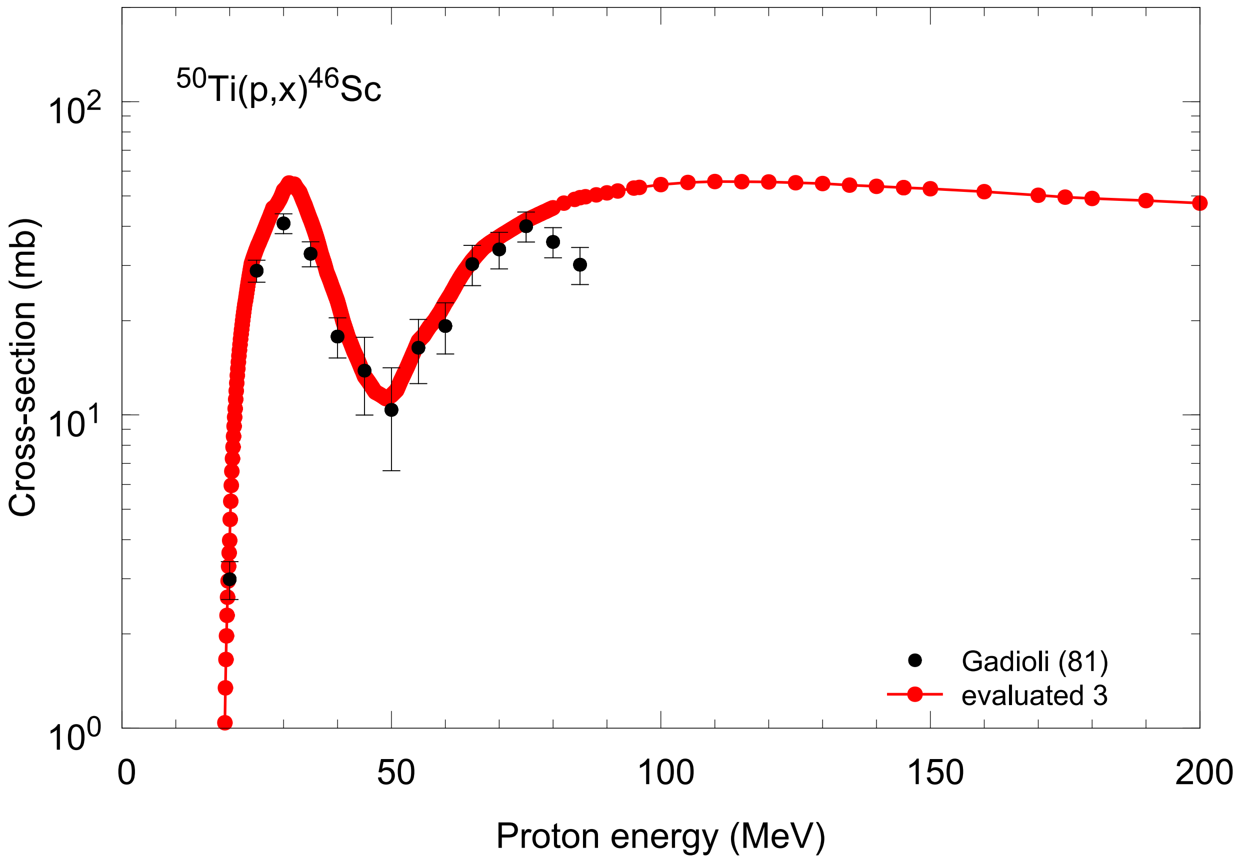

$^{50}Ti(p,x)^{46}Sc$
Cross-section (mb)
10^2
10^1
10^0
0
50
100
150
200
Proton energy (MeV)
Gadioli (81)
evaluated 3

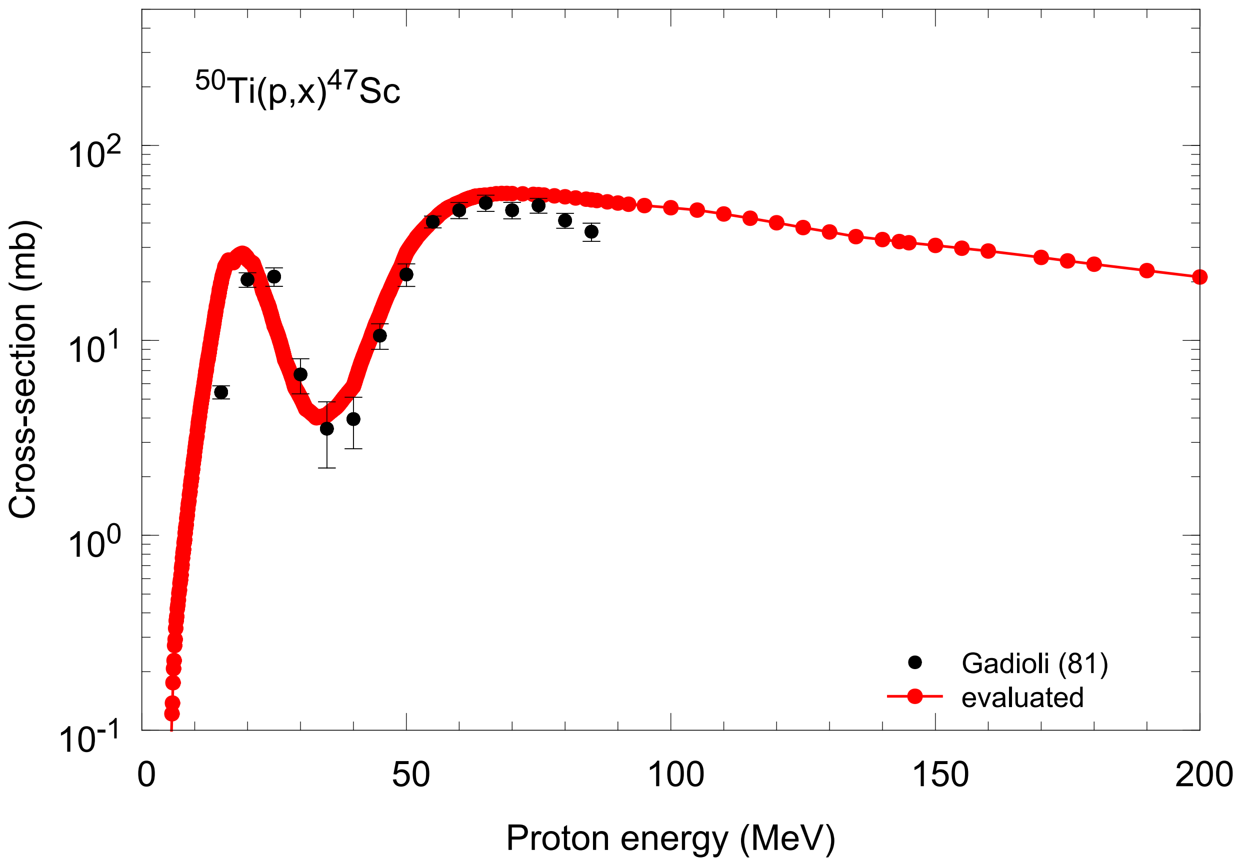

$^{50}Ti(p,x)^{47}Sc$
Cross-section (mb)
10^2
10^1
10^0
10^{-1}
0
50
100
150
200
Proton energy (MeV)
Gadioli (81)
evaluated

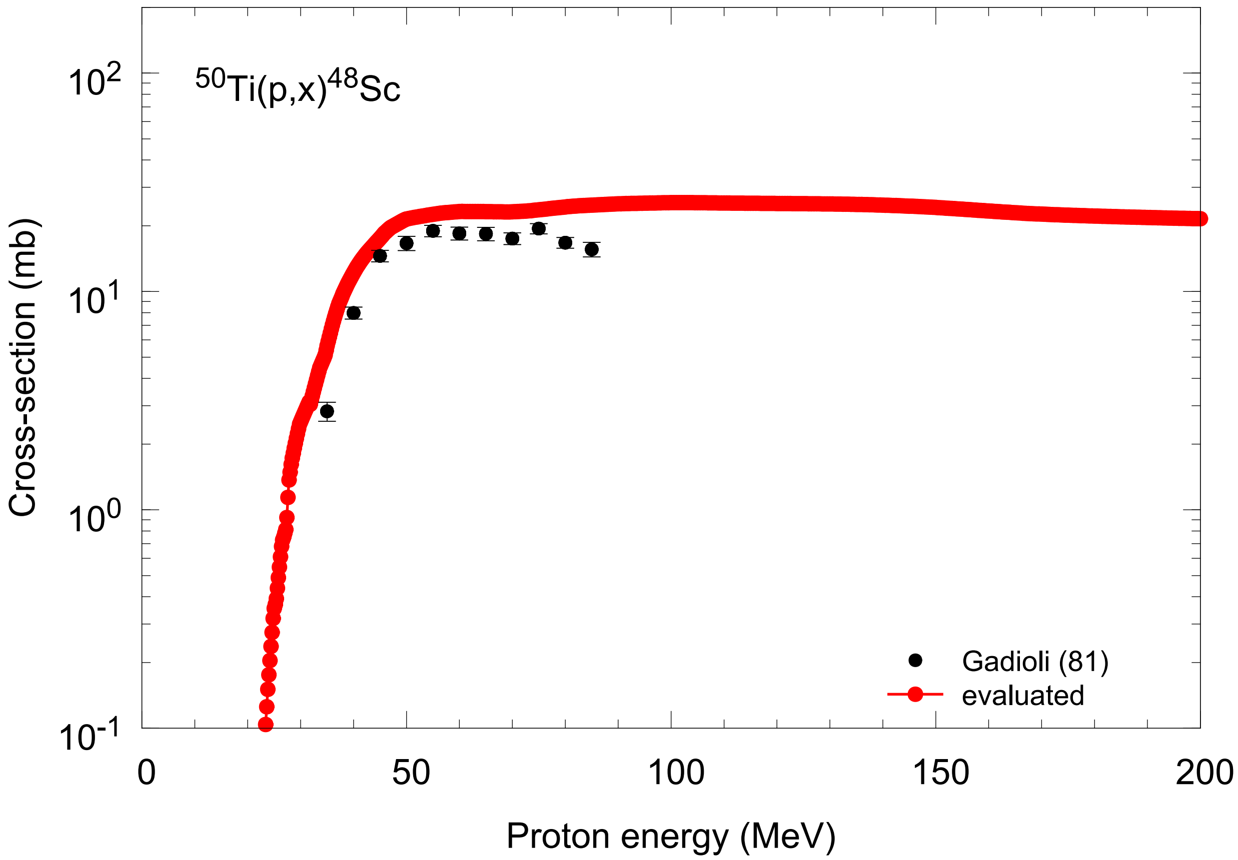

$^{50}Ti(p,x)^{48}Sc$
Cross-section (mb)
Proton energy (MeV)
Gadioli (81)
evaluated

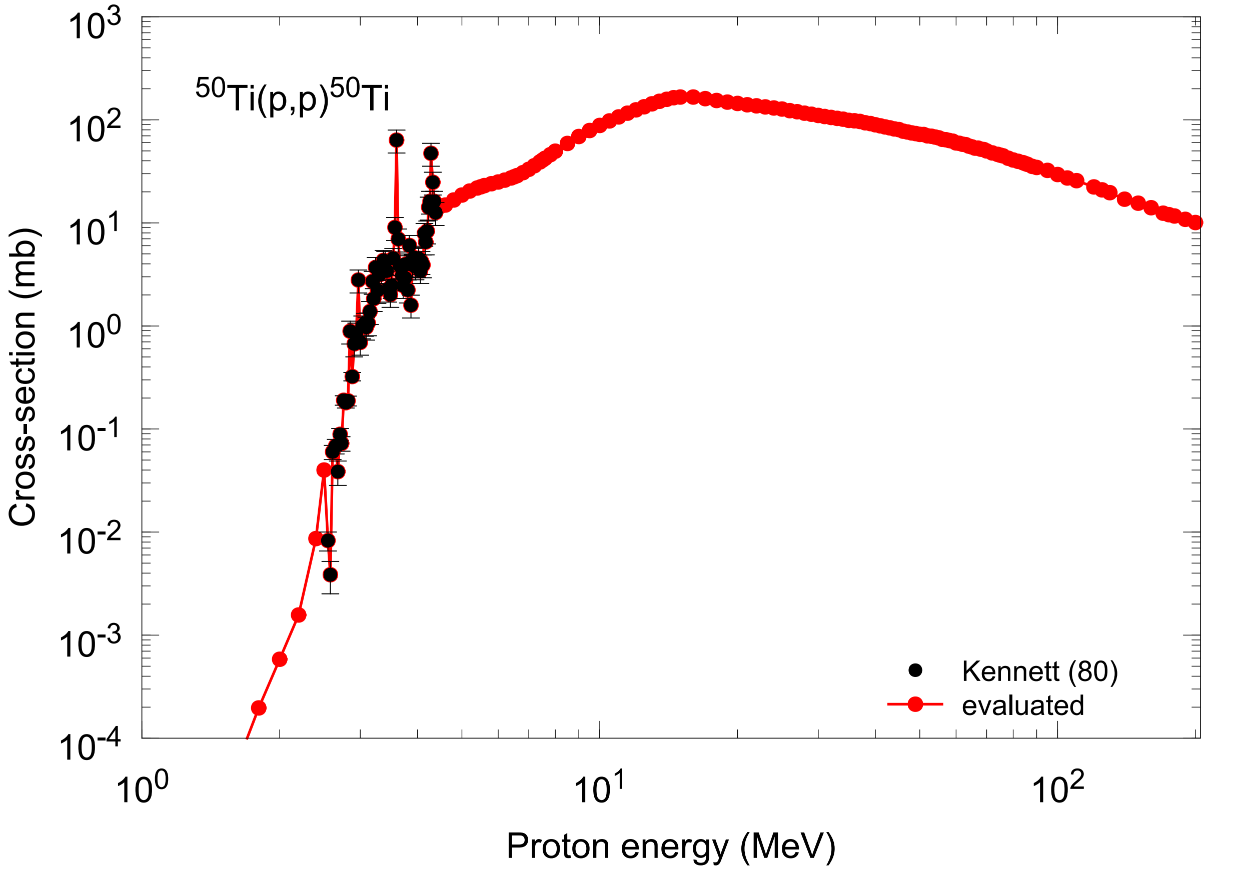

$^{50}Ti(p,p)^{50}Ti$
Cross-section (mb)
Proton energy (MeV)
Kennett (80)
evaluated

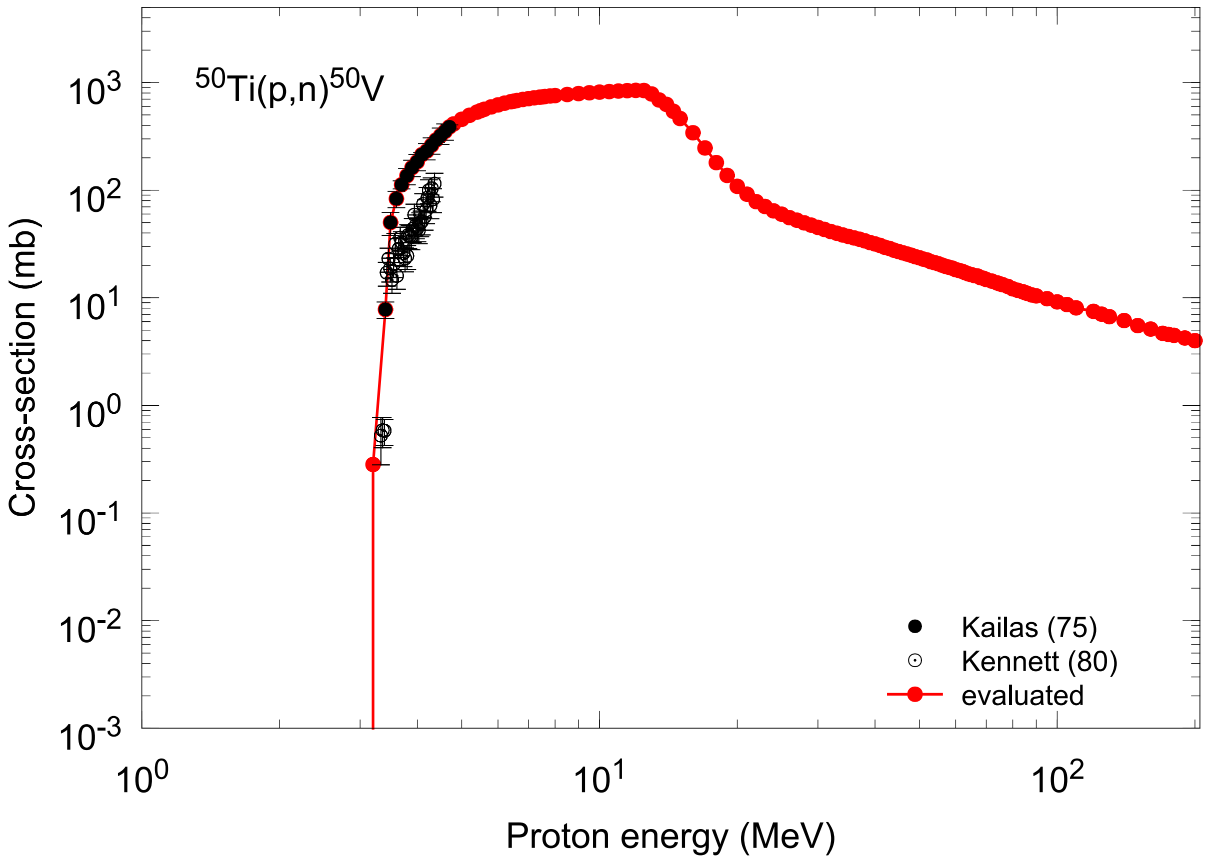
$^{50}Ti(p,n)^{50}V$
Cross-section (mb)
Proton energy (MeV)
Kailas (75)
Kennett (80)
evaluated

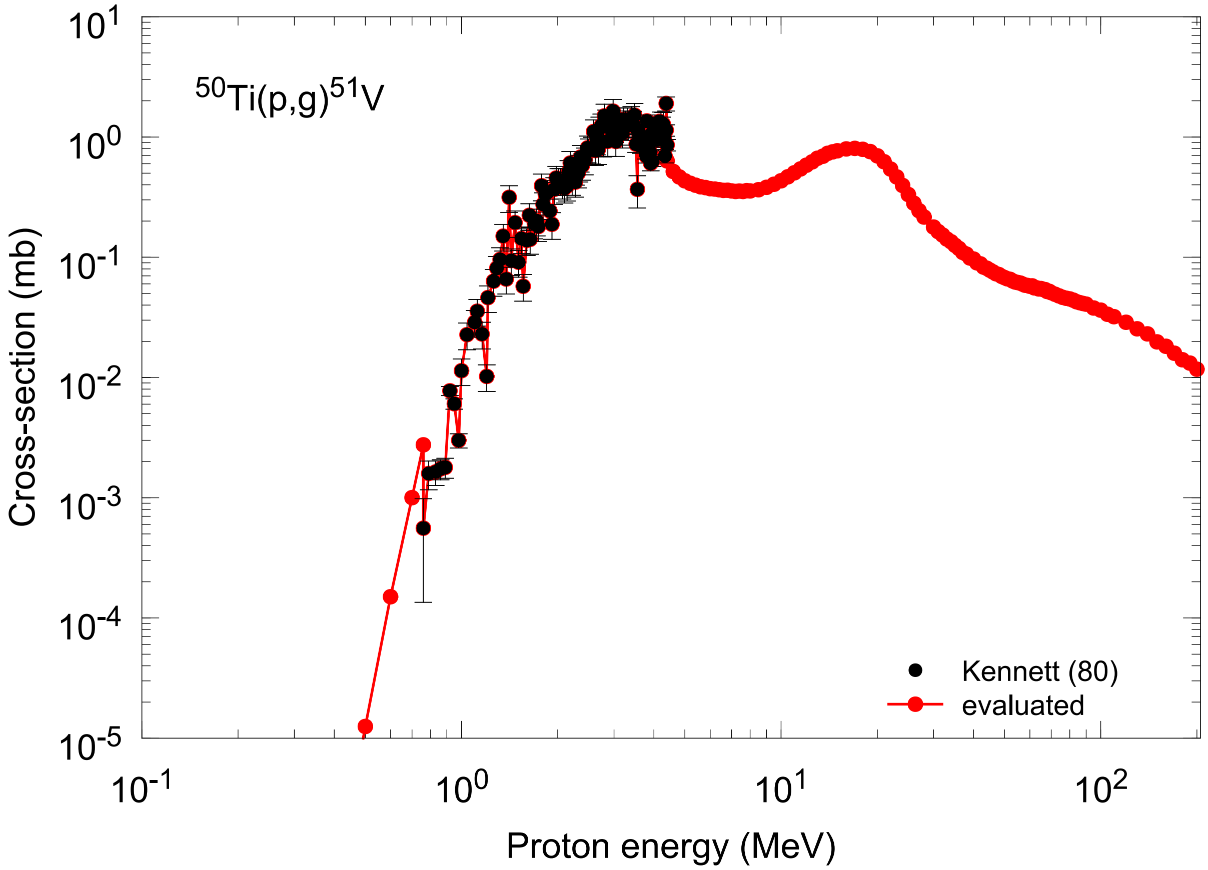
$^{50}Ti(p,g)^{51}V$
Cross-section (mb)
Proton energy (MeV)
Kennett (80)
evaluated

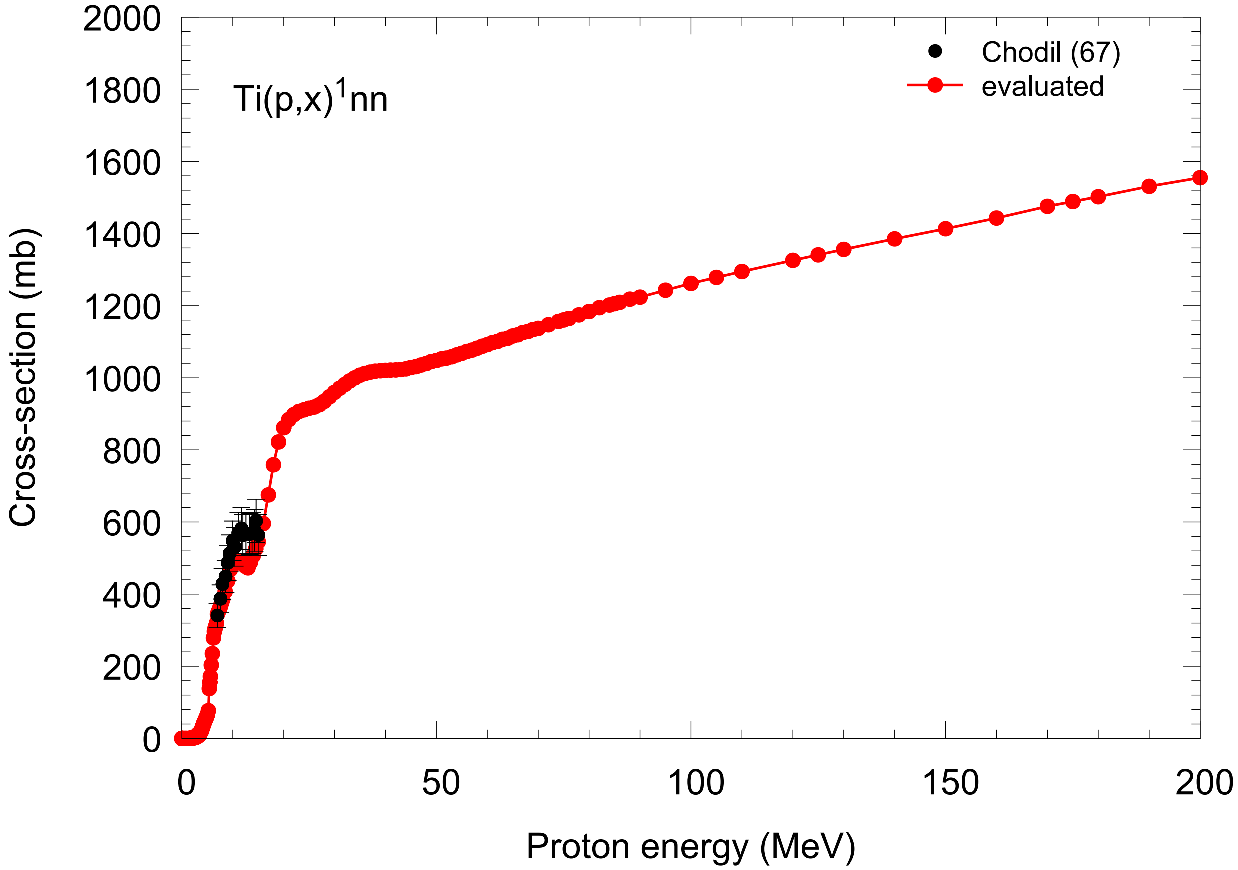

Ti(p,x)^{1}nn
Chodil (67)
evaluated
Cross-section (mb)
Proton energy (MeV)
2000
1800
1600
1400
1200
1000
800
600
400
200
0
0
50
100
150
200

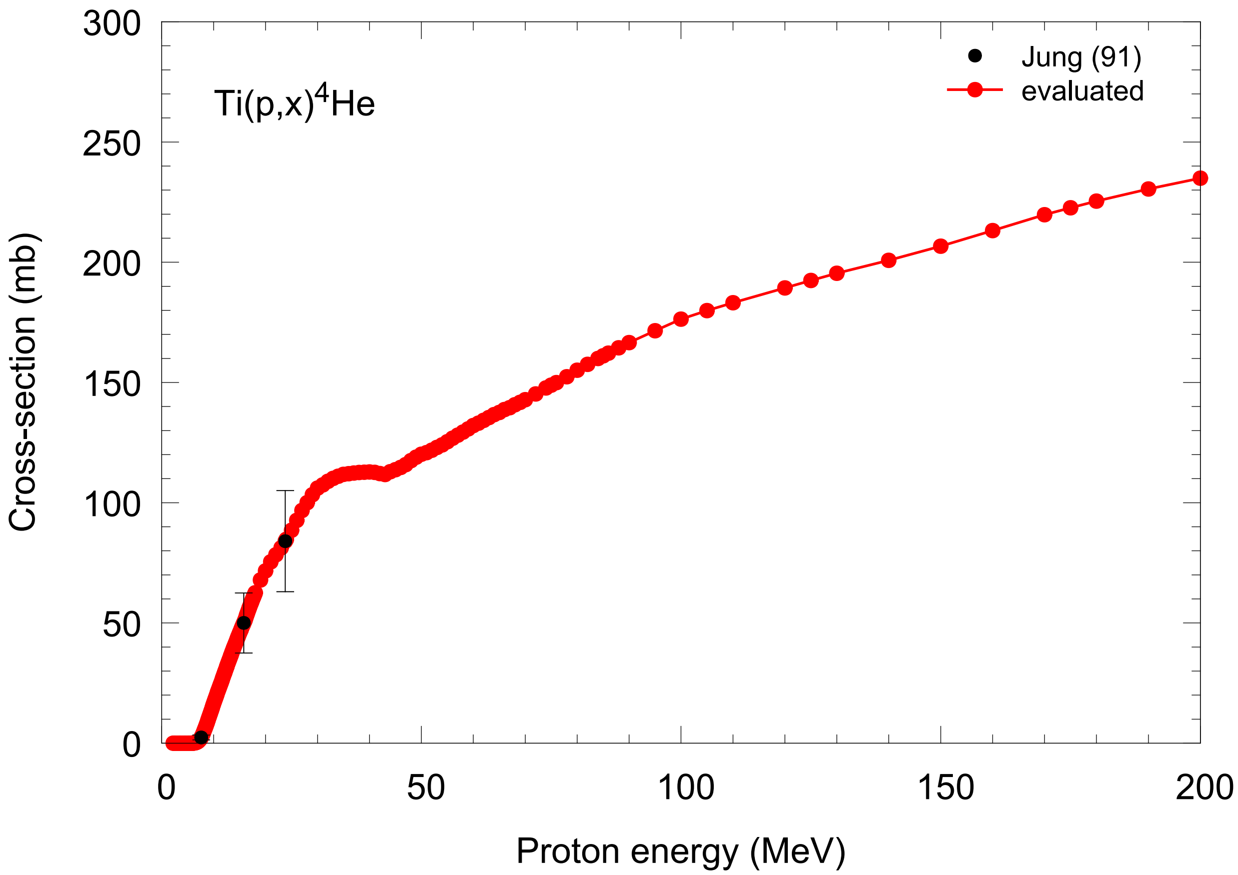

Ti(p,x)^{4}He
Jung (91)
evaluated
Cross-section (mb)
Proton energy (MeV)
300
250
200
150
100
50
0
0
50
100
150
200

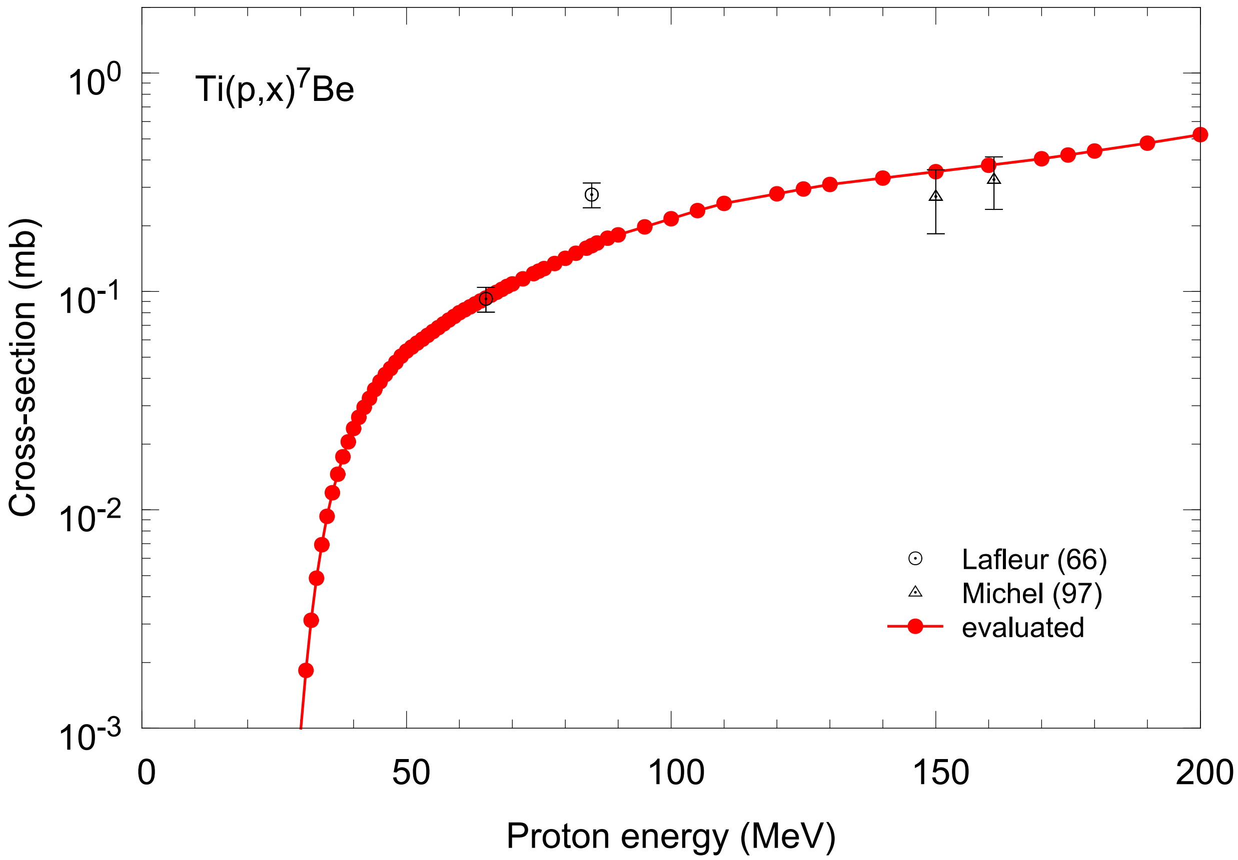
Ti(p,x)^{7}Be
Cross-section (mb)
10^{0}
10^{-1}
10^{-2}
10^{-3}
0
50
100
150
200
Proton energy (MeV)
Lafleur (66)
Michel (97)
evaluated

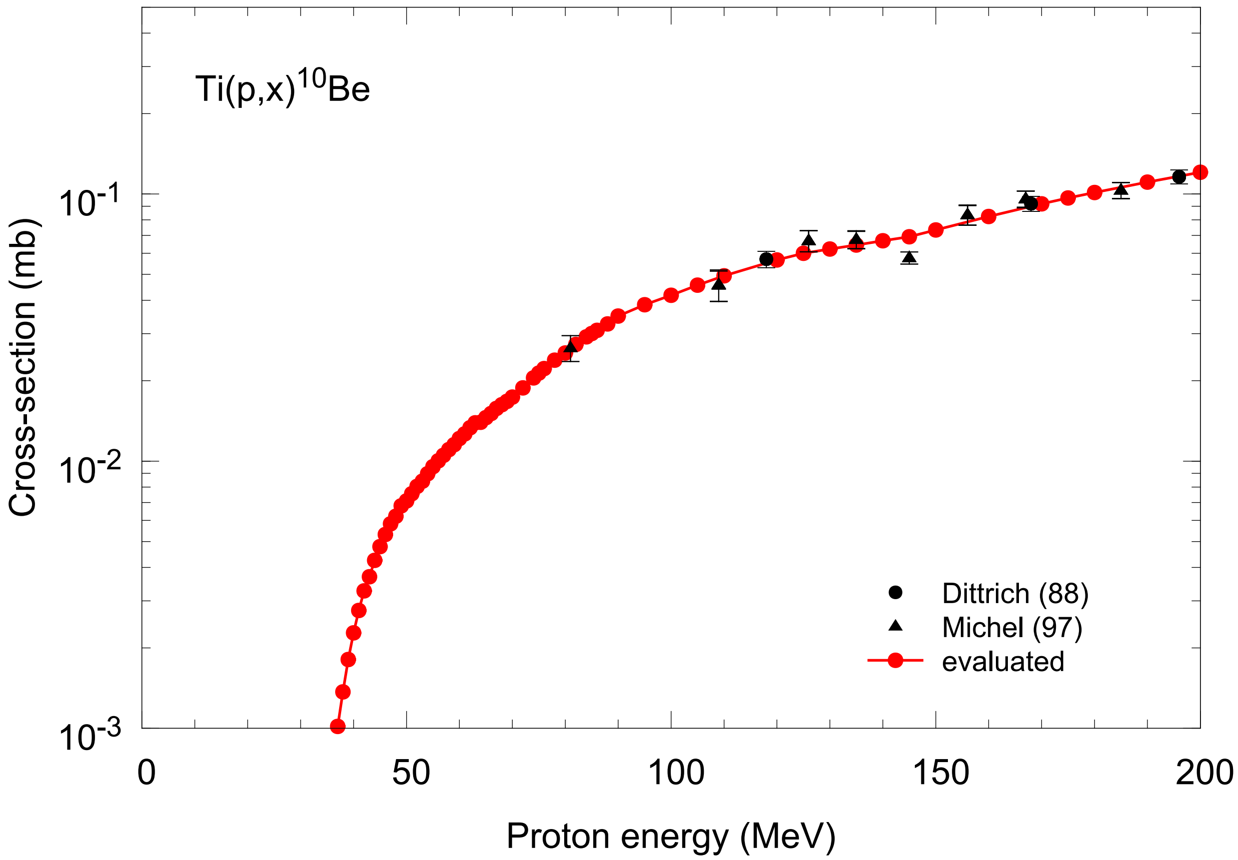
Ti(p,x)^{10}Be
Cross-section (mb)
10^{-1}
10^{-2}
10^{-3}
0
50
100
150
200
Proton energy (MeV)
Dittrich (88)
Michel (97)
evaluated

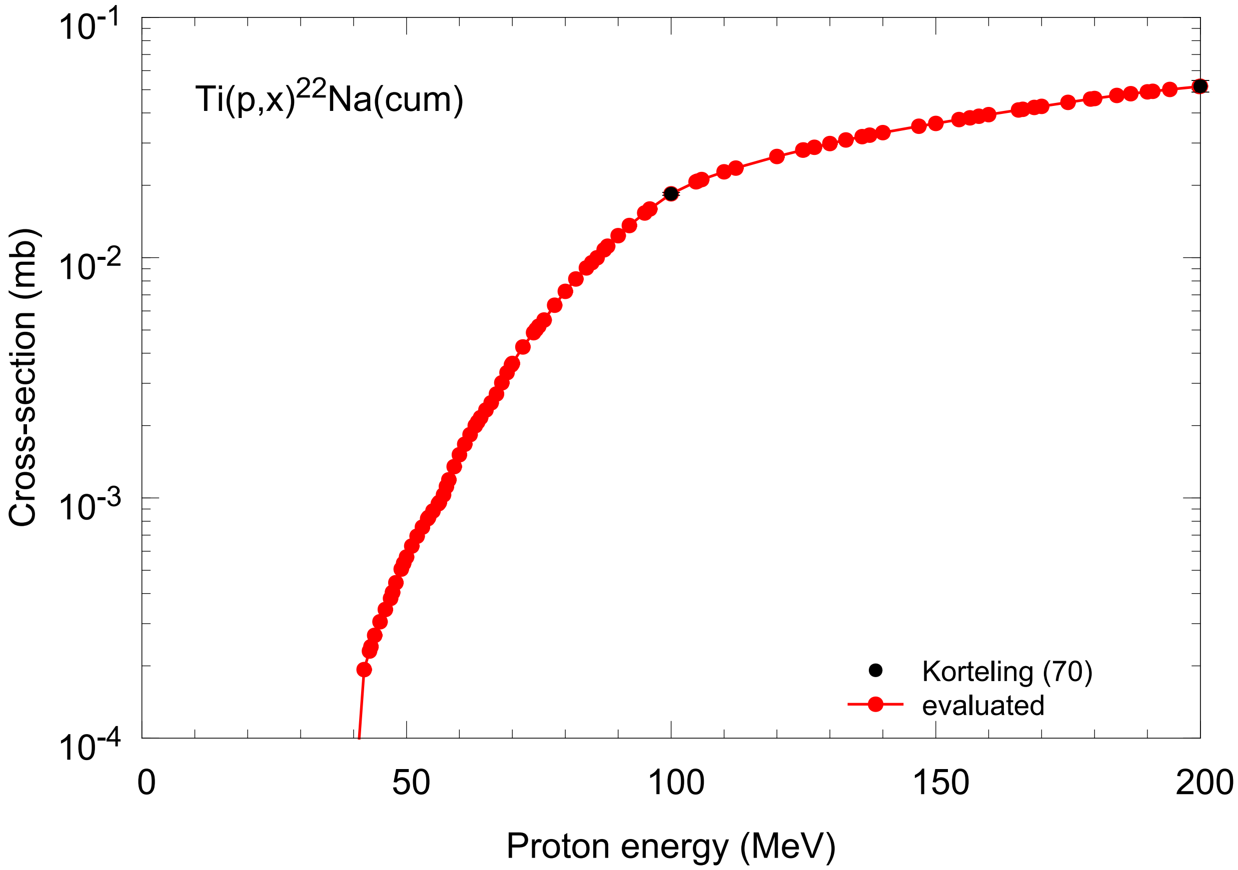
Ti(p,x)^{22}Na(cum)
Cross-section (mb)
Proton energy (MeV)
Korteling (70)
evaluated

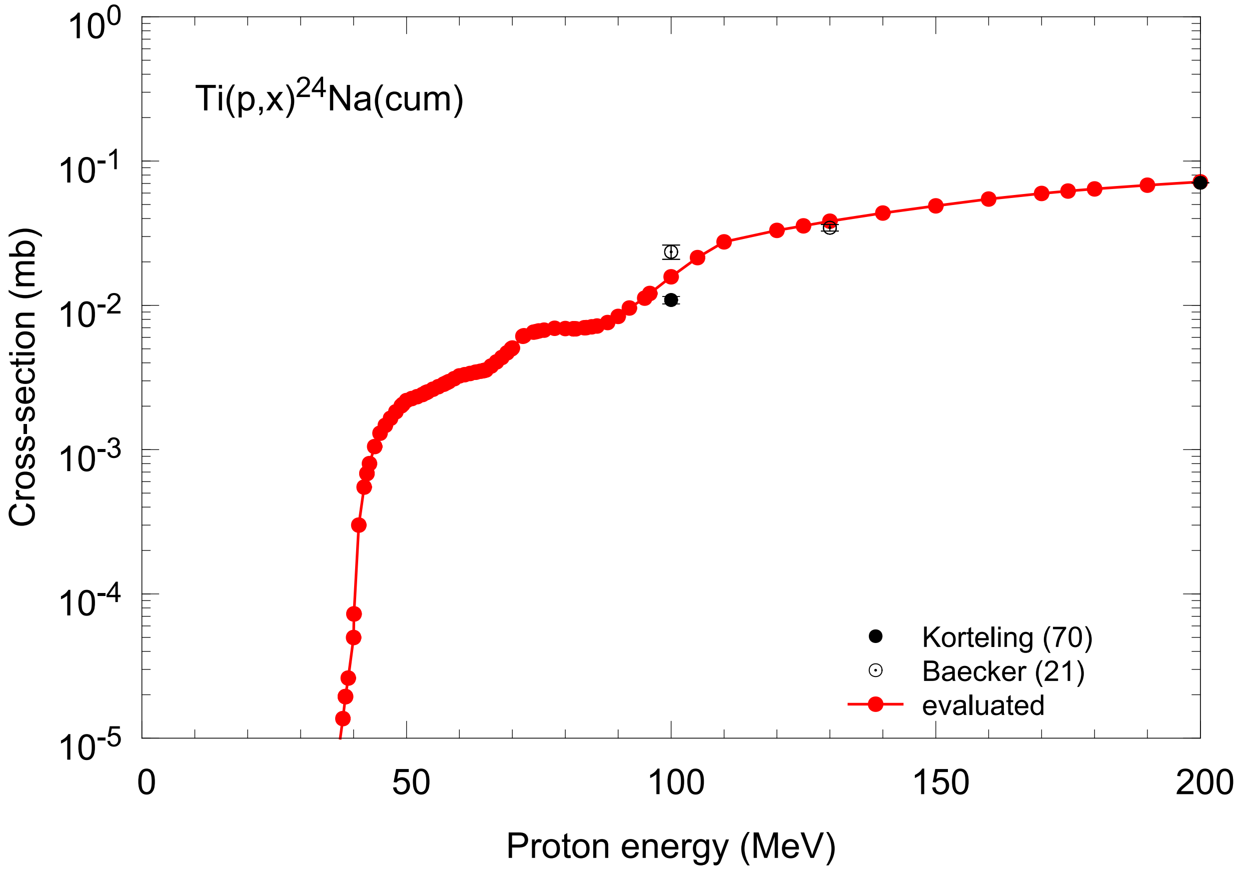
Ti(p,x)^{24}Na(cum)
Cross-section (mb)
Proton energy (MeV)
Korteling (70)
Baecker (21)
evaluated

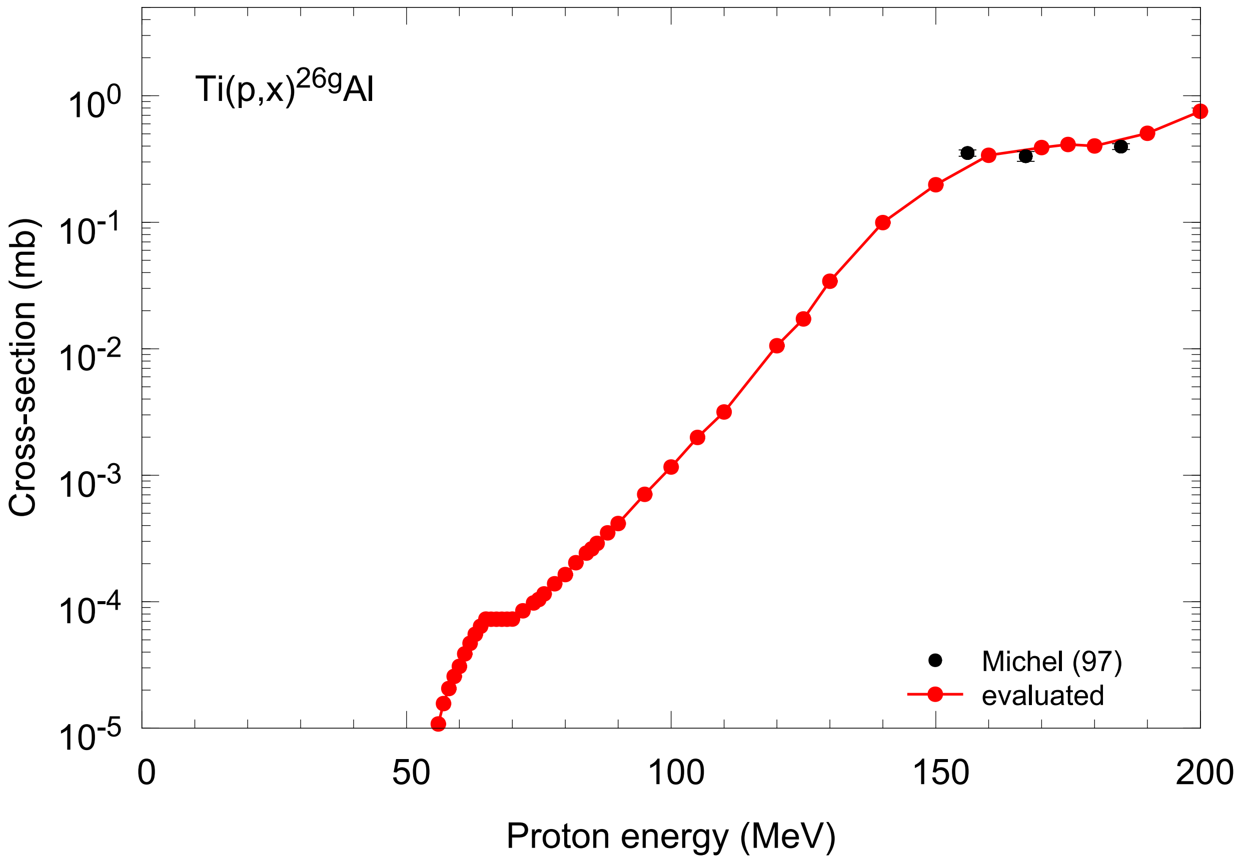
Ti(p,x)^{26g}Al
Cross-section (mb)
10^{0}
10^{-1}
10^{-2}
10^{-3}
10^{-4}
10^{-5}
0
50
100
150
200
Proton energy (MeV)
Michel (97)
evaluated

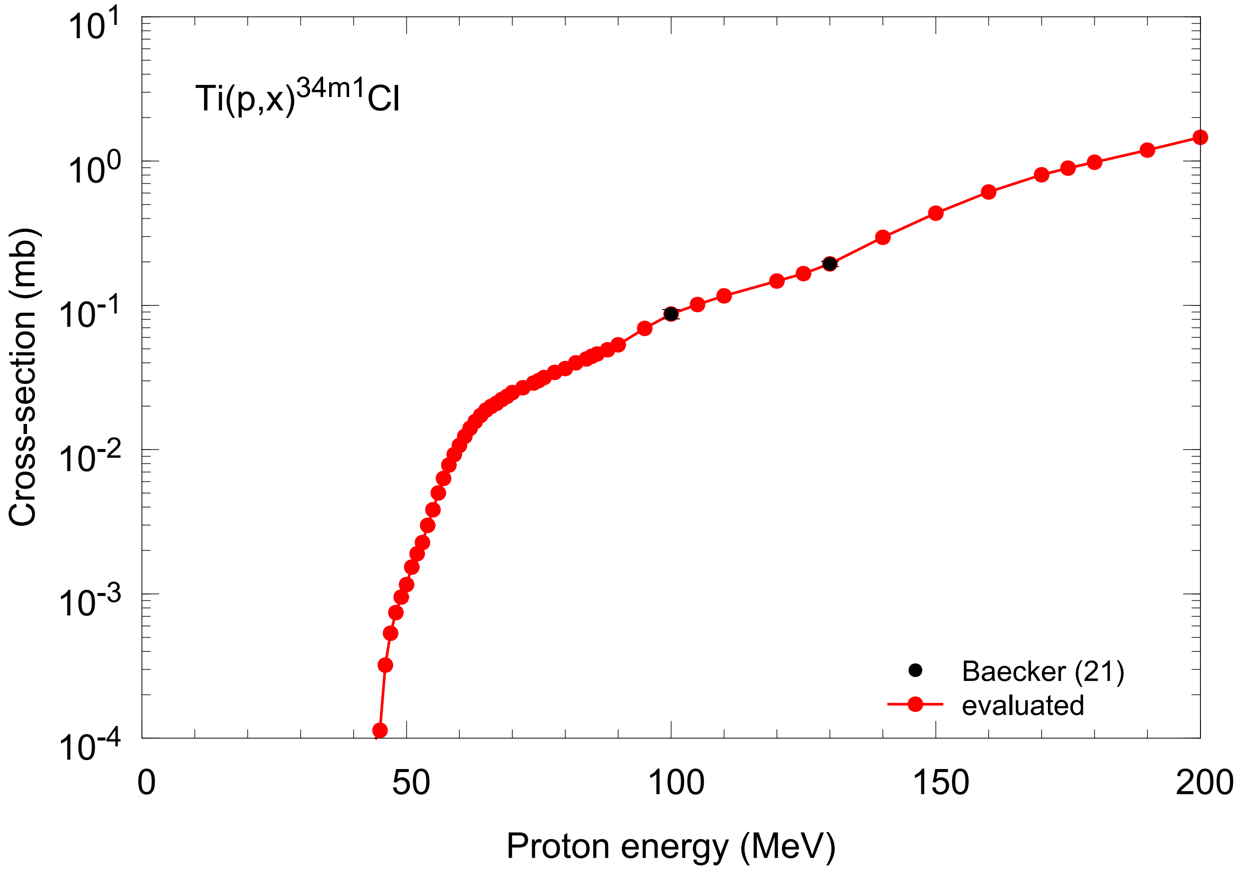
Ti(p,x)^{34m1}Cl
Cross-section (mb)
10^{1}
10^{0}
10^{-1}
10^{-2}
10^{-3}
10^{-4}
0
50
100
150
200
Proton energy (MeV)
Baecker (21)
evaluated

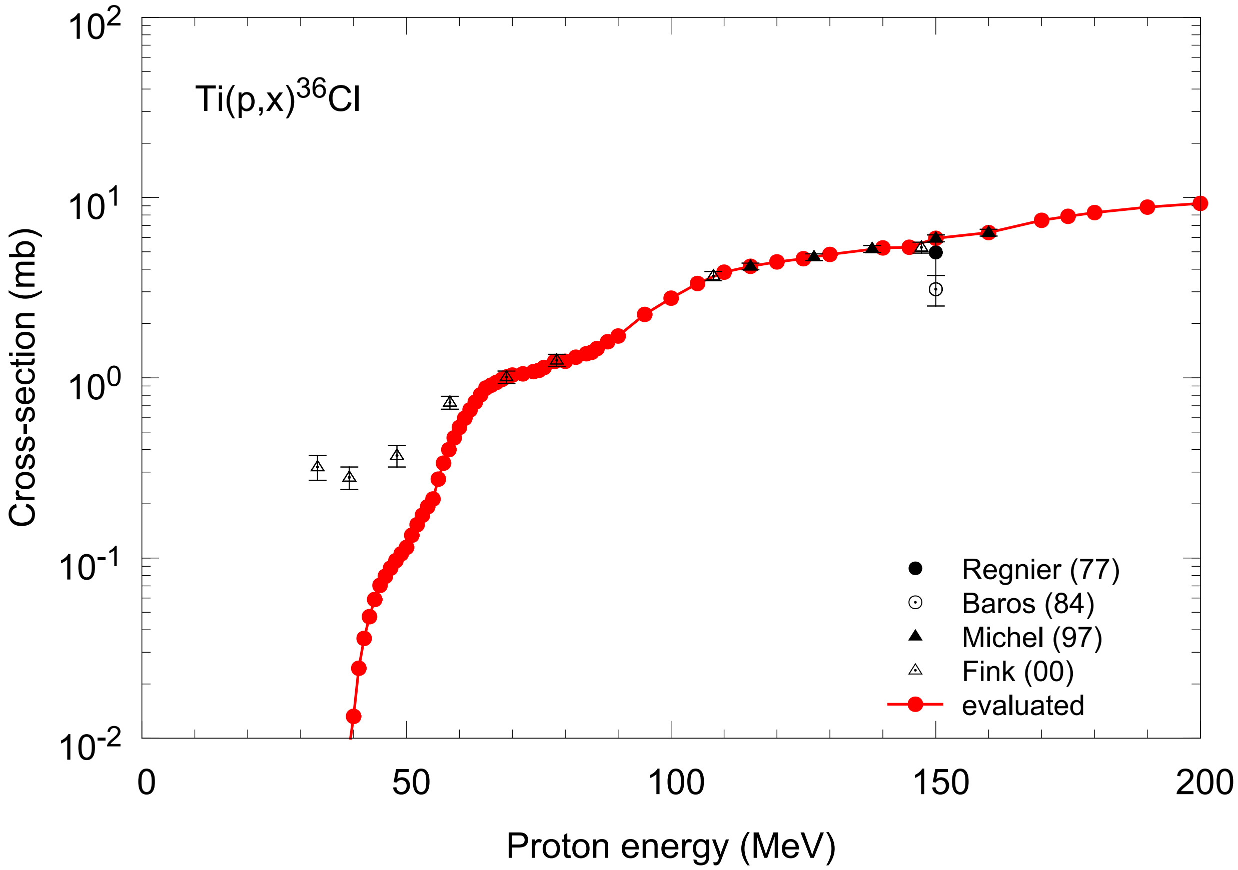
Ti(p,x)^{36}Cl
Cross-section (mb)
Proton energy (MeV)
Regnier (77)
Baros (84)
Michel (97)
Fink (00)
evaluated

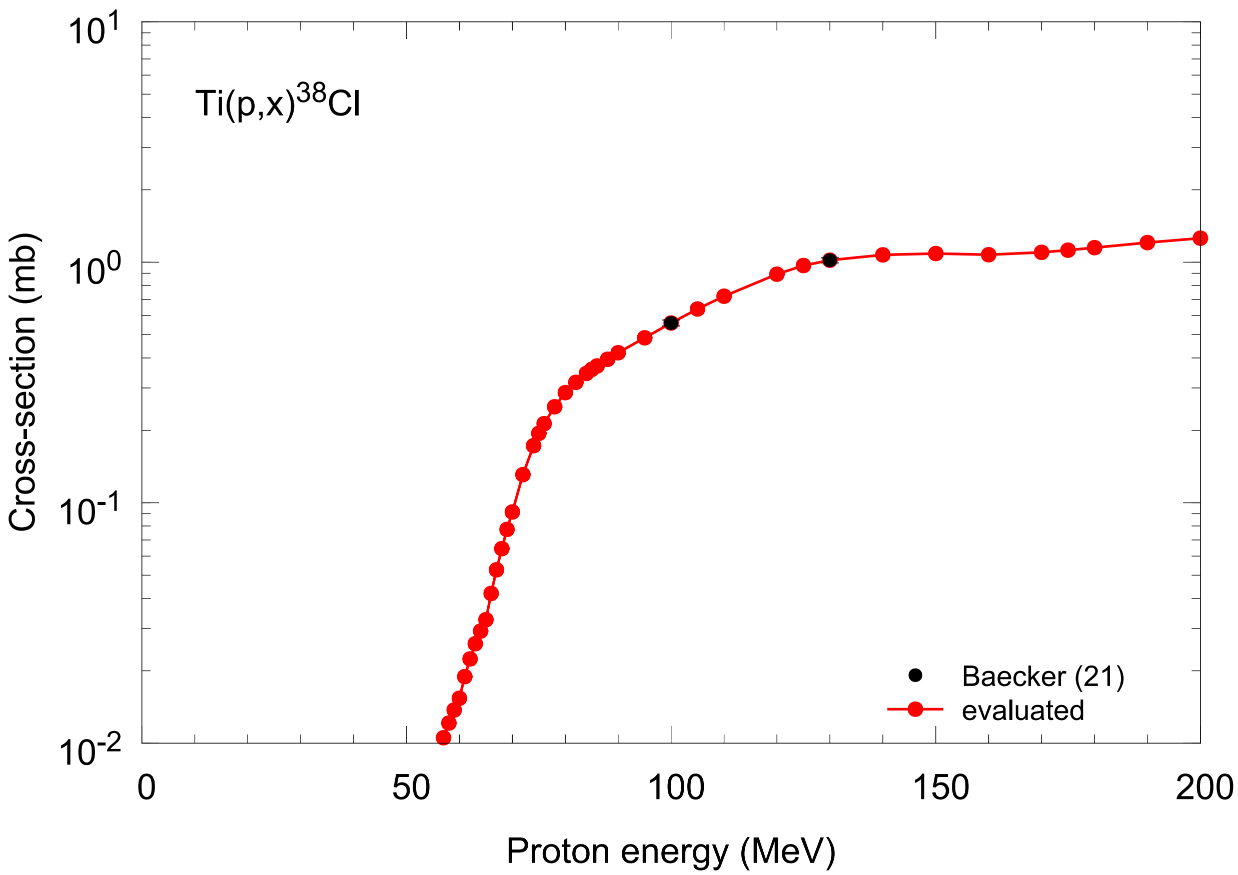
Ti(p,x)^{38}Cl
Cross-section (mb)
Proton energy (MeV)
Baecker (21)
evaluated

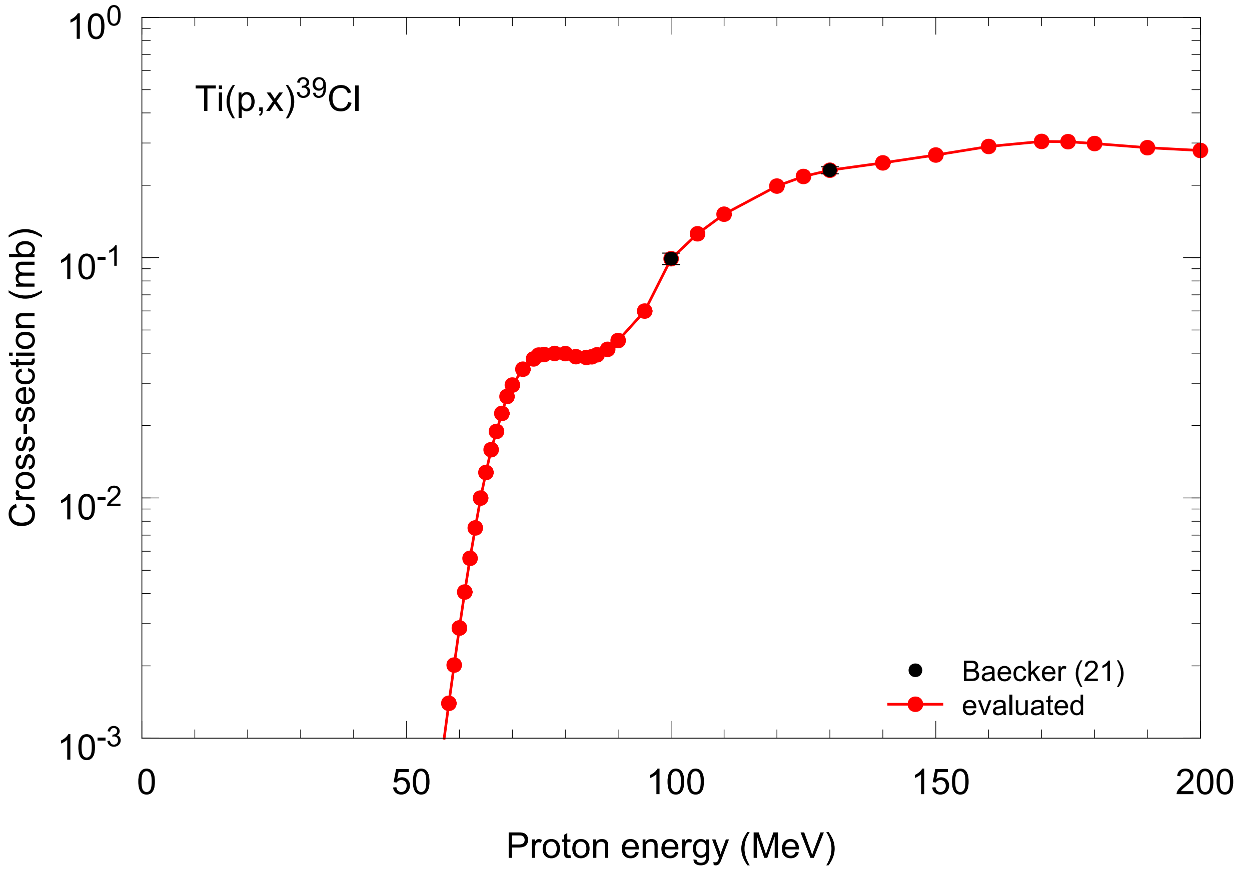

10^0
10^{-1}
10^{-2}
10^{-3}
Cross-section (mb)
Ti(p,x)^{39}Cl
Baecker (21)
evaluated
0
50
100
150
200
Proton energy (MeV)

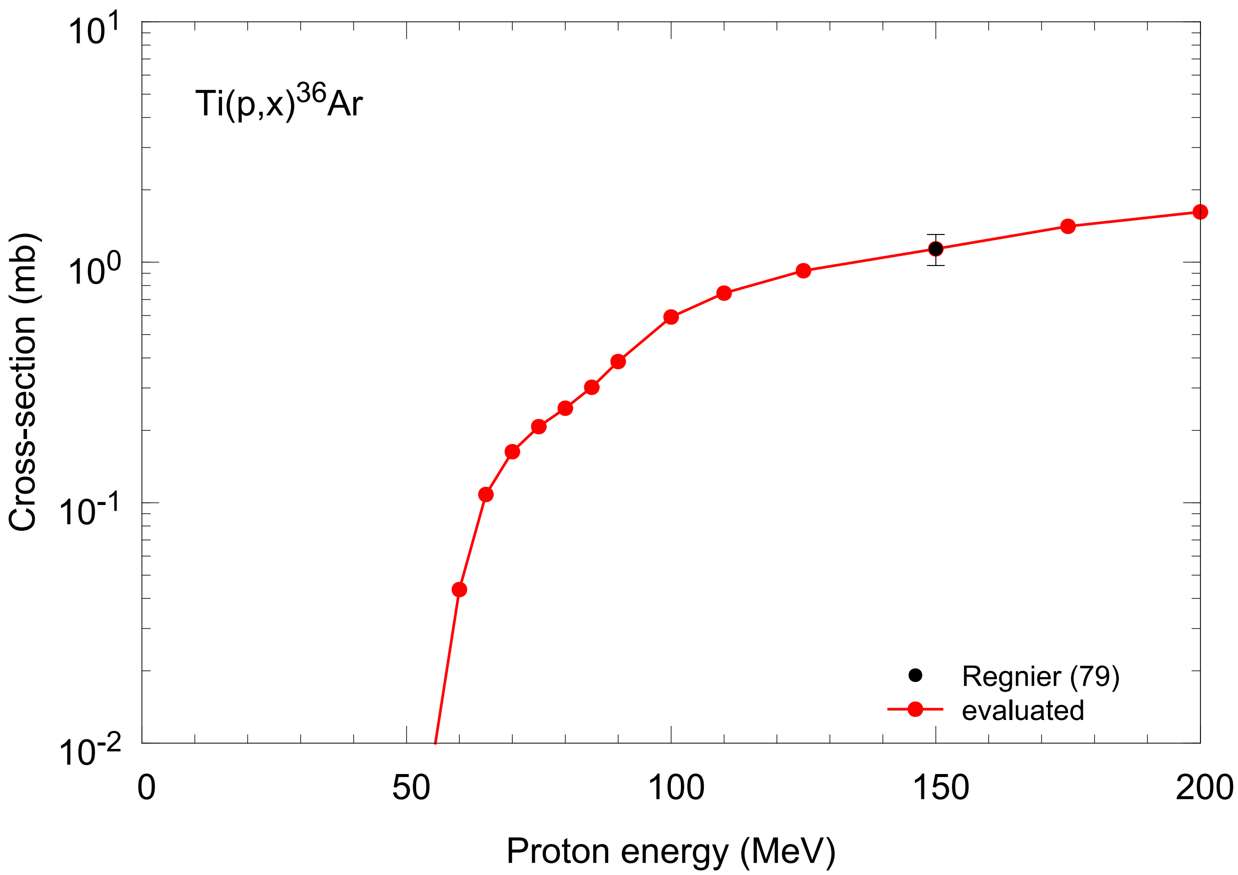

10^1
10^0
10^{-1}
10^{-2}
Cross-section (mb)
Ti(p,x)^{36}Ar
Regnier (79)
evaluated
0
50
100
150
200
Proton energy (MeV)

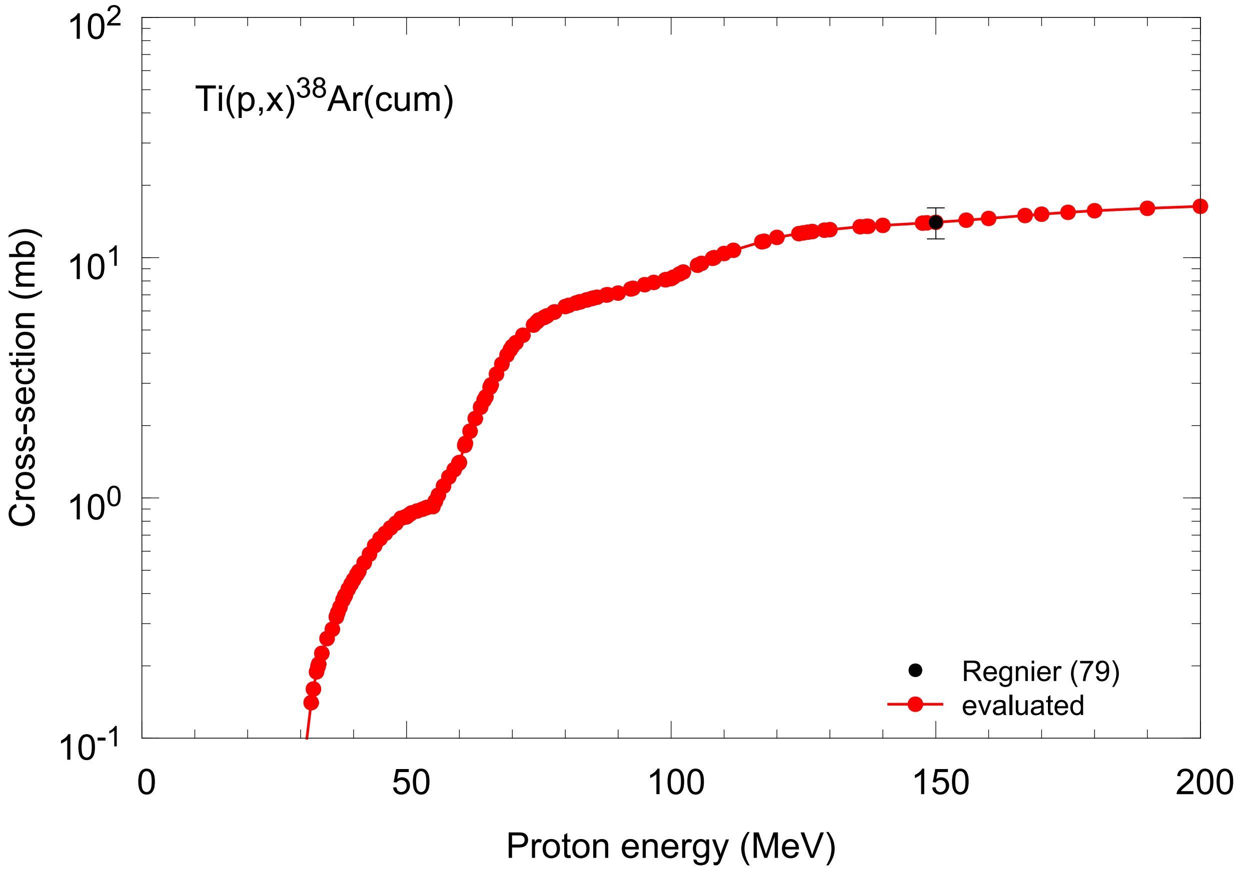

Ti(p,x)38Ar(cum)
Cross-section (mb)
Proton energy (MeV)
Regnier (79)
evaluated

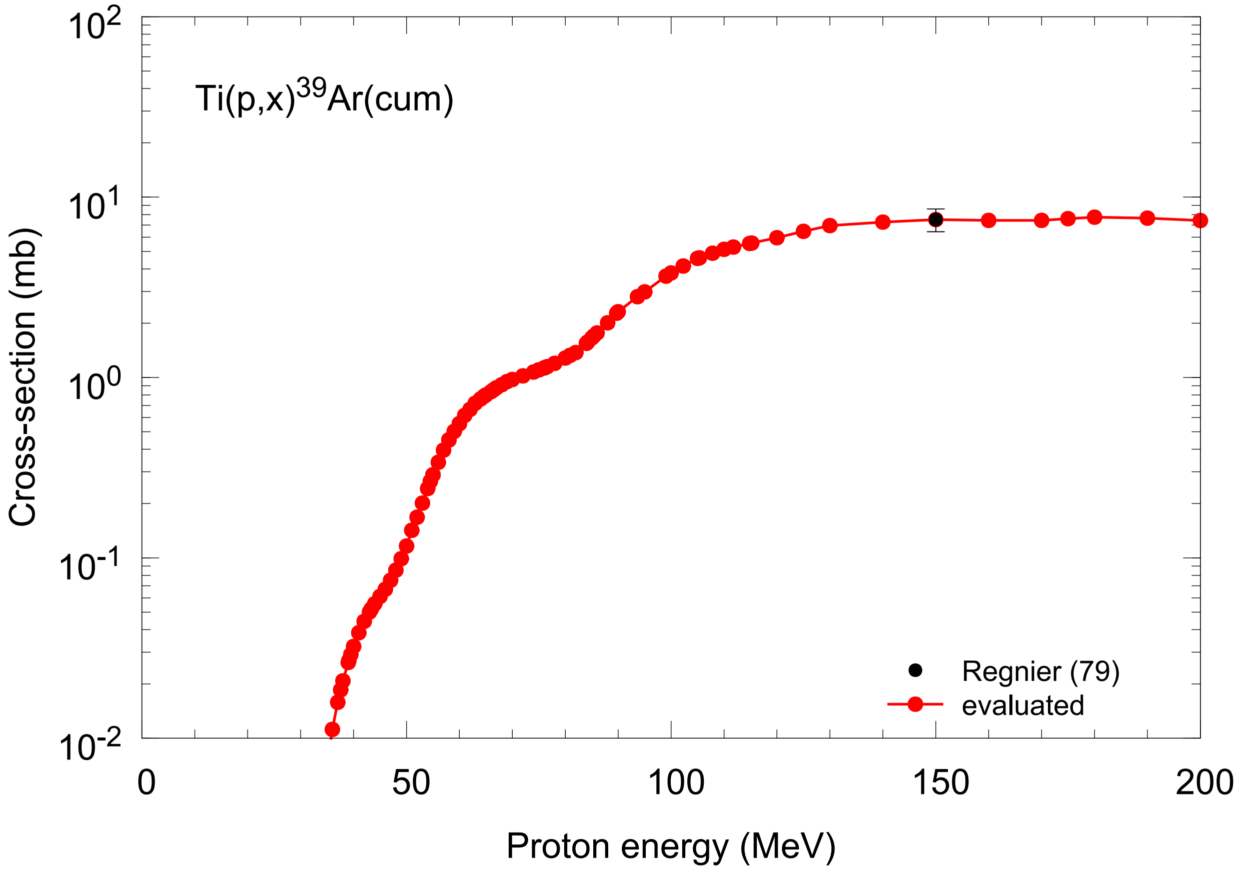

Ti(p,x)39Ar(cum)
Cross-section (mb)
Proton energy (MeV)
Regnier (79)
evaluated

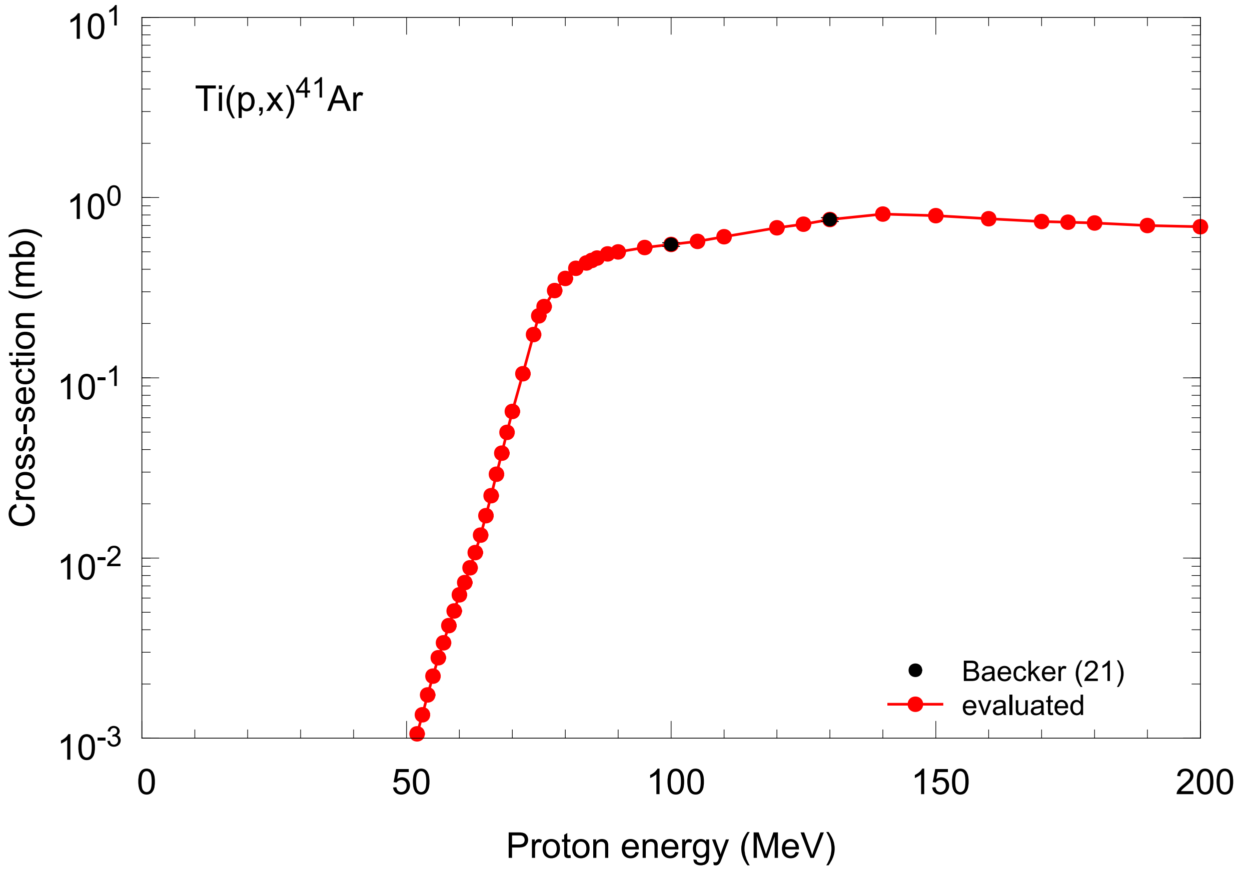

Ti(p,x)^{41}Ar
Cross-section (mb)
Proton energy (MeV)
Baecker (21)
evaluated
10^{1}
10^{0}
10^{-1}
10^{-2}
10^{-3}
0
50
100
150
200

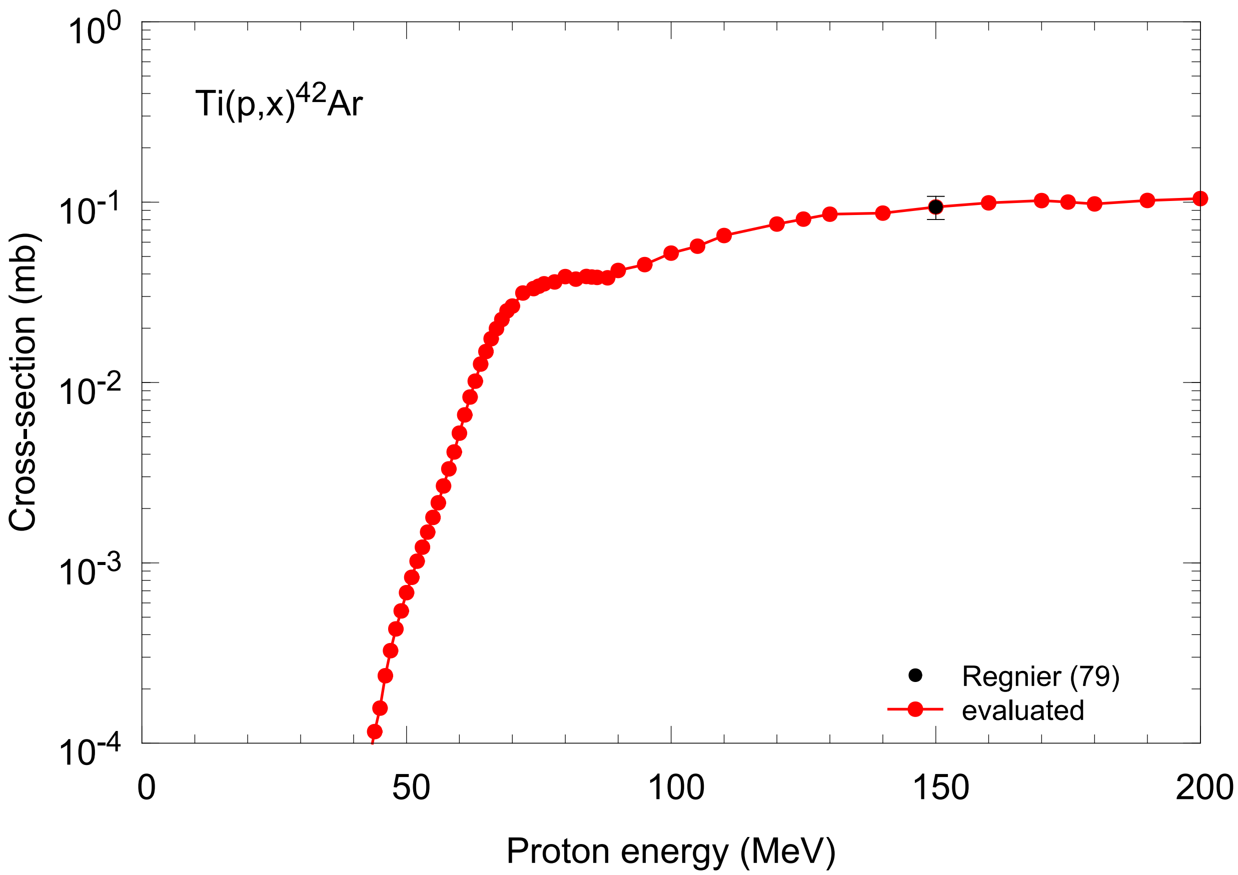

Ti(p,x)^{42}Ar
Cross-section (mb)
Proton energy (MeV)
Regnier (79)
evaluated
10^{0}
10^{-1}
10^{-2}
10^{-3}
10^{-4}
0
50
100
150
200

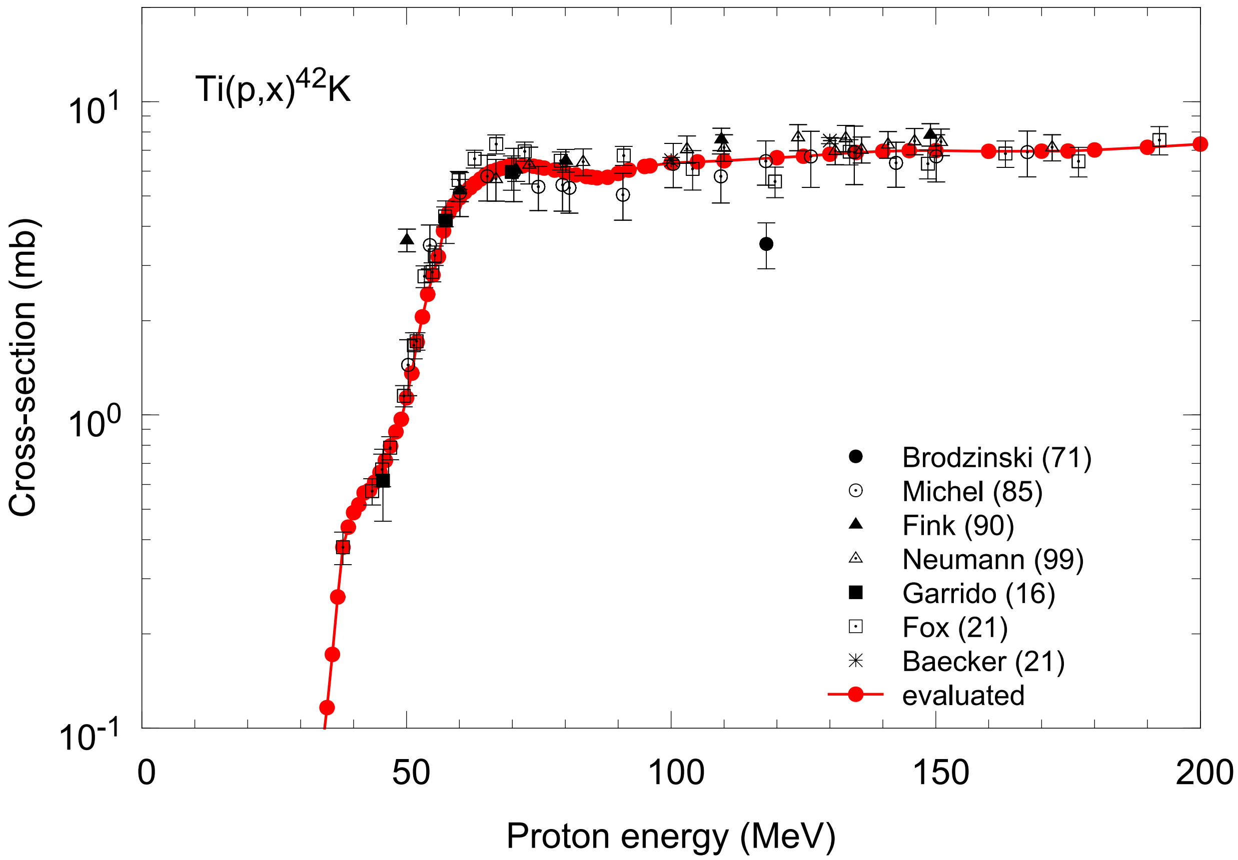
Ti(p,x)^{42}K
Cross-section (mb)
10^{1}
10^{0}
10^{-1}
0
50
100
150
200
Proton energy (MeV)
Brodzinski (71)
Michel (85)
Fink (90)
Neumann (99)
Garrido (16)
Fox (21)
Baecker (21)
evaluated

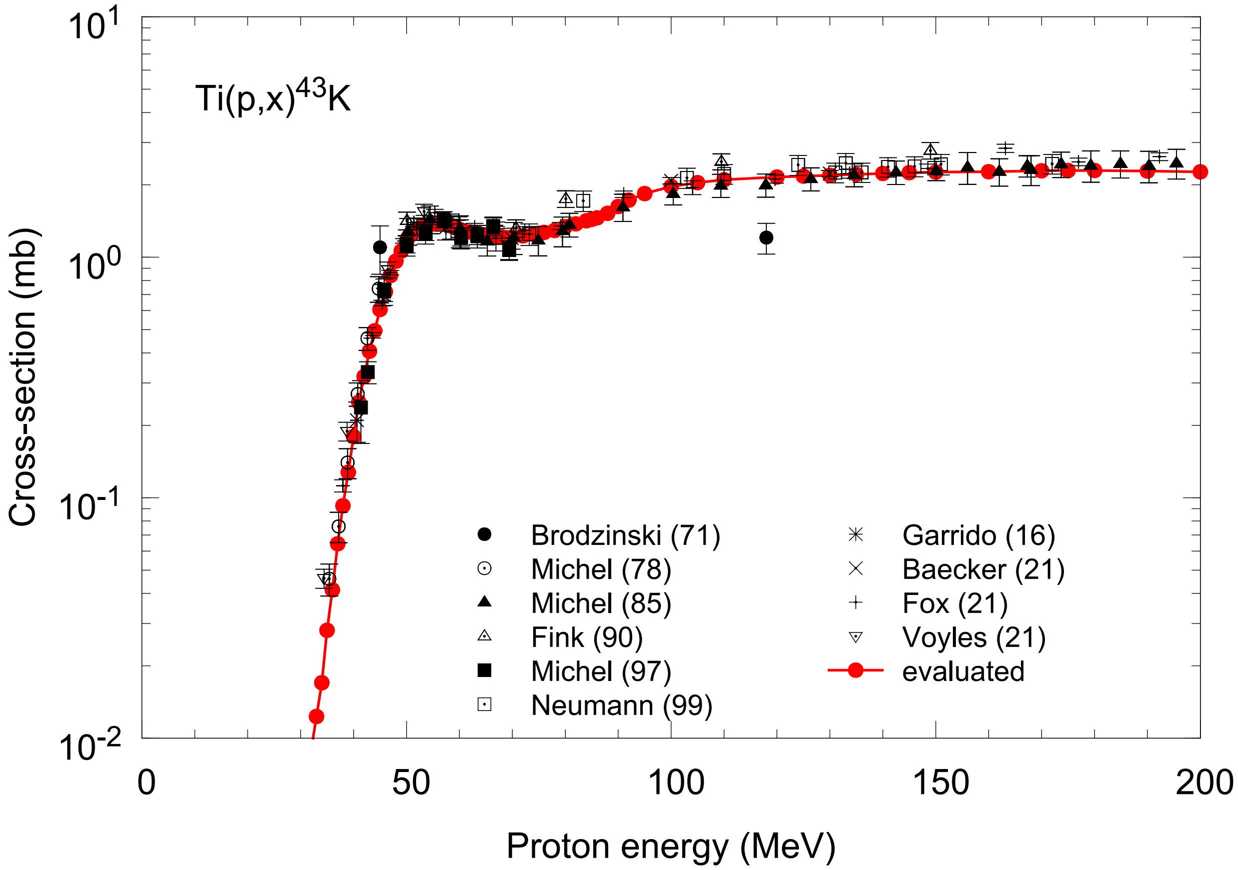
Ti(p,x)^{43}K
Cross-section (mb)
10^{1}
10^{0}
10^{-1}
10^{-2}
0
50
100
150
200
Proton energy (MeV)
Brodzinski (71)
Michel (78)
Michel (85)
Fink (90)
Michel (97)
Neumann (99)
Garrido (16)
Baecker (21)
Fox (21)
Voyles (21)
evaluated

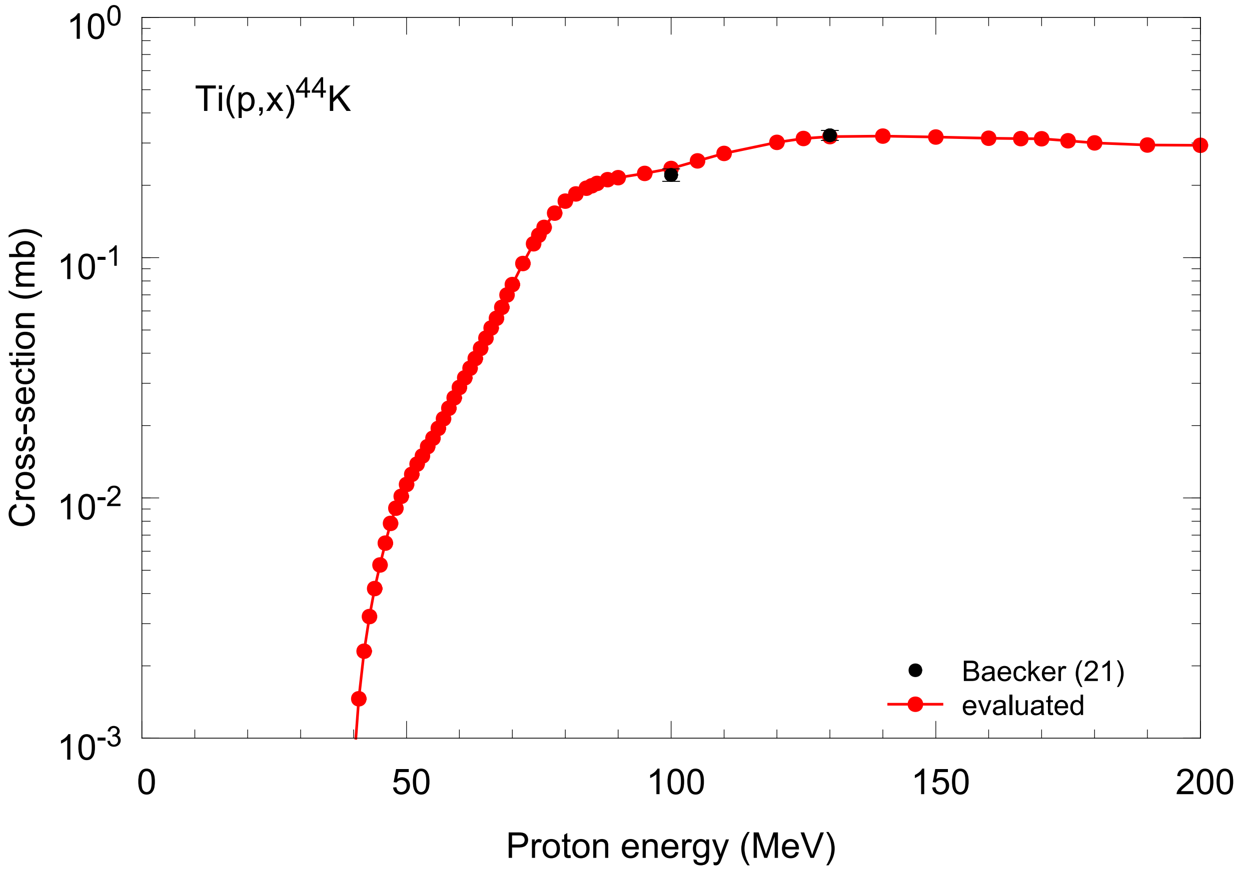

Ti(p,x)^{44}K
Cross-section (mb)
10^0
10^{-1}
10^{-2}
10^{-3}
0
50
100
150
200
Proton energy (MeV)
Baecker (21)
evaluated

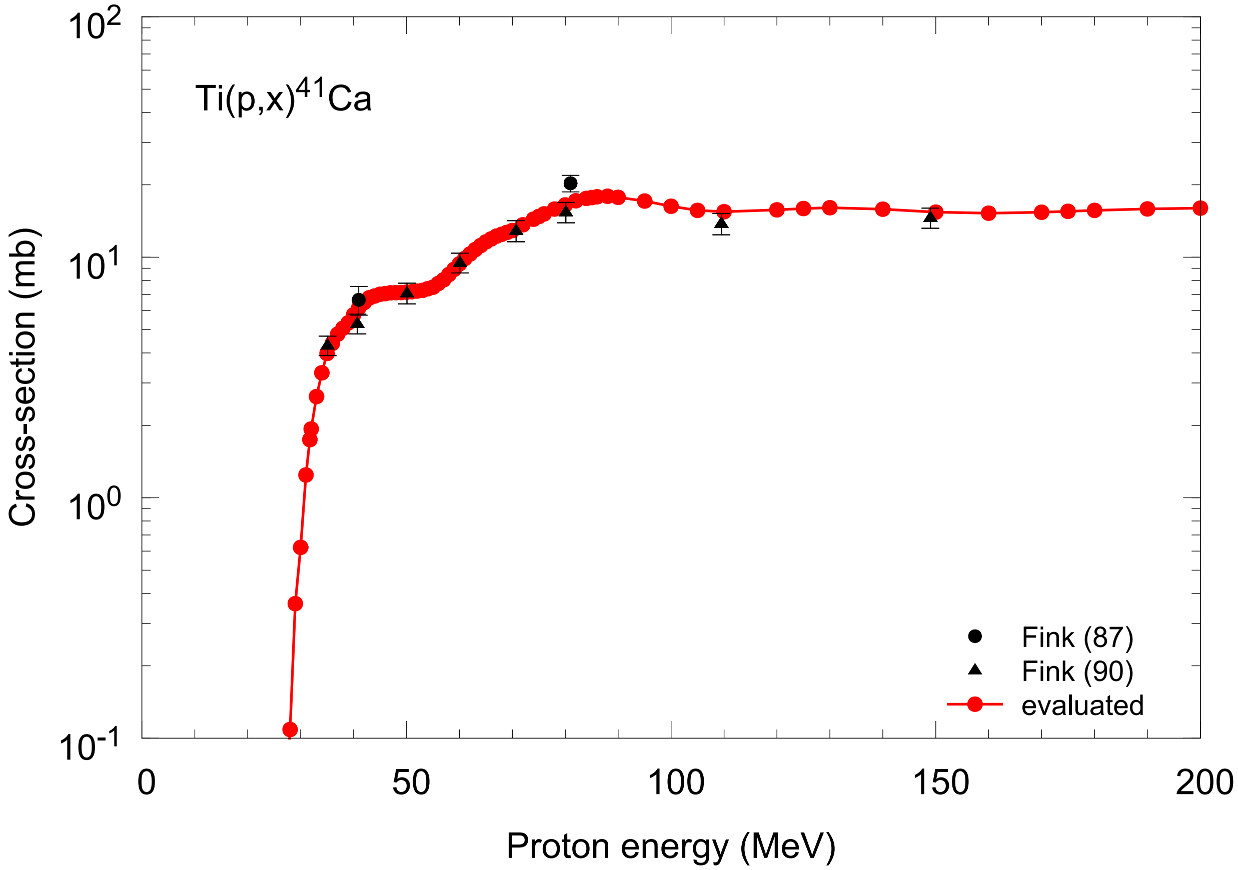

Ti(p,x)^{41}Ca
Cross-section (mb)
10^2
10^1
10^0
10^{-1}
0
50
100
150
200
Proton energy (MeV)
Fink (87)
Fink (90)
evaluated

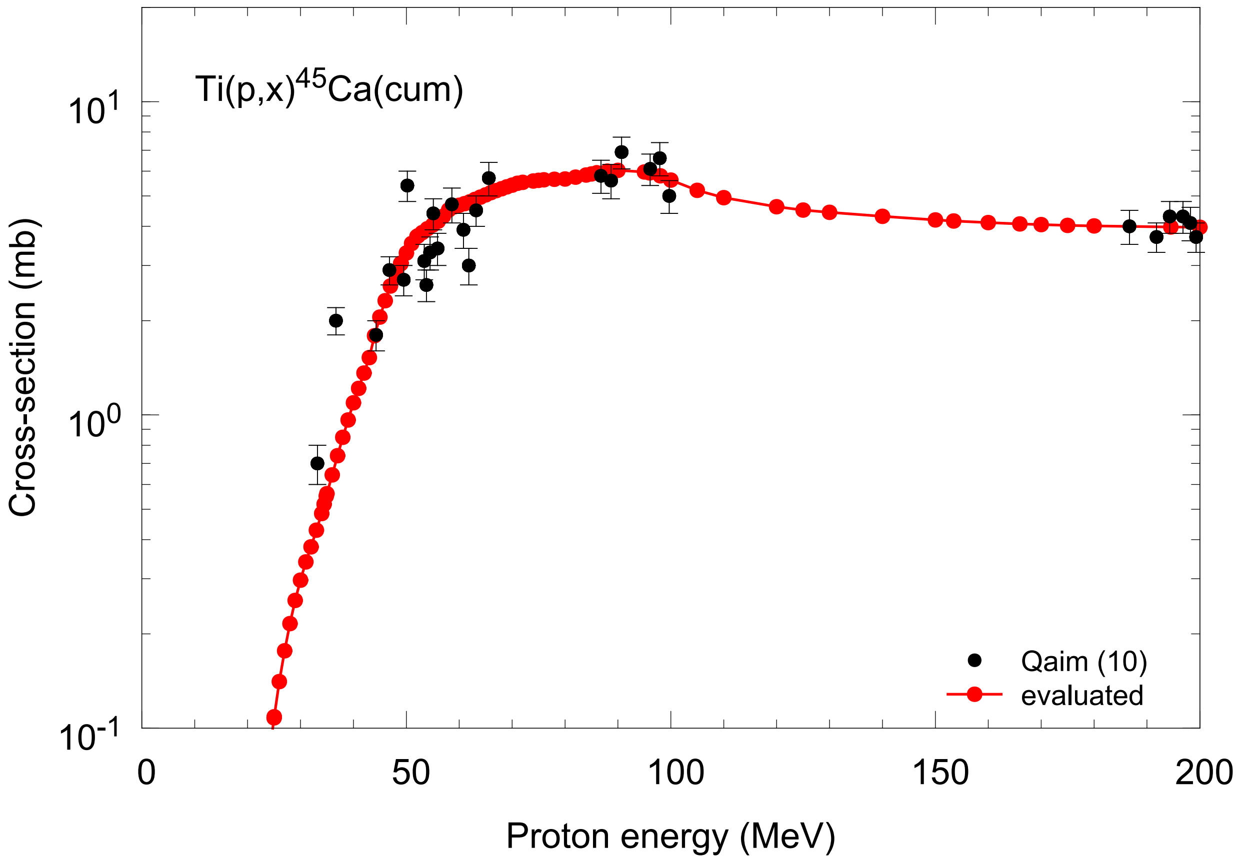

Ti(p,x)^{45}Ca(cum)
Cross-section (mb)
10^{1}
10^{0}
10^{-1}
0
50
100
150
200
Proton energy (MeV)
Qaim (10)
evaluated

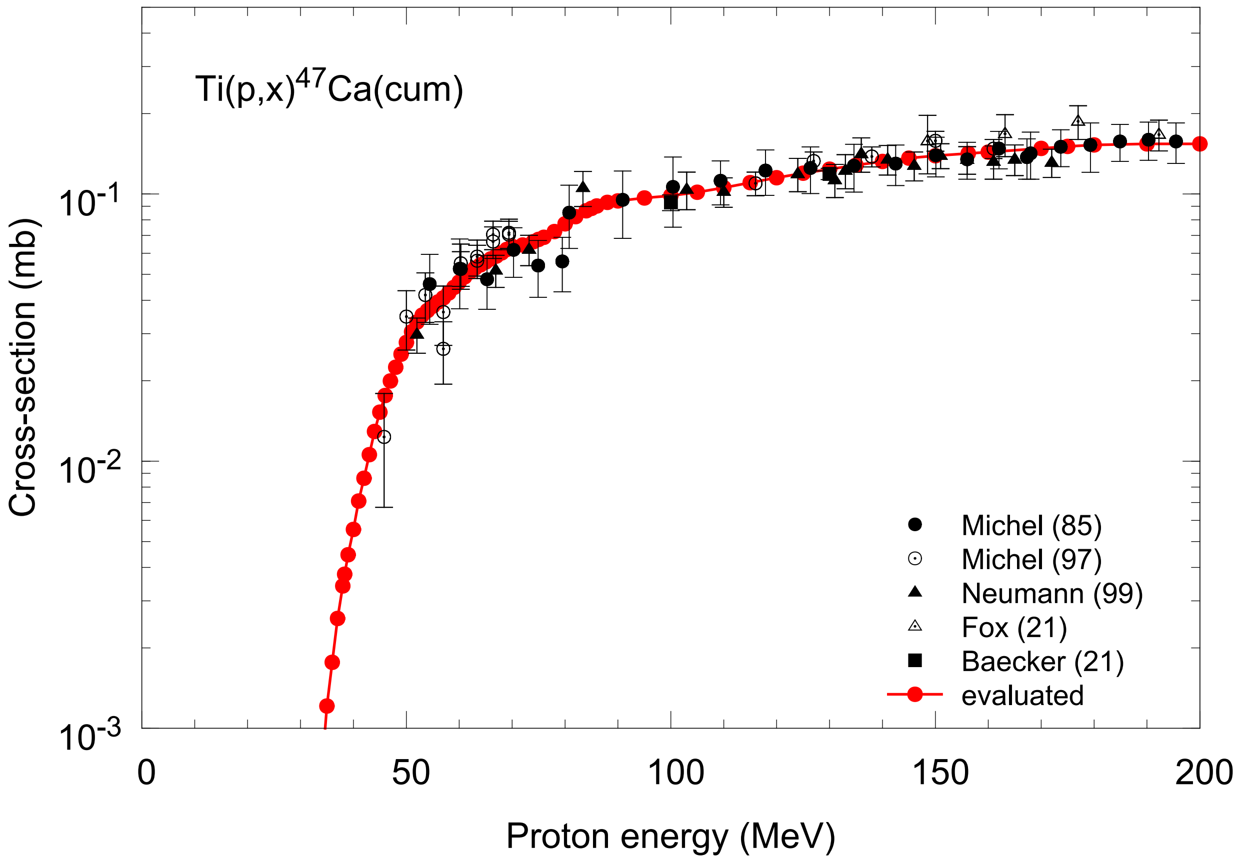

Ti(p,x)^{47}Ca(cum)
Cross-section (mb)
10^{-1}
10^{-2}
10^{-3}
0
50
100
150
200
Proton energy (MeV)
Michel (85)
Michel (97)
Neumann (99)
Fox (21)
Baecker (21)
evaluated

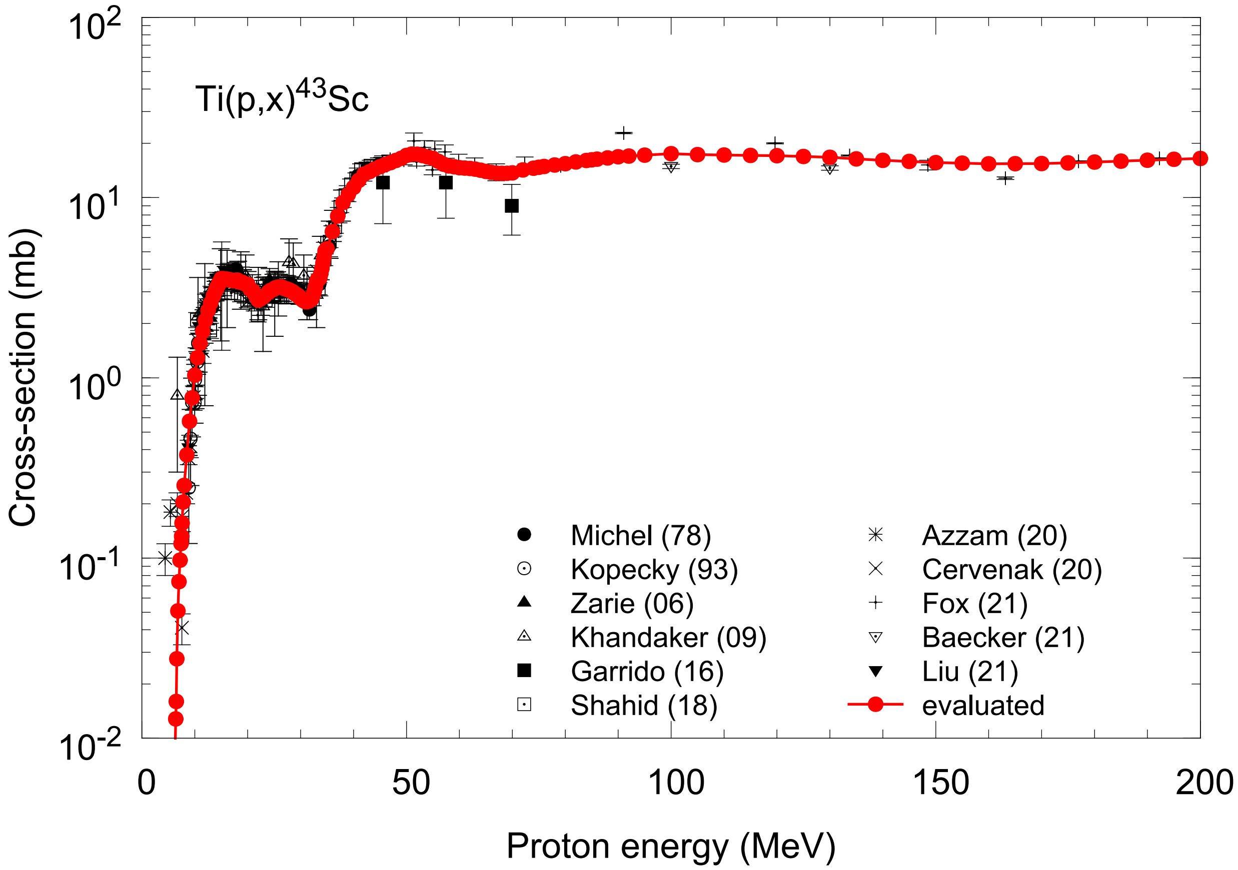

Ti(p,x)43Sc
Cross-section (mb)
Proton energy (MeV)
Michel (78)
Kopecky (93)
Zarie (06)
Khandaker (09)
Garrido (16)
Shahid (18)
Azzam (20)
Cervenak (20)
Fox (21)
Baecker (21)
Liu (21)
evaluated

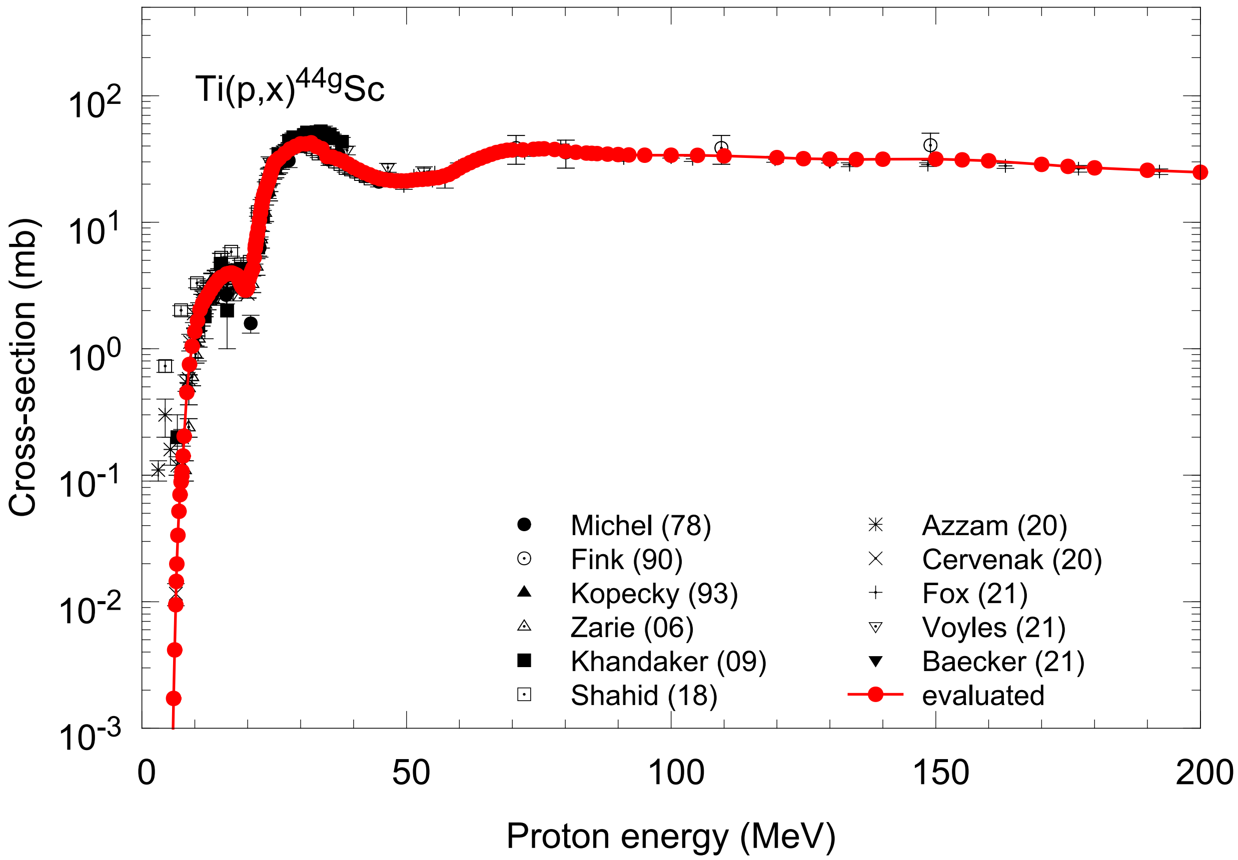

Ti(p,x)44gSc
Cross-section (mb)
Proton energy (MeV)
Michel (78)
Fink (90)
Kopecky (93)
Zarie (06)
Khandaker (09)
Shahid (18)
Azzam (20)
Cervenak (20)
Fox (21)
Voyles (21)
Baecker (21)
evaluated

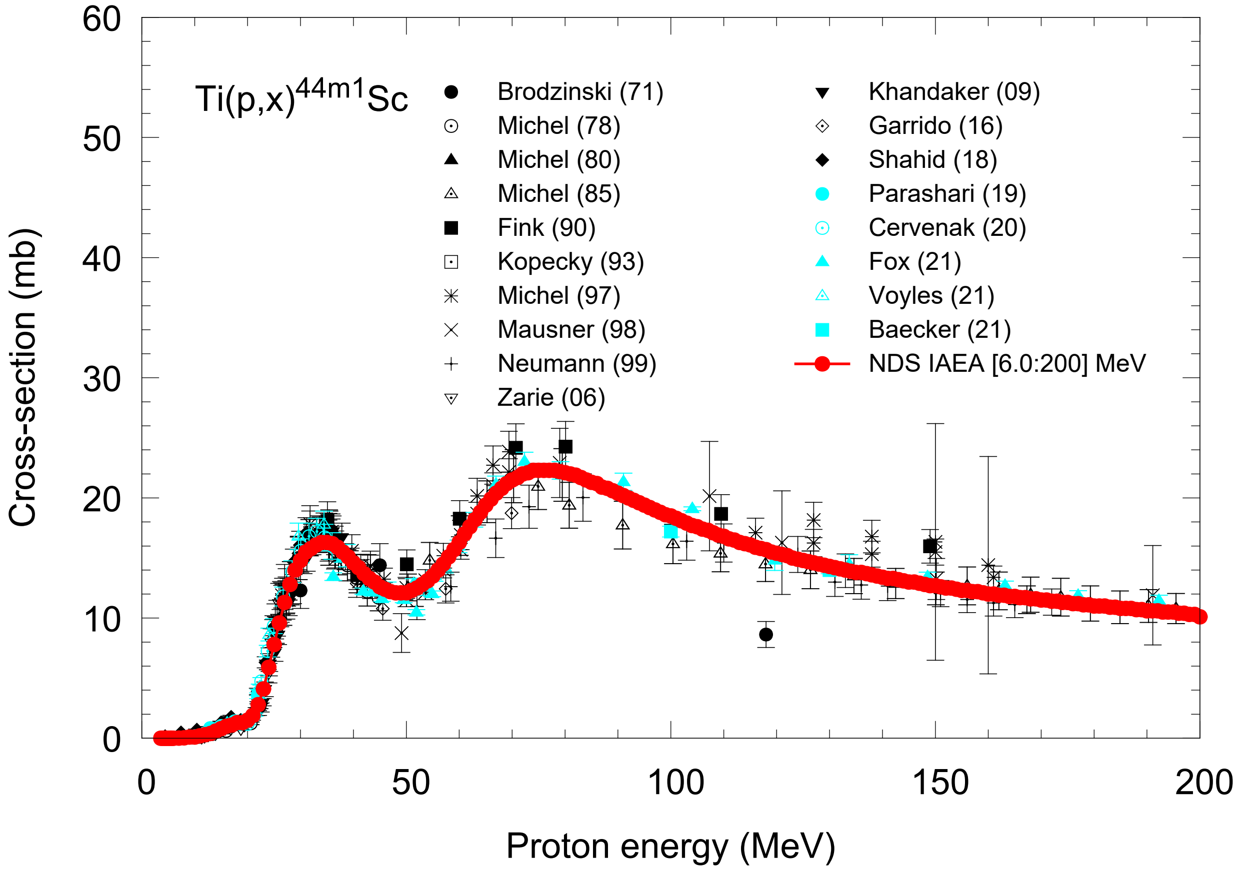
Ti(p,x)44m1Sc
Brodzinski (71)
Michel (78)
Michel (80)
Michel (85)
Fink (90)
Kopecky (93)
Michel (97)
Mausner (98)
Neumann (99)
Zarie (06)
Khandaker (09)
Garrido (16)
Shahid (18)
Parashari (19)
Cervenak (20)
Fox (21)
Voyles (21)
Baecker (21)
NDS IAEA [6.0:200] MeV
Cross-section (mb)
Proton energy (MeV)
0
10
20
30
40
50
60
0
50
100
150
200

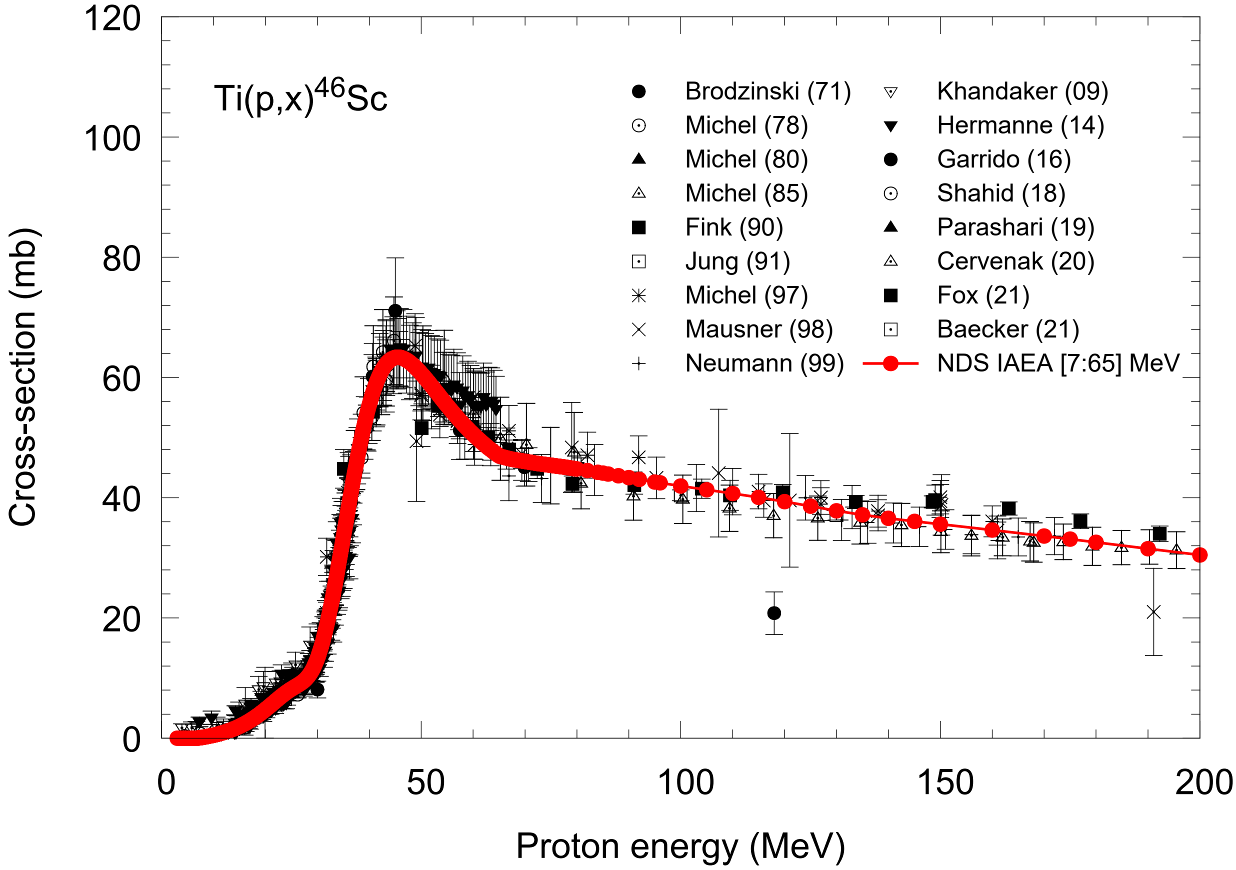
Ti(p,x)46Sc
Brodzinski (71)
Michel (78)
Michel (80)
Michel (85)
Fink (90)
Jung (91)
Michel (97)
Mausner (98)
Neumann (99)
Khandaker (09)
Hermanne (14)
Garrido (16)
Shahid (18)
Parashari (19)
Cervenak (20)
Fox (21)
Baecker (21)
NDS IAEA [7:65] MeV
Cross-section (mb)
Proton energy (MeV)
0
20
40
60
80
100
120
0
50
100
150
200

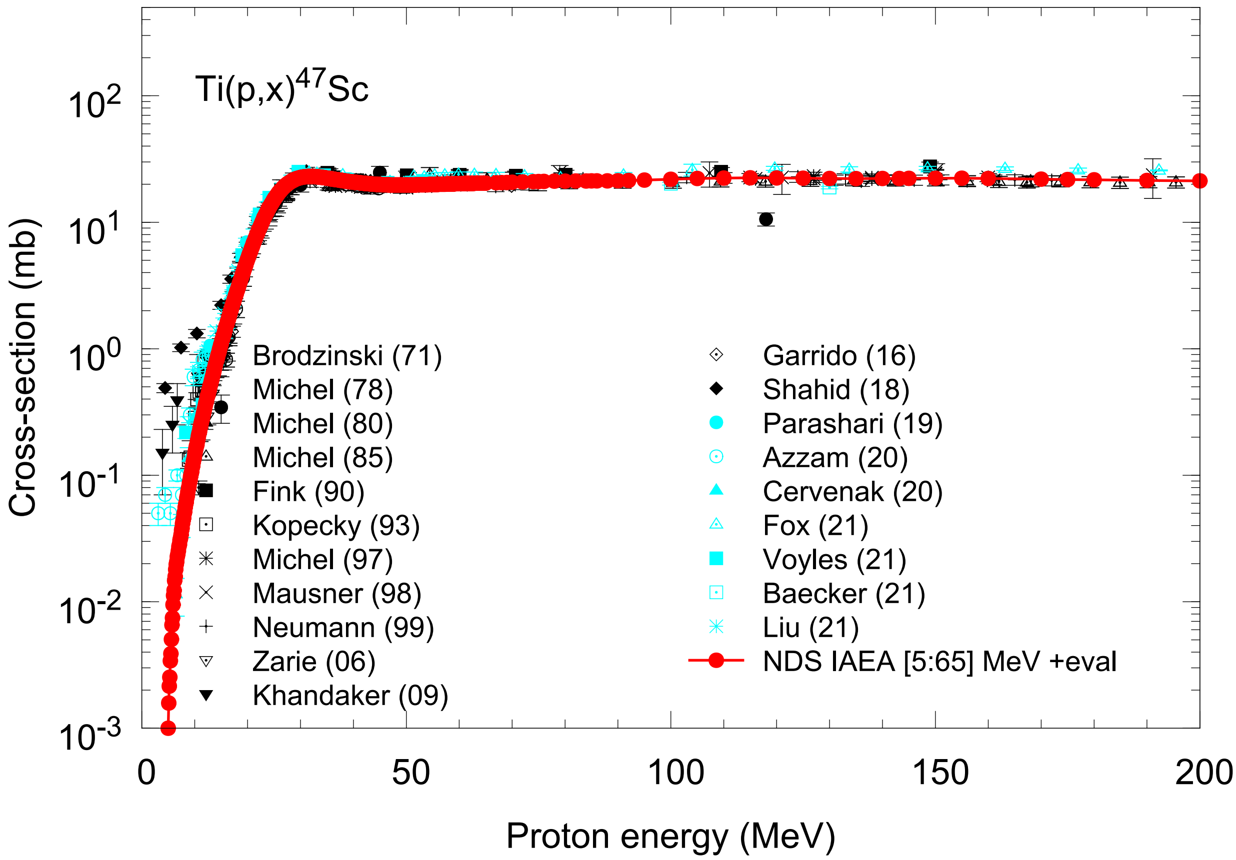
Ti(p,x)^{47}Sc
Cross-section (mb)
Proton energy (MeV)
Brodzinski (71)
Michel (78)
Michel (80)
Michel (85)
Fink (90)
Kopecky (93)
Michel (97)
Mausner (98)
Neumann (99)
Zarie (06)
Khandaker (09)
Garrido (16)
Shahid (18)
Parashari (19)
Azzam (20)
Cervenak (20)
Fox (21)
Voyles (21)
Baecker (21)
Liu (21)
NDS IAEA [5:65] MeV +eval

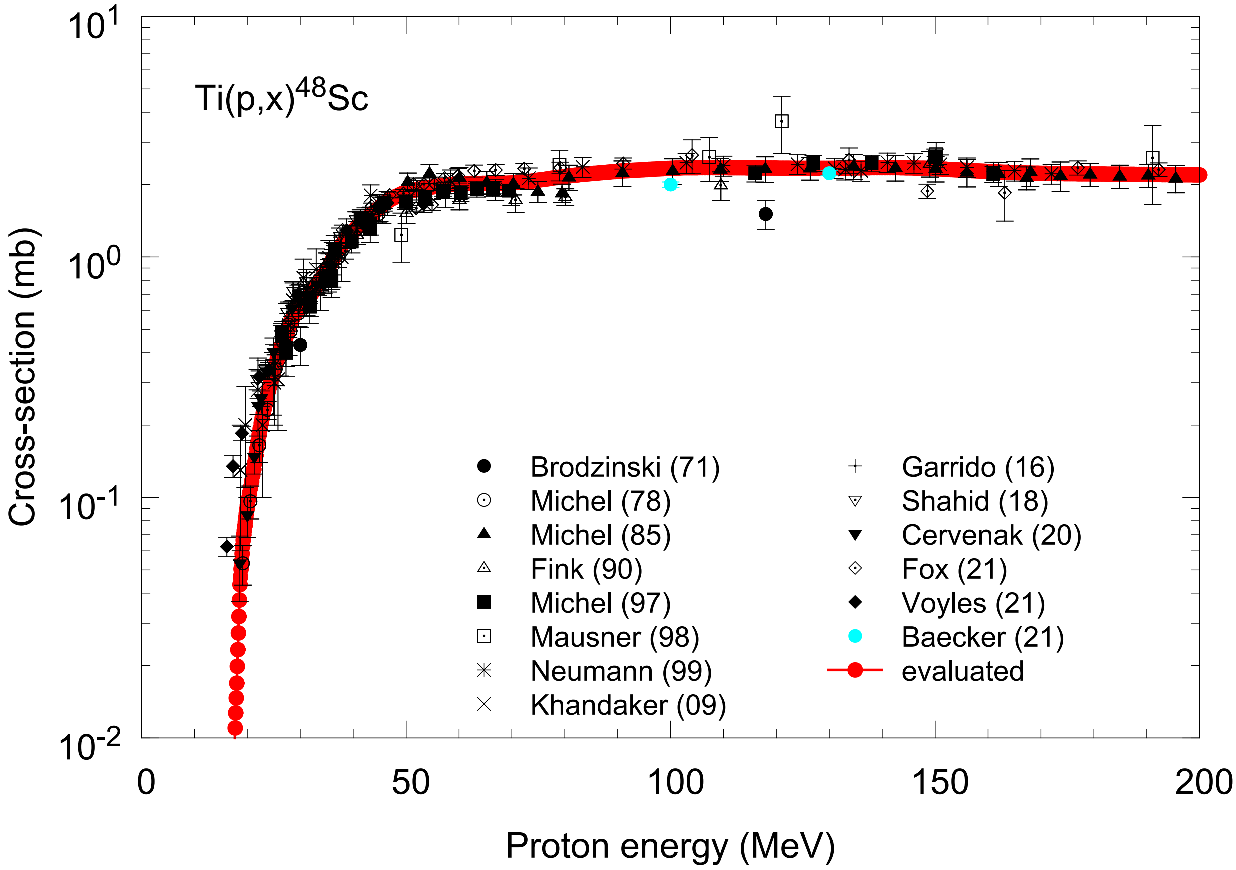
Ti(p,x)^{48}Sc
Cross-section (mb)
Proton energy (MeV)
Brodzinski (71)
Michel (78)
Michel (85)
Fink (90)
Michel (97)
Mausner (98)
Neumann (99)
Khandaker (09)
Garrido (16)
Shahid (18)
Cervenak (20)
Fox (21)
Voyles (21)
Baecker (21)
evaluated

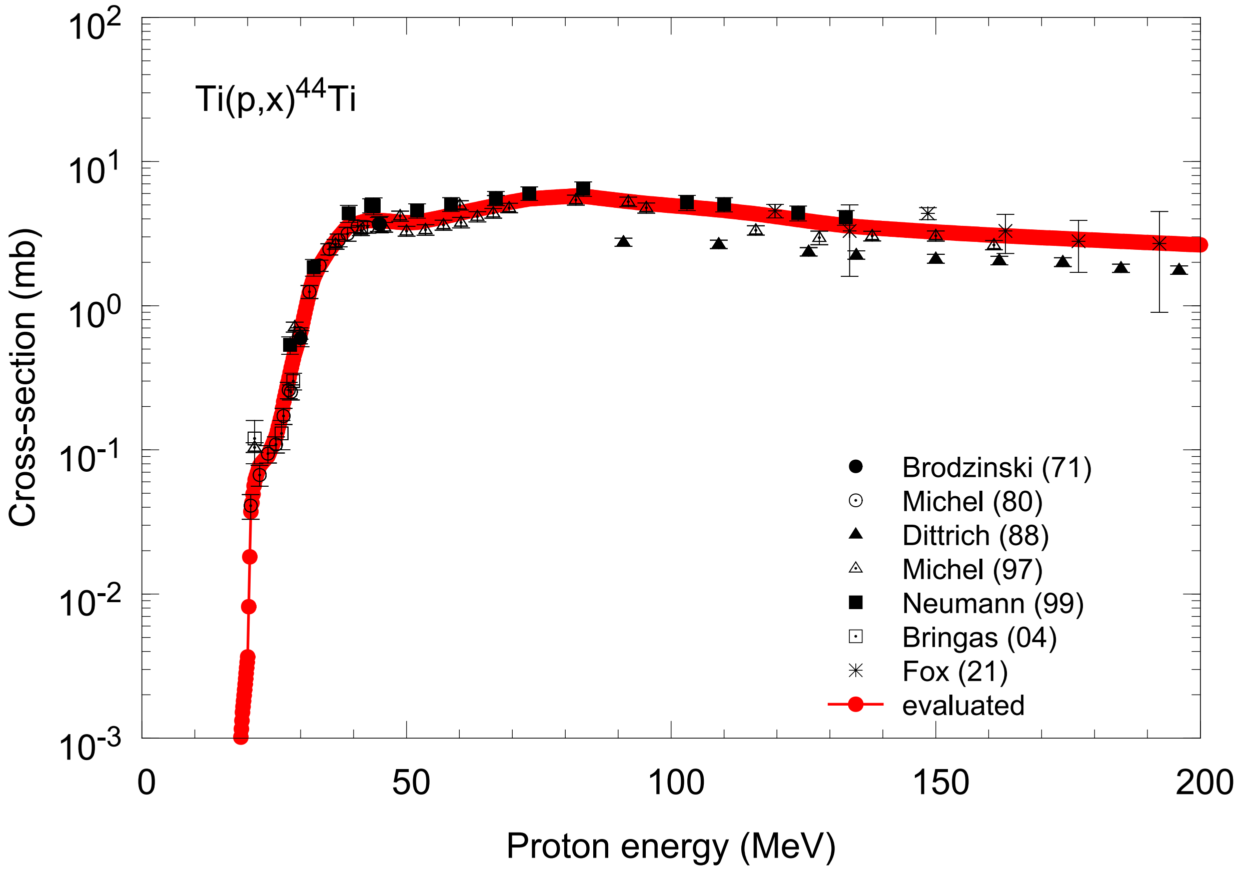
Ti(p,x)^{44}Ti
Cross-section (mb)
Proton energy (MeV)
Brodzinski (71)
Michel (80)
Dittrich (88)
Michel (97)
Neumann (99)
Bringas (04)
Fox (21)
evaluated

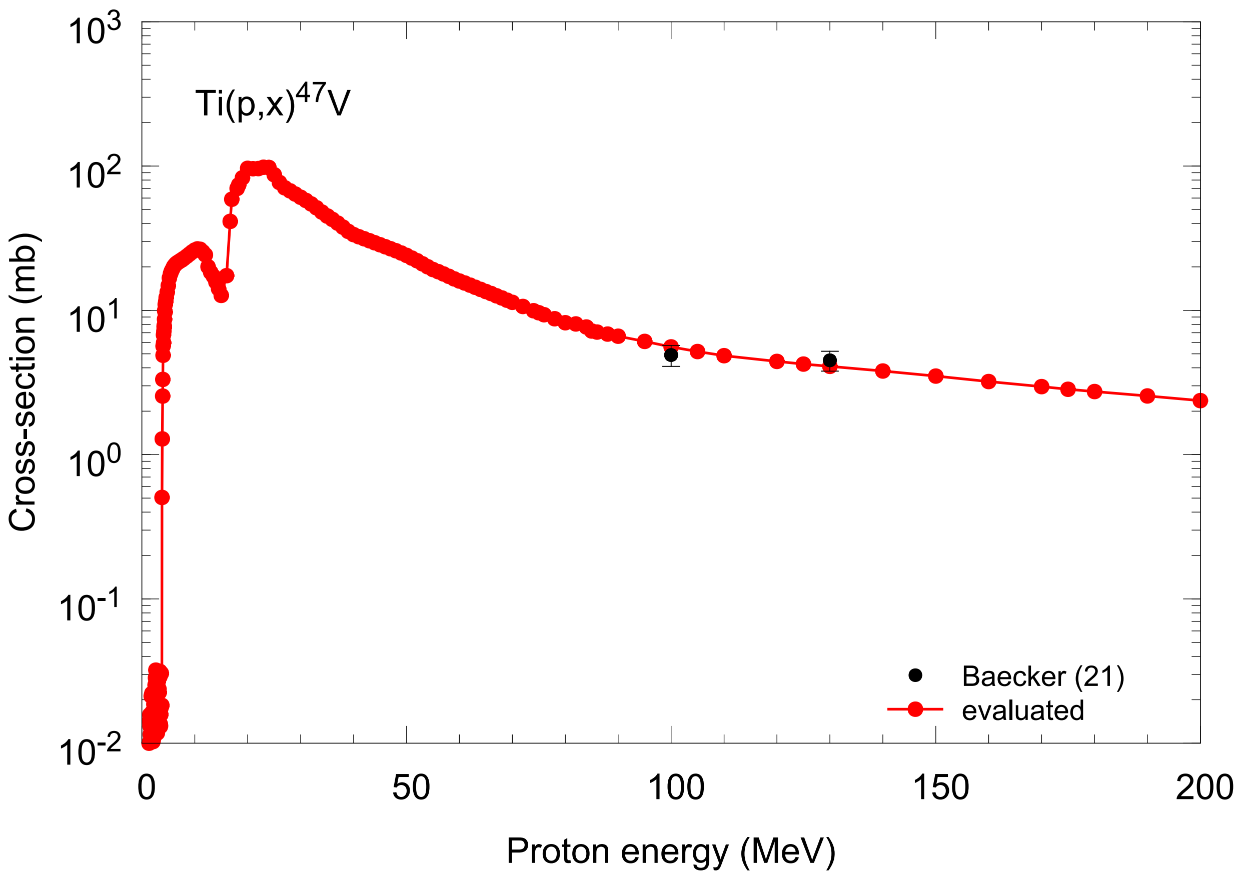
Ti(p,x)^{47}V
Cross-section (mb)
Proton energy (MeV)
Baecker (21)
evaluated

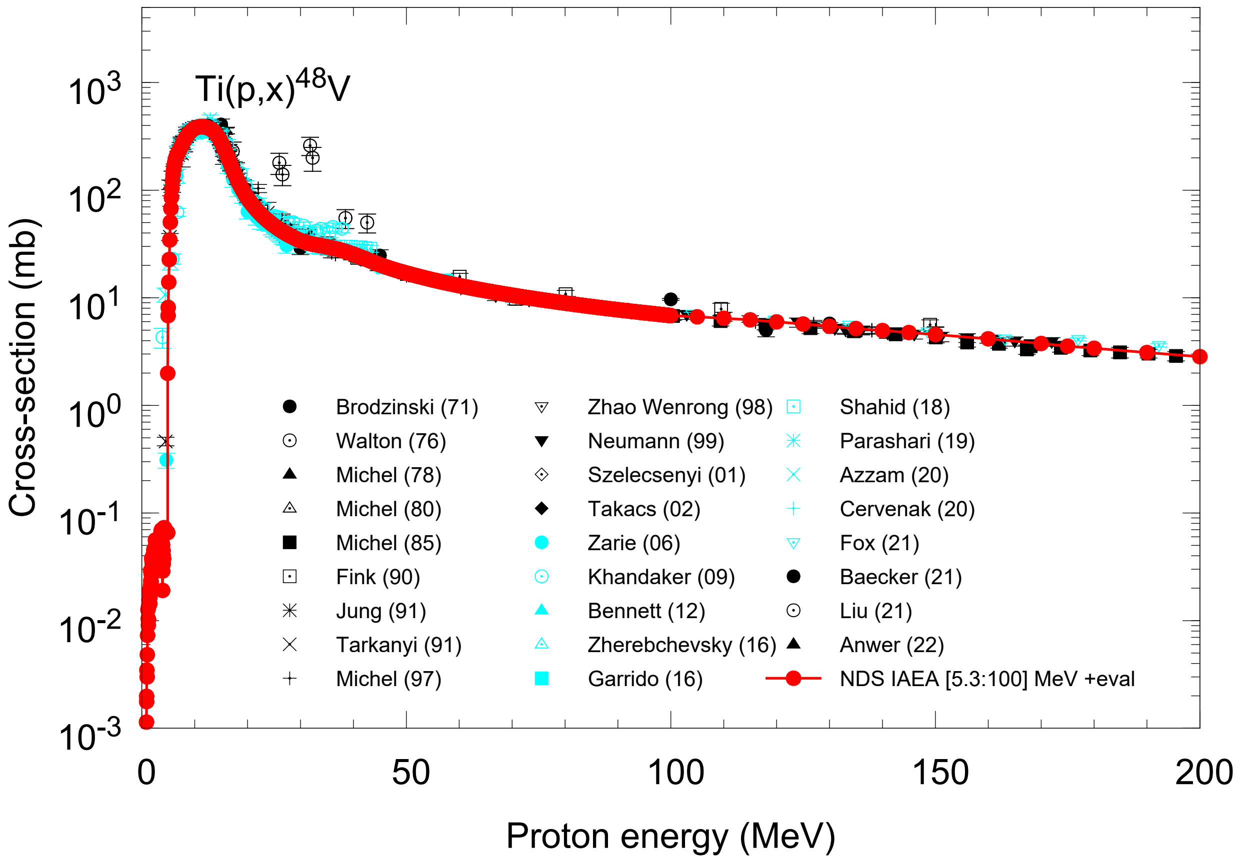
Ti(p,x)^{48}V
Cross-section (mb)
Proton energy (MeV)
Brodzinski (71)
Walton (76)
Michel (78)
Michel (80)
Michel (85)
Fink (90)
Jung (91)
Tarkanyi (91)
Michel (97)
Zhao Wenrong (98)
Neumann (99)
Szelecsenyi (01)
Takacs (02)
Zarie (06)
Khandaker (09)
Bennett (12)
Zherebchevsky (16)
Garrido (16)
Shahid (18)
Parashari (19)
Azzam (20)
Cervenak (20)
Fox (21)
Baecker (21)
Liu (21)
Anwer (22)
NDS IAEA [5.3:100] MeV +eval

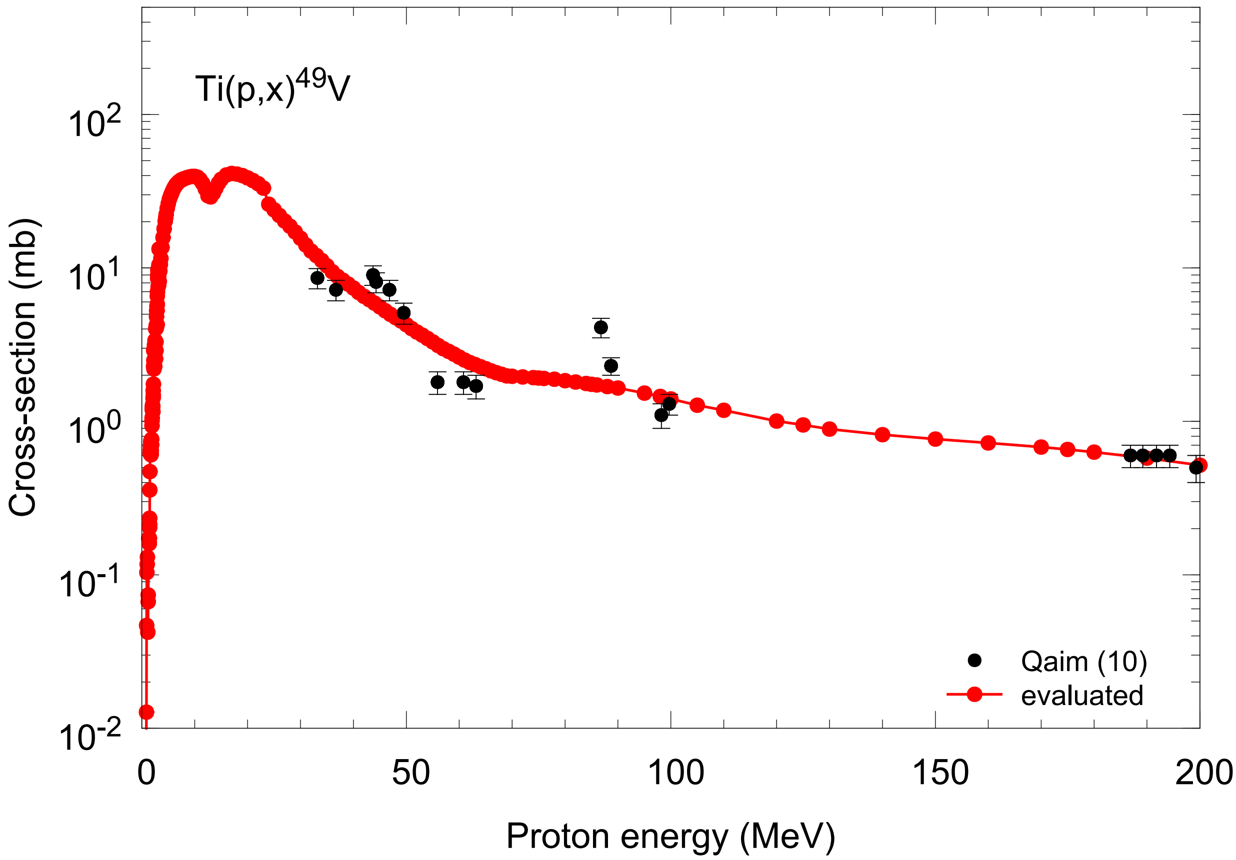
Ti(p,x)^{49}V
Cross-section (mb)
Proton energy (MeV)
Qaim (10)
evaluated

KIT Scientific Working Papers
ISSN 2194-1629